

## **Tibet and High-Asia**

*Results of Investigations into High Mountain Geomorphology,  
Paleo-Glaciology and Climatology of the Pleistocene  
(Ice Age Research) (IV)*

The reconstruction of the Ice Age glacier expansions was begun by the author in the western foothills of High Asia, in the south-eastern Kuhrud mountains (Zagros), in the years 1973 and 1974. Since 1976 he was able to carry out a series of scientific research trips and expeditions for periods of from one to four months in Tibet and its surrounding mountains concerning the same, but broader question. These undertakings, which in part led to remote areas which had scarcely ever been investigated, were logistically difficult and expensive. They have been financed by the Deutsche Forschungsgemeinschaft (DFG), the Max-Planck-Gesellschaft (MPG), the Academia Sinica, the Russian Academy of Sciences, the Volkswagen-Stiftung (VW-Stiftung), the Deutsche Akademische Austauschdienst (DAAD), the University of Göttingen and by private means. The initially astonishing observations with respect to unexpectedly low glacial traces of the glacier margin and the related very extended glacier areas in the subtropics, became more and more established in the meantime, though they provoked vehement protest at the outset. Since 1990 they have been confirmed by the results of other scientists and research groups – especially in China – and integrated in the international cartographic project. Nevertheless, and in spite of increasing efforts to describe and understand the geomorphology, the Ice Age glacier cover and the related climatic and ecological changes and upheavals on the part of both our own and other research groups, this bare, wild, remote and in consequence scarcely settled section of Asia is too extended to finalize our investigations once and for all. After all, High Asia between the Hindukush and East-Kuenlun and between the Himalaya and Altai extends over approximately 4 million km<sup>2</sup>. Due to the energy-rich geometry of its global radiation intake, it occupies an important position – if not a key-function – for the onset of Ice Ages and the climatic history in the Pleistocene.

The four papers of this volume seek to deliver a further contribution to physical-geographical knowledge and Ice Age research. With that they follow the tradition of the first three volumes ‘Tibet and High-Asia’ (I–III), which have been presented by *GeoJournal* at intervals of three years since 1988. Most of the empirical data of the studies have been acquired during field campaigns over several months to Tibet (PR China), Kirghizia, Pakistan, India and Nepal.

M. Kuhle’s contribution addresses the Last Glacial glacier history of the Pamir, of the Nanga Parbat massif, of North- and Central Tibet and of South Tibet with the Himalaya. During the investigation of these test-areas, which surround large sections of Tibet, and thus amount to undertaking spot-checks, work focussed on registration of the maximum pre-historic glacier expansion as well as detailed regionally-extended revision of the theory that Tibet had almost been completely covered by an ice sheet. – In the valleys and forelands of the today still rather heavily glaciated mountain-massifs of the Tian Shan and the Karakorum, the investigations of S. Meiners distinguish between Late Glacial ice margins or glacier expansions from the Holocene (Neoglacial) and Historic lateral- and end moraines.

The methodical linkage of her glacio-geomorphological analyses of the moraine sequences and for the important purpose of supra-regional comparison is an as exact as possible calculation of the ELA (snow-line) depression. L. Iturrizaga presents a further empirical investigation, the observations of which stem from the north-western Karakorum. The work deals with the influence of climatic, geomorphological and glacial processes on traffic routes and settlements with their fields and irrigation installations. Based on field-data, these first three contributions are chronologically connected because they concern the Ice Age to Historical glacier history and its geomorphological consequences for the human settlement of the mountain region. The research of B. Bielefeld concerns a physical and mathematical deductive calculation of the Last Glacial Maximum (LGM) energy loss of the earth. This calculation is based on the global rise in the albedo by Ice Age glacier surfaces. The High-Asian glacier surfaces are included, indicating their involvement in the global cooling. The study thus comments the hypothesis, according to which the glaciation of Tibet, linked with the uplift above the snow-line, might have been the impulse and the true trigger of the Pleistocene Ice Ages.

In this place the editor wishes to thank those Chinese, Russian and German colleagues who worked with him in the field, or participated closely in realising the results presented here through organisation, their expert support and their advices. Among others these included Prof. Wang Wenjing, Prof. Xu Daoming, Prof. Xie Zichu, Prof. M. G. Grosswald and Prof. M. B. Dyurgerov, as well as the honorary experts of the above-mentioned institutions.

Grateful mention is due to the founder of *GeoJournal*, Dr. W. Tietze, whom the editor wishes to thank for his untiring encouragement and supervision of the publication of our research results in this series of 'Tibet and High-Asia' – the printing of which has been technically of the highest quality. In addition the editor wishes to express his thanks to the managing editors, Prof. H. van der Wusten and Prof. O. Gritsai, as well as Mrs. P. D. van Steenbergen for the painstaking publication and printing of this volume. Thanks also deserve the various authors for their contributions.

*Matthias Kuhle*  
*Göttingen, October 1996*

## **The Sino-German Joint Expedition to S Tibet, Shisha Pangma and the N Flank of Chomolungma (Mt. Everest) 1984 – Expedition Report**

*Kuhle, Matthias, Prof., Dr., University of Göttingen, Institute of Geography, Goldschmidtstr. 5, D-3400 Göttingen, FR Germany;*

*Wang Wenjing, Prof., Dr., Academia Sinica, Institute of Glaciology and Cryopedology, Lanzhou, PR China*

*(Presented at the International Symposium on Tibet and High Asia, October 8–11, 1985, Göttingen, FR Germany)*

**ABSTRACT:** The Sino-German Joint Expedition consisted of a group of 8 scientists from the Lanzhou Institute for Glaciology and Cryopedology and the Institute for Plateau Biology in Xining (China) as well as 3 participants from the Geographical Institute of the University of Göttingen (FR Germany). The research expedition to S Tibet and the N slope of the Himalayas was undertaken from August to November 1984, supported by technical personnel and yak herders.

During the 87-day field campaign studies were done in the Transhimalayas, Tibetan Himalayas, and High Himalayas on Shisha Pangma (8046 m) and under specific aspects on Chomolungma (Mt. Everest, 8848 m). The participants of the expedition worked 63 days at altitudes above 6000 m and 6500 m. The highest altitude reached during the collection of data was 7100 m, i.e. the E face of Chang La leading to the N summit of Mt. Everest. Results were attained in the areas of Pleistocene research, recent glaciology (glacier movements, ablation, albedo and firn-ice temperature measurements), neoglacial and recent glacier history, cryopedology (debris drift measurements), botany and vegetation geography. Additionally, geocological data on all significant climatic parameters at high altitudes were collected. This work was documented on 16-mm sound movie film in cooperation with the Institute for Scientific Films (IWF, FR Germany). The expedition results were presented and discussed at the International Symposium on Tibet and High Asia, October 8–11, 1985, in Göttingen.

### **On the Tradition of New Research on High Asia in the Peoples Republic of China and the Federal Republic of Germany**

The Lanzhou Institute for Glaciology and Cryopedology of the Academia Sinica founded in 1958 has now been sending expeditions for field research between Tien Shan in the N and the Himalayas in the S for over 20 years. Highlights were the first studies done on Shisha Pangma (1964) and Chomolungma (Mt. Everest, 1966–1968) (Shi Yafeng et al. 1966; Lanzhou Institute 1975, 1977). Since 1981 several of the Tibetan glacier and permafrost areas have been researched in cooperation with foreign scientists (Xie Zichu, Zhou Youwu et al. 1986). While research together with Japanese glaciologists was occupied in that year with the Tien Shan

glaciers, work with scientists from the FR of Germany concentrated on NE Tibet (Qinghai-Xizang plateau) and the E portions of Kuen Lun (including Animachin), Datsaidan Shan, Kakitu and Quilian Shan, and the mountain chain inbetween (Hövermann and Wang Wenjing 1982; Kuhle 1982a, b). This 4-months undertaking by the 1st Sino-German Joint Expedition 1981 commenced a multiyear cooperation with the Geographical Institute of the University of Göttingen (Kuhle 1985a).

At the Göttingen Institute this tradition is only half as old and began in 1973 and 1974 with glacial-geomorphological reconstructions and cryopedological research in the mountains of SE Iran (Kuhle 1974, 1976) in order to then extend research further to the E in 1976 to the central Himalayas including the Dhaulagiri and Anna-

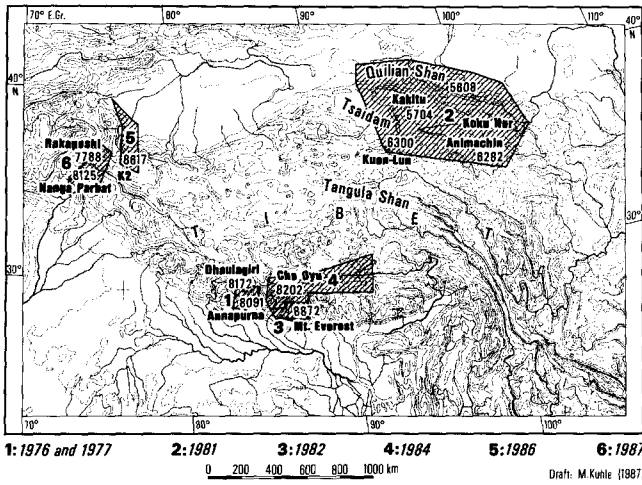


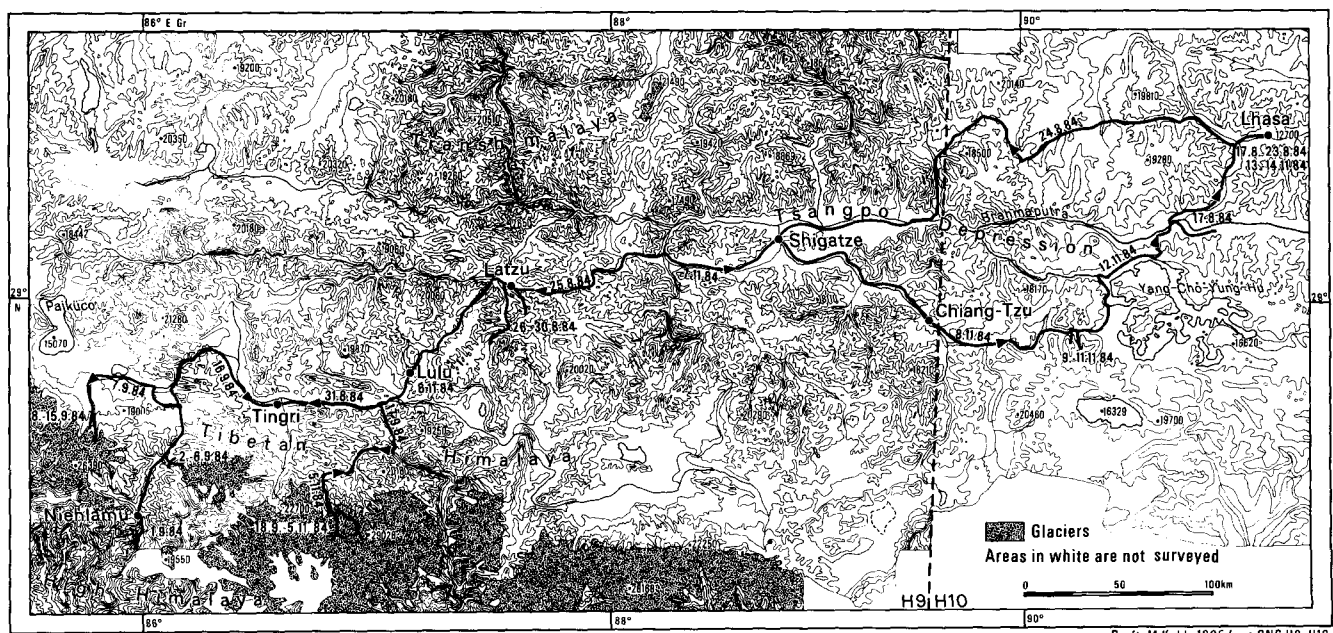
Fig 1

purna Himalayas (Kuhle 1977/78, 1979, 1979/80). The 4-months Himalayan expeditions of 1976 and 1977 also led to the N slope of the main ridge and to S Tibet. The regions studied were practically unknown in terms of their geomorphology, glaciology and vegetation, and the fact that several of the valley sections visited were set foot on for the first time substantiates the lack of knowledge here compared with other mountains and highlands of the world (Kuhle 1982c, 1983a; Mieke 1982). All the more reason why it was important to maintain contact with the classic high-mountain geography in the Alps and to employ all possible observations for comparison with other periglacial regions of the world, e.g. arctic, subarctic and the Andes. Thereby, new data and

findings can be better explained and classified. In 1981 the aforementioned 1st Sino-German Joint Expedition followed. The Chinese side was directed by Prof. Wang Wenjing and the German by Prof. Dr. Jürgen Hövermann. This expedition enabled the scientists to make the 1800 km jump to the N slope of this great highland. In 1982 the Germans were again working on the S margin in the Mt. Everest region (Kuhle 1983b, 1986a, b; Mieke 1986). All of these multimonth field campaigns were financed by the German Research Society (DFG), the Max Planck Society (MPG) and the Academia Sinica. Fig 1 reveals that for working areas 1, 2 and 3, area 4 is an important void to be filled on a NS profile for the problem of the Pleistocene glacier cover in Tibet, which is the key paleoclimatic problem for the studies of Prof. Kuhle.

An essential condition for studying the lowest sub-recent ice margin positions is sufficiently deep valleys in addition to the height of the glacier catchment area. This is found on the marginal slopes of high Tibet in the S in the high Himalayas (Fig 1, nos. 1, 3) and in the N in Kuen Lun and Quilian Shan (Fig 1, no. 2). Area 4 fulfils this topographic requirement through the deepening of the Tsangpo valley. Within area 4 it cuts into the highland down to 3700–3900 m asl. Thus, the Tsangpo depression between the Transhimalayas and the Tibetan Himalayas in S Tibet (Fig 2) is for Pleistocene research the same as what the Tsaidam depression between Kuen Lun and Quilian Shan, which cuts down to an altitude of 2850 m, in area 2 is. Between areas 4 and 2 the depressions are lacking. The plateau rises over 5200 m asl, and on its surface there are the recent, even more glaciated mountain groups, such as the 6500 m high Tangula Shan.

Fig 2



### Preparation for the 1984 Expedition

The expedition plan, based on previous research and the aforementioned considerations, was conceived in 1981 and 1982. The final agreement on the work program, number of participants, stages, dates and expedition route was made in Beijing in March 1984. The areas of Pleistocene research, recent glaciology, neoglacial and recent glacier history, cryopedology, geomorphology of rapid mass movements, botany, plant ecology at high altitudes and ecological data collection at the highest altitudes were decided upon. A 16-mm sound movie film was planned to document the work, in cooperation with the Institute for Scientific Films (IWF). Dipl. Geographer J.-P. Jacobsen, one of the expedition participants, received a training program in camera techniques at the IWF during the preparation for filming. The evaluation, analyses and dating of the samples taken is to be done at the Lanzhou Institute, the Institutes of Geography, Mineralogy, Geobotany at the University of Göttingen, and at the State Survey for Soil Science of Lower Saxony in Hannover, FR Germany. The scientific and expedition equipment was made available by the Lanzhou Institute, the University of Göttingen and German manufactures of measuring and climatic instruments. The financial basis was provided by the Academia Sinica, the German Research Society and the Max Planck Society. The German group departed on August 12, 1984, and joined the Chinese colleagues on August 17 in Lhasa, who had been underway for several weeks with the expedition vehicles from Lanzhou through N and central Tibet.

### The Expedition

The Chinese team was comprised of eight scientists, technicians and a base camp manager, including Prof. Wang Wenjing, Prof. Xu Daoming and Prof. Zheng Benxing from Lanzhou and Prof. Huang Rongfu from the Institute for Plateau Biology in Xining. The German participants were: Prof. Dr. Matthias Kuhle, Dr. Georg Mieke and Dipl. Geogr. Jens-Peter Jacobsen from the Geographical Institute in Göttingen. A cook, three drivers and two helpers completed the expedition team. From the base camp our work at high altitudes was supported by Tibetan yak herders and their pack animals. We drove 2500 km with three cross-country vehicles with all-wheel drive, including a 3-axle truck which made several supply trips. Five base camps were built as starting points.

During the 87 days field campaign studies were done in the following regions: Transhimalayas, Tibetan Himalayas (particularly in the mountains E and W of Chalamba La and E of Utsang Wei at a max. altitude of 6138 m; in the Latzu massif or Quilagugahai Shan and Ladake Shan or Hlako Kangri, ca. 6800 m and 6482 m, respectively; in the massif of Lankazi or Nagartse and



Fig 3 Members of the Sino-German Joint Expedition to S Tibet, Shisha Pangma and the N flank of Chomolungma (Mt. Everest) 1984, left to right, standing: Dipl.-Geogr. Jens-Peter Jacobsen, Cook, Prof. Dr. Matthias Kuhle, Engineer Li, Driver Wang, Driver Li, Dr. Georg Mieke, Prof. Wang Wenjing; in front: Yak-drivers Pemba, Dorji, and Kanza.

Nangkartse, 7188 m or 7191 m, respectively) in the high Himalayas in the Sun Kosi traverse valley (Bote Chu with portions of the group W of the Rolwaling Himal reaching 7038 m asl), on Shisha Pangma (8046 m) and above all on Mt. Everest (Chomolungma, 8848 m) and N of the adjacent massifs. The scientists working at high altitudes stayed 63 days at altitudes over 5000 m and 16 days at altitudes over 6000 m for collecting data. Kuhle attained the highest altitude of the expedition (7100 m) by climbing the E wall of Chang La leading to the N summit of Mt. Everest and the lower portion of the SE ridge of Changtse. The expedition ended on November 20, 1984. Research was facilitated by the extremely good weather. The results presented here were discussed at the International Symposium on Tibet and High Asia from October 8–11, 1985, in Göttingen (Höllermann 1986; Kuhle 1986c).

### Detailed Account on the Expedition

For initially adjusting to the high altitudes a stay in Lhasa at 3700 m was planned for August 17–23. This first jump in altitude is considerable, as was confirmed

by the very dangerous case of pneumonia which a Chinese colleague caught. After two days he was brought to the hospital where he was put on an oxygen apparatus. He joined the expedition four weeks later but was not allowed over 5500 m altitude. Precaution was also taken particularly against infections of the respiratory tract. In combination with the unusual altitude they can also lead to edema. A German member of the expedition caught a cold and had a temperature of over 39° C (102° F) within a very short period of time. For this reason he was immediately treated with penicillin and was back on his feet again in just a few days.

We used the stay in Lhasa for three 1-day field trips into the granite areas of the Tsangpo tributary valleys. On August 24 and 25 the expedition then crossed several passes in the Transhimalayas W of Lhasa, including the 5300 m high Chalamba La. On the way, detailed surveys were made, and several samples of important erratics were collected. Moving slowly up the roads and the Tsangpo valley and passing Shigatse, the convoy reached the Lazu military station at 4030 m asl. From this point on, work was done until August 30 on the N slope of Ladake Shan with an intermediate camp at 4800 m up into the congelifluction zone (Fig 2). The climb continued from the highest settlement named Phu Shar (4300 m) into a largely unmapped region. The botanist Prof. Huang Rongfu and the three Germans were supported by four porters. The other Chinese participants were already preparing for the Shisha Pangma campaign. In addition to surface temperature measurements, radiation measurements and plant ecology studies the features of recent, extremely glaciated mountain topography – reminiscent of the Scandinavian Alps – were surveyed. On August 31 the group crossed over into the W parallel valley, the Mangaphu Chu and Lho Chu, into Mapu La with light new snow (5220 m; 5439 m according to Howard-Bury 1922) and collected glacial till and erratic samples up to Lulu military station (4350 m). Following the Bhong Chu from 4300 m to 4500 m asl to the W and passing the Tingri settlement, the road from this S parallel valley of the Tsangpo gains the altitude of the 5100 m high Thong or Tung La (5480 m according to Howard-Bury 1922) curving more and more to the S. From here on, the route follows the Bo or Bote Chu (Sun Kosi) from its origin over the main ridge of the Himalayas to Damu on the border between China and Nepal at 2100 m asl. All Chinese and Germans then joined in Nylamu and ventured into the region of the great 1981 avalanche which took over 100 human lives and destroyed the "Friendship Bridge" on the road to Kathmandu. Prof. Huang Rongfu had to be taken to the hospital in Damu due to a gastro-intestinal disorder.

#### Work on Shisha Pangma

The three German participants, the cook and later the Chinese colleagues lived at first from September 2–6

in a camp at 4300 m asl at the mouth of an E tributary valley of the Bote Chu, N of the main Himalayan chain in the Tibetan Himalayas. From here and an intermediate camp at 4760 m field work continued to 5540 m asl and telemetric measurements were taken up to the upper summit region at 6500 m (Fig 1). These studies were documented on film and the topographical context of the extensive mountain areas concerned were recorded with several panshots.

After the base camp had been moved on September 7 about 70 km WNW to an altitude of 5020 m on the N slope of Shisha Pangma (8046 m), two higher camps at 5300 m and 5550 m were built on the tongue of the Yepokangara glacier during the increasingly better weather of the post monsoon season. Detailed studies were done on the great late-glacial outwash aprons of the N slope of the Himalayas up to an altitude of 6000 m. From the foot of the mountains they run out onto the plateau remains of S Tibet at 5000 m asl. The N side of Shisha Pangma was specially chosen for this work because it is one of the rare regions where the high Himalayas come in direct contact with the plateau without intervention by the Tibetan Himalayas – as is the case for example N of Mt. Everest. Such a mountain foreland situation is the topographical precondition for outwash apron formation. At the same time, the outwash aprons of these glaciogenic foreland deposits were selected because they were not only situated in the permafrost zone at the time of formation, but also still lie in this zone today. As a result, the outwash apron slopes have been smoothed out by solifluction rather than deeply eroded, and thus are better preserved.

Triangulations with the Geodimeter 122 were done for the first time on this field campaign. This was done to redetermine the height of Shisha Pangma. Additionally, automatic climate measuring stations were operated at the three camps, and infrared temperatures, glacier tongue positions and ice pyramid positions were measured. The transport of supplies to camp 2 (5550 m) was eased with the help of yaks and two Tibetan herders, who also helped with the field work by carrying measuring equipment.

The supplies brought were supplemented by milk, butter, cheese and two sheep. We bartered them from the partly nomadic Tibetans who spend the four months of summer on these highest pastures with their herds. Two of the Chinese expedition members went hunting daily and shot hare, ptarmigan (*lerwa lerwa*) and pigeons (*columba rupestris*). Later, on Mt. Everest, large wild sheep (*ovis hodgsoni*) were also hunted. At the base camp the helpers, cook and the drivers were not only plagued with ailments such as troubled sleep, dizziness, loss of appetite and nausea, but also persistent altitude sickness which was accompanied by intensive headaches and lasted for weeks, even during the time at the Mt. Everest camp. The cook finally had to be taken to the Lulu military station where he recovered at 4300 m asl and did not join us again.

## The N Slope of Mt. Everest

On September 16 our work on Shisha Pangma was completed and the equipment was transported to Lulu. Part of the expedition had already departed the day before. On September 17 the three heavily loaded vehicles crossed over the 5200 m high Panga La between the Bhong Chu (basin of Lulu) and the Dzakar valleys and the latter was then followed up into the Rongbuk valley. The monsoon season ended prematurely in 1984, and with only a few short-lived interruptions the good weather continued on into November, till the conclusion of our 50-day studies at Mt. Everest. After we had left behind the deeper sections of the Dzakar Chu (4300–4550 m asl), in which the buckwheat and barley harvest was in full swing, there were three small obstacles to overcome before reaching the tongue of the Rongbuk glacier where the base camp was to be built. The deep Rongbuk river had to be crossed, which was no problem for the first cross-country vehicle and the equipment truck. However, water began to flow into the third vehicle. Only after the passengers had waded to the other shore did the driver succeed in getting the vehicle to the dry bank in low gear and with full throttle. The strenuous uphill drive in rock of the valley floor overheated the motors again and again so that they died and were very difficult to start again. Finally, a large moraine block had rolled down from above the Rongbuk monastery and blocked the way for the wide truck. It took many hours to build a detour around this large block. In the remaining sunlight we were able to set up several tents for sleeping at 5170 m asl in the forefield of the glacier. On September 18 we finished construction of the base camp and installed the measuring equipment (Fig 4). Part of this work involved constructing the stand with the Geodimeter, which was to be in operation for more than 40 days, and the accompanying reflections on various solifluction slopes. The remaining reflectors on the Rongbuk glacier, which were used to make the finest measurements of the decreasing movements at the boundary zone toward the static ice and extended up to 2.6 km into the ice flow, were installed over the next few days.

## The Central Rongbuk Glacier

After short exploratory climbs camp 1 was set up on the central Rongbuk glacier (Fig 4). It stood in the orographically right marginal depression at 5500 m asl and was built with the help of yaks, as important means of transport. The 100 m high steep innerslope of the moraine caused problems for the pack animals and here they lost four loads. The fallen aluminium cases were badly damaged and the valve on our oxygen equipment was broken. Until the beginning of October work was conducted from camp 1 onto the central Rongbuk glacier up to the N face of Mt. Everest at 6450 m and over to

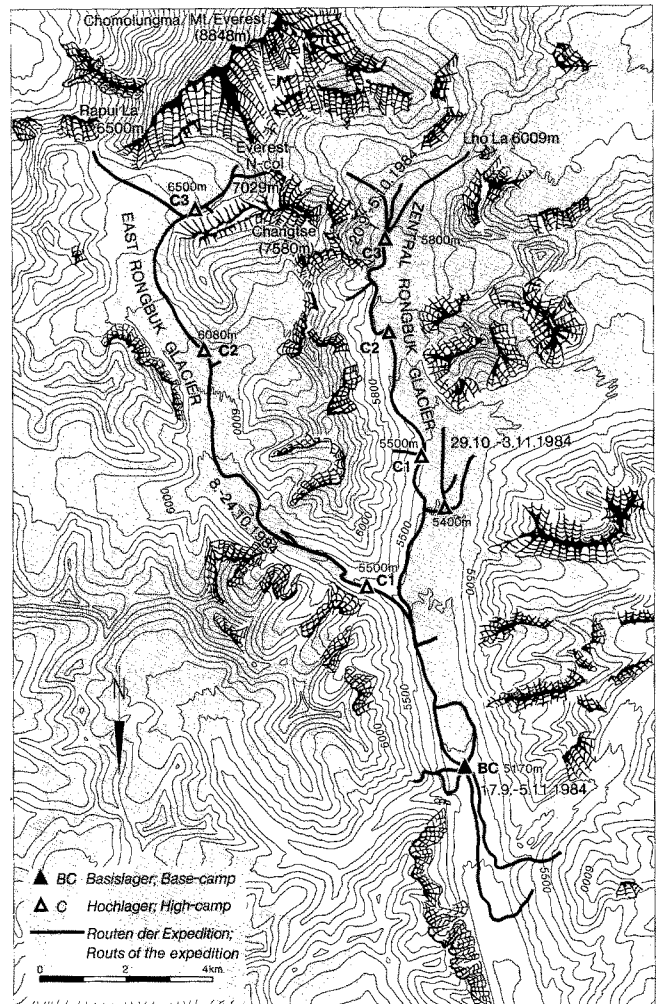


Fig 4

Lho La (Fig 4). Prof. Huang, who was now back on his feet, and a helper joined the German group in camp 1. Two of the Tibetan yak herders set up camp 2, which was built between two ice pyramid chains on the upper moraine, and brought supplies up. Further up on the glacier, the scientists continued with field work as well as supply trips, cooking and building camp 3 at 5850 m asl (Fig 4). This double burden of collecting scientific data on one hand and the logistics on the other, including the transport of 25 to 30 kg loads to the other side through difficult glacier terrain partly covered with broken rock and avalanche, was overcome due to the good weather. During the 15 days of work on the central Rongbuk glacier rock samples, lichen samples and the highest plants were collected and radiation, radiation balance, humidity, soil temperature, firn temperature and ablation measurements were taken. Ice-, firn- and rock-surface temperatures were measured up to 8700 m asl.

During this time, a Chinese group under the direction of Prof. Wang worked on measuring the movements of the central Rongbuk glacier on a profile

at 5400 m. The placement of the measuring rods was impeded by the ice-flow surface caused by cryokarst phenomena.

#### The E Rongbuk Glacier up to the SSE Ridge of Changtse

On October 6 and 7 back at the base camp, the climb over the E Rongbuk glacier was prepared. While several Chinese colleagues were to oversee the measuring equipment at the base camp, a Sino-German working group planned a stay of at least 14 days for research at 6000–7100 m asl. The scientists started on October 8 and were back in the base camp on October 24 after 17 days of work. Camp 1 (5500 m) was solely used for one night during the climb up and later by the three Tibetan yak herders. Camp 2 (6080 m) was used for six days and camp 3 (6500 m) for nine days (Fig 4).

The group was supported by pack animals up to camp 3. The route over the E Rongbuk glacier enabled eight yaks, each carrying 40 kg, to transport equipment twice up to camp 2 at 6500 m. The equipment consisted of instruments, provisions, fuel, two wind-resistant thermal dome-tents, rope and climbing gear and medical supplies including several oxygen tanks. The oldest yak herder, named Pemba, demonstrated his talent in an unusual way by cutting steps into the impassable lower portion of the glacier ice for the yaks. In this manner the smooth, steep slopes of ice were able to be ascended. The hoof injuries of the pack animals had to be disregarded, just as the danger of rockfall. Finally, the group was happy to reach the top without losing any animals and seriously damaging any equipment.

None of the yak herders remained very long or even stayed overnight in camp 3. Porters, helper or a cook did not assist the scientists as they were accustomed to on the other side of the Himalayas, in Nepal. In this context, it was medically interesting to note that the Tibetans who were used to higher altitudes and had their permanent settlements downvalley at 4600 m asl, complained more about problems with headaches, nausea and stomachaches than the scientists. These complaints were apparently to allow them to descend from camp 3 again as soon as possible.

One of the weaknesses in the equipment became very evident during the operations on the upper E Rongbuk glacier, i.e., the lack of walkie-talkies. With the distance of several tens of kilometres and an altitude difference of 2000 m they would have eased the work and above all increased the safety factor at an altitude to which proper adaptation is physiologically no longer possible. However, for financial reasons and more importantly due to problems with space and weight at this altitude we dispensed with them. Yet, after this experience, they were used for the Sino-German Karakorum expedition in 1986 to the 25 km long N K2 glacier.

On October 8 camp 1 was built in the forefield of the E Rongbuk glacier (Fig 4) and on the next day camp 2

on the medial moraine of the N Changtse and E Rongbuk glaciers, below the eastern N Changtse spur (Fig 4). The instruments for measuring radiation were installed and research on the N Changtse and E Rongbuk ice flows was done until October 14 up to an altitude of 6480 m. During this time work was hindered by overcast skies with light snowfall and gusty wind (jet stream) with temperatures down to  $-12^{\circ}\text{C}$ . On October 15 camp 3 was then constructed at 6500 m under the cover of a shallow glacier crevasse, but not out of danger from avalanche and rockfalls of the 550 to 900 m high SSE wall of Changtse. From this point, glaciological, climatological, geomorphological and even plant ecology studies were conducted with wind temperatures of  $-18^{\circ}\text{C}$  (at 6500 m) but under clear skies. In a roped party all areas of both upper firn basins of the E Rongbuk glacier up over the Rapiu La bordering to the E, which connects the Kangchung valley with the E flank of Mt. Everest, were traversed (Fig 4). Thereby, telemetric temperature measurements were taken on the N flank of Chomolönzo and Makalu (8481 m) which were a continuation of the studies on these mountains which began in 1982 from the W.

On October 21 three of the scientists traveled to the foot of the NE wall of Chang La. One of them climbed this flank to the N anticline of Mt. Everest on the SSE ridge of Changtse, while the others took measurements in the W firn basin of the E Rongbuk at 6650 m asl. The climb was eased by a fixed rope left behind by an American expedition to Mt. Everest. From the SSE ridge of Changtse at 7100 m asl the reduction in snow and firn cover with altitude was able to be recorded and mapped in detail due to the suitable distance of 3.5 km from the summit of Mt. Everest and thus the sufficiently shallow angle of the perspective. For observations of this type there is not a more suitable point at this altitude on Mt. Everest.

Jacobsen carried the heavy 16 mm camera with a great expenditure of energy so that good quality pan and still shots were able to be recorded up to altitudes of 6700 m for a scientific film (Kuhle 1985b, 1986d). Mieke also took care of the very hard, nonscientific work at the base camp. A part of this, for example, was the many hours of cooking and melting ice to cover the high daily water requirements of ca. 5 liters per person. These enormous amounts of water fight firstly against dehydration caused by hyperventilation during climbing and work in thin air and relative humidities of no more than 0.13 and 2.52 g/m<sup>3</sup> and secondly against thickening of the blood dependent on the increasing hematocrit values with decreasing amounts of oxygen. Altitude-dependent risks of blood thickening are frostbite of the hands and feet in spite of good clothing, overexertion of the heart, leading to edema of the brain or lungs and internal broken blood vessels, which can lead to cerebral apoplexy and nearly irreversible bleeding in the inner eye (Zink 1978). Apparently as a result of insufficient water intake Jacobsen suffered from very light frostbite of the



feet in spite of his special aluminium-lined double shoes made for high altitudes. On October 23 he complained about slightly troubled vision which originated from damaged blood vessels in the eye as an altitude-dependent sickness, i.e., blood intrusion into the vitreous humor. For this reason he had to take good care of himself from now on, remained at the base camp altitude after the descent and did not participate on the climb to the N slope of Mt. Everest. This eye problem troubled him long after the expedition.

In the late evening of October 24 the scientists reached the base camp with all the equipment from the upper camp and spent the next two days taking repeated measurements with the Geodimeter 122. Some of the Chinese had used the meantime for taking more ice movement measurements at the tongue of the central Rongbuk glacier. With a party of four under the direction of Wang Wenjing they had also set up an upper camp for several days at 5400 m asl for this purpose.

#### The Concluding Work on the N Slope of Mt. Everest

On October 27 and 28 the detailed work on the right and left flanks of the Rongbuk valley outside of the base camp was completed up to an altitude of 5550 m. This work involved collecting samples for radiometric age dating of late- to neoglacial marginal moraine terraces, measuring sprout deformation of dwarf shrubs on creeping waste slopes and completing the collection of plant material.

On October 29 Kuhle and Mieke began the last longer excursion at Mt. Everest to the confluence of the W Rongbuk glacier and the central ice flow. This time they were supported by two Tibetan herders with five yaks and set up camp on the upper moraine of the main glacier (Fig 4). During the six days on the glacier they busily collected data on ice pyramid formation, on upper moraine thickness and thermokarst phenomena with melt water pools and rock-specific cryoconite formations under dark crystalline schist and light tourmaline granite debris along several glacier cross sections. On November 3 the pack animals came again to pick them up. During this time Jacobsen recorded the amount of runoff from the 140 m<sup>2</sup> Rongbuk glacier system at the Rongbuk river.

On November 4 a portion of the expedition personnel dismounted and packed the instruments at the base camp. Some of the scientists used this time to make a previously postponed trip up to the mouth of the tributary valley with the tongue of the NE Gyachung Kang glacier (7975 m) at 5650 m asl. Following the 50 days of field work at Mt. Everest the descent from the base camp to 5170 m was planned for the afternoon of November 5. Although the weather was still good, there was a growing danger of snowfall beginning in the middle of October and the temperatures decreased to  $-12^{\circ}$  to  $-15^{\circ}$  C even at the base camp, so the date for

descent seemed to be chosen well. The extreme onset of winter in Tibet with temperatures of  $-40^{\circ}$  C and heavy snowfall at the end of October and beginning of November in 1985 confirms just that it was not too early.

#### The Lankazi Massif in the Tibetan Himalayas

On November 6 samples, e.g., varve clays, were collected in the Lulu basin (middle Bhong Chu). One and a half additional days with a stay in Shigatse were necessary to cross the three passes on the road to the E to the Lankazi massif (Fig 2). From November 8 to November 12 the expedition worked in this 7191 m high mountain group of the Tibetan Himalayas with intermittent light snowfall. On the first day work was done from the 5100 m pass road. Work continued on November 9–11 from two higher camps which were set up near the Kang Chüng glacier at 4870 m and 4720 m asl. The geomorphological, glaciological and plant ecology studies concentrated on the 6679 m high Kang Chüng massif for which recently completed topographic maps from the Lanzhou Institute for Glaciology and Cryopedology were available. Thereby the scientists, following a late-glacial marginal moraine terrace into an eastern, N-draining tributary valley for 10 km, reached an altitude of 5300 m. From this point they were able to look out onto and photograph the N flank of an estimated 6500 m high glacier berg which was located outside of the map area and which acted as the catchment area of the aforementioned moraines.

One working group led by Prof. Wang undertook a climb from the Lankazi military station (4500 m) to the very extensive E flank of the Lankazi massif for topographical and glaciological purposes and attained nearly 5000 m altitude. Due to lack of time, however, none of the glacier tongues there, which are still unknown, were able to be reached.

#### Conclusion of the Expedition

On November 12 soil and peat samples were collected on the SW shore of the Yung-Cho-Yung-Hu lake (Yamdruk lake according to Aufschnaiter 1983, 118–119) at 4480 m asl. Then we drove over the nearly 4900 m high Tschü Sü La (Gampa La according to Aufschnaiter 1983, 118) into the Tsangpo valley. We arrived in Lhasa in the evening (Fig 2). The cleaning, drying and sorting of the equipment, instruments and samples as well as the discussion on the procedure and distribution of the evaluation took place on November 13. In the evening the German participants were invited to a joint farewell dinner since the mutual undertaking was disbanded on November 14. With the exception of Prof. Wang who accompanied the Germans to Chengdu and Beijing, the Chinese personnel drove back to Xining and Lanzhou where they arrived 2½ weeks later.

On November 16 Prof. Kuhle was invited to a lecture at the Geological Institute of the Academia Sinica in Chengdu. In conclusion, we had the preliminary discussions for field research at the Minya Konka massif (7590 m) on the E margin of the Tibetan plateau planned for 1991. These discussions were with Prof. Li Jian and Li Tianchi, who visited the Geographical Institute in Göttingen from 1980 to 1982. The travels by train lasting nearly two days through Chengdu of E China offered

informative insights into the old Far East cultural setting which the Germans particularly enjoyed after the months in uninhabited areas. In addition to recreational and sightseeing tours during the last two days in Beijing there was a banquet at the Chinese Academy of Sciences in honor of the joint expedition as an official conclusion at which there were also representatives from the German Embassy.

## References

- Aufschnaiter, P.: Peter Aufschnaiter, sein Leben in Tibet. Innsbruck 1983.
- Bruce, C. G.: Mount Everest. Der Angriff 1922. Basel 1924.
- Dyhrenfurth, G. O.: Zum dritten Pol. Die Achtausender der Erde. München 1952.
- Finch, G. I.: Der Kampf um den Everest. Leipzig 1925.
- Höllermann, P.: Neuere Forschungen über Tibet und Hochasien. Bericht über ein Symposium in Göttingen 1985. Erdkunde 1 (1986)
- Hövermann, J.; Wang Wenyong: First Sino-German Joint Expedition to Qinghai-Xizang (Tibet) Plateau 1981. In: Wannagat, U. (ed.) Sitzungsber. u. Mittl. der Braunschw. Wissensch. Gesellsch. Sonderheft 6, Die 1. Chinesisch-deutsche Tibet-Expedition 1981. Braunschweig-Symposium 14.–16. 4. 1982, Göttingen 1982.
- Howard-Bury, C. K.: Mount Everest. Die Erkundungsfahrt 1921. Basel 1922.
- Kuhle, M.: Vorläufige Ausführungen morphologischer Feldarbeitsergebnisse aus dem SE-Iranischen Hochgebirge, am Beispiel des Kuh-i-Jupar. Ztschr. f. Geomorph. N. F. 18, 4, 472–483 (1974)
- Kuhle, M.: Beiträge zur Quartärmorphologie SE-Iranischer Hochgebirge. Die quartäre Vergletscherung des Kuh-i-Jupar. Gött. Geogr. Abh. 67, V. I, 1–209, V. II, 1–105 (1976)
- Kuhle, M.: Über Periglazialerscheinungen im Kuh-i-Jupar (SE-Iran) und im Dhaulagiri-Himalaya (Nepal) sowie zum Befund einer Solifluktionsobergrenze. In: Coll. sur le Périglaciaire d'Altitude du Domaine Méditerranéen et Abords, Strassbourg 1977, pp. 289–309, Strassbourg 1978.
- Kuhle, M.: Settlements on the Southern Slope of the Dhaula-Himal. A Contribution to the Settlement Geography of the Nepal-Himalaya. Nepal Research Centre Miscellaneous Papers 33, 1–36 Kathmandu 1979.
- Kuhle, M.: Klimageomorphologische Untersuchungen in der Dhaulagiri- und Annapurna-Gruppe (Zentraler Himalaya) 244–247. Tagungsber. u. wiss. Abh. 42. Dt. Geographentag 1979, Wiesbaden 1980.
- Kuhle, M.: Erste Deutsch-Chinesische Gemeinschaftsexpedition nach Tibet und in die Massive des Kuen-Lun-Gebirges (1981) – ein Expeditions- und vorläufiger Forschungsbericht. Tagungsber. u. wiss. Abh. 43. Dt. Geographentag 1981 in Mannheim, 63–82. Wiesbaden 1982a.
- Kuhle, M.: An Expedition to an Unexplored Region of Tibet. German Research, Reports of the DFG 3/82, 26–29 (1982b)
- Kuhle, M.: Der Dhaulagiri- und Annapurna-Himalaya. Ein Beitrag zur Geomorphologie extremer Hochgebirge. Z. f. Geomorph., Suppl. 41, 1 1–229, 2 1–184, Geomorph. Karte 1:85 000. Berlin-Stuttgart 1982c.
- Kuhle, M.: Der Dhaulagiri- und Annapurna-Himalaya. Empirische Grundlage. Ztschr. f. Geomorph. Suppl. 41, 1–383. Berlin-Stuttgart 1983a.
- Kuhle, M.: DFG-Forschungsbericht der Expedition von Aug. bis Nov. 1982 in die Mt. Everest-Südabdachung. 1–23, 1983b.
- Kuhle, M.: Glaciation Research in the Himalayas: A New Ice Age Theory. Universitas 27, 4, 281–294 (1985a)
- Kuhle, M.: Die Südtibet- und Mt. Everest-Expedition 1984 – Geographische Untersuchungen in Hochasien. 16 mm-Farbfilm, Dauer: 42', Kamera: J.-P. Jacobsen, produziert in Zusammenarbeit mit dem Inst. f. d. Wiss. Film (IWF), Göttingen 1985b.
- Kuhle, M.: Absolute Datierungen zur jüngeren Gletschergeschichte im Mt. Everest-Gebiet und die mathematische Korrektur von Schneegrenzberechnungen. In: Tagungsber. u. wiss. Abh. 44. Dt. Geographentag 1985 in Berlin, Wiesbaden 1986a.
- Kuhle, M.: Former Glacial Stades in the Mountain Areas surrounding Tibet- in the Himalayas (27°–29° N: Dhaulagiri, Annapurna, Cho Yu and Gyanchung Kang areas) in the south and in the Kuen Lun and Quilian Shan (34°–38° N: Animachin, Kakitu) in the north. In: Joshi, S. C. et al (ed.) Himalayan Research & Development, Himalayan Research Group, Vol. Nepal-Himalaya-Geo-Ecological Perspectives. 1986a.
- Kuhle, M.: New Research on High Asia, Tibet and the Himalayas. The International Symposium on Tibet and High Asia on Oct. 8–11, 1985 in Göttingen. GeoJournal 12, 3, 341–343 (1986c)
- Kuhle, M.: Die Südtibet- und Mt. Everest-Expedition 1984. Film-Kommentar und Erläuterungen. In: Publ. zu wiss. Filmen, Sektion Geographie, Inst. f. d. Wiss. Film, Göttingen 1986f.
- Miehe, G.: Vegetationsgeographische Untersuchungen im Dhaulagiri und Annapurna-Himalaya. Dissertationes Botanicae 66, 1, 1–224, 2 1–152 u. Abb., Karten (1982)
- Miehe, G.: Die Höhenstufen der Vegetation am Mt. Everest. In: Tagungsber. u. wiss. Abh. 44. Dt. Geographentag 1985 in Berlin, Wiesbaden 1986.
- Norton, E. F.: Bis zur Spitze des Mount Everest. Die Besteigung 1924. Basel 1926.
- Shi Yafeng et al.: A Photographic Record of the Mount Shisha Pangma Scientific Expedition. Peking 1966.
- Xie Zichu; Zhou Youwu et al.: Selbstdarstellung des Lanzhou-Instituts für Glaziologie und Cryopedologie und seiner Geschichte. Lanzhou 1986.
- Lanzhou-Institut: Wissenschaftliche Ergebnisse der Mount Jolmo Lungma- (Mt. Everest-) Expedition 1966–68. Peking 1975.
- Lanzhou-Institut (1977): A Photographic Record of the Mount Jolmo Lungma Scientific Expedition. Peking 1977.
- Zink, N.: Ärztlicher Rat für Bergsteiger. Stuttgart 1978.

**Maps**

General map of Hedin's travels in Tibet 1906–1908 (1:3 000 000, designed and drawn by O. Kjellström 1909, Leipzig).

The Transhimalayas (1:1 500 000, drawn from the original map of Sven Hedin by O. Kjellström 1909, Leipzig).

Atlas of the Polish Peoples' Republic (sheets 77 and 78, 1:2 500 000, Warsaw 1971.)

Preliminary map of the route of the 1921 Mt. Everest Expedition (1:750 000, by H. T. Morshead, Basel 1922.)

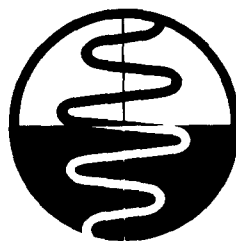
Mt. Everest and the Tschomo Lungma group (1:63 360, drawn by C. Jacot-Guillarmod using the photogrametric photo by R. E. Wheeler and H. Singh, Mt. Everest Committee of the Royal Geographical Society and the Alpine Club, English Mapping Office, Basel 1925.)

Topographic map section of the northern slope of Shisha Pangma (1:50 000), surveyed on the 1964 Chinese Shisha Pangma Expedition, Lanzhou Institute of Glaciology and Cryopedology, Academia Sinica, Peking.

Chomolungma (Mt. Everest) map (1:50 000) of the 1966–1968 expedition "The comprehensive Expedition to the Qinghai-Xizang Plateau". Academia Sinica, Peking 1979.

# Geophysik Consulting GmbH

delineation of subsurface layer boundaries  
 detection of groundwater level  
 magnetic anomalies, cavities  
 evaluation of dynamic elastic parameters  
 pipeline surveys  
 marine site and route surveys  
 prospecting for mineral deposits, sand, gravel, clay etc.



refraction seismics on land with P- and S-wave generation  
 marine reflection seismics  
 geoelectric measurement (sounding and mapping)  
 land and marine magnetics  
 electromagnetic surveys (VLF, radar)  
 oceanographic measurements

Bureau for Applied Geophysics

Marthastraße 10, D-2300 Kiel 1 Germany Telefon (04 31) 67 24 24

## Geomorphological Findings on the Build-up of Pleistocene Glaciation in Southern Tibet and on the Problem of Inland Ice –

### Results of the Shisha Pangma and Mt. Everest Expedition 1984

Kuhle, Matthias, Prof. Dr., Universität Göttingen, Geogr. Inst., Goldschmidtstr. 5, 3400 Göttingen, FR Germany

#### The Area under Investigation and Presentation of the Problem

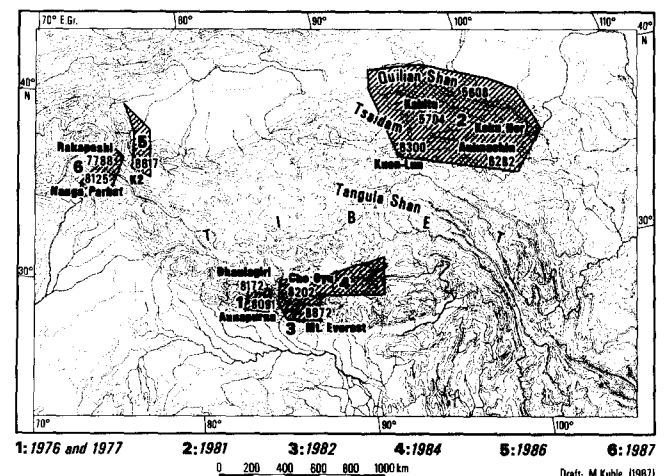
The evaluation of the findings made in 1984 is part of a complex of problems which the author had also investigated in the course of six other research expeditions to Tibet and the High Himalayas (1976, 1977, 1981, 1982, 1986, 1987). Extending from August till November 1984<sup>1)</sup>, the expedition permitted previously unexplored parts of the Tibetan Himalaya, of the Tsangpo Depression and the Transhimalaya rising to the N of it to be included in the investigations of another section of the N slope of the High Himalayas, i.e. the N slopes of the Shisha Pangma and Mt. Everest (Fig 1).

The aim of the expedition was to attempt a reconstruction of the lowest pre-historic glacier margins in the N slopes of Mt. Everest and Shisha Pangma, as well as in seven mountain groups of the Transhimalaya and the Tibetan Himalaya N and S of the Tsangpo between 28° and 29° 50' N, as well as between 85° 24' and 91° 13' E. In the area under investigation, the High Himalaya rises to 8874 m, with the massifs of the Transhimalaya and the Tibetan Himalaya explored here reaching 6000 to 7200 m. In the Tsangpo valley the lowest areas descend to 3700–3800 m<sup>2)</sup>.

At this still great altitude of the lowest surfaces of S Tibet, which constitute a topographical limit for the climatic possibility of even lower locations for ice margins, the problem of recording those which are actually the lowest, i.e. glacier locations of the High Glacial, arises. This applies especially to very great

altitudes of glacier-catchment areas. However, it must be taken into account, that the upper limit of glacier-catchment areas underwent a climatic lowering during the Ice Age which ran parallel to, and at a constant distance from, the equilibrium line (Kuhle 1985, 1986a, b). A topographical limit of the lowest glacier margins is only missing in the S slope of the Himalaya where the Bo Chu (Sun Kosi) descends to 1000 m asl. This problem did not occur in the remaining hitherto researched areas under investigation, such as NE Tibet (Fig 1, no. 2) where the Tsaidam depression descends to about 2900 m, and the Gobi desert N of the Quilian Shan (Richthofen Mountains) extends below 1400 m. In the areas covered by the expeditions of 1976–1987 (Fig 1, nos. 1, 3 & 6), and in the NW (Fig 1, no. 5), the Ice Age glaciers were also

Fig 1 Location of the area of the 1984 Expedition (No. 4) in relation to those of the author between 1976 and 1987 (Nos. 1, 2, 3, 5, 6).



1) The expedition was financed by the Deutsche Forschungsgemeinschaft, the Max Planck-Gesellschaft and the Academia Sinica.  
2) Altitudinal data in accordance with ONC H-9, 10 1:1,000,000 and aneroid measurements.

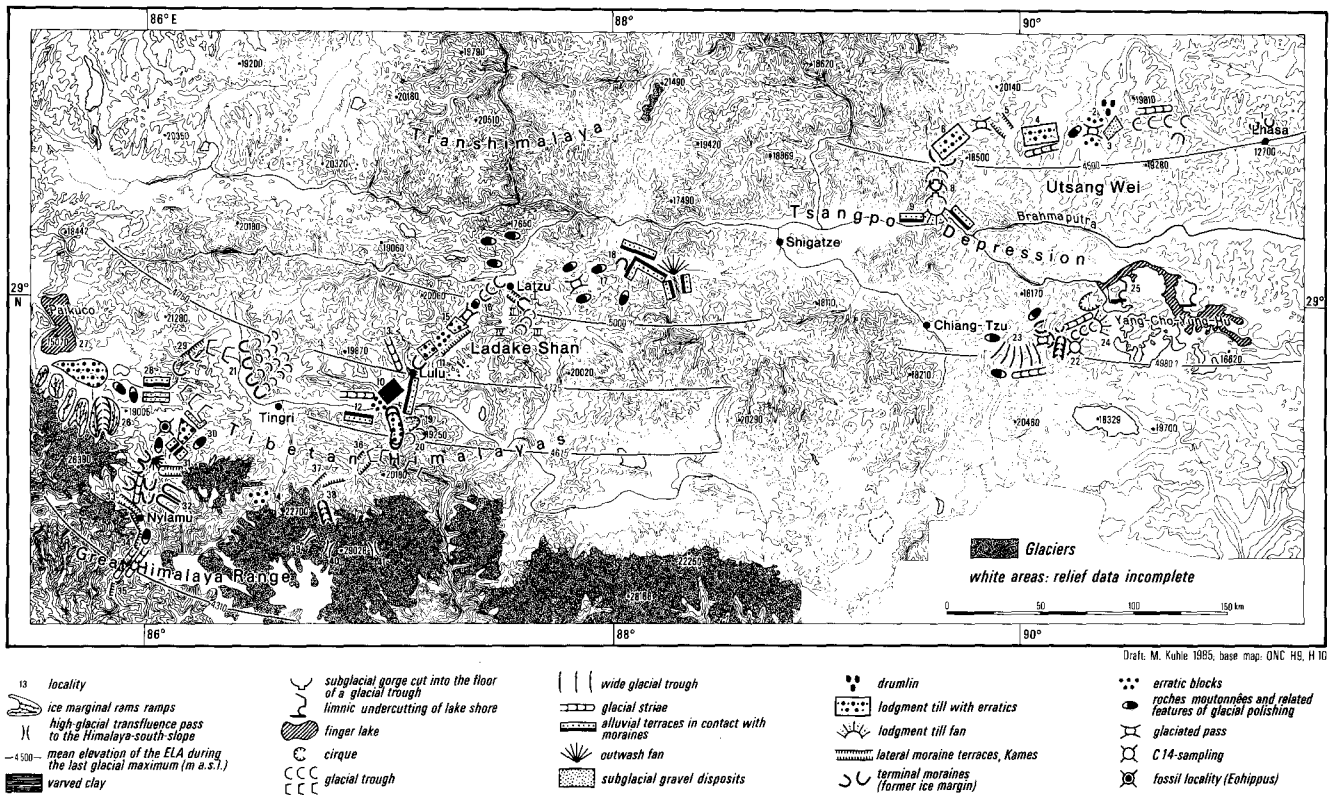


Fig 2 Glacio-geomorphological map of the 1984 investigation area in S Tibet; (Explanation in text).

able to deposit their climatically lowest moraines along the entire S slope of the Himalayas, which in some places drops to 600 m. In this way the findings of the fieldwork carried out there complement the results presented here. On the other hand, the area explored in 1984 plays a significant role as a gap in Central Tibet, which touches upon the Transhimalaya and follows the Tsangpo depression.

### The Method of Calculating the Line of Equilibrium as a Means of Reconstructing Pre-Historic ELAs

The calculation of the levels of equilibrium lines can be carried out with the methods used by v. Höfer (1879), Brückner (1886), Richter (1888) and Kurowski (1891), and their variations developed by Louis (1955), Kuhle (1980, 1982, 1986b), that is by Gross et al. (1977), since only they are based upon factors which are more or less obtainable in the absence of glaciers. These factors are the mean altitudes of the crest frames (v. Höfer) or the highest summit altitudes (Louis; Kuhle) and the lowest location of ice margins (terminal moraines), as well as the superficial extent of the accumulation and ablation areas (Kurowski; Gross et al.), but also the difference of the angle between the average slope of the area of accumulation and ablation. (Kuhle 1988c).

Due to insufficiently exact large-scale topographic maps, methods based on the division of areas are not suitable for the area under investigation. Moreover, the possibility of variations are too great and range from  $AAR = 0.5$  (1:1) to  $0.85$  (1:5.66) from accumulation area to ablation area, as was demonstrated by Meier (in Müller 1980, p. 93) in the case of North American glaciers with an even balance. The accuracy of the v. Höfer method can therefore not be improved upon in the case of the area under investigation. Like its derivative methods of calculation (cf. Kuhle 1986b, p. 41), its application provides sufficient precision in conjunction with the topographical maps available for S Tibet. The author therefore intends to confine himself to the v. Höfer method and, in cases of pre-eminent avalanche feeding, to its variation according to the "maximal method" (Kuhle 1982). The maximal method substitutes the mean altitude of the crest frame with the highest point of the catchment area, and sets it in arithmetical relation to the lowest location of an ice margin. The chosen approach recommends itself by its lucidity, and is intended to avoid a mixing of methods, being based upon the principle of supra-regional comparability: not only all the equilibrium line reconstructions (ELA, GWL) carried out by the author in High Asia, but also the majority of calculations of other authors, or their compilations in v. Wissmann (1959), were conducted in accordance with v. Höfer (1879).

### Lowest Ice Margin Locations and Equilibrium Lines in the Transhimalaya (North Utsang Wei, to the North of the Tsangpo) (Fig 2 and Tab 1)

Joining the Lhasa valley immediately N of the town, a northerly tributary valley contains moraine complexes which run from two third-order valley ends in a southerly and subsequently, from the larger basin, in a SW direction down to 4250 m and 3950 m asl ( $29^{\circ} 43' N / 91^{\circ} 04' E$ ; Fig 3), even reaching a valley floor of a higher order in the last case. With a mean altitude of c. 5200 m for the catchment area, the *orographic equilibrium line* for the SE aspect is calculated as occurring at 4725 m, and for the SW exposition at 4575 m asl. The *climatic equilibrium line* near Lhasa at the time of the *last High Glacial period* accordingly ran at about 4500 m (Fig 2, no. 1).

It was noted in the Tibetan Himalaya N (i.e. to the leeward) of the Dhaulagiri-Himal that an expositional lowering of the equilibrium line by 300 m from the S to the N aspect had occurred (Kuhle 1982, p. 170, 1983). At a corresponding latitude, under comparable conditions of incoming radiation and equal annual precipitation (Jomosom 270 mm/y, Gyantse 271 mm/y and Lhasa 437 mm/y) the climatic equilibrium line would here, too, be found to run 150 m below the orographic equilibrium line on a S exposition. In the case in hand the climatic equilibrium line is thus to be assumed as being 75 m lower than the orographic equilibrium line on a SW exposition.

Extending over tens of kilometres, the E and W slope of the Shüke oder Chalamba La (pass to the W of Lhasa,  $29^{\circ} 41' N / 90^{\circ} 15' E$ ) furnish firm indicators of the existence of pre-historic ice flow networks with *glacier thicknesses* of c. 1200 m in valley-branch flows in the form of erratic findings (Fig 2, no. 2). Biotite-granite blocks with K-feldspar (albeit without chlorite) over a dark Mesozoic rhyolite bedrock (with chlorite) have been found up to 100–150 m above the height of the pass (5300 m) (Fig 4 & 5). Analogous parent rock of probably pre-Miocene age does not occur in the area. According to the geological map presented by Gansser (1964, Plate 1) they only appear at the surface in the Lhasa area, 80–100 km further to the E. This implies transport from the E over tens of kilometres. The topographic arrangement of the erratics also indicates an ice-sheet which swept across the watershed of the pass without a break in the characteristic manner of an ice-stream-network. Rounded and polished mountain ridges rising to 5600 m and steep rock walls towering above them are confirmation of the reconstructed ice level.

Up to 50 m high remnants of ice marginal ramps, esker-dams or kame remnants found to the E of the actual culmination of the Chalamba La at an altitude of 4300 m are already regarded as phenomena of the sub-glacial disintegration of the High Glacial ice cover, just as transverse and lateral moraines between glaciers breaking up into several lobes are considered as belong-

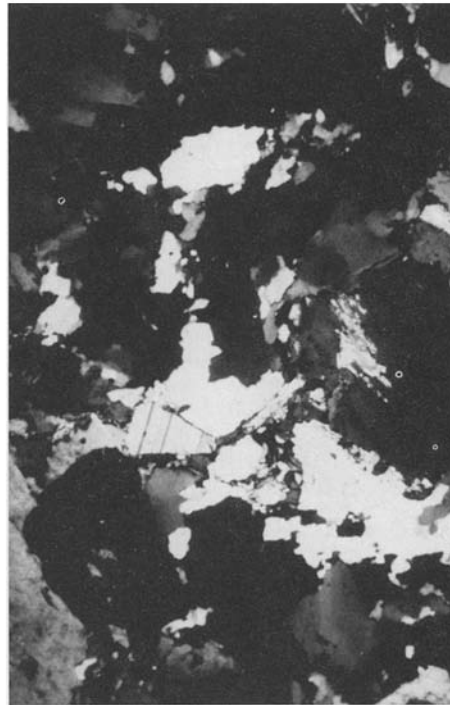


Fig 3 Moraine complex some decametres thick in the form of a terminal moraine between 3950 m in foreground and 4250 m in the middleground of the photograph (X) in a tributary valley near Lhasa (S exposure  $29^{\circ} 43' N / 91^{\circ} 04' E$ ; cf. Fig 2, No. 1). The incisions in the moraine are cutting up to 50 m deep through the diamicton. It lies on granite. The glacier tongue flowed from a corrie-like valley-end at 5200 m from the upper right and pushed the terminal moraine like a pedestal. Photo: M. Kuhle.

ing to the Late Glacial age ( $29^{\circ} 41' N / 90^{\circ} 15' E$ ) (Fig 2, no. 3) On the W fringe of this wide, intra-montane basin there are drumlin-like accumulations.

All of these accumulations are in the centre of the basin. On the edges where tributary valleys present themselves at the 4500 m-high basin floor, ice marginal ramps (*bortensander*) (Kuhle 1984, 1989) and intersecting *outwash cones* are evidence of later, Late Glacial glacier stages. The mean level of the catchment area equals 5400–5600 m here. Higher up in these valleys there are still more recent *dumped end moraines*, which resulted from the block glacier phases as the last stage before the retreat of the ice (v. Klebelsberg 1948; Höllermann 1964; Kuhle 1982). This does not refer to periglacial “block glaciers”.

W of the Shüke or Chalamba La, and down to at least 4430 m asl, the floor of the descending valley and the adjoining N/S basin is covered with ground moraines containing erratics and a lot of interstitial material (Fig 2, no. 4) ( $29^{\circ} 35' N / 90^{\circ} 00' E$ ). In some places the boulder clays are tens of metres thick. Though more than a kilometre wide, the entire floor is covered by the ground moraine deposits. The small present-day stream has not yet succeeded in a fluvial transformation of the ground moraine above 4580 m. Only downstream has



**Fig 4**  
Thin section of the solid rock of the Chalamba La (Col 5300 m asl 29°41'N 90°15'E; cf. Fig 2, No. 2) upon which lie the erratics of Fig 5. This is a rhyolitic rock with crystals of quartz, albite-oligoclase, mica and chlorite and is hydrothermally altered. Its eruptive character is shown by its macro-crystalline features (xenocrysts of twinned feldspar) embedded in an amorphous matrix. Laboratory photograph: A. Heydemann and M. Kuhle.

**Fig 5** Thin section of an erratic block from the Chalamba La (see Fig 4 and Fig 2, No. 2). This is a biotite-granite i.e. an acid plutonic rock (light block) of quartz (dark, wavy extinction), biotite, albite-oligoclase and potash feldspar crystals with a macro-crystalline structure. This structure and its different mineral composition (the granite with potash feldspar, the solid rock rhyolite with chlorite) show that these blocks are glacially transported erratics. Laboratory photograph: A. Heydemann and M. Kuhle.

the increasing discharge led to the flushing out of some of the fine material between the boulders, though even here they cannot be distinguished from an ablation moraine with absolute certainty.

As far as the glacier retreat stages of the Late Ice Age are concerned, two tongue basins of 4800 m and 4650 m are closed off by frontal moraines, which are particularly well preserved (29° 38' N/90° 10' E) (Fig 2, no. 4). The present-day glacier, which had caused the formation of the two tongue basins in the past, is situated at the foot of the dominating and well over 6000 m high peak. A tributary valley on the right hand had provided a link with the valley which descended in a westerly direction from the Shūke La.

Fifteen km S of the 6138 m (20, 140 ft) high summit there is a valley leading W and up to the 4900 m high Zu Ka La, where kame terraces or paraglacial embankments have been preserved at altitudes around 4550 m (29° 44' N/89° 54'E). Besides boulder clay, they tend to be sandy accumulations, indicating a prolonged, Late Glacial ice deposit, followed by the formation of dead ice (Fig 2, no. 5).

In the valley floor areas on both sides of the Zu Ka La this is followed by covers of ground moraine extending over a distance of 10 km S of the culmination (to approximately 29° 43' N/89° 45' E; Fig 2, no. 6).

Away from this valley, which is called Orio Matschu, towards the S and in the direction of the Tsangpo valley and further down, a significant bipartite valley cross-section starts at about 4380 m; its lower part is box-like, while the upper part presents a trough-like extension;

such bipartite profiles are to be attributed to glacial formation in the upper part and to simultaneous sub-glacial meltwater erosion, together with lateral undercutting, in the lower part. It is a formation which developed only below the level of the High Glacial equilibrium line (Kuhle 1982 p. 50, Fig. 97, 1983a, p. 117, 227). Its extent is explained by a major discharge of the Ice Age network of ice streams, i.e. of the Tibetan inland ice, for the box shape appears to be set 50–100 m deep in the trough floor. Valley shoulders (rock terraces) separate it from the trough flanks, which are at times only slightly concave or straight.

Moraine accumulations some 4340 to 4300 m high occur 202 km away from Lhasa (by road) (29° 37' N/89° 39' E, Fig 2 no. 7). Below them slightly terraced, stratified glacio-fluvial drift, with many rough blocks, take over. They are evidently outwashed moraine deposits. Outwash moraine material may be observed in the openings of all the side valleys up to 4250 m.

About 20 km down valley at the basal level of about 4070 m, there is a moraine accumulation on the true left-hand bank, which forms a polymict terrace, with rounded as well as faceted blocks embedded in an ample matrix of fine material (not outwashed) that runs down-valley over several kilometres (29°28'N/89° 37'E). On the valley side of these moraines, large mudflow- and alluvial fans from side valleys have been piled-up in a kame-like fashion on the probably Late Glacial ice fringe of the valley glacier – itself probably already reduced. Reaching heights of 100–120 m, these conical shapes break off more or less immediately, though sometimes in

Fig 6  
Late-glacial end-moraine (××) in the Orio Matschu valley with its base at 4020 m (29°27'N 89°38'E; Fig 2, No. 8). The walls of the moraine are formed of large blocks in a matrix of fine loamy material. The true left wall (× right) carries a wash of loess. Below this terminal position lies an outwash fan forming a low terrace (◆). Photo taken into the valley by M. Kuhle.



Fig 7  
High or Late-glacial outwash fan (No. 5) forming 35 m to 60 m high terraces at the outlet of the Orio Matschu valley (29°21'N 89°36'E, 3820 m; Fig 2, No. 9) in the Tsangpo valley; the Tsangpo on the right. If in fact the outwash fan No. 5 is of maximum glaciation age this shows that then the Tsangpo valley was free of ice (cf. Fig 8). Photo: M. Kuhle.



three or four steps, towards the bottom line of the main valley.

Four kilometres down-valley from that moraine there are wall moraines with basal altitudes of about 4020 m (29° 27' N/89° 38' E, Fig 2, no. 8; Fig 6). Two lower gravel terraces of more recent origin penetrate the walls, which continue to block half the valley.

Further on down-valley (29° 25' N/89° 36' E) and interlocking, and at times modified by mudflow substratum, or by single mudflow events from a side valley on the left, there are accumulations which attain thicknesses in excess of 200 m. They consist of polymict blocks of mixed degrees of roundness without suggesting any sorting. In up-valley direction, as well as down-valley, they change into graded valley fills with four terrace levels. In this profile the valley floor of the Orio Matschu shows considerable deposits. The lowest, and therefore belonging to the High Glacial stage, of these ice margins of the glacier systems concerned have been found at about 3900 m asl, on the S slope of what older maps present as the Nien-tschen-tang-la mountain group, 6–10 km from the Tsangpo, and with peaks rising to 6138 m (Fig 2, no. 9). With a mean altitude of 5400 m for the catchment area, the *orographic line of equilibrium* becomes calculable at 4650 m asl. The precise and lowest ice margin has been established by terminal moraine walls, followed by terraces of outwash plains or ice contact stratified drift, respectively.

The terraces of outwash plains of this true left-hand tributary valley of the Tsangpo continue in the 35–60 m high terrace system of the main Tsangpo valley (Fig 7).

Together with traces of glaciers in the Tibetan Himalaya S of the Tsangpo a picture evolves of two ice-stream systems of the High Glacial stage (Fig 74, 12 and 13), both of which just failed to reach the Tsangpo with the lowest edges of their outlet glaciers. Between the two glacier areas, though itself free from ice, there was thus a glacio-fluvially marked valley trough, with floors of stratified drift at altitudes of about 3800–3900 m running parallel to the latitude. Two terraces can be clearly distinguished (Fig 8). The upper one (60 m,



Fig 8  
Outwash terraces No. 5, 60 m (probably maximum glacial) and No. 4, 20 m (late-glacial) in the central Tsangpo valley (29°21'N 89°34'E; cf. Fig 2, No. 9) at 3800–3900 m asl (cf. Fig 7). These contain well rounded components in part well-sorted gravels in the outwash (sandr). Tsangpo in the foreground. Photo: M. Kuhle.





**Fig 9**  
The Tsangpo trough; alluvium with flood plain and river (29°20'N 89°33'E; 3830 m). Where the flood plain ends a terrace a few metres high has developed (▼) and above, running out on it, is an alluvial fan (■). The patches of aeolian sand on the slopes (●) show the semi-aridity of this environment (with an annual precipitation of 200 mm) at an elevation a little below the potential tree-line (4300 m) and the permafrost-line (4700 m). The pleniglacial glacier flowed from the ice-smoothed rock domes and ridges (◆) down into the Tsangpo valley.  
Photo: M. Kuhle.

no. 5) has hitherto been attributed to the last High Glacial, whereas terrace number 4 (20 m) is considered to be the result of the late glacial Ghasa Stadium (I) (Kuhle 1982, p. 118). According to computer modelling of the ice dynamics by Herterich and Kalov (1988) based in turn on the author's glacio-geological data (Kuhle 1986c, 1987a), this E section of the Tsangpo valley could well have been filled with glacier ice during the last High

Ice Age. Geomorphological evidence for such filling is not, however, available so far (Fig 9). Since the Tsangpo valley bottom line exceeds 4600 m, an ice bridge between the Transhimalaya ice (I 2) and the most southerly complex of the Tibetan ice of the Tibetan Himalaya (I 3) must be assumed as being W of 86° E.

#### **Lowest Positions of Ice Margins and Equilibrium Lines in the Tibetan Himalaya (South of the Tsangpo) (Tab 1)**

Just as alluvial fillings of the Tsangpo valley point to lack of glacier cover during the last Ice Age as long as they remain undated, so do varves in the Lulu basin indicate a complex in the Tibetan Himalaya that remained free of ice during the late Ice Age in any case (Fig 2, no. 10). The floor of this basin is situated at 4300 m, and the glaciolimnic terraces are preserved time and time again over tens of kilometres. They end in a front with fan-like deltaic deposits towards the basin (Fig 10 ↓).

#### **The Glaciolimnic Sediments in the Lulu Basin as a Representative Sample**

The up to 60 m thick varves were subjected to detailed investigation. Fig 11 shows the annual stratifi-

**Fig 10** Glacial-lake deposits of a late-glacial ice-dammed lake (▼) on the N slopes of the Lulu basin. The lake terrace is 60 m high and lies with its edge in a terrace flight of deltaic deposits from tributary valleys (↓). The lake deposits are easily eroded and the deeply eroded channels contrast with the very small gullies above its floor (28°38'N 87°04'E; Fig 2, No. 10; cf. Fig 11–16). Photo at 4300 m. M. Kuhle.



cation of 0.2–0.5 cm thick layers. Medium silt (MS) and clay prevalence (C) are characteristic indicators of strata laid down in summer and winter (Fig 12, above right and below left). Frenzel (in a private communication dated 13. 6. 88) had subjected the samples to electron-microscopic screening and, by comparing them with fermented loam material from N Scandinavia, interpreted and then confirmed them as being glaciolimnic. He recognized characteristic “chattermarks” (Fig 13) and curved breaks with sharp, glaciogenic fracture edges (Fig 14 and 15) in the angular quartz grains of the strata put down in summer and winter. These sharp edges also indicate the absence of aeolian polishing, the results of which may range from tarnishing to rounding-off down to the grain size of the summer strata. The author regards the wealth of small clay mineral plates in the summer strata as the typical “mineral grain peak” (fine grain peak) of the bimodal grain size distribution of glaciogenic material (Dreimanis & Vagners 1971). This peak is even more evident in the fine spectrum of this secondarily (i.e. limnically) enriched material than in the primary boulder clay of the actual moraines (Fig 16). In general the wealth of clay minerals is initially dependent on the existing bedrock in the denudation area and its pre-glacial periglacial conditioning process. The comparison with the samples Frenzel (cf. above) had taken in N Scandinavia are evidence of this; in spite of pedogenesis (they come from a depth of only 4–7.5 cm) they present a smaller proportion of clay mineral. It must, however, also be noted in principle that these combinations of sediments, which are proportionally rich in fine grains, can only be the result of the grinding glacier action. In the Tibetan varves under consideration, the new formations of clay mineral through pedogenesis can be excluded, as the material has been taken from a depth of 45 m. There is no indication of soil formation (Fig 10 & 11).

These paraglacial (glacio-fluvial and glaciolimnic) and solifluctual sediments on the metamorphic bedrock of the slopes became Holocene and are still being blown out. Thus blown sand floors with ripple markings and hummocks came to cover the pebble terraces with thicknesses ranging from a few decimetres to several metres (Fig 12, top left). The aeolian character is revealed through the comparison with purely glacio-fluvial sediments (Fig 17).

**Some Observations on the Glaciation of the Lulu Basin and the Southern Slope of the Lazu Massif (Ladake Shan)**

A striking terrace of outwash material (15–20 m high) has been deposited in the Lulu basin from the Lulu valley (Fig 2, no. 10). It dovetails with the glaciolimnic sediments but, being about 40 m lower, it does not attain their height of deposits. Composed of plutonic and metamorphic gravel, some the size of a head (60%

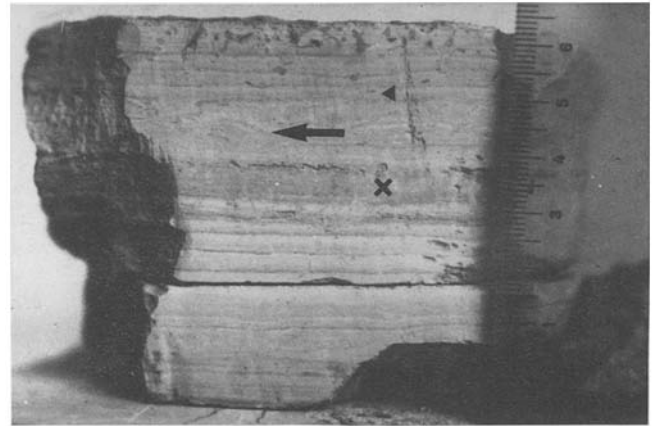
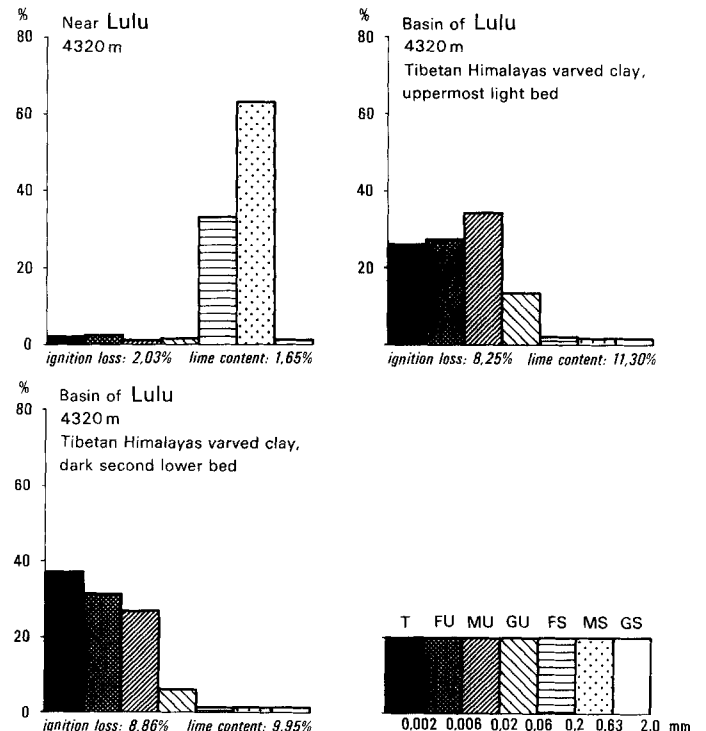


Fig 11 The lake deposits in the Lulu basin are up to 60 m thick (cf. Fig 10). They have all the characteristics of rhythmites of glacial origin and are obviously varve deposits. The yellow intercalations (10YR 7/6) are 1–2 mm thick (▲) and alternate with light grey bands (5Y 6/1) 1–5 mm thick (×). They contain weak colour transitions to light grey (cf. Fig 12 grain size analysis of winter and summer layers). Some of the bands show push features (←). Laboratory photo: M. Kuhle and J. Peters.

rounded, 38% with smooth edges: Reichelt Method, 1961), the terrace becomes a diamictitic boulder clay cover towards the valley. This change in material is evidence of the position of a valley glacier ice margin at an altitude of 4350 m (S slope of the Lazu massif, Fig 2,

Fig 12 Particle size analysis from the Lulu basin (28°38'N 87°04'E) of the aeolian sediments in mounds on the outwash terraces (upper left) and late-glacial varve sediments (cf. Fig 11).



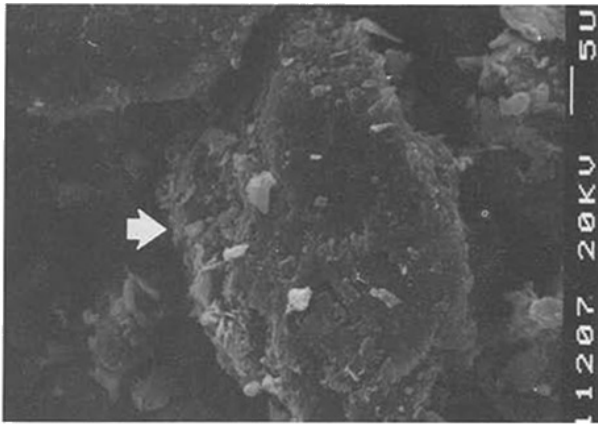


Fig 16

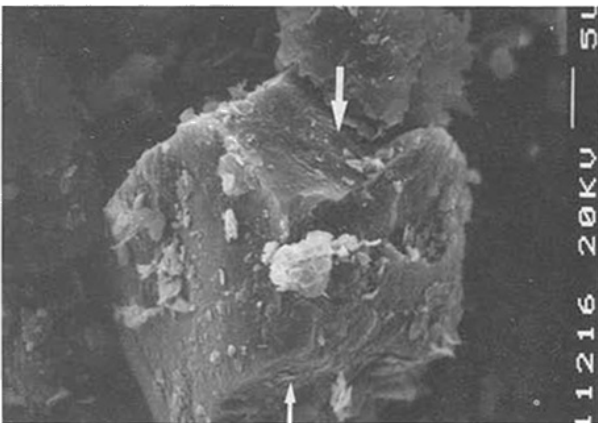


Fig 15

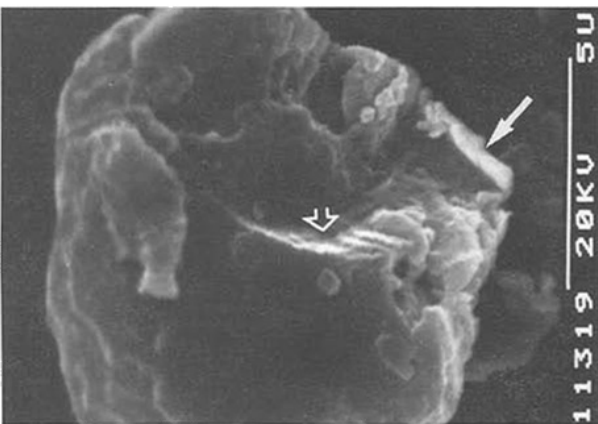


Fig 14

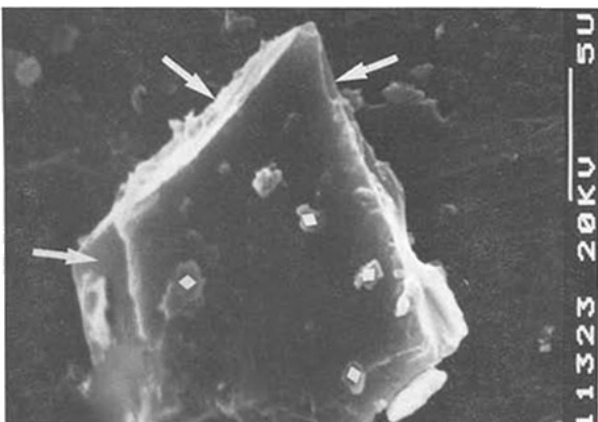


Fig 13

Fig 13 Glacially modified quartz particles with some little-modified clay mineral particles (◆◆) from the winter layer T (clay) of the varve sediments of Lulu (4320 m) (cf. Fig 11 and 12). There is no sign of aeolian or periglacial working. Fracture surfaces of this kind (←) on quartz particles are typical of the 'Gärlehme' of Scandinavian ground moraine. Scanning-electromicrograph and analysis: Laboratory B. Frenzel.

Fig 14 Quartz particle, also from the winter varve layer of Lulu (4320 m) dominated by clay. The grain shows typical crescentic cracks (↵) and impact surfaces (←; chattermarks). Here, too, there are no rounded edges which would denote aeolian or periglacial modification (cf. Fig 11 and 12). Scanning-electromicrograph and analysis: Laboratory B. Frenzel.

Fig 15 and 16 Samples from the Lulu basin summer varve deposit (dominated by medium silt fraction; Fig 11 and 12) at 4320 m. The large quartz grains show smooth impact surfaces (Fig 15 ←) and are like wedge-shaped chattermarks typical of glacial transport. The grains are plastered with clay minerals derived from the glacier milk suspension. These also form even an overall-layer on those of the summer deposits (Fig 16 ↗). Newly formed clay minerals do not occur since these samples have never been affected by pedogenesis (weathering) due to the great depth – 10–45 m below the surface – from which they were taken. Scanning-electromicrograph: Laboratory B. Frenzel.

no. 11, 28° 45' N/87° 14' E). It shows an orographic ELA-lowering up to a maximum of 1275 m to an altitude of 4725 m. However, for the time being and as a matter of care the position of the ice margin is still to be classified as of High Ice Age, although it is likely that the entire Lulu basin was filled with a glacier. This is indicated by very large granite blocks (longitudinal axes of up to 3 m) in a matrix of fine material at the present level of the river (4300 m) (Fig 2, no. 12). They present the picture of an outwashed moraine, and are W of and outside the axis of the mouth of the Lulu valley. It may in fact be the moraine material transported by mud-flows, since it cannot be entirely ruled out that moraine lakes in the catchment area burst their banks. Under conditions of an ice-filled Lulu basin however, the striking rock polishing on the upper slopes, even on outcropping metamorphic slopes in the Shegar Tsong basin (4400 m) adjoining in the NW, could be explained by the polishing action of glacier masses which were several hundred metres thick (Fig 2, no. 13). The under slopes are now being dissected by regressive linear erosion. The notion of the Lulu valley being completely filled with ice is supported by Odell's (1925, p. 331) reconstruction of the complete glaciation of the Tingri basin (28° 35' N/86° 35' E) to the W. On the Phusi La (pass at 5411 m) (Fig 2, no. 14), S of the Tingri basin Odell found some boulders with ammonites 300 m above the Kyetrak glacier, which is now taking a N course from the Cho Oyu massif. The fossil permits the rock to be unequivocally identified as being Jurassic. It was an erratic, as pre-Jurassic metamorphic-crystalline bedrock series occur at that particular place. The boulders therefore originated in the Jurassic area 30 km to the N. Odell concluded from the erratic and the geological situation that there must have been ice-flow powerful enough to over-run watersheds and to reverse the direction of the Kyetrak glacier towards the S; coming from

the High Himalaya, it now flows N. He takes this as an indication of the ice-cover of S Tibet during the High Glacial stage. The author's own findings appear to point in the same direction. In the local context it implies that the component which ran off to the S and reached the Phusi La must have come from the Lulu basin. A landscape of glaciated knobs immediately on the edge of the Lulu or Tingri basin – like the one near Shegar Tsong – is equally evidence of considerable glacier cover and filling. Attention must also be given to the fact that the recent tongue of the Kyetrak glacier terminated at 4980 m. This is only approximately 700 m higher than the floor of the Tingri basin (4300 m). Thus an ELA depression of merely 350–400 m already made it accessible for the Kyetrak glacier. This implies that a depression of a maximum of 700 m is required for the filling of the basin with glacier ice (see below). The reorientation to the S would have taken place at this point, together with some of the run-off via the Phusi La, not only the Nangpa La (5700 m) into the Rongshar valley.

Just as the erratic on the Phusi La provides evidence, so can other findings of erratica in the Lulu valley not be explained in any other way than by glaciation that filled in the relief (Fig 2, no. 15). Here, above 4350 m (cf. above) there are boulder clays in glacial bank formations (wall forms, Fig 18), as well as valley floor fillings with very large biotite and two-mica granite blocks (longitudinal axes 1.5–4 m). These diamictites are on top of bedrock basalts into which the valley has been cut, and were deposited at least 170 m above the valley floor on the flanks of a trough and on rock ledges (Fig 19–23). More and more widely spread out, and almost reaching the 5200 m high Latzu pass (28° 54' N/87° 27' E), these ground moraines are unambiguous evidence thanks to sedimentological criteria: the rounded and light-coloured blocks of acid-plutonic rock are embedded separately in a fine, sandy to loamy-clayey matrix. This moraine cover is at least 10 m thick and superimposed upon those hydrothermally decomposed basic bedrock volcanics.

Although of comparable significance, the connection (the geomorphological sequence) with the corresponding wealth of denudation forms has generally been neglected, due to the difficulty of visualizing (and describing) topographic-geomorphic relationships: the Latzu pass borders on a classic landscape of polished basins and swells with wide-ranging trough profiles (Fig 24). It presents all the elements of Scandinavian glacial denudation landscapes (such as the Kebnekaise or Sarek massifs at 67° N, albeit 4000 m lower). The glacially scoured rocks are dressed with a shallow (i.e. decimetres thick) layer of conglifraacts. Steeper slopes experienced a more forceful periglacial transformation to frost-smoothed slopes (conglifluction slopes). Glaciated ridges have been slightly pointed by frost cliffs where the slopes of partition valley interfluvies intersect. As in Scandinavia, the periglacial morphodynamics have tended to leave a concordant and thus slight mark on the glacial relief (Fig 24).

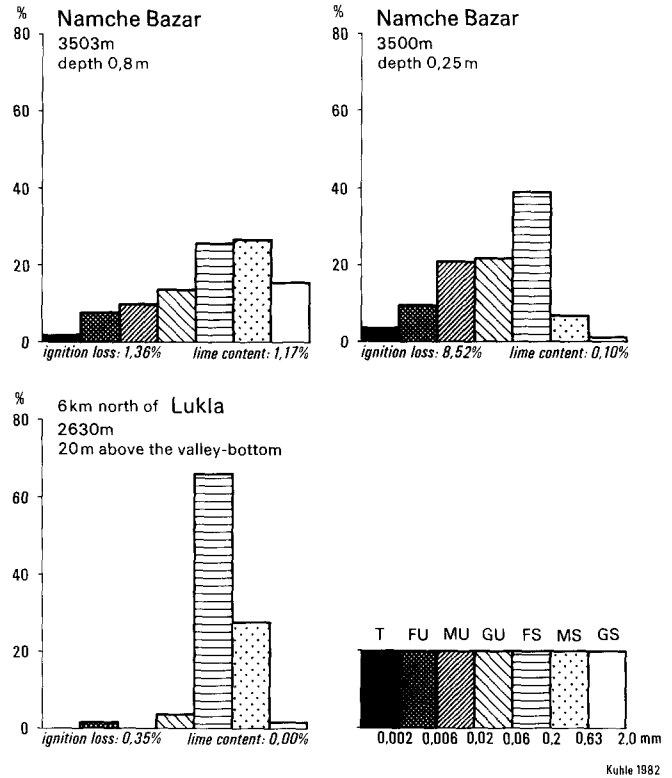


Fig 17 Representative example of glacio-fluvial sediment from the paraglacial sandr on the S edge of Tibet (Khumbu Himal; 27°42'–51'N 86°43'E). These are late-glacial paraglacial sands (Ghasa I stadium or Pre-Ghasa stagnation ● 1/2) deposited in the marginal depression alongside of the some ten-kilometre outlet glaciers originating from the S Tibetan ice stream system (Fig 75 and 76, 13). Characteristically fine sand is prominent, while in case of aeolian sands medium sand is dominant (cf. Fig 12). The microscopic analysis showed that most grains in these sandrs are unreworke and they have travelled only a short distance.

Fig 18 Ground moraine ridges in Lulu valley (Latzu massif S slope 28°48'N 87°14'E 4950 m; Fig 2, No. 15, cf. Fig 19–23). The large, light coloured morainic blocks are of granite with biotite and two-micas. The country rock shows them to be far-travelled erratics. They lie on basic volcanic rocks and 'swim' in a fine loam-rich ground mass. This is typical of ground moraine (lodgement till). Photo to N: M. Kuhle.



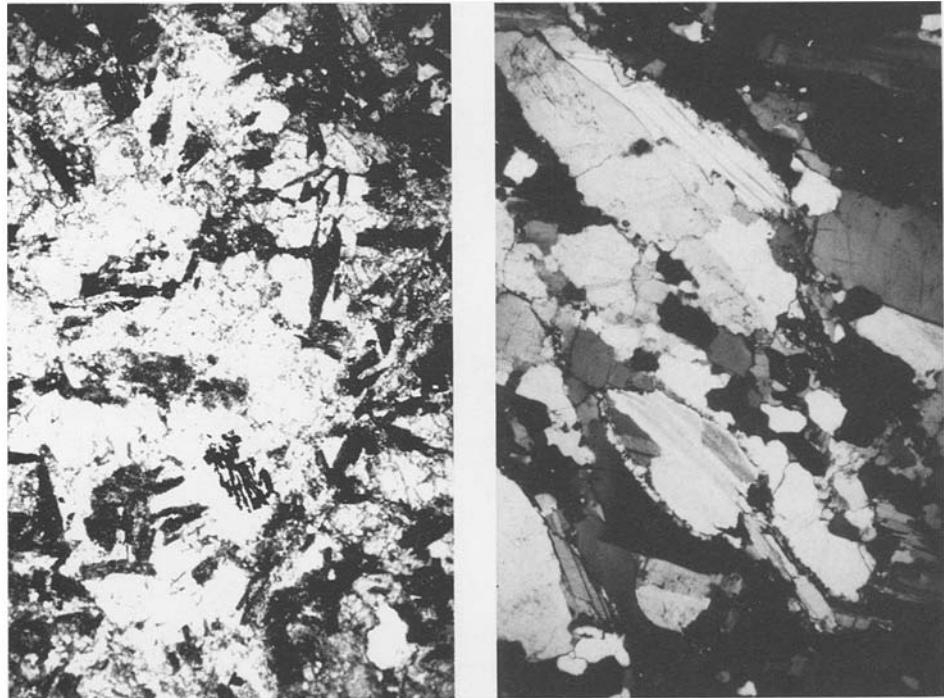


Fig 22

Thin section of the basalt country rock of the Lulu valley (Fig 19). It is a much decomposed basaltic rock in which the pyroxenic components are hydrothermally chloritised and carbonatised. Laboratory photograph: A. Heydemann and M. Kuhle.

Fig 23

This thin section of the erratic two-mica granite (Fig 21) shows the diagnostic macro-crystalline structure of plutonic rocks (Fig 22 and 23 have the same scale). Laboratory photograph: A. Heydemann and M. Kuhle.



accumulation below 4200 m, which may be of glacial origin, but evidence for this is lacking. The lowest undoubtedly glacial end moraines are to be found below the Phu settlement at an altitude of 4200 m (Fig 2, no. 16); ( $28^{\circ} 58' N/87^{\circ} 38' E$ ). The mean altitude of the catchment area of the adjacent summit region being at 5500 m, the ELA depression would be 900 m. The orographic ELA ran at 4850 m asl (Tab 1). The ice margin is classified as belonging to the Late Glacial Ghasa Stage (I) (after Kuhle 1980, 1982). The entire landscape here has gentle features, and is provided with glacially scoured upper slopes and granite block coverings so that the relief appears to have once been completely dominated by ice (Fig 25). There is no evidence, however, of an even lower ice margin position. Higher

up the Phu valley, at 4500 m and 4700 m, and again at 5000 m asl, more Late Glacial tongue basins join in; they are surrounded by striking granite block walls (Fig 25 and 26). They are classified as the Taglung Stadium (II), the Dhampu Stadium (III) and the Sirkung Stadium (IV) (according to Kuhle 1982) with ELA depressions of 750 m, 650 m and 500 m respectively.

Strikingly rounded mountain tops and ridges were observed in metamorphics in the areas to the S of the military station at Lattu ( $29^{\circ} N/87^{\circ} 45' E$ ) and on the 4500 m high Suo La (Solotse La) pass from the Lattu valley to Shigatse up to altitudes of 4700 to 5500 m asl (Fig 27, Fig 2 no. 17). Reference to such forms in soft sedimentary rock introduces contradictory arguments: 1. Soft sedimentary rock can also easily be rounded

Fig 24

Glacial landscape of eroded hollows and ridges in the pass over the Lattu massif (Ladake Shan) at 5200 m (cf. Fig 2, No. 16  $28^{\circ}57'N 87^{\circ}27'E$ ). The Lattu pass is set in a broad trough-like profile that reaches up to 6000 m. The area was completely ice covered. Photo to NW: M. Kuhle.





(1)	(2)	(3)	(4)	(5)	(6)	(7)	(8)	(9)	(10)	(11)	(12)	(13)	(14)	(15)	(16)	(17)	
Lan-Kazi-Massiv Tibetan Himal. 7193 (7223)	28°52'N 90°08'E	N	6430	5705											5855	present ice margin at 4980 m; name of gl.	
	28°53'N 90°08'E	N	6430	5705			VII	4790			5610				5760	"; Kang-Chüng gl.	
	28°53'N 90°08'E	N	6430	5705				4800			5615				5765	S <sub>(m)</sub> -depression 95 m "; S <sub>(m)</sub> -depression 90 m	
	28°53'N 90°08'E	N	6430	5705			VII	4810			5620				5770	"; S <sub>(m)</sub> -depression 85 m	
	28°53'N 90°08'E	N	6430	5705				4830			5630				5780	"; S <sub>(m)</sub> -depression 75 m	
	28°53'N 90°08'E	N	6430	5705			VIII	4860			5645				5795	"; S <sub>(m)</sub> -depression 60 m	
	28°53'N 90°08'E	N	6430	5705				4870			5650				5800	"; 17th cent.?	
	28°53'N 90°08'E	N	6430	5705			IX	4880			5655				5805	"; 19th cent.? S <sub>(m)</sub> -depression 50 m	
	28°52'N 90°08'E	N	6430	5705				4900			5665				5815	"; 19th cent.? S <sub>(m)</sub> -depression 40 m	
	28°52'N 90°08'E	N	6430	5705			X	4920			5675				5825	"; 20th cent.? S <sub>(m)</sub> -depression 30 m	
	28°53'N 90°11'E	N	5900	5705?			V	4730			5315				5465	recent S <sub>(m)</sub> taken from glacier in the west parallel valley (Kang-Chüng glacier)	
	28°53'N 90°11'E	N	5900	5705?			VI	4820			5360				5510	S <sub>(m)</sub> depression 337 m	
	28°52'N 90°11'E	N	5900	5705?			VI	4836			5368				5518	S <sub>(m)</sub> depression 337 m	
	28°52'N 90°11'E	N	5900	5705?			VI	4870			5385				5535	S <sub>(m)</sub> -depression 320 m	
	Everest-N slope	28°25'N 87°00'E	N	7300	6235	5910		4380			5840					5990	local. lower Zambu S <sub>(m)</sub> -depression 245 m near Zambu
		28°17'N 86°58'E		7300	6235	5910		4550			5925					6075	
28°15'N 86°48'E		N	7300	6235	5910		4780			6040					6190	S <sub>(m)</sub> -depression 200 m opposite to a recent glaciertongue in 5180 = rec. climat. S <sub>(m)</sub> at Everest main ridge	
Dzakar Chu, upper Arun valley; 8874															6333		
E of the basin of Man-ko-pa Tib. Him. c. 5800	28°44'N 86°27'E	W	5300	5900		4400			4850			1050			4750	glaciation type: ice stream network; deeper ice margin, covered by sediments possible	
Shisha Pangma-E-SE slopes 8046; middle Bo-Chu (transverse valley)	28°17'N 86°01'E	E	5600				4100			4850					4900	steep hanging	
	28°09'N 85°59'E	W	5800				4100			4950					4900	short valley glacier	
	28°06'N 86°00'E	SE	7100				3670			5385					5450	after Kuhle (1982) a recent valley gl., 35 km long Nylam Phu glacier; near settlement	
							3380			5240					5305	Choksum at the main ridge of the Himalayas (Dhaulagiri-Annapurna)	
lower Bo-Chu (Sun Kosi Khola) 8046	27°56'N 85°56'E	S	7100	6250		1600			4450			1900		4310	gorge-glacier up to Friendship Bridge-local. = recent climat. S <sub>(m)</sub> at Shisha Pangma main ridge		
														6313			
														-6260			



(1)	(2)	(3)	(4)	(5)	(6)	(7)	(8)	(9)	(10)	(11)	(12)	(13)	(14)	(15)	(16)	(17)
Shisha Pangma N slope 8046	28°46'N 86°09'E 28°35'N 85°45'E 28°32'N 85°07'E 28°30'N 85°07'E 28°28'N 85°08'E 28°28'N 85°08'E 28°27'N 85°08'E	NE N N N N N N	6500 7100 7100 7100 7100 7100 7100 7100 7100 7100 7100 7100	5705 6325 6325 6325 6325 6325 6325 6325 6325 6325 6325 6325	•½-I I-III II-IV II-V V-VI VI-VII VII-VIII	4500 5015 5210 5300 5415 5455 5495			5500			850? 5375	950	5415 6260 -6313 5993 6090 6135 6193 6213 6233	(4) is uncertain, bec. high gl. ice marg. is 60–70 km away from the highest catchment area S <sub>(m)</sub> -depression 170 m S <sub>(m)</sub> -depression 125 m S <sub>(m)</sub> -depression 67 m boundary of hist. stage S <sub>(m)</sub> -depression 47 m 17th cent.? S <sub>(m)</sub> -depression 27 m 19th cent.?	
N slope of the whole Lankazi massif 6679	28°51'N 90°11'E 28°52'N 90°06'E	NNE N	5900 6000 6000 6000	5705 5595 5595 5595					4870 4910 4980			5435 5455 5490		5855 5745 5585 5605 5640	present ice marg. at 5510 m; local. 6084 m peak NNE-face; Kang-Chüing-N-gl.; present ice marg. at 5190 m; S <sub>(m)</sub> -depression from 160, 140, 105 m;	
E slope of the whole Lankazi massif 7193	28°44'N -29°10'N 90°21'E -91°04'E	E	5500 -5855	5745 -5855		4460			4980			765 -875		4980	20 m is the assumed depth of the Yang- Cho-Yung Hu, a glacial piedmont lake but presumably it is much deeper. It is not clear whether it is the deepest part of a high glacial ice margin or the deepest part of a later glacial stage	

1) after v. Wissmann (1959): climatic snowline

The present day overall climatical snow line (here used equivalent to equilibrium line altitude = ELA) in S Tibet and the N slope of the Himalayas between 28° to 29°50'N and 85°24' to 91°13'E runs at approx. 5900 m asl based on fifteen values. Assuming that the deepest ice margin positions found in this area belong to the last High Glacial (Würm) the snow line during the Ice Age ran at about 4820 m based on eight values. When, however, an Ice Age *climatic* snow line is extrapolated from these eight values we come down to 4720 m. Thus the High Glacial snow line (ELA) depression was as much as 1080 m or 1180 m respectively.

Fourteen late and post glacial stages were identified although the features were not everywhere found in completeness. The boundary between late and neo-glacial stages is most likely situated at a snow line depression of 67 m to 95 m. The onset of glacial stages in historical times is assumed to coincide with a snow line depression of some 55 m.

Presupposing stable humid conditions a snow line depression of 1180 m would mean a Pleistocene cooling of the warmest month by 7.1° C in S Tibet. However, according to own measurements in this area a gradient of 0.8° C/100 m could be correct, and thus a cooling of about 9.4° C would not be unlikely.

periglacially; 2. their very softness should have encouraged and left behind different forms, such as acute dissection by linear erosion and the outwashing of ravines which, in spite of periglacial influences, had a dominant effect in the more recent past, and continues to do so – if the previous glacial formation had not come down to us (Fig 27).

*Sedimentary rock and glacier polish: a comparison with the Arctic*

Here, as in numerous other places of the S Tibet ice cover, sedimentary rock indicates a geomorphological landscape character which presents an equivalent to the sedimentary rock of W Spitzbergen (i.e. Dicksonland on Svalbard, cf. Kuhle 1983b) including its post-glacial, periglacial-fluvial reshaping with funnel erosion and box valleys with braided river gravel floors. The only difference is that, in oceanic Spitzbergen, at 79° N, perennial patches of snow occur far below the present glacier tongues, despite a comparable annual precipitation of 250 mm. In subtropical S Tibet they rarely occur a little below or even at the equilibrium line level.

The rough texture of the metamorphic sedimentary rocks in place can be the result of 1) a post-glacial frost-weathering which always has a powerful effect on them in the continental highland. Granites in glaciated knobs on the Kakitu massif in N Tibet, though still beneath ice during the Late Glacial stage, were shown to be affected by considerable post-glacial rock disintegration (Kuhle 1987a, p. 205, Fig 17; p. 231, Fig 32). Sugden and John (1976, p. 196, Fig 10.4) even instance it for less weathering-intensive areas like Scotland, where glaciated knobs have by now become nothing short of anti-flow dynamic castellated rocks. Although not during an initial periglacial fragmentation but at a later point, in the course of a disintegration into rough blocks, the gross voluminous structure of the granite even proves to be of advantage, whereas finely weathered metamorphics retain the large structures more effectively (Fig 29, 41). 2) In the case of the Tibetan glaciation areas there is no need to assume that initially the surfaces of the rock ridges were substantially polished by glacier action; on the contrary, over vast stretches, the ground-ice of the semi-arid and therefore very cold Tibetan ice (cf. above) was firmly frozen to its rock base, so that the traces of abrasion must already be *primarily* rated as small within the specific context of the Ice Age climate.

Observations on Prehistoric Ice Covers between Shigatse (29° 17' N/88° 54' E) and Suo La (29° 09' N/88° 02' E)

Situated at the same level as the Tsangpo valley, the S parallel valley (between the Changma and Silung settlements; see ONC 1:1,000,000, H-9, and Fig 2, no. 18) is filled with large alluvial fans side-valleys and a

broad alluvial floor, now used for agricultural purposes. 70–90 km (by road) W of Shigatse discordantly and shallowly deposited reddish-brown weathered glacio-fluvial – and possibly even glacial – sediments occur on diagenetically consolidated, disturbed and probably Late Tertiary (or even Neogene?) sedimentary rocks. They definitely belong to the Pleistocene and form ridges tens of metres high. At km 93 (29°14'N/88°14'E) and at the altitude of 4160 m the track reaches the level of a terrain of conspicuously softly rounded forms, executed in more or less distinct banks of limestone and to be interpreted as a classical landscape of glaciated knobs. It is essential to note that the landscape has undergone recent dissection into gullies and gorges, which confirms the prehistoric formation of the glaciated knobs.

Here at 88° E the N outlet glaciers of the Tibetan Himalaya stretched down to about 4100 m (Fig 2, no. 18), failing to reach the Tsangpo level by a small amount. This confirms (see above) that, with rising valley levels of the Tsangpo and its immediate parallel valleys further W between 87° and 86° and the existing, correspondingly great altitudes of the catchment areas, the Tsangpo furrow had been reached by the outlet glacier tongues of the ice-stream network and the inland ice, and W of 86° E had also been infilled. This is the area from whence I3 was connected with I2 (Fig 75).

Glacier Traces in the Pang La Massif, South of the Lulu Basin (28° 30' N/87° 07' E)

On the N side of the massif, in the valley descending to the N of the Pang La, covers of rough quartzite blocks reach down to at least 4500 m, and form dumped end moraines (28° 33' N/87° 05' E) (Fig 2, no. 19). The entire broad valley floor up to the pass at 5200 m consists of moraine fields, the substrata of which experienced solifludial shifts of a few tens of metres during the Holocene. With a mean altitude of the catchment area of 5400 m, calculations show an orographic lowering of the equilibrium line to 4950 m, and corresponding ELA depression of at least 800 m. On the S slope moraine deposits in the shape of walls of quartzite blocks tens of metres thick (Fig 28; 28°26'N/87°06'E) and slope dressings with glacial diamictites were found as far down as 4250 m asl (Fig 2, no. 20). This moraine substratum already flanks a somewhat larger side-valley (Fig 29) which the Pang La valley joins, and which in turn reaches the Dzakar Chu at the settlement of Tushidzom. Valleyward findings of erratics 270 m above the valley-bottom line near the Nyomdo settlement confirm the position of the ice margin there. This results in a glacier surface slope which does not allow the glacier to terminate above 4250 m. From the confluence of the tributary valleys at the Nyomdo settlement a mature trough-profile manifests itself (Fig 29). The trough valley leads down from the highest peak (5867 m)



Fig 25



Fig 26

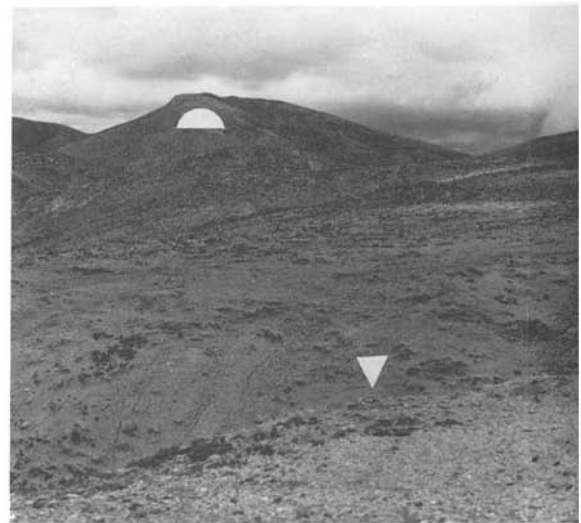


Fig 27



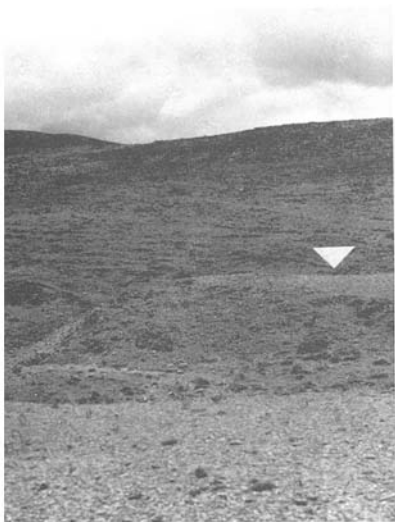
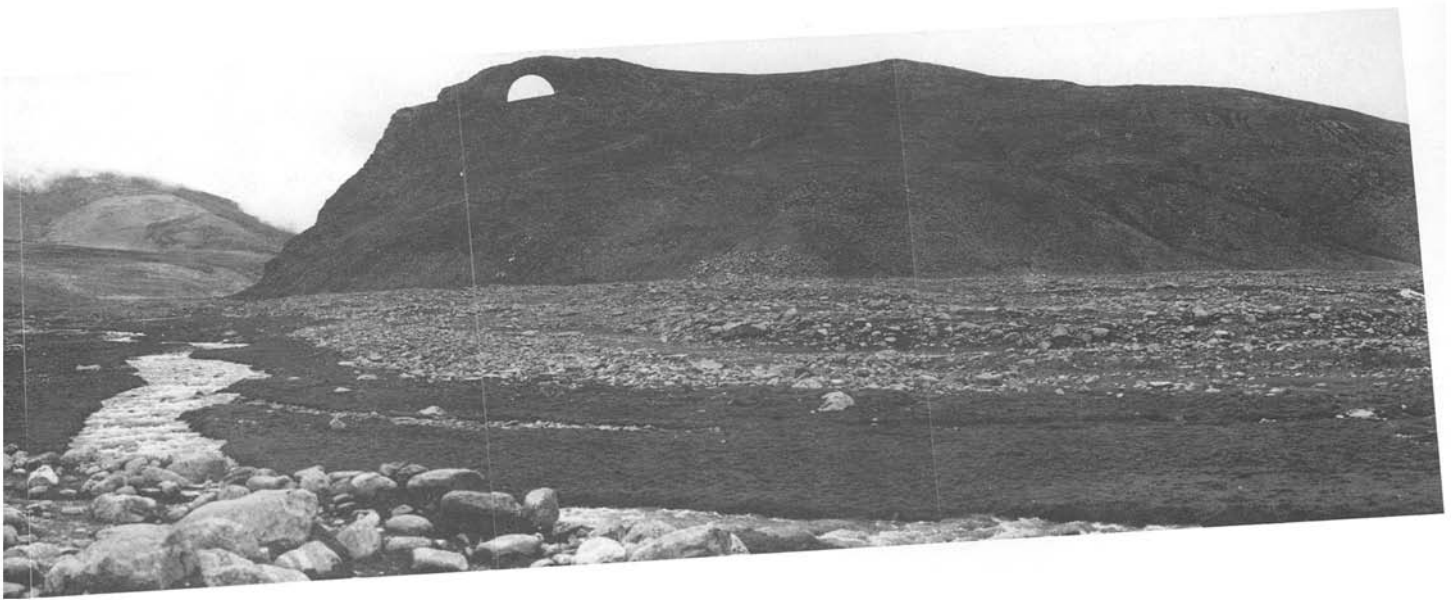


Fig 28

Fig 25

The glacial landscape of the central Mangar valley (Phu valley) in the north slope of the Latzu massif (Ladake Shan 28°54'N 87°39'E; viewpoint 4420 m, centre of panorama up-valley to WSW, cf. Fig 26). The valley floor (fore- and middle-ground) is covered with a granite block loam (ground moraine deposit) of the late-glacial stages I (Ghasa stadium) and II (Taglung stadium). The metamorphic rock ridges here (▲▲) have the characteristic shape of roches moutonnées and were completely overridden by the ice (Dhampu and Sirkung stadium). They project through ground moraine remnants; (cf. Fig 2 left of No. 16 III, IV). Photo: M. Kuhle.

Fig 26

Looking down the middle valley of the Mangar (see Fig 25) towards the NE from 4700 m. In the middle-ground are late-glacial morainic deposits modified glaciofluvially (▼). III shows the end moraine of the Dhampu stadium (late-glacial) which is also shown in down-valley direction in Fig 25. II marks the remains of a lateral moraine of the Taglung stadium (late-glacial). During the maximum glaciation the area was completely ice-covered which produced the whalebacks (▲). Photo: M. Kuhle.

Fig 27

Roche moutonnée landscape (▲) at 4500–4700 m on the Solotse La (Suo La) S of the Tsangpo valley (Fig 2, No. 17; 29°04'N 87°59'E). Periglacial solifluction sheets lie on the glacially scoured weak metamorphosed sedimentary series. Today they are dissected by deeply incised gullies (▼▼). Photo: M. Kuhle.

Fig 28

View from 4400 m to the NNE (centre of panorama) upwards to the area of the confluence of the two component streams of the Ice Age Dzakar Chu glacier (Fig 2, No. 20; cf. Fig 29); right is the settlement Nyomdo, left are lateral moraines with large blocks of quartzite (●). In the background similar erratic blocks overlie the in situ flysch series (↓). The true left valley side is glacially scoured, the etchings being smeared with ground moraine (▼). Glacial striations occur generally, as well as on the true left side (▲). Photo: M. Kuhle.



Fig 29

Fig 30



Fig 31





Fig 29  
Panorama (centre to the E) from 4400 m (Fig 2, No. 20; 28°27'N 87°09'E; cf. Fig 28). The valley of Nyomdo is a glacially formed trough valley. The fields of the settlement are located on impermeable ground moraine (◆◆). The valley is picked out by well-preserved striations along sedimentary layers (→). The smoothing of the surface (●) up to and over the surrounding heights indicates a complete covering of glaciers of the 'Panga La massif'. Photo: M. Kuhle.

Fig 30  
From Panga La (28°30'N 87°06'E) at 5200 m in the S Tibetan mountains to the S to the Himalayas and Mt. Everest. In the middle a large open corrie (●) is cut into metamorphic rocks N of Dzakar Chu (Fig 2, No. 19). The recent glacier tongues (●●●) lie only 1000 m above the valley floor of the longitudinal Dzakar Chu where it is most deeply incised (⚡). As the results of the (reconstructed) depression of the equilibrium line altitude by about 1200 m at the glacial maximum the relief was then completely full and overflowing with an ice stream network flowing from the Himalaya (Fig 75 and 76, I3). Photo: M. Kuhle.

Fig 31  
View from 4430 m towards the ENE (centre of panorama) to the W slope of the massif in the E of Man-ko-pan (28°44'N 86°27'E; Fig 2, No. 21). Both the trough valley (above ●) and the rounding of the summits show that the relief has been completely covered by a network of ice streams or an ice sheet (Fig 75 and 76, I3). Small ice streams flowed from the hanging trough valleys (above ●) to combine in the basin of Man-ko-pan (foreground). Photo: M. Kuhle.



Fig 32 From Tschü Sü La (4880 m) above the Yang-Cho-Yung-Hu (Yamdruk lake) towards the WSW to the 7193 m (7223 m) Lankazi massif (28°56'N 90°07'E; Fig 2, Nos. 24, 25); (---) shows the recent orographic snow line (equilibrium line altitude); (●●) mark the recent glacier tongues (in the ablation zone) facing E. The lake (at 4480 m) is a postglacial filling of a glaciated surface (shown by rounded hills ●, and corries ×). This is shown by the steep shores freshly cut into the slopes (↘). Photo: M. Kuhle.

of the Pang La massif. Its profile polishes metamorphic stratified rock. In the valley running S from the Pang La, as well as in its tributary valleys, broad, flat, corrie-like glacier beds have been formed (Fig 30, foreground). Flysches with marls and argillaceous schists occur with vertical stratification. They have been smoothed by basic glacial polishing across the outcrop curvatures and are superimposed upon by ground moraine tens of metres thick (Fig 28, background). These are drifts of large, rounded quartzite blocks with a crust of ferro-manganese (up to  $2 \times 3 \times 3$  m), which are separated by a fine, sandy, at times also clayey matrix, lilac blue in colour. Well-rounded blocks occur beside others with rounded edges. A solifluidal layer of moving drift has formed within the uppermost metre of the moraine. On the approximately 5500 m high arêtes and peaks, the affected light-coloured quartzites occur. Having filtered through from higher altitudes, or been broken down into block covers, they occur in sections, superimposed upon partially eroded soft flysches as relatively weathering-resistant residues. The moraine blocks were picked up by the glacier at this point, and transported well over 16 km away. Besides the lowest, distinct ice margin position at 4250 m (see above), another one had been formed at 4500 m, so that equilibrium lines at 4825 m and 4950 m result. The higher one is classified as belonging to the Late Glacial stage (Ghasa Stadium I) (see Tab 1). Since they occur on southerly aspects, the appropriate climatic ELAs are to

be stated as occurring 150 m lower at 4675 and 4800 m asl.

Due to the absence of present glaciation in the Pang La massif it is difficult to estimate the recent climatic ELA. However, it does run S of the Dzakar Chu at about 6000 m (Fig 30, background), so that 5900 m constitutes a likely figure, which points to an Ice Age ELA depression of 1225 m (5900–4675 m) and a Late Glacial one (Stage I) of 1100 m (5900–4800 m).

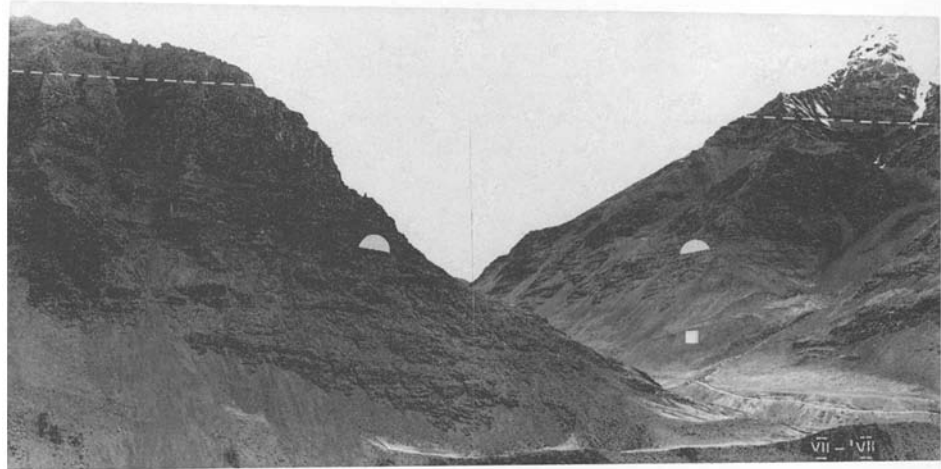
Greater equilibrium line depressions, i.e. lower ice margin positions, cannot be dealt with within the representative section of the Pang La massif under investigation here, since at the altitude of 4250 m the Dzakar Chu, a W branch source of the Arun valley (main valley running in a W–E direction) has been reached. This valley has been glaciated from the Himalayan N slope (Mt. Everest group; see below; Fig 30, background) during the Late and High Glacial Period. This implies that there was an ice-stream network without further ice margin locations N of the Himalayan ridge.

#### Traces of Glaciation in the Massif East of the Man-ko-pan Basin (28° 44' N/86° 27' E)

This c. 5800 m-high massif N of the Tingri basin is now likely to be entirely free of glacier (Fig 31), or at most occupied by very small corrie glaciers and perennial snow patches. The recent climatic equilibrium line thus runs at 5900 m (no higher, however). During the Ice Age there was glaciation of the type of an ice-stream network which filled the entire relief; all valley troughs are evidence of this (Fig 31). At the valley exits to the S and W ground- and end moraine ramps take over (Fig 31 ●●). There is a similarity between these and remnants of ice marginal ramps (cf. Fig 41) and pedestal moraines (dam moraines), on which the glacier builds up its own drift foundation by transporting and depositing lateral moraines (Kuhle 1982, vol. 1, p. 84, vol. 2, Fig 82; 1983a, p. 238). The trough-profiles extend down to 4600 m asl, and at 4400 m the moraine ramps become submerged below the more recent (recent Late Glacial?) glacio-fluvial drift sediments of the Man-ko-pa basin or the Tingri basin (Fig 31, middle ground; Fig 2, no. 21). With the mean altitude of the catchment area at 5300 m, the orographic equilibrium line on the W side is calculated as being at 4850 m, in accordance with a climatic ELA around 4750 (Tab 1). It has hitherto not been possible to prove in situ that this is a Late Glacial lowering of the equilibrium line, though the author records it as likely as the basins of Tingri and Lulu which join on in the E must have been filled with ice during the Ice Age (cf. above), and this catchment area is situated here at a similar altitude. Moreover, the ELA depression of 1050 m during the maximum Ice Age would be disproportionately low in comparison with lowerings in the vicinity.

Fig 33

View from Kang Chüng valley at 5200 m of the main valley leading down eastward (right) from the Lang La (Lankazi massif 28°57'N 90°11'E). At the glacial maximum this accidented area was filled up to the summits with a network of ice streams at least 1000 m thick (Fig 75 and 76 I3). This is shown by the lateral striations on the laminations of the metamorphic rocks (●). (---) indicates the minimum thickness of the ice. VII-VII marks the moraines of the Kang Chüng glacier known historically; these are younger than 790 ± 155 and older than about 320 years. (■) shows other moraines known historically and up to neoglacial age (younger than 4160 and older than 320 years). Photo: M. Kuhle.



The Glaciation of the Lankazi Massif (28° 56' N/90° 07' E; Tab 1)

On the N-facing Kang Chüng glacier in the Lankazi massif (Fig 32) which rises to 7193 (7223) m in the 5150 m high area of the Lang La (28° 57' N/90° 11' E) in the Tibetan, or Inner Himalayas, it was possible to distinguish at least nine historical glacier locations, all of which were more recent than 790 ± 155 BP (Fig 33). All these stages occurred within a maximum equilibrium line depression of less than 100 m as compared to the glacier tongue of the time, which does not descend further than to 160 m above the lowest of these moraine formations (Tab 1). In accordance with the Kuhle nomenclature (1982, p. 118) they are classified between Stadium X to

the more recent Dhaulagiri Stadium (VII) and down to the Middle Dhaulagiri Stadium (VII).

Neo-Glacial moraine chains were observed and mapped as extending into the mouth of the main valley of the parallel E valley (feeding into the Lang La valley, which descends in an easterly direction) (Fig 34, 35). They occur as far down as 4730 m (Fig 2, no. 22). The unnamed high peaks of the immediate catchment area rise to 6600 m, and the mean altitude of the ridge surrounds will be about 5900 m. The equilibrium line of the N face accordingly ran at about 5315 m, and at the time of that ice margin position thus 390 m lower than the recent equilibrium line (which is at about 5705 m). With reference to this equilibrium line depression a classification as Neo-Glacial or late Late Glacial is

Fig 34 A valley E of and parallel to the Kang Chüng valley seen up-valley towards the S; at its end is a completely glaciated peak at some 6600 m (left background: Fig 2, No. 22). Viewpoint at 4960 m. The sides of the valley here, as in all valleys parallel, are glacially scoured to considerable heights (●, cf. Fig 33, 35, 36, 38, 39). The well-developed lateral moraine terraces with sporadic alpine vegetation on each side of the centre line of the valley and the end moraines (foreground) are from a neo-glacial stadial position (Nauri stadium V or Older Dhaulagiri stadium VI ?). Photo: M. Kuhle

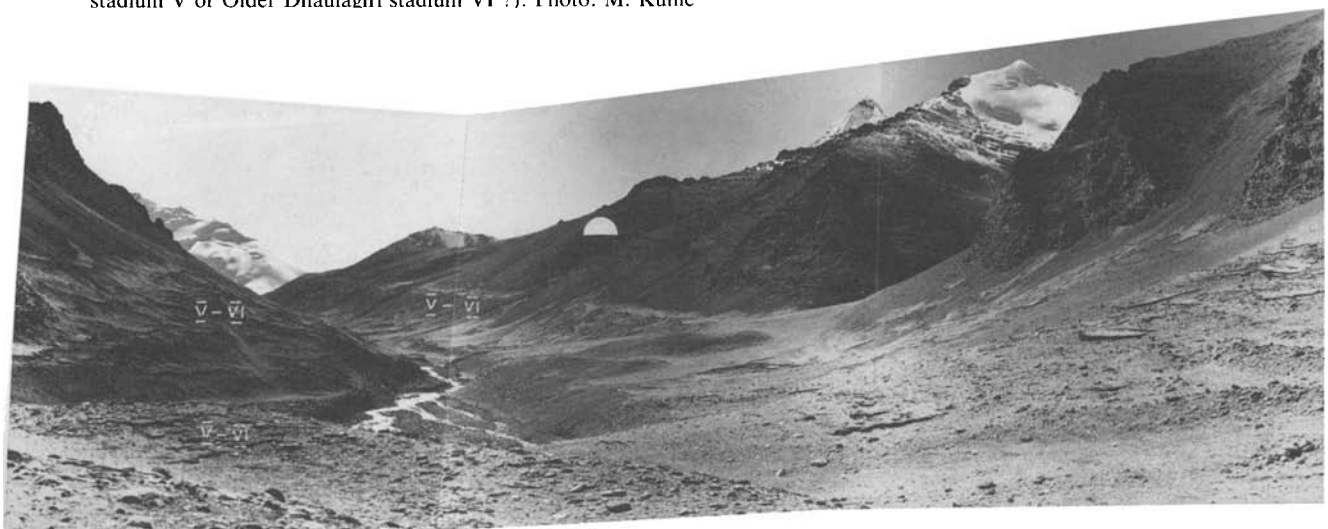






Fig 35 The valley parallel to the Kang Chüng valley to the E seen from 5300 m (see Fig 34; 28°54'N 90°10'E) looking down-valley to the N. The high peak (◆) reaches 6500 m. (▲) shows the remains of the lateral striations on the laminations of the easily weathered metamorphic rocks. The bluffs and arêtes (▼▼) are the remains of the earlier slopes of this trough valley landscape eroded by ice in maximum glaciation times. The moraines in the valley floor are of neoglacial age (V–VI). (↓) shows the location of C14 dating (790±155 BP; Fig 2, No. 22 ○) in the main Lang La valley. The neoglacial end moraines (×) are at 4730 m. Photo: M. Kuhle.

appropriate. It has not been possible to establish the minimum age of the moraines with the aid of C-14 analyses. Under the cold-arid conditions, there is a lack of sufficient organogenic substratum. At the exit of the E parallel valley of the Kang-Chüng North Glacier to the Lang La valley (28° 53' N/90° 11' E) it was possible to date one of the samples, taken at a depth of 0.6 m from a few metres-high outwash plain terrace, at 790±155 BP (14C content 90.6±1.7% modern; analysis by M. A. Geyh, 30. 5. 85) (Fig 2, no. 22; Fig 35 ▼). Both the position of the ice margin down valley at 4730 m and the ELA depression of 390 m are thus shown to be older, and therefore classified as Nauri Stadium V (Kuhle 1982, p. 159, 160). This also provides a clue for the fact that the ELA depressions of 390 m and more are of Neoglacial age at least (for Himalaya cf. Kuhle 1986d, p. 438–454; 1987b, p. 200–205). The formation of humus from alpine turf which has been dated here may admittedly be significantly more recent than the ice margin position in question, for the amount of shifting in the area affected by the confluence of the alluvial plains of two valley glaciers is considerable (Fig 36). It is true that this is the body of a terrace the top of which must have been dispensed within the course of the dissection that goes with the retreat of a glacier, and thus from further interference and the opportunity of providing the most favourable locality for taking samples. The ice margin positions of 4820 m asl, with ELA depressions of 345 to 320 m, are situated further up-valley from the sample locality, i.e. higher, so that they must be classified as probably more recent and thus historical. In principle, however, it cannot be ruled out that they are much older than the formation of soil and humus in question, since soil destruction may not only be due to a crossing glacier, but also to meltwater erosion. For this

reason, though also because of equilibrium line depressions around 300–350 m, they are being classified as three stages of the older Dhaulagiri Stadium (VI) (Kuhle 1987b, p. 205).

W of the Lankazi massif and the Lang La there is a very large and more than 10 km-wide high valley with a valley floor between 4400 and 4800 m (Fig 37). It runs in the direction of the Chiang-Tzu settlement and is enclosed by more than 6000 m high mountain massifs which are currently glaciated. Included amongst these are the main peaks of the Lankazi massif in the region of the Lang La (Fig 37). All the main valleys of the Lankazi massif (where the Lalung and Sutu settlements are located), which run westwards towards the large valley, bear characteristics of relief-filling glaciation. These include glacial scouring on outcropping layer edges in easily splintered metamorphics, as well as glacial grooves several hundred metres above the 4800–5100 m high valley floors (Fig 33–36, 38, 39). Although there has been no certain evidence that also the large longitudinal valley had been completely filled by glaciation, it is highly likely considering its altitude. From both the flanks, large, flat alluvial fans descend (Fig 38), like those observed in glaciated longitudinal valleys of Würm age in Alaska (i.e. the McKinley river N of the Alaska Range, 63°30'N/151°W), in W Greenland (Sarqaqdaalen, Nugsuaq, 70°03'N/52°W; Kuhle 1983c) and in Dicksonland (Western Svalbard, e.g. Idodalen, 78°03'N/52°W; Kuhle 1983b). During the Ice Ages, ice in valleys of this kind would build up to thicknesses of several hundred metres without leaving behind striking glacial traces in the metamorphosed sedimentary rocks, apart from polished triangular areas between the exists of side-valleys and softly-rounded forms (Fig 37 ●●; Fig 2, no. 23).

Fig 36

Looking down the Lang La valley from 4800 m (Lankazi E slope, cf. Fig 33, 35 (in distance), 39). The cross profile of the trough valley is box-like. Above the ground moraine there lie the up to  $790 \pm 155$  year old outwash deposits of the historic glacier (foreground); the river has cut down 1–2 m into the gravels ( $\downarrow$ ). The valley sides are glacially scoured ( $\blacktriangle$ ). Photo: M. Kuhle.



The E slope of the Lankazi massif is characterized by prehistorically totally glaciated, glacialic box valleys with distinctly polished flanks (Fig 33, 35, 36, 39). As in the case of the Alps, Late Glacial and High Glacial glacier-levels cannot be differentiated with precision, but a surface of an ice-stream network at altitudes of around at least 5500 to 5750 m has been established by ridges that have been polished into roundness and intermediate valley divides with upper ice-scour limits (Fig 33, 34, 39 -----). This implies ice thicknesses of about 1000 m. Higher peaks like the Kang Chüng, the Lankazi peak and other high mountains (Fig 33, 35, 37) reach altitudes of 6500 to 7193 (7223) m, and rose another 1000 m above the surface of the ice-stream network. In the opening of the large valley which descends in an E direction and is being accommodated by the track from Lang La, there is a large moraine fan of ground moraine at 4530 m ( $28^{\circ}55'N/90^{\circ}24'E$ ; Fig 2, no. 24). It is tentatively being attributed to the more recent Late Ice Age (Sirkung (IV), Dhampu (III), or Taglung Stadium (II)). As a valley lake, the wide and branching Lake Yamdrok (Yang-Cho-Yung Hu in Chinese; Fig 32, Tab 1) to the E of the Lankazi massif has a certain similarity to the Alpine Vierwaldstätter Lake. It is interpreted as a lake in a terminal basin of the High to Late Glacial genesis (Fig 2, no. 25). Its level is at an altitude of 4480 m, and assuming a minimal lake depth of 20 m, it would have required an ELA depression of 765–875 m in order to have a glacier reach the lake floor. This ELA depression rather suggests a Late Glacial (Ghasa Stadium (I)) rather than a High Glacial classification (Tab 1). The post-glacial filling up of a lake in a former terminal basin is confirmed by the limnic undercutting of the shore with the subsequent formation of striking steep banks (Fig 32  $\blacktriangledown\blacktriangledown$ ) as a new, previously not yet established formation element. Gentle glacialic slopes have been worked upon concordantly by interglacial and post-glacial periods of solifluction (Fig 32  $\bullet\bullet$ ), and have now been given a new formation of a different kind by the undercutting of the lake shore.

The Lankazi E face with an equilibrium line at around 5800 m (Fig 32 ----) and an upper glaciation line at the level at which a shallow relief sets in (Fig 32  $\bullet\bullet\bullet$ ; cf. also Fig 30  $\bullet\bullet\bullet$ ); make the exponential glacier increase clear. Even an ELA depression of only 500 m brought the equilibrium line to 5300 m asl, the glaciers then terminated only 300 m above the level of the lake and the gain in ice area was considerable. It is the altitudinal interval within which large, bowl-shaped corrie basins were polished out (Fig 32  $\times$ ).

#### Lowest Ice Margin Locations and Equilibrium Lines in the High Himalaya

Prehistoric glaciation of the High Himalaya cannot be separated from that in S Tibet and in the Tibetan Himalaya N and E of the Shisha Pangma massif. The two will therefore be treated together.

The Glaciation of the Shisha Pangma Massif with Bo Chu (Sun Kosi) and its Catchment Area (Tab 1)

In the course of our joint 1984 expedition Zheng Benxing included the Shisha Pangma N slope in its 'Geomorphological Map of the Mount Xixabangma Region' (1988), and the author explored it as well (Fig 40, 41). The states of glaciers recorded by the two fieldworkers proved to be identical. Apart from the nomenclature, differences occurred in the estimates of the age of glacialic diamictites.

#### Some notes on the nomenclature and age classification of the stadia

Zheng Benxing designed a local nomenclature of the state of glaciers, with the massifs of Shisha Pangma and Mt. Everest in mind. Here the author attempts to extend his exemplary Dhaulagiri-Annapurna-Himal nomenclature so as to include Tibet and its adjacent mountain



Fig 37

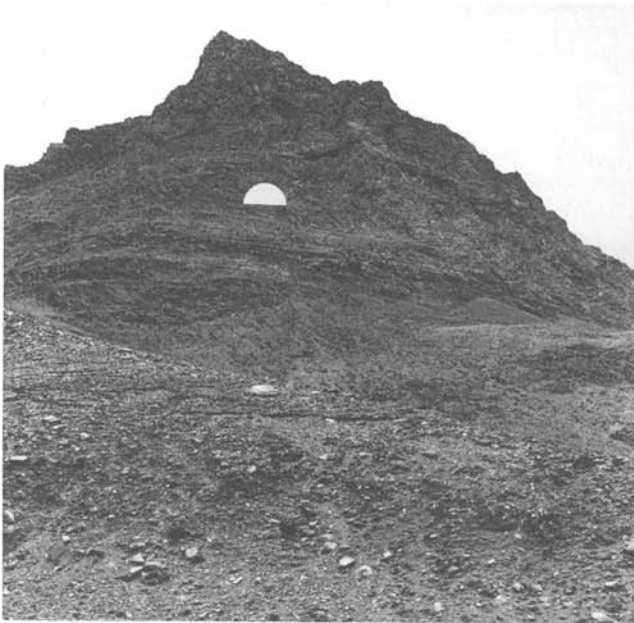


Fig 38



Fig 39



Fig 40

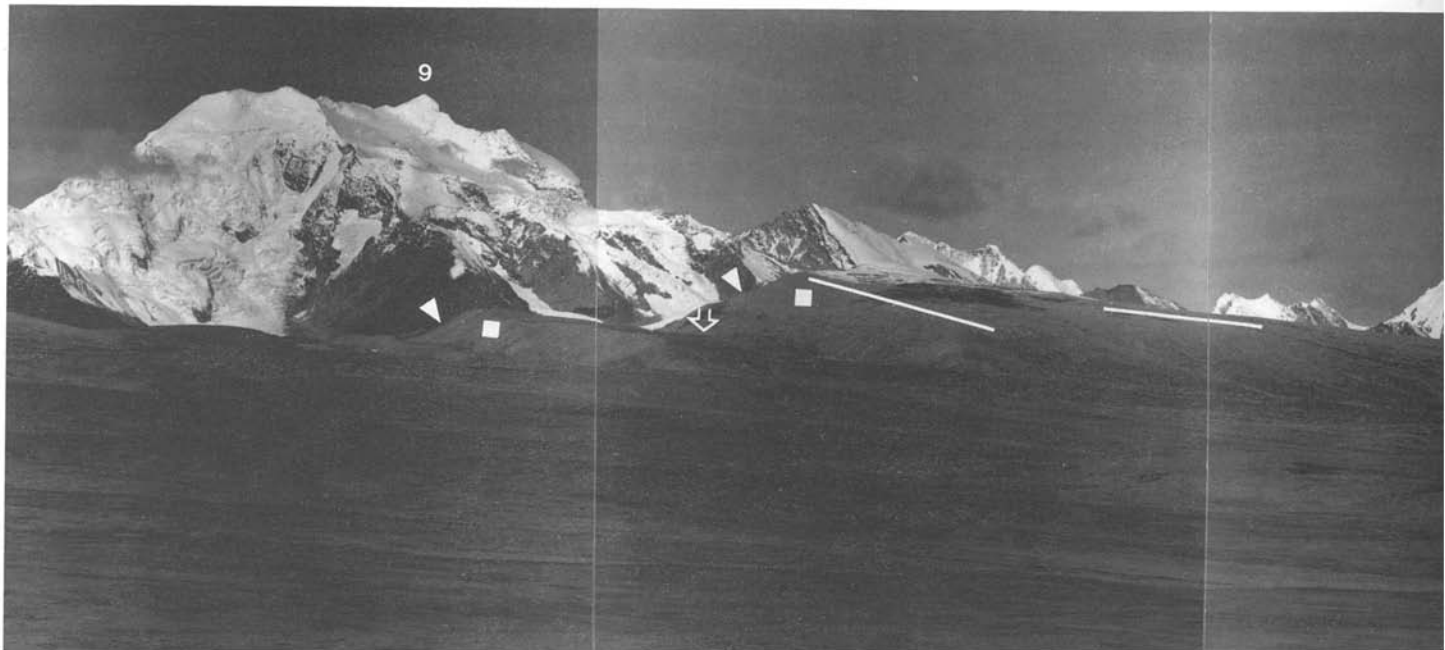




Fig 41

**Fig 37**  
View looking S (centre of panorama) from 4630 m in the large E–W running longitudinal valley that leads from the Lankazi massif (28°51'N 89°54'E; Fig 2, No. 23). The glaciated peak at c. 6600 m to the left lies E of Lang La (c. 5150 m). The view right shows the broad trough-like valley contours towards the W. The valley floor is filled with late-glacial and postglacial alluvium (with portions of outwash ◆ and historical alluvial fans (▼)). The alluvium lies above lodgement till. The slopes show glacial striations (●●) on the weakly resistant metamorphic rocks. These are modified but not removed by solifluction sheets and gully wash (↓). The aspect of the relief recalls that of the ice sheet eroded region of West Spitsbergen or e.g. that of the Kluane mountains in the West Yukon (Canada).  
Photo: M. Kuhle.

**Fig 38**  
Detail of the state of preservation of features produced during the maximum and late-glacial. Sculpturing of strata edges (●) on finely stratified and thus easily weathered crystalline schists (phyllites). True left tributary valley of the Lang La valley (Lankazi massif; Fig 2, between No. 23 and 25; 5100 m). Photo: M. Kuhle.

**Fig 39**  
Glacial shaping of the upper Lang La valley viewed toward the W. (Lankazi massif; viewpoint 5050 m; Fig 2 E of No. 23). The lineations of glacial scouring are well preserved in spite of the slight resistance of the rocks. This shows them to be young and thus probably late-glacial in origin. The level of the ice during the glacial maximum lay above the rounded rock bosses (---). The lateral kamiform terrace (◆) must therefore have been formed along the young, late-glacial valley glacier.  
Photo: M. Kuhle.

**Fig 40**  
N slope of Shisha Pangma (No. 8) seen from 5250 m (Fig 2, No. 26 28°23'N 85°47'E) on the S Tibetan plateau. The high plateau in the foreground is in direct contact with the High Himalayas without interposition of the Tibetan Himalayan mountains. I–VI shows late-glacial to neoglacial stadal positions of the Yepokangara glacier which flowed from Shisha Pangma. Its tongue ends today at the foot of the 8046 m mountain (↓; cf. Fig 42 ×). The moraines I–VI deposited between the lateglacial piedmont glacier tongues are marginal sandr (ice marginal ramps = IMR, × and I). The IMR were raised above the equilibrium line in the post-glacial so that today they have individual ice patches (× and I). This new glaciation shows that Tibet has been uplifted more rapidly than the Himalayas because the recent tongues of the Yepokangara glacier (↓) no longer reach these lowest end moraines.  
Photo: M. Kuhle.

**Fig 41**  
The N slope of the 7299 m Kang Benchen (No. 9) photographed towards the W (centre of panorama) from 5250 m. Its glaciated slopes lead down over 1700 m vertical distance to the High plateau of S Tibet (Fig 2, N of No. 27; 28°40'N 85°34'E). The recent (↓) glacial tongues reach exactly to the base of the marginal sandr (ice marginal ramps or IMR ■■■). These were deposited in the late-glacial. Their ramp-like contours (▼) with a steep front slope facing the mountains (—) are characteristic of such glacial and glaci-fluvial outwash features of semi-arid piedmont glaciers. Photo: M. Kuhle.

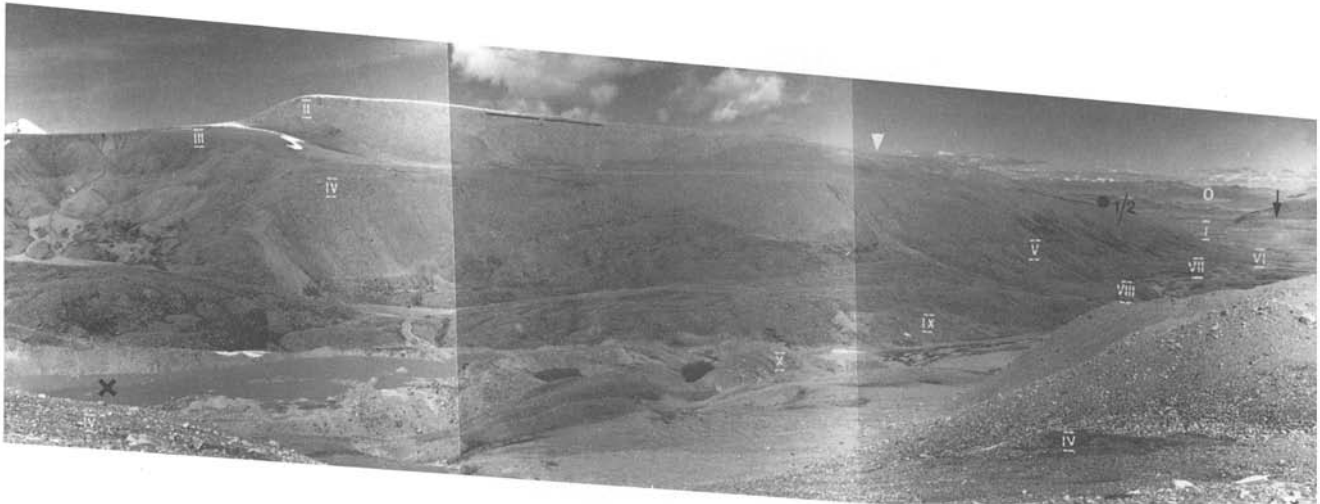


Fig 42 Marginal sandr (ice marginal ramps = IMR, —) seen in cross section from 5820 m towards the W (centre of panorama). These late-glacial (I–IV) and as recent as historical morainic ramps (V–IX) dominate the valley floor (×) by more than 500 m. × marks a glacial lake in dead ice on the tongue of the Yepokangara glacier of Shisha Pangma N slope (Fig 2, No. 26; cf. Fig 40 ◀). The checker-board intermixing of kamiform features and lateral moraines of progressively younger ages is characteristic. This results from the progressive downward contraction and narrowing of the glacier tongues between the marginal sandr deposits (see the succession from II, ● <sup>1/2</sup>, III, IV, V, IX, X). (○, extreme right) marks the area of the ice sheet engulfing the relief (↓), an area of classical roches moutonnées. Photo: M. Kuhle.

systems (Kuhle 1980, 1982, 1983a, 1986d, 1987b). In what follows a comparison of the two systems will be presented.

#### Zheng Benxing

Highest moraine platform of Xixabangma glaciation (middle Pleistocene?)	_____
Higher moraine platform of Nyanyaxungla glaciation (middle Pleistocene?)	_____
Oomolangma glaciation I (Fuqu glaciation I)	_____
Oomolangma glaciation I (Fuqu glaciation II)	_____
Oomolangma glaciation II (Pulao glaciation)	_____
Neoglaciation (all stadia up to the sub-recent terminal moraines are included)	_____
“ ”	_____
“ ”	_____
“ ”	_____
“ ”	_____
“ ”	_____
“ ”	_____
“ ”	_____
“ ”	_____
“ ”	_____
“ ”	_____

#### M. Kuhle

Ghasa Stadium (I) (Late Glacial)	_____
Taglung Stadium (II) (Late Glacial)	_____
Dhampu Stadium (III) (Late Glacial)	_____
Sirkung Stadium (IV) (Late Glacial)	_____
Nauri Stadium (V) (Neo-Glacial, c. 4000–5000 BP)	_____
Early Dhaulagiri Stadium (VI) (Neo-Glacial, c. 2000–2500 BP)	_____
Middle Dhaulagiri Stadium (VII) (Neo-Glacial, more recent than 2000 BP)	_____
Late Dhaulagiri Stadium (VII) (c. 440 BP)	_____
Stage VIII (c. 320 BP)	_____
Stage IX (more recent than 320 BP)	_____
Stadium X (c. 80–30? BP)	_____
Sub-Recent – Recent Stadium (30–0 BP)	_____

In spite of a subdivision into 13 stages, the author's scale still proved to be too small in the forefield of the recent glaciers of the Shisha Pangma N slope (Fig 2, no. 26). It is even possible to establish altogether 16 to 18 steps and stages (Fig 40, I–VI). This applies to the forefield of the Yepokangara Glacier (Fig 42, O–X), the immediate catchment area of which includes the Shisha Pangma main peak.

The author differs from Zheng Benxing essentially in that his assessment of the time for the stage process in the Shisha Pangma foreland is different. There are no absolute data for the area concerned. It is too cold and arid to produce sufficient quantities of organogenic substratum for radio-carbon analysis. Whilst the Chinese age-dating attributes the oldest moraines to the Middle or even the earlier Pleistocene, the author – assessing the freshness of forms – assumes an at most Late-Glacial age, i.e. c. 15,000 BP (Ghasa Stadium I and younger). All the more recent oscillations in the course of the glacier retreat have, accordingly, taken place in post-Glacial times. This agrees with the glacier retreat of the past 13,000 years given for other areas in High Asia (Karakoram, Quilian Shan, Kun Lun, Himalaya) Kuhle 1986, 1987 a, b).

Outside the late-glacial glacier margins mentioned above, which descend at most down to only 5015 m asl (Ghasa Stage I, cf. Tab 1; 28°35'N/85°45'E), marked and well-preserved forms of glaciated knobs occur widely (Fig 42 ▼; Fig 2, no. 26). They rise to fully 5250 m asl, and are evidence of a complete inland glaciation, which subdued the S Tibetan relief. It must be attributed to the last Glacial Maximum of the Ice Age, 18,000 to 30,000 years ago (Fig 42 ○). In accordance with the great altitude of the plateau of S Tibet, which does not fall

below 4500 m anywhere here, a maximum ELA-depression of 850 m to 5415 m can be ascertained (Tab 1; 28°46' N/86°09'E). During the pre-Ghasa stagnations (● 1/2), two glacier locations, which are to be found entered between the High and Late Glacial (Kuhle 1982, p. 153), the glacier tongues which had moved furthest to the N from the High Himalayas down to the plateau, terminated in the tongue basin of the Paiküco (Peiku Tso) lake at about 4500 m asl (Fig 42 ● 1/2; Fig 2, no. 27). They present stages of the retreat from the situation of the all-covering inland ice to a Himalaya N slope-piedmont glaciation that remained into Late Glacial times.

*The complex of problems concerning the ELA-depression and glacial isostasy on the Shisha Pangma*

Compared with equilibrium line depressions of the Late Glacial stages of the Himalayan N face, which attain 700–1250 m (Kuhle 1982 p. 154 et seq.), those of the Shisha Pangma N side are very small. The Ghasa Stadium (I) thus came up with an ELA-depression of from 6325 m to 6060 (6058) m, i.e. of only 265 m (Fig 42, I).

To begin with, this results in objections to the age of the moraines, establishing them as being still more recent than Late Glacial and possibly even as Neo-Glacial (cf. Kuhle 1986d, 1987b). In any case their age can by no means be interpreted as High Glacial or even as Middle Pleistocene, as Zheng Benxing tries to do (see above). Thin section analyses of moraine blocks are evidence even of what are, microscopically, clearly visible iron hydroxide formations which follow hairline cracks as lines. Blocks of coarse-grained Shisha Pangma eye-gneiss were selected (Fig 43). Under the cold and arid conditions the formation of weathering lines of this kind requires more than the 2–4 Ka of the neo-Glacial

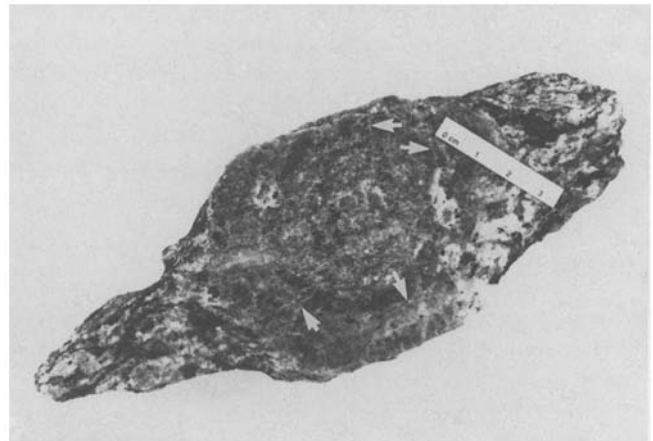
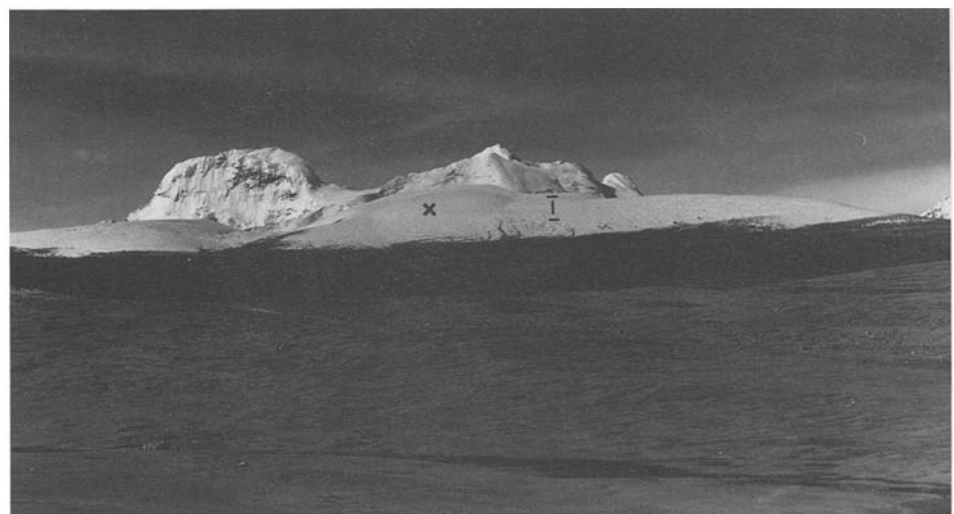


Fig 43 Polished sectioned hand specimen of Shisha Pangma augengneiss. The rock portion is a morainic component of the late-glacial ice-marginal ramps in the Shisha Pangma N slope (locality ● 1/2, Fig 42). Weathering discloses streaks of iron-hydroxides (↓) produced over 9000 to up to 15000 years. They may be followed between the crystals of albite oligoclase and potash-feldspar. The light weathering streaks (↓) are positioned on the cross-wires. Laboratory photograph: M. Kuhle and J. Peters.

fluctuations of the glaciers. An age of 9–15 Ka, however, seems to be right (see below). This raises the question of how it is here that in the immediate vicinity of ELA-depressions of up to 1250 m (on the S side of the Himalaya) of the same age, the Late Glacial (the Ghasa Stadium I, for instance) reached no more than 200–300 m. The answer to this may be helped by the observation that some of the terminal moraines from the Late Glacial are now covered by a glaciation of their own, i.e. are now within or even above the present level of the equilibrium line (Fig 40 × and 44 ×). Evidently the post-Late Glacial uplift has subsequently pushed up the terminal moraines of the rising equilibrium line so

Fig 44 N slope of the western Shisha Pangma mountains (the nameless 6500 m peaks between Shisha Pangma and Risum to the W: 28°38' N 85°39' E, Fig 2, N of No. 27). End moraine of the marginal sandr (IMR) type of the late-glacial (Ghasa stadium I). The surface of the moraine has been lifted above the equilibrium line in the post-late-glacial period so that an hour-glass-like plateau glacier has been produced (×). This uplift is the result of a very intense glacio-isostatic unloading as the Tibetan ice sheet melted. Photo: M. Kuhle.



that the recent glacier tongues terminate fully a mere 500 m above the lowest end moraines of the Ghasa Stage (I) (Fig 42, distance of recent dead-ice lake  $\times$  to I). This leads to the postulate of an uplift since the Late Glacial period, which raised the terminal moraines by several hundred metres, i.e. by perhaps 600 m within 15 Ka, for it is accepted that

$$ELA_{\text{Depr.}} = \frac{t_p - t_i}{2} \text{ (m asl),}$$

with  $t_p$  representing the recent termination of the glacier tongue and  $t_i$  for that of the prehistoric one. This is equal to an ELA-depression of 500–600 m at that time ( $600:2 = 300 + 265 = 565$  m). This is much too low for the Ghasa Stadium (I), which tends to show depressions clearly above 1000 m (Kuhle 1982). This amounts to an indication that either the assumed uplift is still being set too low, or that the lowest immediate moraines of the piedmont glacier on Shisha Pangma belong to distinctly younger Late-Glacial stages than had hitherto been assumed (as shown in Fig 40, 42 and 44). A clarification of this problem calls for the investigation of the cause of this evidently very considerable average uplift of some 40 mm/year or more, and one that is three to eight times greater than Gansser (1983, p. 19, and an oral communication in January, 1983) states for the High Himalaya. Evidence for the much more rapid uplift of the Tibetan plateau, as compared with the 8046 m high massif during the Holocene, can be found here on the Shisha Pangma. Although the large terminal moraine wedges or broad moraine ridges (Fig 40, I and 44, I) of the ice marginal ramps type (ice marginal ramps = IMR; see below) have been raised above the equilibrium line and are superimposed upon by a glaciation of their own (Fig 40  $\times$  and 44  $\times$ ), the mountain glacier tongues (Fig 40,  $\downarrow$ ), the predecessors of which deposited the terminal moraine ramps in prehistoric times, no longer reach the lowest ice margin locations (Fig 42, I). It follows that the Shisha Pangma massif, the catchment area of the mountain glaciers, was not uplifted in the same way as the terminal moraines. The tongue of the Yepokangara glacier (Fig 40  $\downarrow$ ) has now retracted 15 km from these terminal moraines.

The finding of the Eohippus, a denizen of the lowlands, at an altitude of 4900 m ( $28^{\circ}33'N/86^{\circ}10'E$ ), E of the Shisha Pangma, provides general evidence for an uplift of S Tibet of about 5000 m during the past 40 million years. However, at the same time the High Himalaya rose faster than the Tibetan plateau over a longer period of the Late Tertiary and Pleistocene. The antecedents of the Himalayan transverse valleys, which originated in Tibet and – synergetically with the uplift of the Himalaya – cut through the main range, are evidence of this (Hagen 1968; Kuhle 1982, p. 18, 20). How, then, can the suddenly accelerated *post-glacial* uplift be explained in an otherwise constant geological-tectonic situation? Had it not be confined to the post-glacial period only, but persisted over prolonged periods

of the Quaternary, the altitude of the Himalayan peaks would already have been surpassed. The hypothesis of glacial-isostatic uplift offers an explanation – precisely also because of the extremely high rates of uplift (see above), which are otherwise unknown in primary vertical tectonics. Creating an increasing impact, the inland ice on the Tibetan plateau achieved a much more remarkable thickness than the ice in the mountains on its fringe, such as the Himalaya, where the comparatively narrow valley glaciers flowed steeply down to below 2000 or 1500 m asl, losing much of their thickness. This explains the much more significant glacio-isostatic deformation, i.e. the greater uplift as compared with the Himalayas which goes together with de-glaciation. The once faster tectonic uplift of the Himalaya, like the compensatory glacio-isostatic uplift of the S Tibetan plateau edge will have taken place at that time along the same N Himalayan marginal fault as a slip plane.

By contrast with the Himalaya, morphological features of such forced plateau uplift are stepped accumulations of ice-marginal ramps, which slope towards the mountains (Fig 41  $\blacktriangledown$ ). The amounts of uplift previously deduced are limited: partly by the extent of the ice burden in the Main Ice Age through the thickness of the ice. In turn, this is topographically limited by the ice overspill into the south slope of the Himalayas, i.e. by the lowest passes plus several hundred metres. But the large Himalayan gaps like the E Bo Chu (Sun Kosi or Po Ho), or the adjacent Chilung Chu (-Ho) in the W have also by way of outlet glaciers contributed to the lowering of the inland ice level.

A glacio-isostatic depression of 600 m implies a thickness of about 1800–2000 m ( $0.9:3-3.3$  [ $g/cm^3$ ]) of ice. That postulated 600 m of uplift may admittedly also contain 100 m of normal tectonics, so that the necessary thickness of ice could be reduced to 1500 m. On the other hand, it must not be assumed that the glacio-isostatic compensatory movement is already completed, so that the end result will be an uplift of more than 600 m. According to Chen (1988, p. 30, Fig 3) an uplift of 7–10 mm/year was measured in central Tibet. Values such as these are cited by Mörner (1980, Fig 6 and 20) for current vestiges of uplift in the central area of the N European inland ice on the Gulf of Bothnia during the Vistula (Weichsel) period, and by Andrews (1970, Fig 2 – I; Tab. V-1) in the equally central areas of the Laurentian ice in North America. Mörner (1978, Fig 1) assumes uplifts of 500 mm/year for the time soon after the deglaciation 10,500 to 7000 years ago. The analogy for Tibet shows that comparable final uplifts continue to occur, and also that by far the largest part of the isostatic uplift had occurred thousands of years ago and shortly after the melting of the ice.

Thanks to the very thick continental crust in Tibet, which is more likely to have reacted to glacio-isostatic depression en bloc than in a spatially much differentiated way, the 1500–1800 m thick ice here on the very edge of the plateau is not necessarily the pre-condition for the

recorded amount of uplift. Ice-scour limits and moraine deposits with erratics are evidence of minimum ice thicknesses in Central Tibet of 700 m (NE Tibet; Kuhle 1987a) to 1200 m (Transhimalaya, see above) and of 1600–2000 m in the contiguous mountains (Karakoram and Himalaya; Kuhle 1982, 1983a, 1988b, p. 146). Simple surface interpolations according to the pattern of a low dome shape (like those hitherto always hazarded in the case of the N inland ice, as there are no inspired clues there either) give substance to central Tibetan ice thicknesses of up to 2700 m (Kuhle 1988b, p. 143, Fig 2).

Such thicknesses are confirmed by the inland ice models for Ice Age Tibet, established thermally and in terms of flow-dynamics, which Herterich and Kalov (1988; Mainz Lecture, 1987) had, with the aid of a computer, calculated based on data supplied by the author. They show that, after a 10 Ka phase of ice development, with a mean ELA level of 4250 m and an annual precipitation of 120 mm already produce ice thicknesses in excess of 2000 m, though the morphological final equilibrium of the ice dome surface is not yet reached at that stage. If the same conditions persist for a longer time, the ice thickness will increase even further (Herterich, Kalov and Kuhle 1988; in preparation).

The assumption is therefore that there is a more or less rigid, integral glacio-isostatic overall depression and uplift which had manifested itself on the Shisha Pangma N slope in considerable short-term altitudinal differences of the terminal moraine ramps (Fig 44).

#### *Some observations on terminal moraines and ice marginal ramps on the Himalayan north slope*

On the N slope of the Langtang-Himal between Bo Chu (Sun Kosi) in the E and Chilung Chu (-Ho, Gyirong Zangbo or Upper Trisuli valley) the Tibetan High Plateau borders immediately on to the High Himalaya for 60 km (Fig 2, no. 27), which rises 1700 m (Fig 41: Kangpenqin or Kang Benchen 7299 or 7211 m) to 2500 m (Fig 40) above the plateau. This is a rare topographical feature. The norm, as on the Dhaulagiri, on Annapurna and even on Mt. Everest, is that the formation of the S Tibetan Highland proceeds from the Tibetan or Inner Himalaya without intact plateau areas. At the Shisha Pangma the high plateau forms an area at the foot of the mountain on to which 12 recent glacier tongues flow out (Fig 40 ↓ ; Fig 41 ↓↓ ). In prehistoric, i.e. Late Glacial to historic times a more or less distally continuous foreland glaciation had been formed (cf. Tab 1, final glacier levels in the Yepokangara glacier forefield between 5015 and 5495 m asl; Fig 42). At the time the Late Glacial foreland glaciers advanced 10–15 km into the pediplain they formed ice marginal ramps over 600 m-high (Fig 41 ■; Fig 40 × and I; Fig 42 II). They have been deposited as large middle moraine-tricornes. Ice marginal ramps as characteristics of semi-

arid foreland glaciation have also been described in detail from other areas of Tibet (Quilian Shan and Kun Lun) as well as for the Zagros Mountains (Iran), from Alaska, and from the subtropical Andes (Aconcagua Group) (Kuhle 1984, 1987a, 1989). Here, too, they form a combination of moraine diamictites and stratified outwash deposits. Ice marginal ramps tend to have surface inclines of 7–15° (Fig 41 —; Fig 42 —) their fringes consist of several terraces of moraines and paraglacial formations which were once bordered by progressively melting and retreating generations of glacier tongue surfaces (Fig 42 III, IV etc.). This regressive development can be traced back down to the recent glacier tongues at the foot of the mountains (Fig 42 ×). Towards the mountains the ice marginal ramps accompanying the basins of the glacier tongues outcrop into the air (Fig 41 ◀◀; Fig 42 left of II; Fig 40 behind I). The tongue basins of adjacent ice flows coalesce on the edges (Fig 2, no. 26). The sudden decrease of the pushing force of the ice where the glaciers issue from the steep mountain slopes upon an open foreland plain is essential to the formation of IMRs. The glaciers spread over a large area here. Considerably reduced in consequence, the oscillations of the glacier fringes led to relatively stable locations of ice margins with polygenetic sedimentation of heaped diamictites and outwashed moraines from the meltwaters. More or less well sorted, the re-deposited psamites of the latter are laid down on the outer slopes of the terminal moraines. They were transported down the ice marginal ramps into the foreland (Fig 41 —). The ice marginal ramps, which contain Shisha Pangma eye-gneiss blocks up to the size of a room, and some of which are well-rounded components, have dark phyllites at their core. It was surrounded by glacier ice and buried in a bed of moraine and outwash material (Fig 40 ▼ shows the locality of an outcrop).

The surface areas of the ice marginal ramps are now the scene of macroforms of solifluction. Apart from large block flow tongues on the steeper slopes, there are macro-structural frost patterns with diameters of 1–2.5 m (Fig 42 ▼ shows one of the localities). This takes place more than 1000 m above the permafrost line, which is established at 4600 m through the presence of pingos near the Paiküco (Peiku Tso) (Fig 2, no. 27).

#### *Further indications of prehistoric glacier covers in the northern and eastern Shisha Pangma foreland*

Glacier termini (the altitudes of the final position of their tongues) and their ELA-depressions from the pre-Ghassa stagnations (● 1/2) of the early part of the Late Glacial to the Neo-Glacial (V, VI) and historic (VIII–X) glacier locations (the latter are concentrated in the example of the prehistoric Yepokangara glacier) are given in the table (cf. Fig 40; Fig 42; Fig 2, no. 26). The glaciated massive-crystalline knobs which rise





Fig 45 The S Tibetan high plateau N of Nylamu (Fig 2, No. 31;  $28^{\circ}19'N$   $86^{\circ}03'E$ ) seen towards the N from 4800 m; in the left middle ground the irrigated cultivation of the Bo Chu cut down to 4300 m; (●) the roche moutonnée country of the 5200 m Sho La plateau (Sho La pass 5060 m Fig 2, No. 30). This completely glaciated (at the glacial maximum) area is characterised by the post-glacially formed frost debris slopes (periglacially frost smoothed slopes = Glatthänge ↓ and foreground). These forms are a function of the easily weathered metamorphosed sedimentary rocks. Photo: M. Kuhle.

between 5000 and 5250 m or 5300 m ( $28^{\circ}40'N/85^{\circ}47'E$ ) have already been mentioned above (Fig 2, N of no. 26). They present high continental frost-weathering and exfoliation along relaxation joints. Although these destroyed glacial striae and polishings, they did not affect the classically-fashioned form of the glacial knob (Fig 42 ↓).

Further E ( $28^{\circ}40'N/85^{\circ}58'E$ ) there are kame-like deposits running W to E in the area of the Kolmangcheng Hu valley (ONC 1:1,000,000 H-9), which ends in the Mankopa valley in the E (Fig 2, no. 28). Only a few kilometres long, these small-scale gravel ridges consist of very well washed gravels (hard, non-stratified crystalline rocks) and can be regarded as sub-glacial esker-like deposits. The five steps of the gravel ridge terrace, ranging in height from 2–3 m (1) to 5.6–7 m (2), 12 m (3), 35 m (4) and 100–120 m (5) present a secondary undercutting of what was originally a homogeneous sub- or paraglacial gravel body. Corresponding gravel deposits in the form of terraces flanking a valley are to be found to the true left of the 4550 m high gravel floor of the valley. Kame terraces have also been preserved at the openings of small hanging valleys on the true left about 27 km outside the valley ( $28^{\circ}48'N/86^{\circ}09'E$ ) (Fig 2, no. 29). They are situated 150–250 m above the Mankopa river. Deposited inside the banks of the main Mankopa valley glacier (minor flow), these deposits are *so recent* that they have not yet been cleared out by the

streams of tributary valleys. They have not even been cut down to base-level. These are post-High Glacial or Late Glacial accumulations, and evidence of an already considerably lowered ice-level. The glacial knob-like rounding at all levels of the valley flanks is evidence of glaciation which covered the entire relief during the High Glacial period. In this case it is the outcrop curvatures of sedimentary rock which have been preserved in their glacier-polished state. These indications make it likely that the Mingchü Ho (valley N of the Mankoyang massif; ONC 1:1,000,000 H-9), as well as the Tingri basin, which lies 100–150 m deeper down, were filled with ice (see above).

The upper catchment area of the Mankopa valley is a 4900–5300 m high plateau, which is dissected by several shallow valleys, leading to the Jalung Sho La (pass at 5060 m) (Fig 45, background). The plateau (centre:  $28^{\circ}35'N/86^{\circ}11'E$ ) forms the watershed for the Bo Chu (the upper Sun Kosi), the Himalayan transverse valley draining southward. Everywhere on the plateau slopes between 4500 and 4800 m there are exposed remnants of gravel bodies and gravels layers with thicknesses varying from 5–10 m. In the bowl-shaped valley sources on the S slope, for instance, and down to the Bo Chu they are dove-tailed with rough block moraine covers (Fig 2, no. 30) ( $28^{\circ}30'N/86^{\circ}10'E$ , 4800 m asl). They have the character of ice contact stratified drift of the Late Glacial period. At the altitude of 4900 m well-rounded erratic blocks of up to 1.2 m in length may be found. A local ice-cap, or plateau glacier, had evidently remained on the plateau. Triangular in outline, its glacier tongues overlapped into the peripheral valleys from all sides. Lack of thrust from the ice led to deposited end moraines or outwashed glacial sediments in the form of alluvial cones. Whilst on the plateau chalks, chalk-marls and lightly metamorphosed rocks came to the surface, these ramps consist of well-rounded gravel with quartzite, granite and gneiss components. They are the substratum of repeatedly shifted allocthonous moraine material (Fig 2, no. 30). Other than glaciogenic interpretations of the gravel would require the assumption of a complete infilling of the valleys on which they occur to a thickness of several hundred metres. However, this would contradict the mass-balance between the relatively small catchment area available for the processing of scree and the considerable quantity required for the filling-in of the relief. Sedimentary rock at about 4900–5100 m on the plateau is superimposed upon by ground moraine covers of unstratified, crystalline erratics, several metres in length, that have been transported here over considerable distances (Fig 2, no. 30). They can be observed from the track to Nylamu.

Cut down a few hundred metres into the plateau, the curving box valleys or troughs with wide valley floors are typically glacial. They may be compared with valleys in the sedimentary rocks of Spitzbergen (Kuhle 1983b).



Fig 46 Southern Tibet with Tibetan Himalaya N of Nylamu (Fig 2, No. 31; 28°17'N 86°02'E) looking up from 4850 m towards the E. The valley was completely glaciated (----- glacier level). This is shown by the glacial scouring and roches moutonnées (●). The trough-like box valleys formed then from the easily eroded metamorphosed sediments were strongly modified by deposits from gullies and stone chutes (↓). Photo: M. Kuhle.

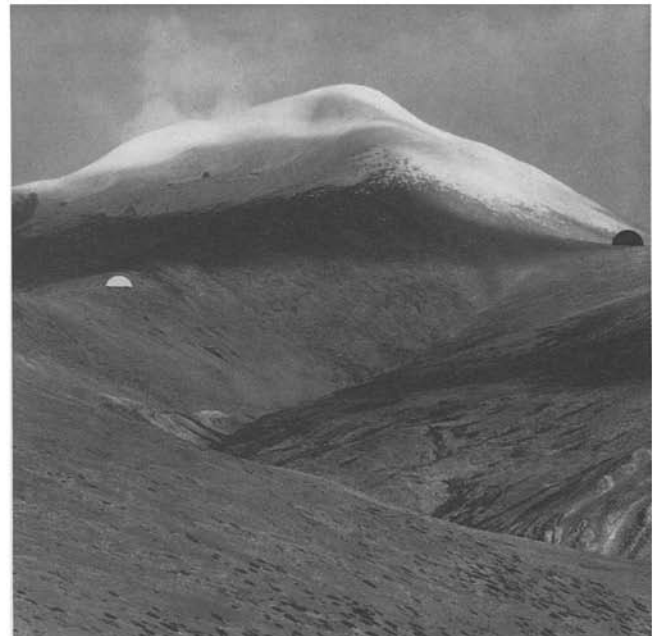


Fig 47 S Tibet, Tibetan Himalayas N of Nylamu with a 6652 m massif (28°18'N 86°20'E; Fig 2, No. 31) seen from c. 5050 m towards the E. The peak carries recent glaciers related to an orographic snow line (equilibrium line altitude) of more than 6000 m. A depression of this line by only 400 m would easily cover the whole area with glacier ice. The scoured transfluence passes (●) indicate a maximum glaciation ice thickness of more than 1000 m related to a depression of the equilibrium line of about 1200 m. Photo: M. Kuhle.

Sub-glacial melt-water erosion is likely to have played a part in their formation, too (Fig 2, no. 30).

The character of the landscape in the area of this plateau and its S slope (Fig 45, Fig 46) is altogether similar to that found in the central areas of Spitzbergen (cf. above), as for example in the sedimentary rock plateaux of Dicksonland (79° N). They, too, have been superimposed upon and shaped by a more than 1000 m-thick inland ice cover during the High Glacial stage (Kuhle 1983b; Troitzky et al. 1979; Boulton 1979). Built up by more or less concordantly bedded sedimentary rocks (sandstones, quartzites), the plateau area is topped by 100–200 m-high, almost scree-less glacial knobs (Fig 45 ●). In the depressions the bedrock is superimposed on by ground moraine boulder clays and in the valleys periglacially smoothed slopes (congelifluction slopes) have developed. They consist of amorphous congelifluction scree covers (Fig 45, foreground), which are interrupted by more resistant outcrop steps (Fig 45 ↓). It is worth noting in this comparison that, after great similarities in their glaciation history, their conformity is primarily based on petrographic foundations. Apart from that an oceanic-arctic climate of freeze-thaw cycles contrasts with a high-continental subtropical one. Not the geomorphology, but the denser plant cover (tundra, dwarf bush heath) as well as the more frequent patches

of perennial snow of the corresponding altitudinal level in the oceanic Arctic, mark the difference whilst precipitation totals (200–300 mm/year) are the same (Fig 45, 46).

A glaciation of this plateau between the Longlonqu river in the N and the Keya river (near the Yali settlement in the upper Bo Chu) in the S requires a lowering of the equilibrium line by at least 800 m (from 5900 to 5100 m). However one must take into account the fact that in pre-glacial times the plateau was situated at a higher level than now (cf. above). The greater altitude of the surface of the ice domes makes it likely that *deglaciation* took place only when the line of equilibrium rose to a level which differs by a mere 600 m from its present location. This points to a deglaciation of this plateau area at about 15–20 Ka BP.

*The prehistoric glaciation of the Bo Chu (Bote Chu, Sun Kosi) and its tributary valleys (Sisha Pangma group's E and SE slope; W flanks of the Rolwalling-Himal and the 6652 m high massif further N in the Tibetan Himalaya: 27° 52' N–28° 30' N/85° 50'–86° 20' E)*

From the 6652 m high massif (28° 18' N/86° 20' E; Fig 47) to the vicinity of the main valley floor (Bo Chu)



Fig 48

Looking down an E tributary valley of the Bo Chu towards the W from 5350 m (Bote Chu, S Tibet 28°20'N 86°07'E Fig 2, No. 31). The glacier level (---) shows that at the glacial maximum the whole area was filled with a network of ice streams. Transfluence passes (▲) in many places were formed by the thick ice masses. Lateral (▼) and end moraines and ground moraine (x) deposits remain from the glacial stadia of late-glacial, neoglacial and historical times. Photo: M. Kuhle.

valley glaciers, probably early Late Glacial, and at most 9 km long, descended in a W direction to about 4100 m asl (28° 17' N/86° 01' E); (Fig 2, no. 31). The sole evidence of this ice stream are the at most 120 m high terraces of lateral moraines (Fig 48 ▼ ▼). With a mean altitude of 5800 m for the catchment area, the orographic equilibrium line is calculated as lying at 4950 m (Tab 1). In this instance the lower of the two ice margin locations was computed. A higher one happened to lie 1 km further up-valley at an altitude of 4250 m, and would have corresponded to an equilibrium line c. 75 m above the first one. Corresponding deposits of ice margins also occur in the S parallel valleys, as well as to the W of the Bo Chu on the E slope of the Shisha Pangma massif.

Now separated from the three recent, up to 3.7 km long, glaciers in the NNW-facing source basins only by neo-glacial or historic dumped end moraines, these glacier locations were classified as belonging to the High Glacial by Zheng Benxing (1988). This is like describing the openly wooded terraces of the lateral moraines of the middle Arolla valley and Zinal valley, or the glacial deposits near Täsch and Saas Grund in the Valais (Alps), as belonging to the High Glacial period because for tens of kilometres there are no marked moraines – or none at all to be found in the large main valley, the Rhone.

Similarly to the alpine region mentioned above, the entire relief had been filled with glaciers to at least 1000 m above the bottom of the main valley. Evidence of this is found in, for instance, the rounded 5030 m-high transfluence pass (28° 20' N/86° 07' E) of the aforementioned valley to the adjacent one further north (Fig 48 ▲). There are distinctly polished flanks and rounded valley shoulders in many places (Fig 46, 47, 48 ▲, ---). Due to the splintering frequently encountered with metamorphics, and to the frost weathering, well preserved polishings on the flanks are rare. Nonetheless, they

have been preserved in the main valley (Bote Chu) at 4300 m asl (Fig 2, no. 31). Fundamentally speaking, this section of the Tibetan Himalaya presents a large-scale landscape of glaciated knobs, of which morphologically speaking the most foreign element is linear and fluvial lateral erosion (Fig 46, 47). If it had been effective throughout the Quaternary in its present intensity, there would now be a steeply-shaped landscape of pointed ridges, steep rock flanks and narrow V-shaped valleys with long stretches of gorges and walls much cut up by the action of water. 10,000 years after deglaciation these form elements already contrast with the periglacial macro-forms conforming to glacial geomorphology. Even small, periodic funnels without catchment areas worth mentioning in precipitation areas of only 150–300 mm/year have since cut deeply into the bedrock once the mantle rock of the practically vegetation-free slopes had been removed (Fig 46, ↓ ↓).

Following up the history of the Late Glacial glaciation further down the valley reveals the tongue basin of the Tsangdong (Fig 2, no. 32). The Tsangdong settlement (28° 15' N/86° 01' E) is located on the valley floor at about 3750 m in the Bo Chu. At Late Glacial times the main valley glacier received its chief supply of ice by way of the Keya valley (confluence of the Bo Chu (28° 22' N/86° 04' E)). It descended from the highest catchment areas of the Shisha Pangma E flank, which must be put at 7100 m asl. The Tsangdong tongue basin is probably as old as the lowest moraines of the W slope of the 6652 m high massif (Fig 48 ▼ ▼); the comparable geomorphological state of preservation also seems to indicate this. A somewhat more recent and less representative glacier tongue basin is situated in a valley chamber about 7 km upstream from Tsangdong at 4050 m (Fig 2, no. 32). It must be regarded as the more recent one of the two Late-Glacial stages occurring on the 6652 m massif (Fig 48 × ×).

Both of the tongue basins are characterized by their more recent stratified drift (outwash plain) fillings. They function as sediment traps and retain the glacio-fluvial washed drift of the immediately preceding stage. During further glacier retreats they were cut up into terraces.

Large terminal moraines were pushed from the mouths of two tributary valleys on the true left into the tongue basin of the Tsangdong (Fig 2, no. 32; 28° 13' N/86° 01' E and 28° 17' N/86° 04' E).

These indicators of ice margins also belong to the Late Glacial system (more recent than the Ghassa Stadium (I)). With the help of the indicator of the relative dating of red-weathering at comparable altitudes above sea-level, the echelons of lateral and end moraines at Nylamu (Nyalam, Fig 2, no. 33), which occur as far down as 3670 m (Fig 49) can be regarded as parallel in time to those of Tsangdong. Pushed out from the Fuqu valley as far as into the main valley (Bo Chu) (28° 06' –09' N/85° 58' –86° 00' E) these diamictites extend up to 3900 m and contain blocks up to the size of houses (Fig 49 ● ●). There is no marked humus stratum, so that the moraine surfaces must have weathered under cold-semi-arid climatic conditions during the Holocene. The abrupt climatic division towards the monsoon-humid Himalaya S slope occurs 5 km up-valley from Nylamu. The tongues of the recent and some 14 km-long Nylamu Phu glacier (Fuqu or Shisha Pangma SSE glacier) and the 7 km-long glacier at the foot of the wall, which flows down an E parallel valley from the Shisha Pangma, are 21 and 23 km away from the Nylamu stadium and more than 1000 m higher. The equilibrium line at about 5400 m (Tab 1, 5385 m) for the Nylamu stadium is evidence of an ELA-depression of 500 m. This corresponds, to a rather small equilibrium line depression on the Himalaya S side for the Late Glacial (cf. Kuhle 1982, 1987a). Even the moraines of the Nylamu stadium the author would possibly attribute to the Sirkung or Dhampu Stadium (III of IV; Kuhle 1982) (Late Glacial) Zheng Benxing (1988) places in the middle Pleistocene. Absolute datings have not been obtained up to now.

In the valley chamber of Nylamu still more, and substantially higher, walls of lateral moraines begin. They are particularly well preserved on the true right-hand side (Fig 49 ■ ■; Fig 2, no. 33). Like the moraine material deposited further up-valley, they are characterized by angular, round-edged, or rounded block components. The moraines are completely covered with green meadow vegetation; their petrography is akin to that of the moraine from the Nylamu Stadium; the polymict composition of blocks include varieties of gneiss including eye gneiss and varieties of granite. There is thus evidence of the Shisha Pangma catchment area belonging to this older glacier stage. These lateral moraines correspond to the end moraine which closes the valley chamber of the Choksum (Shü Shang) settlement at 3380 m asl 5 to 7 km down-valley (28° 06' N/86° 00' E, see Tab 1). The end moraine juts out from the true right-hand valley flank (from the W) towards the deepest

point of the valley (Fig 2, no. 34). The stage is to be regarded as the Taglung or Dhampu Stadium (II or III), and thus as being from the Late Glacial period. Compared to its present position the equilibrium line was depressed by about 650 m. The extreme steepening of the Bo Chu valley profile (Bote Chu or Sun Kosi) sets in between Choksum and Nylamu where the Fuqu or Nylamu Phu valley ends. Above this steepening, e.g. in the tongue like basin of Tsangdong, mud-flows, along with alluvialfans, are reshaping the moraine landscape, whilst below the glacial forms are modified by substantial linear incision (Fig 50). Barrier mountains below Nylamu mark the old level of the valley floor. Glacial polishing had rounded their tops. They received their finish as late as the Late Glacial and are accordingly well preserved, glaciated knobs (Fig 49 ▲). All the post-Glacial slides and mud-flow activities are swallowed up by the very deeply incised valley long profile which continued its formation during the sub-Glacial period, and subsequently rapidly removed by the ample waters of the Sun Kosi river and distributed tens of kilometres further down the valley. The mudflow event on August 28th, 1983 is an example of such a discharge. Caused by a moraine lake in a tributary valley on the true left of the Bo Chu at an altitude of more than 4800 m asl, it killed more than 100 people. It reached the main valley at about 3000 m and proceeded another 2000 m further down. Covering a vertical distance of about 4000 m, cut through the track of the mountain road in two places and destroyed the large suspension bridge (the Friendship Bridge) 20 km down-valley.

The main valley gradient (Bo Chu) over 30 km equals a 2000 m height loss; this explains the enormous tractive powers in the prehistoric valley glacier. They had the effect of polishing the floor much more intensively than the polishing on the flanks which led to the formation of a trough-shaped gorge, or – depending on the intensity – a gorge-shaped trough (Visser 1938, Vol. II p. 139; Kuhle 1983a, p. 155 et seq.). The glacial formation of this valley section is established through the frequently concave profile of the flanks in the gorge, which have been smoothed by glacial polishing (Fig 51 →). The crumbling away of the rock (Fig 50 ◆) and even larger rockfalls have occurred frequently. They are presented here as outcrops of the Khumbu and Kathmandu covers (KU 1–3, KN 2, 3) which consist of gneiss metamorphics (Hagen 1969, p. 129) and slope northward at 20–35° (20–35/10). Obsequent or, respectively insequent in its course, the valley tends towards a V-shape profile, thanks to the structure of its rocks and the collapse of undercuttings induced by crevices. Having reached down to at least 1600 m, that is to the present Kodari settlement (27° 56' N/85° 56' E) (Tab 1) this High Glacial valley glacier remained with its tongue below the equilibrium line (4450 m) for 22 km. The end of its tongue was about 2800 m below the ELA. It follows that the meltwater was able to cause sub-glacial erosion over the same distance. With a surface

Fig 49

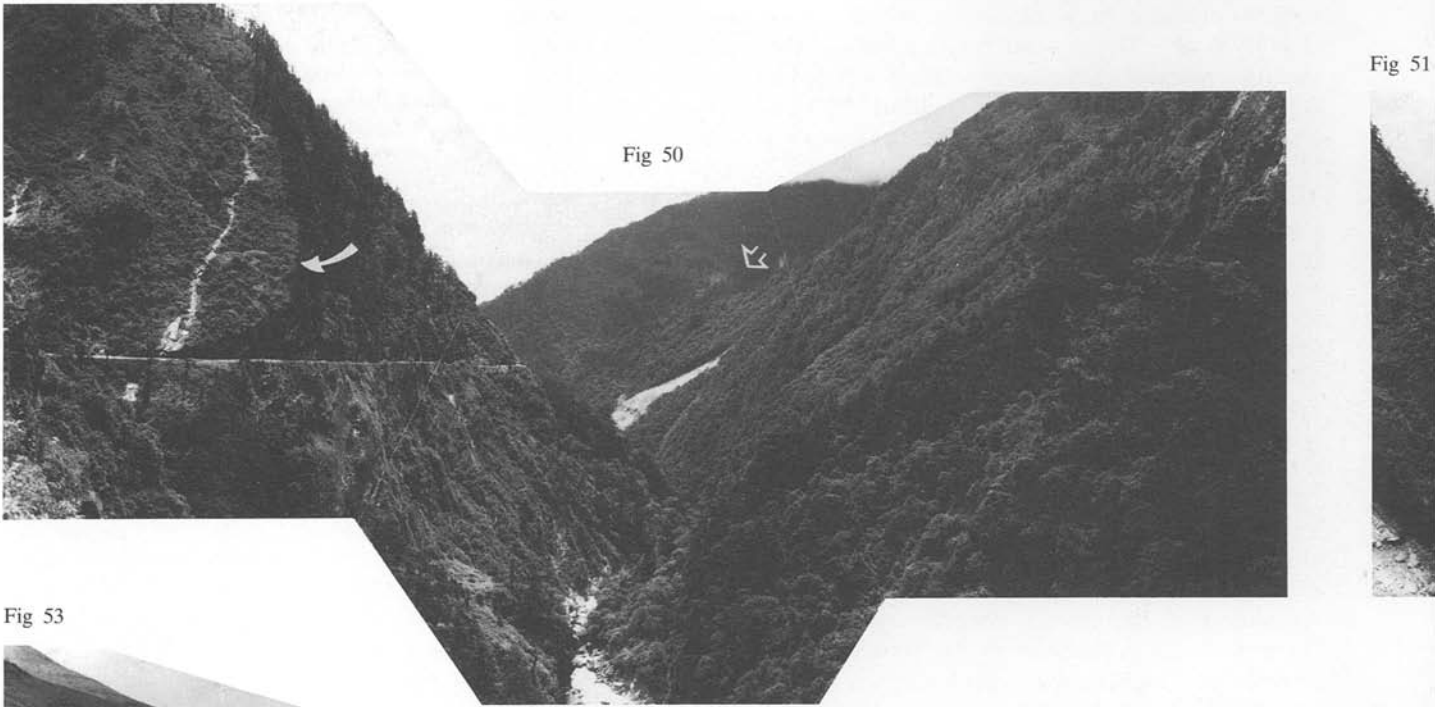


Fig 50

Fig 51

Fig 53





Fig 52



Fig 49

An area of lateral moraines (■●) by the settlement of Nylamu in Fuqu Chu (Fig 2, Nos. 33, 34). View from 3690 m towards the SW (centre of panorama) in the area of the Bo Chu-(Sun Kosi-)transverse through the Himalaya main range. The glaciers from the SE Shisha Pangma (Fuqu glaciers) formerly flowed together in the Fuqu valley (Nylamu valley) and even in the late-glacial reached (■) the Bo Chu main valley (■ well to the left and ▲) and thus the previous Bo Chu glacier. Fig 2 shows (Nos. 33 and 34) the course of the lateral moraines in the valley system. A few kilometres below the confluence of the Fuqu and Bo Chu valleys the glacial accumulations set out due to the steepened relief (well left in the background). Thence far into the S side of the Himalaya lateral scouring and roches moutonnées (▲) indicate the extent of the glaciation at the maximum (Fig 50, 51 and 52; Fig 2, No. 35). Because of the content of the augengneiss and granite these montane moraines are poor in fine material and contain coarser components (● well to the right, outcrop). Photo: M. Kuhle.

Fig 50

The glacially produced gorge of the middle Bo Chu where it breaks through the main Himalaya seen looking southward down the valley from 2700 m (Fig 2, between No. 34 and No. 35). The erosive force of the steeply downhill-flowing maximum glaciation glacier resulted in bottom erosion exceeding lateral scouring. This resulted in a slightly trough-shape concavely scoured V-shaped valley. At the same time at 1500 m below the equilibrium line altitude (snow line) the subglacial melt-water had enhanced erosive force which exaggerated the V-shape. (♣) marks a typical rock fall of post-glacial origin. Photo: M. Kuhle.



Fig 51 Looking up the Bo Chu from the same viewpoint as Fig 50 (28°02'N 85°59'E; 2700 m). (↓) shows the concave scoured slopes of this glacial gorge-like trough. Both contemporaneous and later rock falls account for the roughness of the rock walls (▶▶). Photo: M. Kuhle.

Fig 52 Ravine in the valley floor of the gorge-like trough of the lower Bo Chu or Bote Chu (Fig 2 No. 35) at 1900 m. This ravine with almost straight right-angled walls with later rock falls (↑↑) is cut into the glacially scoured rock floor of the valley (▲). It follows a fault shatter zone. The incision resulted from erosion by subglacial meltwaters under hydrostatic pressure and continues today subaerially. Photo: M. Kuhle.

Fig 53 The Dzakar Chu seen downwards towards the N from 4450 m (Fig 2, No. 36; (28°23'N 86°57'E)). This box-like valley is a trough with a wide outwash-gravel-filled bottom. The valley slopes of metamorphosed sediments are completely rounded up to the inter-valley watershed by glacial scouring (▲▲) (cf. Fig 54). (↓) the settlement Zambu; behind is a similar glaciated relief. Photo: M. Kuhle.

split up by crevasses and ice-falls, the steep glacier tongue had the effect of a very immediate discharge of meltwater from the ice surface to the rocky floor of the valley. As a result of the hydrostatic pressure of the intraglacial water column there was a very intensive erosion and deepening of the valley floor (Tietze 1961). This was further intensified by cavitation corrosion. Easily visible remnants of slickensides show that the Sun Kosi follows a fault which facilitates linear erosion. This permits an explanation of the bipartite cross-section of the Sun Kosi: beneath a trough-shaped gorge profile (gorge-shaped trough) there is an acute and c. 40–100 m deep gash-like cut with almost parallel steep flanks (Fig 52). They form suggestive working edges towards the hanging glacier bed (Fig 52 ▲ ▲). Glacigenic polishings on the upper metres of the gorge and further down into it are evidence of the simultaneity of glacial erosion in the upper section of the profile (Fig 52 above ▲ ▲) and meltwater erosion in the lower one (Fig 52 below ▲ ▲). As a matter of fact the two associated processes are linked in the way of a geomorphological sequence. The sub-glacial erosion through meltwater precedes the glacial polishing. It prepares the detraction and detersion carried out by the glacier by way of renewed resistance to attack, thus making glacigenic deepening come to the fore instead of flank polishing. The gorge-shaped trough profile is therefore not only to be attributed to the considerable gradients of the long profile, but also to sub-glacial meltwater erosion.

Breaks in the compactness of the glacigenically polished flanks are due to petrographic factors. In places where gneiss covers alternate with soft two-mica phyllites, the ample monsoon precipitation causes recent slate slides and mudflows. These expose the hard strata and destroy the road track every year. This may, for example, be observed on the true left-hand flank down-valley from the Damu border station at 1900 m asl (cf. Fig 50 ▼).

The lowest unambiguous glacigenic polishings reach the location of the Friendship Bridge at about 200 m above the valley bottom-line, so that it was possible to reconstruct a terminal position for the glacier tongue at 1600 m (see above Fig 52 ▲). A c. 100 m high terrace of sorted pebbles and diamictites, which must be interpreted as a kame-like paraglacial formation confirms the altitude of the ice margin positions. The orographic equilibrium line is calculated as being at 4450 m asl, the climatic equilibrium line at about 4310 m. These values are about 260–485 m higher than those in the Dhaulagiri and Annapurna parts of the Himalaya some 200 km further W (Kuhle 1982, p. 152). They are regarded as belonging to the last High Glacial period. There are no preserved glacier locations between this, the lowest ice margin position, and the one near Choksum (Shū Shang) which are considered as belonging to the Late Glacial stages II and III (Taglung or Dhampu Stadium). The Taglung or Ghasa Stadium (II or I) and the two pre-Ghasa stagnations (●<sup>1/2</sup>) are likely to have been cleared out completely on account of the steep and narrow contours of the gorge (Fig 50, 51). In the cross-section of the valley at Damu (27° 59' N/85° 58' E) the Sun Kosi flanks are well marked by steep "bottleneck" corries with small and well-rounded barrier mountains (glaciated knobs), which occur as far down as 3500 to 3300 m. They are evidence of a depression of the ELA on the Himalayan S side to well below 4000 m (to c. 3700 m). Due to the inaccessibility of the very steep, wall-like and densely wooded (*Tsuga dumosa*, *Abies spectabilis*, *Rhododendron lepidotum*) valley flanks it proved impossible to establish whether all the remnants of loose rocks preserved in the runnels of the walls are ground moraines or lateral moraines which have been infilled, or scree from the flanks that got stuck in the long profile. On the true right-hand at about 3300 m asl, c. 300 m above the valley bottom-line of the Bote Chu gorge there is polymictic moraine material which plugged a tributary valley (28° 02' N/85° 59' E).

An estimation of the minimum age of the glacigenic forms that have come down to us requires the forced dynamics in the recent mudflow gullies to be taken into account. The humid monsoon climate, together with the melting of the snow, the vertical distance and the absolute altitude of the catchment areas with their prehistoric moraine deposits which can be moved down, all combine to form ideal conditions for these dynamics. Hanging valleys and high altitude basins of prehistoric tarns and nivation niches give way to runnels and gullies. Their steep floors contain mudflow tunnels which are like bottlenecks, U-shaped with cross-sections of 5×20 m. Fresh abrasion levels on the rocks are evidence of mudflow passages up to a depth of 4–5 m in the cross-section, and evidently resulted in considerable corrosion effects. If a body of mudflow suspension comes to a halt in such a tunnel, i.e. does not reach the lowest level of the main valley, the fine material is washed out by the stream. This includes gravel and coarse valley



Fig 54 The Dzakar Chu seen looking upwards from the same valley cross profile as Fig 53. The overwhelming maximum glacial ice cover of this area has led to a considerable valley-wards extension of this roche moutonnée landscape (●●). The comparatively meagre remains of moraines (▼▼) in relation to the appreciable glacial erosion recalls the relationships in the Scandinavian mountains where erosive forms also dominate. Photo: M. Kuhle.

train. However, very large blocks stay where they are and block the landslide runnel. They dam up finer materials or are worked free from beneath by the stream. The tunnel exits of particularly active mudflow passages retreat from the main valley back into the flanks. This is evidence of post-glacial erosion amounting to several tens of metres.

The former Glaciation of the North Slope of Mount Everest from the Rongbuk Valley down to the Middle Dzakar Chu (upper Bhong Chu or Arun Valley;  $28^{\circ} - 28^{\circ} 26' N / 86^{\circ} 38' - 87^{\circ} 15' E$ )

The following comments continue the discussion above (p. 11) on the area N of the Pang La massif. In 1984 the author had had the opportunity of proceeding with investigations up-valley of the Dzakar Chu, starting at the Tushidzom settlement. In the valley cross-section of the settlement, which crosses the 4200 m isoline there are no glacial deposits whatsoever. It is a "box" profile with a kilometre-wide valley train floor, and a flat alluvial fan poured out from the Nyomdo valley provides security from floods for the dwellings and fields of Tushidzom. Here the valley is not dissimilar to the Rhone valley profile at Siders (Valais, Alps), though much more arid. Glacial formations on the valley flanks are not clearly identifiable. The metamorphic bedrock and the heavily folded, flysch-like sedimentary rocks have been broken up into crags, i.e. rock heads and ribs. Post-glacial talus slopes follow on below. Some remnants of lateral moraines have been preserved on the true left hand, about 18 km up-valley at an altitude of about 4350 m and 100 m above the valley train floor (Fig 2, no. 36). The corresponding position of the ice margin may have been situated tens of kilometres outside the valley and has so far escaped reconstruction. (Investi-

gations in the lower Dzakar Chu and Arun valleys are planned for 1989). The extrapolation of a hypothetical Dzakar glacier from these moraine findings, which stretched down to 4180 m, would produce an equilibrium line depression of about 350 (345) m, as opposed to the recent orographic equilibrium line of the Rongbuk glacier system at 6235 m. Taking into account the thermo-dynamic upper limit of the glacier, the ELA runs at 5910 m (Kuhle 1986a, b) (Tab 1).

The estimation of the absolute level of the equilibrium line is difficult here in the Everest region, due to the adjacent catchment areas at very high altitudes – the mean being 7300 m asl – with their special conditions. The definitions of ELA depressions, however, are subject to consistent conditions and are, in consequence, reliable.

An ELA depression of merely 350 m is evidence of the at least recent Late Glacial age of the extrapolated ice margin position outside the Tushidzom valley. (Being too uncertain, i.e. only an extrapolation, it was not included in Tab 1). By comparison with conditions N of Shisha Pangma, a significant post-glacial uplift of the Dzakar Chu, the part of S Tibet that borders on the High Himalayas, must also be assumed here N of Mt. Everest.

There is no change in principle in the geomorphology further up the Dzakar Chu until the valley floor reaches an altitude of about 4500 m. Once again (Fig 53;  $28^{\circ} 23' N / 86^{\circ} 57' E$ ) the very wide valley floor between two steep valley slopes strikes the observer as characteristic, and not unlike those in the formerly ice-covered areas in the interior of West Spitzbergen (i.e. Sauriedalen and Lyckholmdalen in Dicksonland;  $78^{\circ} 27' - 78^{\circ} 45' N / 15^{\circ} - 16^{\circ} E$ ). There, in the Arctic, these valley floor fillings have been deposited near sea-level, i.e. close to the absolute erosion base. Here, in the subtropics, conditions for ample valley floor sediment-





Fig 55 The upper Dzakar Chu seen towards the SW from 4600 m (Fig 2, No. 37). The glacial scouring of the strata (▲) is remarkable insofar as under unglaciated conditions the layer-edges would have been decomposed to rock towers and gendarmes. The present day snow line (equilibrium line altitude) runs some 1000 m above the valley floor in this semi-arid part of S Tibet (outwash plain in foreground). Photo: M. Kuhle.

ation in a thawing-out (apering) region are comparable, thanks to the small gradient of the valley floor and the sedimentary rocks. From the confluence of the Gyachung Kang N valley with the Rongbuk valley ( $28^{\circ} 17' N/86^{\circ} 48' E$ ) to the Tushidzom settlement ( $28^{\circ} 24' N/87^{\circ} 08' E$ ) over a distance of 45 km, the valley floor drops by only 400 m. One ought therefore to imagine an ice-filling during the glacial period which stayed put in this S Tibetan valley grid and, due to a great deal of friction, displayed no impulses of discharge worth mentioning. It merely distributed the Pleistocene inter-glacial debris on the valley floors, but had not scoured it out in the way which is characteristic for steep relief.

One difference between this profile and other valley cross-sections of the Dzakar Chu further down the valley, however, is the much better state of preservation

of glacial fluvial polishings. The outcrops of more or less metamorphic sedimentary rock series have been preserved in their clearly polished, rounded form (Fig 53 ▲▲). They are evidence of a glaciation that included the entire valley. In some depressions remnants of moraines and para-glacial terrace deposits (glacigenic outwash alongside the lateral moraines) have been preserved (Fig 54 ▼▼). Established by lateral moraines or kame terrace remnants on both sides, the nearest ice margin was about 15 km down-valley of the Zambu settlement (Fig 53 ●) at 4380 m asl (Tab 1). It corresponds to an equilibrium line depression of c. 250 (245) m. (Fig 2, no. 36).

Further up-valley there is a glaciated-knob landscape of very large dimensions; its metamorphics with a concordant layer of congelifractions produce soft forms, which are evidence of a large-scale overwhelming of the relief by glaciation during the High Glacial period (Fig 54, 55 ▲). Now only 60 m high, a true right-hand terrace of lateral moraine at 4600 m basic height asl (Fig 54 ▼ left; Fig 56 ▼▼; Fig 2 no. 37) marks another, Late Glacial position of an ice-margin up-valley from the Zambu and Chöbuk settlements at 4550 m, and thus an ELA depression of c. 225 m (Tab 1). A corresponding moraine remnant is preserved on the true left in the exit of the Gyachung valley. Here again the glacier catchment area had been established by the N slopes of Gyachung Kang (7975 m) and Mt. Everest (8874 m). Its altitude is, rather comprehensively, given as 7300 m. Further up-valley it was only possible to reconstruct the glacier arm of the Rongbuk valley.

The next and more distinct end moraine is to be found at about 4780 m asl (Tab 1) in the uppermost Rongbuk valley chamber, up-valley from the bottleneck of the valley in the area of the confluence with the Gyachung-Kang N valley, 400 m lower than the recent terminus of the glacier tongue (5180 m). Evidence for it is provided by boulder clays with very large granite components. Considerable glaciofluvial remoulding has taken place, i.e. it has been integrated into an outwash



Fig 56 True right bank lateral moraine terrace (▼▼) in the upper Dzakar Chu (Fig 2, No. 37, 4600 m) seen looking E. These deposits were formed in the late-glacial around the end of a glacial tongue at 4550 m (equilibrium line depression c. 225 m). Post-glacial solifluction has smoothed the edges of the moraine and softened their bulges. Measurements show that periglacial debris movement on slopes such as this reaches 4–8 cm per year. Photo: M. Kuhle.

terrace on the true right-hand side (Fig 57). The calculated equilibrium line depression amounts to only 200 m. Apart from a likely post-Late Glacial uplift (see above), which is bound to lead to faulty calculation (to too small a value of ELA depressions) this position of the ice margin is about 12 km away from the recent glacier (Fig 2, no. 38). This extension of the glacier tongue can scarcely have been achieved by that small ELA depression of a mere 200 m. The de facto value may have been accordingly distinctly greater. As far as the Rongbuk settlement (monastery) no further lowest ice margin positions can be distinguished. Higher up, however, the valley slopes show accumulation ledges and traces of exarations which are evidence of relief-filling glaciation during the High Glacial like the polishing and scouring facets (glacigenic triangular slopes between the junctions of tributary valleys) which run high up on the valley flanks (Fig 58 ● ●). Post-Late Glacial morphodynamics are extremely intensive in this section of the valley. Quite apart from a nivally-induced periglacial formation, mudflows in tributary valley junctions are very active (Fig 58 ◆ ◆). Large mudflow cones within which extremely large blocks of polymict lateral moraine material was shifted, block the valley from the true right-hand, i.e. produce a chamber. Examples of this may be seen in the three mudflow cones 1, 3 and 6 km down-valley to the N of Rongbuk. All three of them at the exits of recently glaciated tributary valleys with catchment areas at altitudes of 6060–6260 m.

Before going into the question of the most recent prehistoric and probably neo-Glacial and historic states of the glaciers of the Rongbuk glacier system, the author would once more like to draw attention to the considerable glacio-fluvial transformation of the middle Rongbuk valley. At the same time though, the transformed end moraines concerned were not at all distinctly formed – if they existed at all. The cause of this was the direction of glacier discharge which changed during the Late Glacial stage from a prehistoric southerly to an at present northerly flow. The prehistoric ice-filling of the relief from an altitudinal ice-level of more than 6000 to 6500 m asl had consequently to spill over the passes W and E of Mt. Everest on to the S slope of the Himalaya (see below).

*Neo-Glacial and historic positions of the Rongbuk glacier (28° 09' – 12' N/86° 50' E)*

Fig 58 shows the succession of moraines from the most recent dumped end moraine (X–VIII) of the Rongbuk glacier tongue to 1.4 km up-valley from the Rongbuk monastery, where the upper neo-glacial end moraine forms a distinct arch (VI). Whilst stages X–VIII continue to hold dead ice and meltwater ponds and remain in contact with moving ice (◆), stage VI is 2.2 km away from the recent glacier terminus. The zone of dead ice and dumped end moraines (stages X–VIII)



Fig 57 The blocky-loam of the end moraines at 4780 m in the lower Rongbuk valley (Fig 2, No. 38) lies 400 m lower than the recent end of the Rongbuk glacier terminal tongue (Fig 58). The accumulation of granite blocks in the foreground is glaciofluvially modified and included in a younger glacial outwash plain (the terrace forms ◆). These outwash terraces are of neoglacial age (c. 4500–2000 years BP; cf. Fig 58, V–VI). The recent Rongbuk river flows 20 m below the terrace edge. The glacially rounded bosses in the background were maintained in shape by freeze-thaw action (periglacial) and covered with frost debris with a maximum thickness of one metre. View down-valley: M. Kuhle.

is about 1 km wide. The discharge of the meltwater from the recent glacier snout occurs about 1 km upstream of the dead ice tongue, thus dividing it from the glacier ice still on the move (Fig 58 ×). Between the outer slope of stage VIII (after Kuhle 1982: a more recent Dhaulagiri Stadium) and the inner slope of stage VI (older Dhaulagiri stage) a classic kame field (● ● ●) has formed. Having been built up from surface moraine which broke through the former basal ice, the conical kames are 4–10 m high. Even an esker-like subglacially formed remnant of a meltwater terrace, a 6 m high drift platform (Fig 58 ■), which extends in the direction of the valley, is part of the inventory of this tongue basin. The tongue basin is filled with more recent outwash material of the stages VIII–X (–4, –5), and of recent outwash deposits (–6), as well as with recent fans of mudflow and alluvial drift (◆). This resulted in the almost complete obliteration of rudimentary end moraines of an intermediate middle Dhaulagiri stage 'VII or an oldest more recent Dhaulagiri Stadium VII. 1.9 km away from recently flowing ice, this stage can be extrapolated by way of lateral moraines on the true left (Fig 58, 'VII or VII). They are submerged below that more recent drift deposit. The difference in basal altitudes from the recent

Fig 58

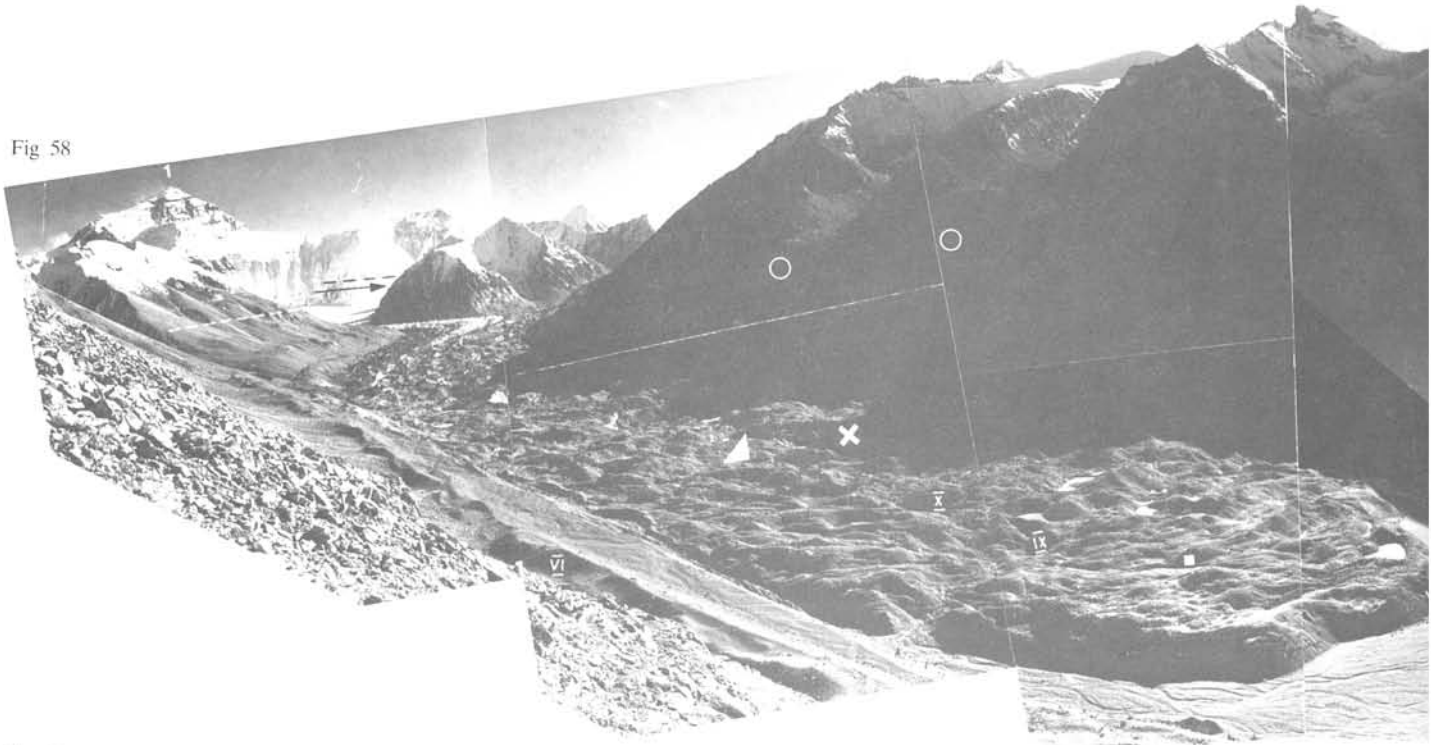


Fig 59

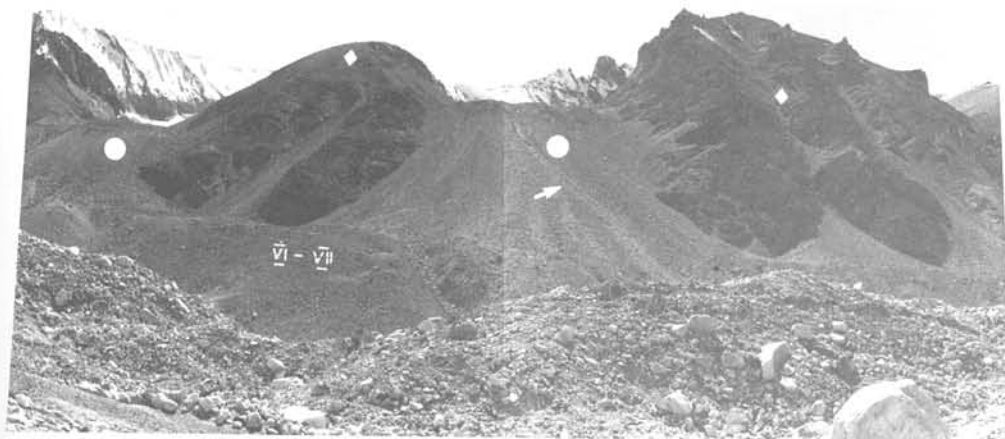


Fig 60



Fig 58 Panorama of the Rongbuk valley towards the S showing Mt. Everest 8874 m (No. 1; Fig 2, No. 40) above the almost 18 km long Rongbuk glacier. In front of it towards the right it is joined to its historical to neoglacial glacier tongue basin (VIII–VI). Towards the N down-valley lie the late-glacial moraines (III) (Fig 2, No. 38). Far right (▼▼) there stretches the mountainous area of S Tibet which was completely glaciated at the maximum. The glacier flow direction in this section of the Rongbuk valley has been completely reversed to the N today as compared with that to the S through the main crest of the Himalaya in maximum and late-glacial times (→). Photo from 5530 m; M. Kuhle.

Fig 59 Looking S from 5650 m from the confluence area of the Rongbuk valley with that of the Rongtö over the Rongbuk glacier to the left and the Rongtö glacier to the right. Mt. Everest 8874 m is at 27°59'N 86°56'E (No. 1). Both ice streams, with their considerable cover of debris, are in retreat. The significance of debris accession from the slopes above the glacier surface is clear. In a few thousand years the intense freeze-thaw climate of S Tibet is able to destroy the lateral striations of the valley sides (cf. Fig 60). Photo: M. Kuhle.

Fig 60 True left slopes of the upper Rongbuk valley near the central Rongbuk glacier (in the foreground; Fig 2, between No. 38 and No. 39). Pedestal moraines (●●) project from two parallel hanging valleys above the neoglacial to historical lateral moraines (VI–VIII; cf. Fig 58, ○○). The recent glacial ice traverses the upper 30 m of the pedestal moraine slopes as far as their edges. Thence the meltwater runs down in thin channels (↗) and forms a kind of sandr skirt or transitional cone (or very steep ice marginal ramp). The quantity of weathering debris on the intervening rock slopes (◆◆) is significant. Periglacial weathering is thus shown to be important even in the morainic deposits surrounding these relatively small glaciers. Photo: M. Kuhle.

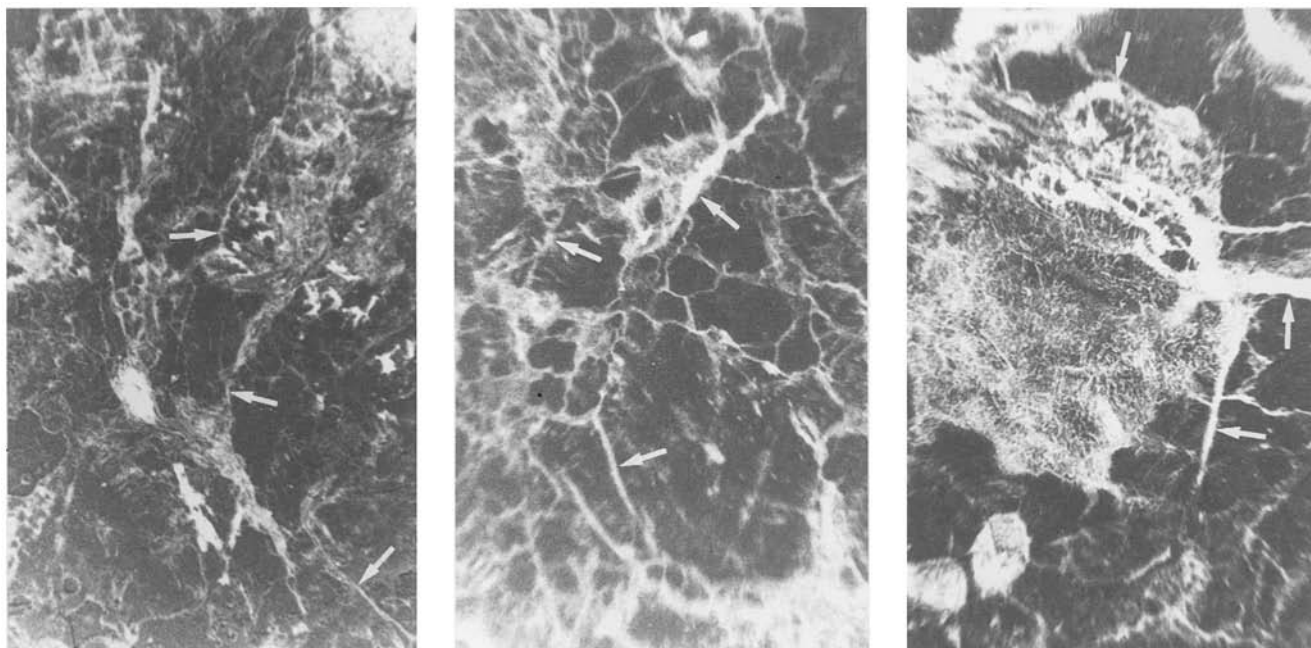


Fig 61 Thin section of a granite morainic block at 5200 m on the upper moraine of the Rongbuk glacier (Fig 58 ■ left; Fig 59 ■ left). The illustration is 4.1 mm long. The iron hydroxide veins on the bounding surfaces of the crystals (oriented along the cross-wires) are only detected in the microscope (—→). They are not visible macroscopically on the debris particles of the upper moraine which is only a few hundred years old; (cf. in contrast Fig 62 and 63). Laboratory photo: A. Heydemann and M. Kuhle.

Fig 62 and 63 Thin sections (1 mm long portions) of the same granite variety of moraine components as Fig 61, but from the 5650 m lateral moraine terrace of the Dhampu stadium (Fig 58 ■ right III; Fig 59 ■ right). The weathering period of at least 7000 years more in comparison to Fig 61 resulted in a macroscopically visible red colouration of the whole surface of the section. The veins of iron hydroxide on the crystal surfaces are appreciably broader (—→). Laboratory photograph: A. Heydemann and M. Kuhle.

glacier tongue to the position of the ice margin of stage VI is about 50 m (5180–5130 m asl). This allows a maximum equilibrium line depression of c. 25 m to be calculated for these historic to Neo-Glacial ice margin deposits. These strikingly small equilibrium line depressions are contrasted by ELA depressions of 280–470 m on the Mt. Everest S slope (Cho Oyu S slope, Kuhle 1987b, p. 205, Tab 2) during the past 2000 to 2500 years, or 150 m during the past 440 years. It is highly likely that this difference can be explained by the post-Late Glacial uplift of the Himalaya N side and S Tibet (cf. above). The glaciated Rongtö valley, which joins on the true left-hand, contains the corresponding moraine sequence to the main valley (Fig 58 VIII–X, VI). The recent glacier tongue of this c. 10 km long Rongtö glacier, with a maximum altitude of 7516 m for its catchment area terminates at 5500 m (28° 09' N/86° 49' E, Fig 59). The basis of the moraine surrounding the prehistoric tongue basin is at about 5410 m, so that the ELA depression is the same (Fig 59, VIII–X, VI). Terminating at a greater altitude in accordance with the lesser altitude of its catchment area (mean: c. 6550 m) the glacier of the tributary valley, like numerous other tributary glaciers of the Rongbuk valley system (Fig 60 ● ●), has aggregated a large pedestal or platform moraine with steep ice marginal ramps (IMR; continuous and transition cones;

Kuhle 1988) into the mouth of the main valley (Fig 58 ××). This platform moraine is situated 350 m above the main valley floor.

In comparison with the mass of glacier ice, the amount of debris collected for these platform moraines is uncommonly large; it is the effect of the increasing debris deposits of regressing glaciers (with a negative mass balance), which is a corollary of the increasing surface covering of such ice streams with debris. There is a cumulative concentration of debris in the valley glacier as it retreats in the course of centuries or even thousands of years (cf. below).

1.2 km down-valley of the Rongbuk glacier stage VI on the true right-hand lateral moraines of a stage V (Nauri Stadium) are preserved over a distance of 800–900 m. The Rongbuk monastery has been erected upon them. Corresponding lateral moraines have also been preserved on the true left-hand; both terminate in the same valley cross-section. Descending much more steeply, their upper edge (Fig 58 ↙ V) contrasts with Late Glacial lateral moraines of stages IV, III and possibly even II (Sirkung-, Dhampu- and Taglung stages), which continue further down the valley. The ice margin of the Nauri stage (V) lay at about 4950 m, c. 230 m below the recent altitude of the ice margin; this points to an ELA depression of 115 m.

*Some notes on the problem of dating moraines in the area of the Rongbuk glacier system*

There are no absolute datings. Due to the recent root penetration all the C-14 analyses carried out on the shallow soil formations beneath the meadow vegetation in altitudes of up to 5500 m failed, or indicated ages of only a few decades. In most cases it was possible to relativize these moraine ages geomorphologically or glaciologically as being too recent. Weathering permits a relative dating beyond the geomorphological method of dating moraines, which takes its bearings from succession, altitude above and distance from the actual body of ice. It was possible to establish at least two intensities of iron hydroxide formations with the aid of granite components on moraines (Fig 61–63). The Recent to sub-Recent, i.e. at most a few hundred years-old upper moraine of the Rongbuk valley glacier at 5200 m (Fig 58 ■ on the left) does not yet show macroscopically any iron hydroxide precipitation, and only very little microscopically (Fig 61 →). The moraine terrace at 5650 m, i.e. 450 m above the recent glacier surface in the same valley chamber (Fig 58 ■ right-hand), already shows distinct iron hydroxide colourings (Fig 62 and 63 →) and not only along the larger hairline fractures. The components of this moraine generation present a complete rust colouring, which is optically clearly visible when under the microscope. The location of these findings on the corresponding moraine terrace (Dhampu Stadium III) (Fig 58 ■ right-hand) is evidence that this weathering intensity is to be attributed to the middle Late Glacial Dhampu stage (III). A corresponding weathering intensity has been diagnosed with the help of thin sections of the very large eye-gneisses in the ice marginal ramps of the N slope of the Shisha Pangma (locality: Fig 40 III or IV), where the iron hydroxide formations continue from the grain boundaries far into the large albite-oligoclase and K-feldspar crystals (Fig 43 →). Near the surface the period of weathering may also have been at most about 9,000–15,000 years here.

Besides related or corresponding massive crystalline rocks (granite, gneiss), comparable edaphic conditions, which stand for the cold-arid climate of S Tibet, can be regarded as fulfilling the conditions for comparison of that sort. Comparisons were made between vegetation-free locations especially where there is no iron mobilisation by humic acids.

The geomorphological conformity of the entire moraine sequence from the neoglacial stage to the historic moraine formations on the S slope of the Mt. Everest group a mere 20–30 km away (Kuhle 1986d, 1987b) points to a greater age for moraine terraces IV and III than the 4000–4500 BP attributed to the moraines of the Nauri stage (V). These absolute age marks gained from the rich organogenic substratum of the S slope were ‘parallelized’ by means of the degree of corresponding geomorphological preservation and on the basis of the sequence of the moraine succession on the N



Fig 64 East Rongbuk glacier seen looking N down-valley from 6030 m. (Fig 2, halfway between No. 38 and No. 41). The viewpoint is on the medial moraine (●) between the confluent Changtse glacier and the main component of the East Rongbuk glacier from the NE slope of Mt. Everest (Fig 67, 68). The layer of debris protects the glacier ice from ablation so that the protected mounds (●) stand above the white unprotected ice (right); (cf. Fig 71, in contrast Fig 70). In the background (■) is an advancing corrie glacier. Photo: M. Kuhle.

slope. A study of the forelands of comparable glaciers proved to be useful for this. In terms of size and type the Rongbuk glacier is very similar to the Ngozumpa glacier, and therefore suitable for a comparison. The result is the following age sequence:

- Sirkung stage (IV) and older (Late Glacial) = older than 4000–4500 years
- Nauri stage (V) = 4000–4500 years
- older Dhaulagiri stage (IV) = 2000–2400 years
- middle Dhaulagiri stage (‘VII) = 2000 years
- recent Dhaulagiri stage (VII) = c. 440 years
- stage VIII = c. 320 years
- stages IX and X = less than 320 and more than 30 years old
- sub-Recent to Recent = less than 30 years old

Evidence of these stages is provided in Fig 58 and 59. A comparison of levels permits them to be traced in many places in the area of the Rongbuk glacier system, as for instance in the area of the E Rongbuk and the far E Rongbuk glacier confluence S of the 7071 m summit. During the deposition of the moraine in the Nauri and the older Dhaulagiri stages (V and VI), probably even well into the historic stages (‘VII–IX), the tongue of the small glacier in the hanging valley extended as far as the E Rongbuk glacier (Fig 64 V and VI). Downstream the

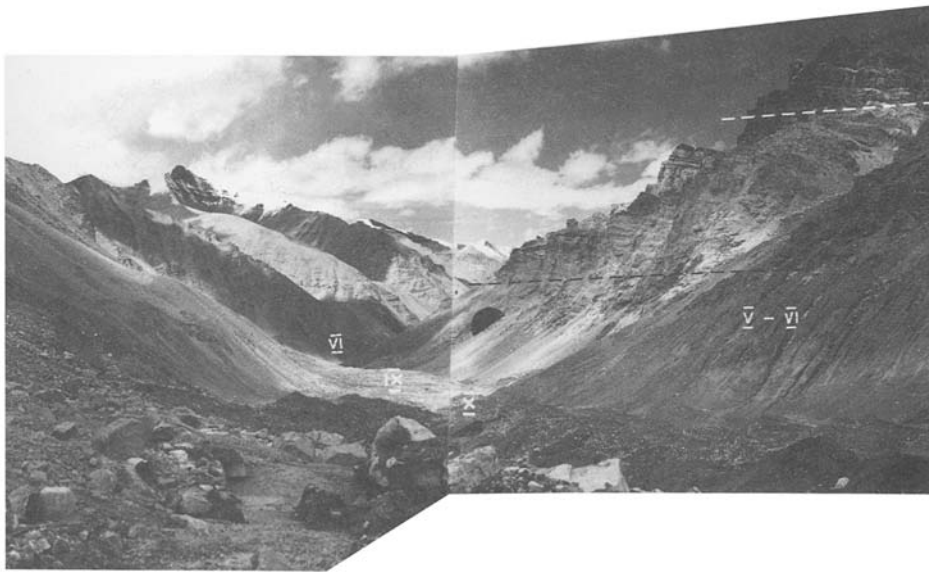


Fig 65  
Debris covered lower East Rongbuk glacier (×) seen from 5750 m valley outwards towards the WNW at the confluence with the central Rongbuk valley (Fig 2, central between No. 38 and No. 41). Trim lines of the neoglacial (--- black) and late-glacial (--- white) on the migmatite rocks of the true right valley slope which is strongly weathered and joint eroded. Photo: M. Kuhle.

E Rongbuk glacier follows a narrow stretch in the valley, so that no lateral moraines, but polished areas have been preserved at the corresponding level on the true right-hand (Fig 65 ●). At 5500 m asl the E Rongbuk glacier tongue is now 2.2 km away from the confluence with the central Rongbuk glacier (Fig 65 ×). During stages VI or VII it still reached it by way of a platform- (dam-) moraine. A historical tongue basin, filled with ice even 30 years ago (× – sub-Recent) is 300–500 m long (Fig 65 X-IX).

The relative heights of the neoglacial to historic remnants of lateral moraines decrease in direction of the upper glacier areas. A few hundred metres up-valley, they get closer and closer to the recent glacier surface until they come together in their source area in just a few, in two, or even a single level. Moraine levels are accordingly best differentiated in the vicinity of the present glacier tongue end (Fig 58, 59).

#### *Some notes on the subdivision and geomorphology of the Recent and sub-recent Rongbuk glacier surface*

By comparison with alpine glaciers, glacier morphology on Mt. Everest above the equilibrium line only differs in respect of the steepness of the catchment area. At its source the central Rongbuk glacier is surrounded by the 5 km-wide and up to 2500 m high N wall of Mt. Everest, the 3 km-wide and 1300 m-high S wall of Changtse (Fig 66), as well as secondary head-walls like the Khumbutse (6636 m) and Lingtren (6714 or 6697 m) walls. Relief conditions are similar above the ELA on the E Rongbuk glacier, where a 3.5 km-long and up to 1800 m high headwall between the E shoulder of Mt. Everest (8390 m) and of Changtse (7580 m) closes off the valley (Fig 67). N and S of the glacier basin the

Everest spurs and the ENE spurs of Changtse follow on over a 3 km distance with 600 m to more than 1500 m high ice flanks. Though not in contact with Mt. Everest, even the W Rongbuk glacier has very steep catchment areas, like the 1500 m high Gyachung Kang ESE flank, and the walls of other high peaks like the Pumori (7145 or 7170 m) with its N wall (Fig 69). This topography causes a considerable proportion of avalanche feeding of the glaciers. Avalanche erosion supplies the ice on the head-walls with debris. This explains the considerable surface moraine cover of the glacier tongues. Since head-wall areas tend to be only a few hundred or thousand metres away from the equilibrium line in up-valley direction, the surface moraine cover already begins just below the equilibrium line in *down-valley direction*.

This is a factual situation which contradicts the method of calculating the equilibrium line in accordance with Lichtenecker (1938), as it assumes the course of the equilibrium line to be generally 50 m above the place where the highest internal moraine appears (recovers by thawing) and becomes a surface moraine. According to observations conducted by the author, however, the internal moraine emerges to the glacier surface below the equilibrium line the sooner the fewer days the debris from the headwall is covered by snow from primary precipitation. How deeply it is covered by fresh snow depends on the time it takes to reach the equilibrium line, and thus on the distance to the foot of the wall (the point of impact of avalanche debris).

Surface moraines increasingly covering areas further down the glacier not only have the effect of changing the energy flow at the glacier surface, but also of a qualitative leap, geomorphologically speaking. A surface moraine which continuously increased its thickness also becomes a protection against ablation. Whilst thicknesses of debris deposits are not more than a few centi-

metres, the surface moraine still forms a concave depression let into the glacier surface; the cryoconitic effect of the debris – heated by insolation – has the effect of melting and moulding a box-shaped moraine channel down to 10 m deep in the surrounding, debris-free reflecting ice (Fig 70 and 69 ●). This form of melting away can be observed in the middle moraine of the E Rongbuk glacier, starting at an altitude of about 6300 m (Fig 70 ●) and descending over 3.3 km to 6000 m asl (Fig 71 ↓). From that point onwards the surface moraine becomes so thick (at least 20–30 cm, and exceeding 50 cm in some places) that it isolates the underlying ice from radiation. After this profile has been reached, the surface of the middle moraine thus returns to the level of the detritus-free ice (Fig 64 and 71 ●). For the next 3–4 km, down to 5800 m, the moraine-covered ice overlaps the open ice on both sides as a ridge that is gradually increasing in breadth (Fig 71, foreground).

At the same time it ought to be borne in mind that the other side of this melting balance is presented by the forced thawing down (and evaporating) of a glacier surface already broken down into ice pyramids (Fig 69). This multiplication of surfaces (and of the extend of the overall ice – surface) increases ablation as a result of the enlargement of areas open to very dry air passing through them. Further upwards the compact ice surface of the glacier remains intact (Fig 66). On a sunny day a specific humidity of 4.2 g/kg was measured directly on ice pyramid surfaces at 5650 m, and of merely 1.0 g/kg at the same time at a distance of 2 m. This humidity gradient is evidence of the great ablation efficiency of the air passing between the pyramids. At 6500 m and a somewhat greater distance from the glacier the dryness of the air temporarily fell to 0.2 g/kg, and even to a minimum of 0.13 g/kg.

This points to a bilateral change in the balance of the longitudinal profile of the glacier. Ablation in the vicinity of the equilibrium line is intensified by the thin cover of debris, and kept low by the still intact surface of the open ice (Fig 70 ■ ■). Further down the thickening cover of debris exerts an increasingly isolating effect, whilst areas of the glacier surface roughened up by ice pyramids dwindle with increasing speed (Fig 64).

The phenomenon of ice pyramid formation is almost independent of the moraine content of the ice. Ice pyramid fields on the tongue of the far-E Rongbuk glacier (Fig 72 ●), containing little surface moraine, are evidence of this. This ice stream arises in a saddle glacier with comparatively little relief as the W component. Although its catchment area reaches 7227 m asl, there is a complete absence of avalanche feeding. This is a case of the relief-specific, glacier-typological leap (Kuhle 1986b) from the ice streams of the High Himalayas to those of the Tibetan Himalaya (Inner Himalaya), which is marked by the near absence of steep walls. The feeding of the Tibetan glaciers is almost exclusively due to primary precipitation.

The formation of ice pyramids is interpreted as specific to subtropical climates, and attributed to the steep angle of radiation at 28° N. Radiation-intensifying factors are the great altitude above sea-level with its extremely radiation-transparent atmosphere (Kuhle 1988a, b), and the position in the monsoon-lee on the N side of the Himalayas, which reduces precipitation and clouding. The Khumbu and the Ngozumpa glaciers on the S slopes of Mt. Everest and Cho Oyu also carry ice pyramids, though to a lesser extent. They, too, find themselves already in the precipitation shadow of the Himalayan chains extending in front of them (with the 6000 to almost 7000 m high peaks of the Kangtaiga, Amai Dablang, Tramserku and others) and receive less than 600 mm of precipitation a year. In general the development of ice pyramids can be observed on all the glaciers of the Himalayan N slope, on the massifs of the Shisha Pangma, as well as on those of Mt. Everest. They appear even in places where small hanging valleys or corries lack breaks in slope which would cause the disintegration of the glacier surfaces (Fig 71 ■ ▼); Fig 64 ■). However, the author regards the vertical discontinuity surfaces of joints and fissures which develop to wide crevasses in the area of large ice falls as the structural protoform inside the glacier for the subsequent development of ice pyramids. This would imply an absence of ice pyramids in small joint-free hanging glaciers, and they are indeed much more markedly represented on large glaciers like the Rongbuk, which are detritically composed of numerous components, with many ice-falls (Fig 69, 72 foreground). But less deep crevasses, of smaller extension, are evidently also sufficient for the formation of ice pyramids. Thanks to their very low viscosity, they occur in almost all cold hanging glaciers, and cause the formation of ice balconies (Fig 71 ■ ▼).

A longitudinal profile of the central Rongbuk glacier provides a clear outline of the genetic series, and thus of the formation of ice pyramids: ice crevasses occur at the level of the equilibrium line and above (Fig 66 ■; below the N wall of Mt. Everest, the W wall of Changtse, as well as E of the Khumbutse and Lingtren walls). Below the scarp section or other unevennesses in the glacier bed they mend again and section by section gets covered by snow (precipitation). As they are not entirely frozen together, the progressive melting process below the equilibrium line prefers and thus emphasizes the fault cracks as they move down-valley (Fig 73 ↓). Radiation follows the intra-glacial network of crevasses and makes the unbroken blocks stand out residually (Fig 73 ◆). Besides tension crevasses running across the direction of movement, there are also longitudinal fractures in the ice resulting from differing flow velocities. This explains the rectangular to almost square ground-plan of the pyramids (being parallelogram-like distorted in case of shear-stress). But before this is revealed, ice walls begin to form across the glacier at first (Fig 70 ◆), which are separated by increasingly deep furrows frequently filled





Fig 66

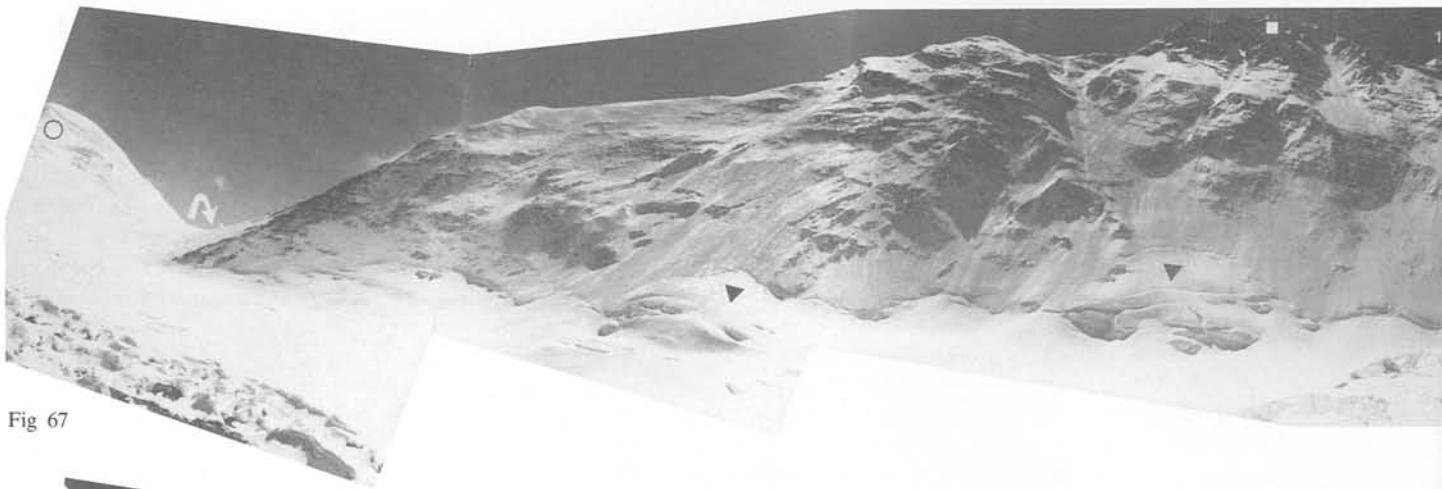


Fig 67

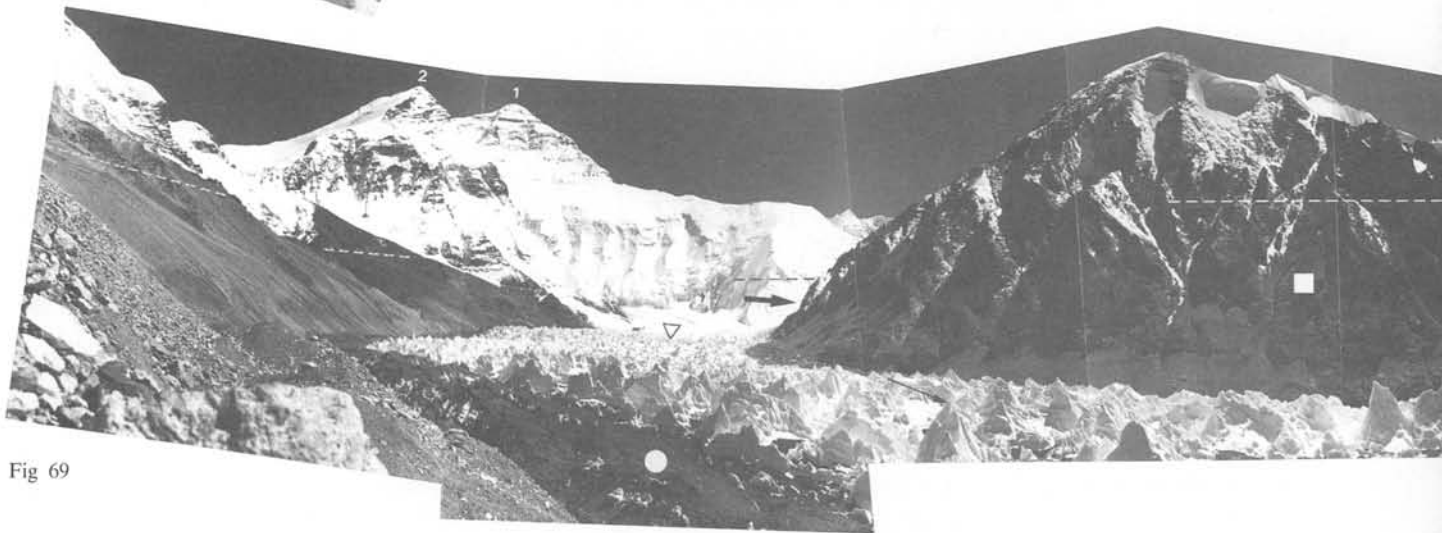


Fig 69

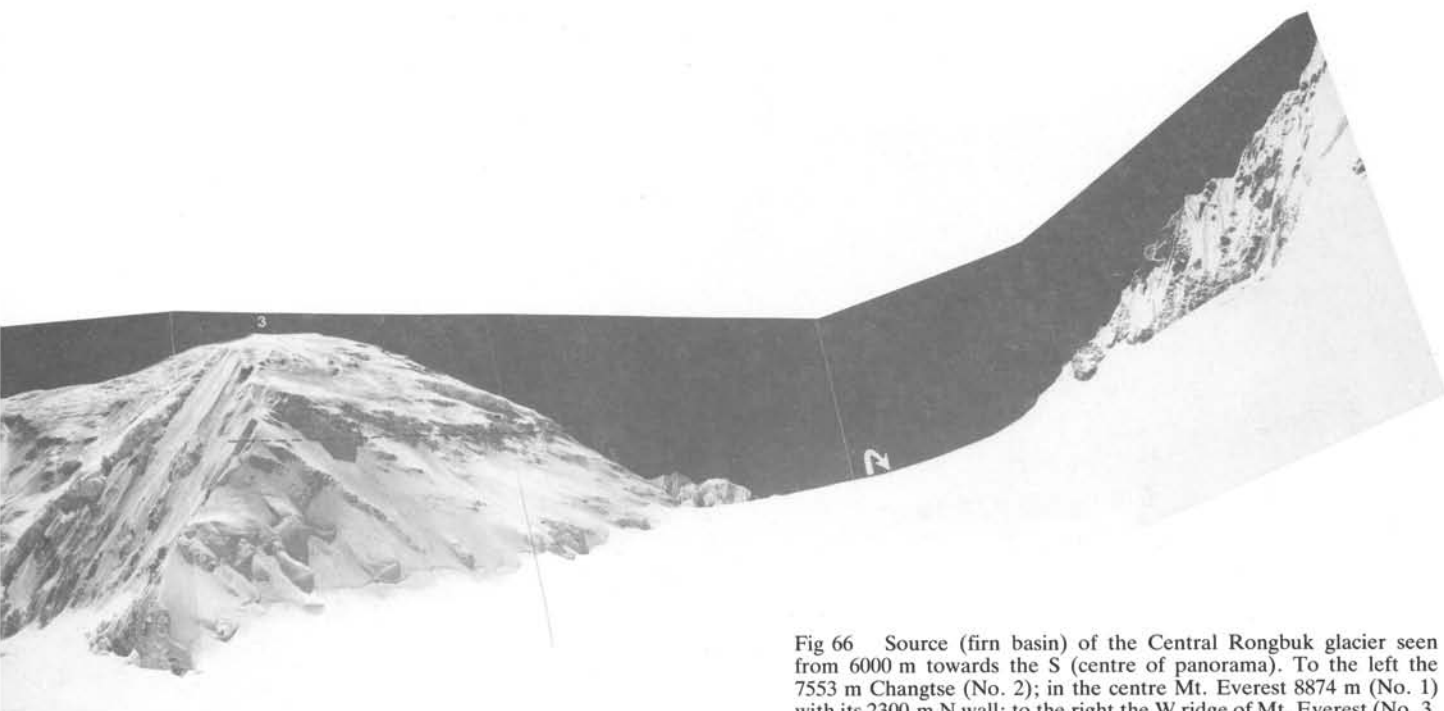


Fig 66 Source (firn basin) of the Central Rongbuk glacier seen from 6000 m towards the S (centre of panorama). To the left the 7553 m Changtse (No. 2); in the centre Mt. Everest 8874 m (No. 1) with its 2300 m N wall; to the right the W ridge of Mt. Everest (No. 3, 7205 m) which falls to the 6009 m Lho La (▲) (Fig 2, No. 40). Here the Rongbuk glacier overflows on to the Khumbu glacier on the S slope of the Himalaya. (---) marks the level of maximum glacial surface in this area of glacial pass breaching (cf. Fig 74). Avalanches are responsible for at least 50% of the supply to this source basin. Photo: M. Kuhle.

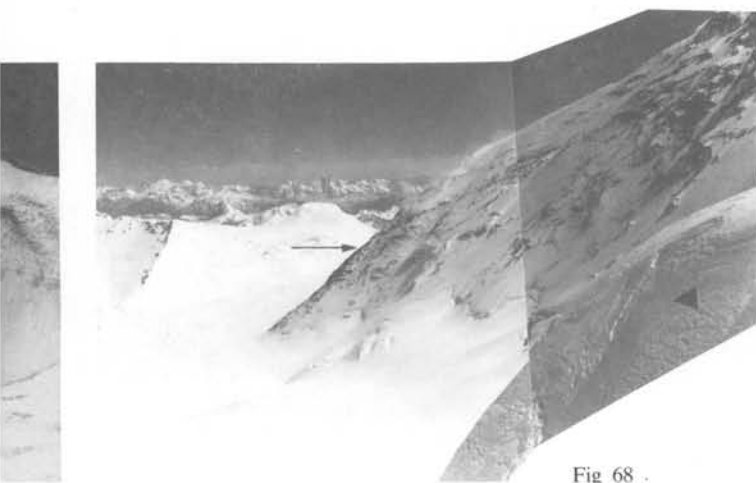


Fig 68 .

Fig 67 Panorama of the East Rongbuk source basin with the 6500 m glacial breach Rapiu La (Raphü La ▲; Fig 2, No. 41; Fig 68) leading to the S slope of the Himalaya; view from the true left edge of the glacier at 6510 m towards the NE (centre of panorama). The avalanche supply is largely from the up to 1800 m high E part of the Mt. Everest N wall, coming from the 8395 m high NE ridge of Mt. Everest (■). Typical avalanche cones are formed at the foot of the wall (▼▼). To the right above is the main peak of Mt. Everest at 8874 m (No. 1). Although the 6833 m peak NE of Rapiu La (○) is covered with glacier ice some decametres thick the ice covering the slopes of the Mt. Everest N wall decreases steadily above 7200 m where rock comes to the surface. The only partial snow cover is that blown into gullies (left and right of ■). Photo: M. Kuhle.

Fig 68 The central source region of the East Rongbuk glacier seen from 7030 m on the N col of Mt. Everest. (→) shows the transfluence of the present glacier ice (much thicker during the pleistocene) across the Rapiu La (Raphü La; Fig 2, No. 41) in the S slope of the Himalaya. This same overflow limited the maximum glacial accumulation of ice on the edge of the S Tibetan plateau to only a few hundred metres more than at present. In the foreground (♣) are the persistent lee side cornices (with ice cores) of the Changtse SSE ridge. In the middle distance (right) the eastern N wall of Mt. Everest falls from its 8395 m NE-spur into the firn basin. Behind are the glacier mountains of the Tibetan Himalaya. Photo: M. Kuhle.



Fig 69 Panorama showing the relationship of the central (left) and W Rongbuk glaciers, one of the major recent valley glacier systems of the Himalaya N slope, seen from 5520 m towards the SW (centre of panorama) (Fig 2, between No. 38 and No. 40). The valley of the Central Rongbuk glacier ends at the summits of Mt. Everest (No. 1) and Changtse (No. 2, 7553 m) 11 km away. The pleistocene surface (---) of the glacier system was controlled by the Lho La transfluence pass (→, Fig 2, No. 40) as is shown by the lateral moraines and the undercutting in the country rock. In the area of the at least 12 km long W source glacier (W Rongbuk glacier ▲) further transfluence passes led to the reversal of the outflow direction of this portion of the flow during the glacial period (Fig 2, No. 39) The central mountain spur at the confluence (■) shows the great post-glacial modification of the lateral scouring (below ---) by frost weathering and gullying. Photo: M. Kuhle.



Fig 70

Medial and surface moraines (●) of the E Rongbuk glacier viewed down-valley from 6300 m towards the NNE (Fig 2, halfway between No. 38 and No. 41). To the left (■) a footwall and slope glacier component from the E slope of Changtse; to the right (■) the intact surface of the E Rongbuk glacier not so far ablated into ice walls and pyramids. Above here the medial moraine (●) is only a few centimetres or decimetres thick so that the dark debris particles experience daily temperature increases and thus promote ablation. Therefore the dark bands of medial moraine (●) are more deeply melted into the glacier surface than the bounding light ice surface (■; contrast Fig 64 and 71). Where patches of snow and firn persist and slope glaciers occur the strata-etched slopes (background ▽) are polished and smoothed. Where no snow-shed activity or glacial bottom scouring occur steep arrowhead slopes and rock steps are typical (□). Photo: M. Kuhle.

with internal moraines. It is true, too, that irregularities (due to shear-stress) in the form of diagonal bridges have created connections between the alignments of the walls. They are attributable to small-scale fluctuations of velocity in the glacier. Some kilometres down the glacier longitudinal furrows have been added and separate the walls into pyramids. At first the pyramids are truncated (Fig 73 ◆), i.e. standing out, they still conform to the glacier surface (Fig 69 ▽). As they melt down the pyramid flanks consume more and more of these small remnant areas until they meet at one point (Fig 72 ▲; 69 ▼). Yet further down the glacier, as a function of the width of the pyramid base, the ice pyramid peaks are

lowered at different speeds. From this point onwards the former level of the glacier surface in the sense of an “upper denudation level”, which is lowered simultaneously by melting, is subject to an irregular dissolution i.e. the speed of melting differs from pyramid to pyramid (Fig 69, foreground, right-hand side ooo; Fig 71, right and left ○○○).

Ice pyramids occupy an intermediate position in the transition from an unbroken snow surface above the equilibrium line to the complete covering with surface moraine in the lowest section of the glacier tongue. In this the surface moraine dovetails with the white areas of ice pyramids in a linkage pattern of counter-flow. The

Fig 71 View from the ridge of the medial moraine of the E Rongbuk glacier (●, Fig 2, between No. 38 and No. 41) at 5800 m upward to the SE to the Rapiu La (↓) No. 41. To the right (No. 1) the rocky upper 800 m of the N slopes of Mt. Everest in front of which is the firn-covered NE ridge of the 7553 m Changtse (No. 2); left (No. 3) a nameless peak of the Tibetan Himalaya at 7050 m. This carries relatively gently inclined slope glaciers typical of S Tibet (■). The true right bank walls of the trough valley of the E Rongbuk glacier (left on both sides of ▼) are broken up by frost weathering into abrupt steps, ridges and gullies. The medial moraine components (●) with their considerable debris thickness stand above the mean level of the white ice with its ice pyramids (○) because they protect the ice below from ablation. Photo: M. Kuhle.





Fig 72 The geomorphological and glaciological phenomena of S Tibet provide a picture of cold-arid climatic conditions. The frost smoothed slopes (Glatthänge ■■) are the result of the great freeze-thaw frequency of subtropical highlands and mountains. Snow patches are only to be seen in summer after monsoon snowfalls. These lie high above the ends of the glaciers, generally only above the equilibrium line (above ■ right). The up to 30 m high ice pyramids of the ablation region of the glaciers (↑) are the result of a maximum global radiation of over 1200 W/m<sup>2</sup> together with an absolute humidity of only 0.15 to 2.01 g/m<sup>3</sup> (at 200 cm above the surface) as measured during the 1984 expedition. The low temperature results in low fluidity of the ice, resulting in the strange forms of the pyramids and their persistence. The ice flows as discrete blocks. View from the medial moraine of the E Rongbuk glacier at 5800 m (Fig 2, between No. 38 and No. 41) towards the E to the far east Rongbuk glacier (●). Photo: M. Kuhle.

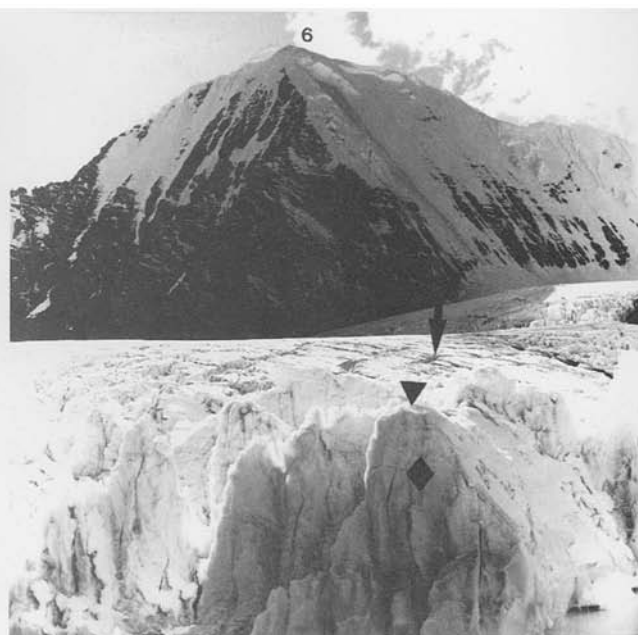


Fig 73 View WNW from 6060 m from the E Rongbuk glacier (Fig 2, between No. 38 and No. 41) over the Changtse glacier to the 6855 m peak (No. 6). The development of the compact ice surface (↓) into ice walls (◆) is here obvious; further down-glacier this allows the formation of ice pyramids (Fig 71 ○○○ to the right). Photo: M. Kuhle.

ice fields decrease as they move down, whilst the areas with debris increase in size (Fig 64, 69, 71) until (from 5400 m asl on the central and W Rongbuk glacier) the ice pyramids thin out completely and the glacier tongue is entirely covered by surface moraine (for another 5 km on the central Rongbuk glacier) (Fig 58, 59, 65). The author would wish to make the point that the ends of the ice pyramid bands on the glacier fluctuate more readily than does the debris-covered glacier snout. This allows smaller climatic fluctuations to be registered than those of the larger valley glacier permit. Consequently they provide a less disturbed picture of the specific climatic conditions. Since the 1:50,000 mapping of the central Rongbuk glacier in 1966 (Academia Sinica 1979), the lowest ice pyramid spurs have retreated about 1.1 km, whilst the glacier terminus at most has witnessed a minor up-valley shift of the dead ice line.

In general, even on the Yepokangara glacier on Shisha Pangma the retreat of ice pyramids shows a negative balance for recent valley glaciers of more than

10 km in length (Fig 59). The same is indicated by the increasing deposition of debris (Fig 59, 65) of even small tributary glaciers (cf. above, Fig 60).

*Reconstruction of ice levels and ice overspill into the southern slope of the Himalayas: some observations on the overall picture of prehistoric glaciation in South Tibet*

The valleys of the Himalayan S slope, like the Rongbuk valley and the Dzakar Chu, its continuation, as well as the valley which continues the Kyetrak glacier on the Cho Oyu, slope gently and in conformity with the gradient their recent valley glaciers flow N, just as they did in historic and neoglacial states and back in the Late Ice Age. The northerly direction of the flow was coupled with equilibrium line depressions of just a few hundred metres. Due to the postglacial glacio-isostatic uplift it is not possible to determine the ELA depression more precisely by way of moraine remnants in the Dzakar Chu, up to which the glacier discharge in a northerly direction took place. In any case the equilibrium line depression at which a glacier discharge towards the N was possible, may well have been greater at that time than at present, since glacio-isostatically the relief N of the Himalaya must have been situated at an even lower altitude.

Previously, during the older Late Glacial period and probably still during the glacial state of the Dhampu-



Fig 74

View at 5300 m to the NE to the Lho La (▲) from the S slope of the Himalaya (S of the watershed) and the Khumbu glacier (Nepal in the foreground; Fig 2, No. 40) (cf. Fig 66). To the left (No. 5) is the 6640 m Khumbutse, in the centre (No. 2) Changtse (7553 m) and to the right (----) the undercutting below the W spur of Mt. Everest showing the maximum glacial surface. The S flowing overflow glacier was thus 400 m thicker. Even today part of the Rongbuk glacier ice still flows across the Lho La (-Pass ▲) at 6010 m to the Khumbu glacier breaking as avalanches from the overhanging ice ledges (■). Photo: M. Kuhle.

(III) or Taglung stage (II), but certainly during the Ghasa stage (I), the entire relief had been infilled with ice. At that time the glacier discharge must have taken a course to the S. Ice-fillings in the valleys N of the High Himalaya had reversed their flow direction once they had reached a certain thickness of many hundreds of metres. In the course of this process, which extended from the Early to the High and Late Glacial period, their surface came to slope southwards instead of northwards. This shift of the ice-shed from the Himalaya to the N can be compared with the N European glacial ice-shed shift from the Scandinavian Alps to the inland ice-dome in the SE. At present it is merely a matter of hanging glaciers on the Himalayan flanks, whereas the ice ages saw massive glaciers flow through (and leave) the High Himalayas. Present glacier feeding is restricted to the slopes of the High Himalayas, whereas it then took place to the N in the area of the S Tibetan ice-stream network, which filled the relief of the Tibetan Himalaya (Kuhle 1982, 1983). This shift in feeding areas even went so far that the then outlet glaciers received almost no ice from the walls of the High Himalayas, at least less than is now available. At that time the thermal upper limit of glaciation (cf. Kuhle 1986a) running parallel to the equilibrium line, had been depressed by more than 1000 m to an altitude of about 6000–6200 m. The surface of the outlet glaciers tended to be at least at this altitude, and usually even higher, so that dry, i.e. glacier-free, walls rose above these glacier streams. On the Cho Oyu it was the now also glaciated Nangpa La (5717 m) to the W, and in the Mt. Everest area, as the more closely defined area under investigation, the passes

of the Rapui La (6500 m; Fig 67 ▲ ; 68 →) to the E, and Lho La (6009 m; Fig 58, 69 →, 66, 74 ▲) to the W of the mountain, which opened the way for the discharge of those outlet glaciers on to the S slope of the Himalayas. Reference must also be made to the 5860 m high Nup La and the 6147 m high pass between Mt. Everest and Cho Oyu (Fig 69 ▲). All these glacier passes are in one line with the Himalayan main ridge and together they form the present-day ice-shed (Fig 2, no. 39, 40, 41), so that one can no longer speak of an overflow from the N slope to the S slope. Nonetheless, they do give the impression of such a prehistoric overflow through the fact that the glacier surfaces, especially those of the central Rongbuk glacier on the Lho La (Fig 66 ▲) and the E Rongbuk glacier on the Rapui La (Fig 68 →, Fig 2, no. 41) are almost horizontal, and that the ice in the pass zone accumulates increasingly before discharging. The process of an overflow from the N slope is thus suggested by these passes, the Himalayan S slope of which is characterized by a steep drop with ice balconies tens of metres thick. The thickness of the glacier at the time of the prehistoric overflow across the Lho La has a witness in the glacial undercutting on the W shoulder of Mt. Everest (Fig 58 -----; Fig 69 -----; Fig 66 -----; Fig 74 -----). The upper limit of glacial scouring runs at about 450 m above the present Lho La. The level at 6400 m is about 300 m above the highest right-hand side E moraine terrace on the upper central Rongbuk glacier (Fig 69 -----; Fig 59 ······; Fig 58 -----).

The moraine at about 6100 m is evidence of the most recent Late Glacial stage, during which the glacier over-

flow into the S slope persisted. It is about 5.3 km from the fully 100 m lower overflow of the Lho La (Fig 2, no. 40). On the one hand it depended on the altitudes of these four overflows how thick the glacier above was and how much ice flowed across them and down on to the S slope. On the other hand, it also depended upon their location in relation to the general direction of main valley axes and main valley discharge to the S. Although the Nup La (Fig 2, no. 39) is 200 m lower than the Lho La, the latter, being an extension of the main valley line of the Rongbuk valley, presented a much better discharge route for ice than the Nup La, situated at right angles to the extension of the W Rongbuk valley. It follows that the main discharge must have been by way of the Lho La (Fig 2, no. 40). Highest of all is the Rapui La (Raphü La, 6510 m) at the end of the E Rongbuk valley (Fig 2, no. 41). Its location is only marginally less favourable than that of the Nup La. However, overflow was least here due to its height.

Large-scale evidence of an almost relief-filling ice-stream network glaciation N of the High Himalayas, i.e. in the Tibetan Himalaya, has been preserved in the mountain ridges rounded by glacial forms of polishing. A good example is the terrain N of and down-valley of the Rongbuk valley (Fig 53–55, 57). The glacier discharge through the Rongbuk valley southwards to the High Himalayas and through it, is shown by Late Ice Age lines of ice scouring on the true left-hand in the central Rongbuk valley ( $28^{\circ} 16' \text{ N}/86^{\circ} 48' \text{ E}$ ), which are inclined to the S in contrast to the valley gradient (Fig 58 ▼▼). On the Himalayan main ridge the level of the High Glacial ice surface was at an altitude of 6200 m and 6400 m. Towards the N, the Dzakar Chu region in the Tibetan Himalaya, it rose to approximately 6500 or 6600 m.

This interpretation of the reversal of the glacier discharge as a result of the Ice Age filling of the relief with glaciers explains the scarcity of moraines in the Rongbuk valley, outside the neoglacial glacier locations. The absence of moraines here is in marked contrast to the large-scale, substantial moraine cover in the N foreland of the Shisha Pangma group a mere 120 km further W (cf. above). The floor of the Rongbuk valley was accordingly covered by several hundred metres of near-motionless ice. There were therefore little or no debris deposits. Only the upper ice strata, being at a higher level, were able to follow the small gradient to the transfluence passes into the S slope. The tongue levels of the remnant glaciers only followed the actual relief of the valley landscape after far-reaching deglaciation had taken place. Only then was the aggregation of moraines intensified. This development set in with the more recent Late Glacial period (stages III and IV) and continued during neoglacial time (V–VII).

The prehistoric ice overflow into the S slope also explains the relatively low height of the oldest lateral moraine terraces above the recent Rongbuk glacier. These moraines are only fully 600 m above the present

surface moraine (Fig 58, 59, 69 —). The small prehistoric ice thickness of about 600 m below the recent ELA is out of the question for such a shallow valley floor gradient without overflow towards the S. Without overflow an enormous build up of ice would have occurred in this valley grid even in the Late Ice Age, for this valley cross-section at the time of the moraine deposits was at or above the level of the ELA. This is the climatically optimal altitudinal area for glacier build-up. This build-up of ice was consequently prevented by the overflow passes leading to the S slope of the Himalaya.

The collective findings concerning the topography explain the reasons for the striking paucity of traces of glacial accumulation on the N slope of Mt. Everest and the contrast they present to an Ice Age equilibrium line about 1200 m lower than today (see Tab 1).

### Summary Review of Equilibrium Line Depressions in South Tibet and Climatological Conclusions

In the area under investigation, the recent orographic equilibrium line fluctuates between 5700 and 6325 m. This applies to the Transhimalaya at  $29^{\circ} 43' \text{ N}$  and the N side of the High Himalayas in the precipitation shadow of the main ridge at  $28^{\circ} 26' \text{ N}$ . The mean average value to be cited as the integral, i.e. the macro-regional climatic equilibrium line, is around 5900 m (see Tab 1). The mean value of the High Glacial equilibrium line depression is 1100–1200 m, so that the integral climatic equilibrium line must have been at an altitude of 4700 m. This depression value very likely still is too small in comparison with the ELA depressions 300 km further W, where, N of the Dhaulagiri and Annapurna Himalaya values of 1530 m, orographically even 1630 m, were found (Kuhle 1982). In places where glaciers were able to penetrate the Himalayan main ridge and descend steeply on the S slope, the detailed analyses show an orographic ELA depression of up to 1900 m. This value applies to the Bo Chu in the Shisha Pangma massif. This is the only location where it was possible to survey the terminus of an outlet glacier in the area of the 1984 investigation. But even the ELA depression for the Ice Age Khumbu glacier (Dudh Kosi glacier on the S slope of Mt. Everest), which flowed down to at least 1800 m, to the Lumding – Drangka confluence ( $27^{\circ} 38' \text{ N}/86^{\circ} 42' \text{ E}$ ) (Kuhle 1988b; Heuberger 1986, p. 30) was about 1400–1500 m. This additional information supports the findings that an ELA depression of 1200 m is likely to be on the low side of operational values for S Tibet. It is confirmed in detail by local and orographic values of the Transhimalaya at Lhasa as well as in the Tibetan Himalaya (see Tab 1). It must, moreover, be taken into account that values like those E of the Man-ko-pa basin and from the Latzu massif have been added to those of the High Glacial period, in order to be on the safe side, but probably belong to the Late Glacial

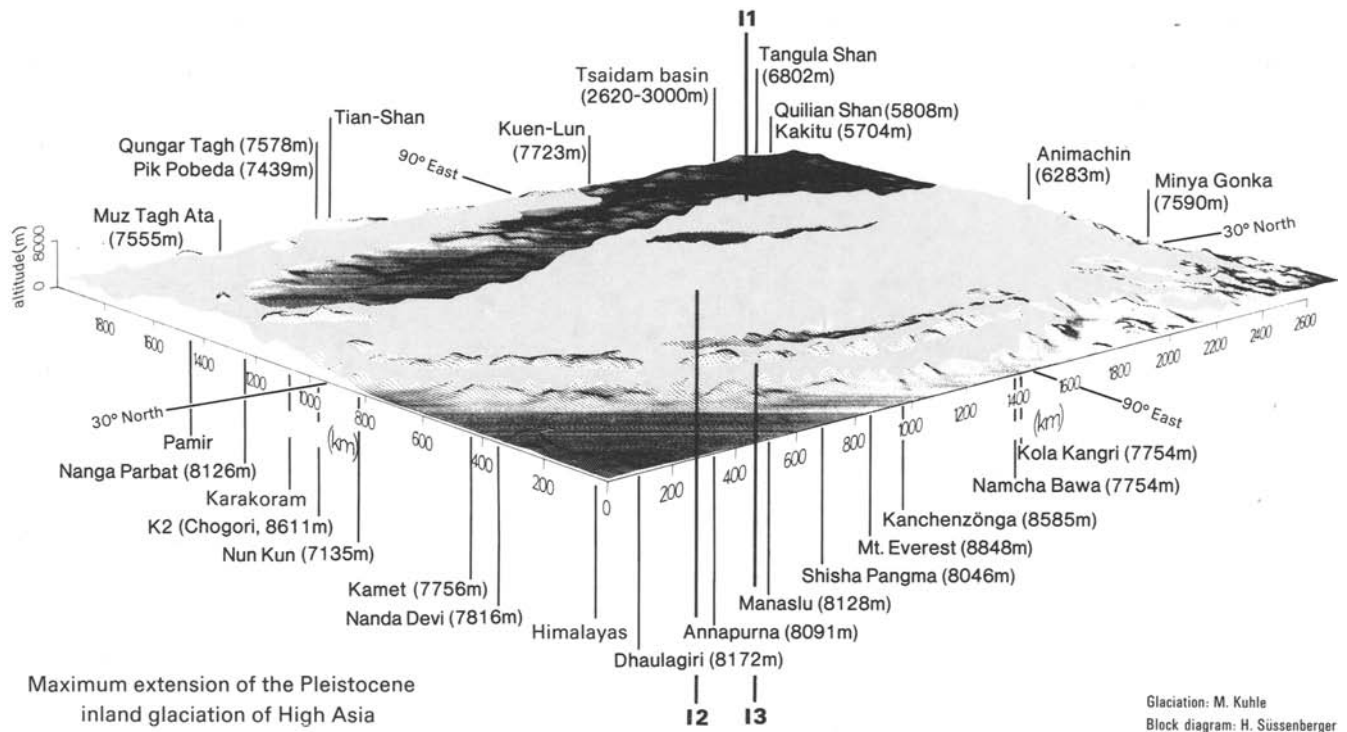


Fig 75 Fig 1 (which includes all the areas investigated so far) shows that the glacier surface in Tibet (with its surrounding mountain systems such as the High Himalayas in the S) covered 2.4 million square kilometres. In addition a network of ice streams occurred towards the NW in the adjacent Tien Shan range. The glacier area reconstructed in this paper lies in the area of I2 and I3 N of Shisha Pangma and Mt. Everest and also N of the ice-free Tsangpo valley (cf. Fig 76).

period. In the basin of Man-ko-pa an ice margin position on the basin floor at 4400 m was taken into account, though there is a near certainty that the entire basin was filled with ice during the Middle Ice Age (see above). A distinctly lower equilibrium line would accordingly have to be assumed than in a case where a glacier merely reaches the basin floor. Such a lower equilibrium line can, however, not be reconstructed. This touches upon one of the major problems of palaeo-climatology concerning equilibrium line reconstructions in the regions of the Tibetan Plateau: all the equilibrium line values are merely minimum figures. From the stage at which glaciation reached the level of the plateau, even a complete inland ice cover was able to establish itself without having a *single* lower moraine as evidence.

Assuming a mean gradient of  $0.7^{\circ}\text{C}/100\text{ m}$ , which, according to the author's measurements (Kuhle 1988a) applies to the K 2 glacier between 4100 and 5300 m asl, and is characteristic of cold-arid high mountain climates, the ELA depression indicates a High Glacial lowering of temperature of  $8.4^{\circ}\text{C}$  for the warmest month. This estimate is based on recent conditions of radiation and of hygric relationships (Kuhle 1983, p. 90). This degree of cooling is, if anything, too low a value when taking into consideration that it must have been drier during the High Glacial period than now, thanks to global cooling and the atmosphere's lower humidity capacity. Long-

term means of annual precipitation, which can now be measured in the lowest valley locations of the area under investigation fluctuate between 270 mm (Gyantse, 4000 m) and 440 mm (Lhasa, 3730 m). As a result of the Tibetan ice sheets reducing or completely preventing the monsoon, they must have been lower then. A prevailing shallow cold high pressure area with katabatic winds must be assumed to have been stationary over the Tibetan ice. On the 1986 expedition to K 2 (Karakoram) from the N annual temperature of  $-9^{\circ}$  to  $-10^{\circ}\text{C}$  were ascertained at the level of the equilibrium line, and the same values are known to occur on the Shisha Pangma N slope (cf. Ding Yongjian 1987, p. 10, Tab 3). (For comparison: the Alpine values are around  $-3^{\circ}$  to  $-4^{\circ}\text{C}$ ). Thanks to increased aridity the Ice Age Tibetan glacier may, if anything, have been even colder. These considerations indicate a summer cooling down by a likely  $10^{\circ}\text{C}$  or more.

In the area under investigation the annual  $0^{\circ}\text{C}$  isotherm runs between 5000 and 5500 m, which is the same as the mean altitude of the termini of valley glacier tongues. (At the altitude of 4000 m the annual temperature is  $5^{\circ}$ – $6^{\circ}\text{C}$ ). According to the measured data mentioned above, the  $-10^{\circ}\text{C}$  isotherm must have been at about 4700 m or still somewhat lower during the Ice Age, with the  $0^{\circ}\text{C}$  isotherm running at an altitude of at most 3800–4300 m. It is likely that the  $0^{\circ}\text{C}$  line had

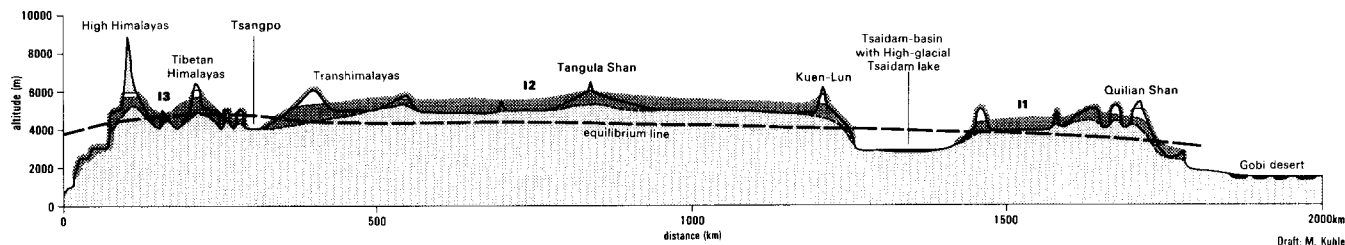


Fig 75 Fig 1 (which includes all the areas investigated so far) shows that the glacier surface in Tibet (with its surrounding mountain systems such as the High Himalayas in the S) covered 2.4 million square kilometres. In addition a network of ice streams occurred towards the NW in the adjacent Tien Shan range. The glacier area reconstructed in this paper lies in the area of I2 and I3 N of Shisha Pangma and Mt. Everest and also N of the ice-free Tsangpo valley (cf. Fig 76).

been shifted markedly lower still by the glacial self-intensifying cooling process.

Late and neoglacial glacier development, successive equilibrium line uplifts since the High Glacial period, and the corresponding warming up in S Tibet may be gathered from Tab 1 by analogy with these arguments.

#### The Ice Age Glacier Cover in South Tibet and Its Indicator Value for the Reconstruction of the Tibetan Inland Ice as a Whole

High Glacial equilibrium line depressions of around at least 1200 m defined by ice margin positions of smaller prehistoric glaciers, together with glaciated forms of valleys and polishings, are evidence of an almost total glacial cover for the Transhimalaya, the Tibetan Himalaya, and the High Himalaya (Fig 75, between Shisha Pangma and Kanchenzönga). In terms of typology this glaciation is to be classified as an ice-stream network. Individual peaks and ridges rose above the glacier surfaces. This is a function of the extreme relief energy, especially in the High Himalaya. In the region of I 3 (Fig 75, 76) the proximity to the S escarpment of Tibet exerts its influence. Discharge was greatly accelerated here. The ice level inclined southwards towards the overflow passes of the High Himalayas. For this reason extreme build-up of ice was impossible. Circumstances in the Transhimalaya were similar. It formed the escarpment of I 2 (Fig 76) to the Tsangpo furrow, which was probably free of ice in its E section. From the central inland ice sheet in Tibet, the basis of which was more than 5000 m asl (Kuhle 1985, 1986c, 1987a, 1988b) outlet glaciers flowed through the transverse valleys of the Transhimalaya, almost reaching the Tsangpo down at 3950 m (Fig 75, 76, I 2). Evidence of the glacier level dropping to these ice margins is supplied here, as in the High Himalayas, by nunatak-like pointed ridges. They rise several hundred metres above the ice level. In the Transhimalaya there was consequently an ice-stream network as well. The finding of erratic blocks along its constituent streams is evidence of glacier thicknesses of at least 1200 m. These statements on the Transhimalaya

apply only to the section E of  $86^{\circ}$ – $87^{\circ}$  E, however, which was investigated in 1984, and in particular to the Nientschen-tang La. Further W the valley floor of the Tsangpo rises to 4600 m asl, and must have been completely filled with ice according to the reconstructed equilibrium line depression. It is likely that the greatest ice thicknesses in S Tibet formed here. Ice thicknesses building up in the course of this development through back-damming assisted the progressive integration of the Transhimalayan ice-stream network into a continuous inland ice I 2/I 3. There must have been a transitional zone between  $87^{\circ}$  and  $86^{\circ}$  E where ice just about filled the Tsangpo valley. It was, however, still part of the ablation area, i.e. it contained glacier areas below the equilibrium line. In this section of the E–W profile of this transitional region, the Tsangpo valley reaches an altitude of about 4300 m and extends only 400 m below the Ice Age ELA.

It has not hitherto been possible definitively to exclude the possibility that some of the S parallel valleys between  $86^{\circ}$  and  $88^{\circ}$  E, like the Tingri and Lulu basins, were free from ice during the High Glacial period, although their floors are situated around 4300–4400 m asl. With an ELA around 4700 m, this would imply that 300–400 m lower valleys in the vicinity of the 6000 m-high mountains, at present still glaciated, – more than 8000 m high mountains in the case of the Tingri basin – would have remained unglaciated. This would be highly unlikely, and indeed difficult to explain, especially since the glacier tongue fronts would have undergone approximately twice the amount of depression undergone by the ELA. A comparison: in the W Alps, as for example in the case of the Rhone valley, a very large longitudinal valley with mountains rising 2000 m above the ELA and a floor that was found to have been 1600 m below the Ice Age equilibrium line, was filled completely with ice (1600–2000 m thick). How could it have happened that this filling should not have taken place in the lowest valleys 300–500 m below the ELA, and with the catchment areas rising to at least 1300 m above the former? Even greater aridity fails to explain this.

The significance of the investigations in S Tibet for the reconstruction of the entire Tibetan ice sheet is to be



found in the southernmost, and thus warmest, position in the highland (Fig 1, no. 4). This selective experimental arrangement of nature permits statements to be made which go beyond the area under investigation in the narrow sense. In the S, the equilibrium line today attains its greatest altitude in Tibet altogether – by rising to 6000 m or beyond. If it was possible to obtain evidence of large-scale prehistoric glacier cover here, it is simultaneously proof of a Tibetan glaciation further N. This deduction is supported by the following facts: 1) The recent ELA inclines towards the N – as it must have done in prehistoric times as well, due to the planetarian decrease in temperature. 2) The mean altitude of the central plateau rises from the area under investigation in S Tibet to large continuous plateaux at altitudes between 5000 and even 6000 m in the N (on the Mayer Kangri 33° N/86° E, for instance). 3) These plateaux are up to 7000 m high mountains, some of which have considerable recent glaciations including plateau glaciers, on top. These functioned as “crystallization centres” for a large-scale build-up of glaciers already at a time when the ELA depression was only 300–500 m. 4) Precipitation increases from 200 mm on the leeward side of the High Himalaya, i.e. from the Tibetan Himalaya, to 400 mm/year on the Transhimalaya and in the central high plateau in the N.

Based on the findings made in S Tibet, these four points were the confirmation and completion of the results of a prehistoric inland ice-cover of Tibet of approximately  $2.4 \times 10^6$  km<sup>2</sup>, which were obtained in W and N Tibet (Kuhle 1987a, 1988b).

### Summary

The last Ice Age (Würm) glacier cover was reconstructed on the basis of standard geomorphological

indicators in S Tibet between the S slope and N slope of the Himalaya by way of the Tibetan Himalaya to the Transhimalaya (28°–29° 50' N/85° 40'–91° 10' E). At the same time, though subject to varying density of data, the process of Late and Post-Glacial deglaciation to Neo-Glacial and Recent glacier cover was considered. Evidence of an almost total glaciation of S Tibet was found in indicators like glaciated knobs, trough valleys with pronounced flank polishings and limits of glacial scouring on nunataks, as well as in findings of erratics, lateral moraines, end moraines, and terraces of outwash plains. This total glaciation took the form of an ice-stream network and attained a thickness of at least 1200 m. Ice-free to about 87°–86° E, the Tsangpo valley with its sander deposits occupied the gap between the glacier areas of the Tibetan and High Himalayas in the S (I 3) and those of the Transhimalaya in the N (I 2). In the light of recently glaciated Late Glacial terminal moraines and ice marginal ramps it has been possible to estimate a glacio-isostatic uplift of c. 400 m during  $10 \times 10^3$  years (an average of 40 mm/year) following deglaciation. It is about 3 to 8 times greater than the tectonic uplift of the High Himalaya. The post-glacially intensified uplift of the S Tibetan Plateau by comparison with the High Himalaya is attributed to the much greater glacier burden during the Ice Age.

In the area under investigation a High Glacial ELA depression (equilibrium line altitude depr.) of at least 1200 (1180) m was reconstructed for a mean altitude of about 4700 (4716) m asl. Assuming constant hygric conditions and a gradient of 0.7° C/100 m, the temperature drop at the time would have been 8.4° C. Since precipitation during the Ice Age must, if anything, have been less, a drop in summer temperature of about 10° C may be regarded as probable.

### References

- Andrews, J. T.: A geomorphological study of post-glacial uplift with particular reference to Arctic Canada. (1970)
- Boulton, G.: Glacial history of the Spitsbergen archipelago and the problem of a Barents Shelf ice sheet. *Boreas* 8, 31–57 (1979)
- Brückner, E.: Die Hohen Tauern und ihre Eisbedeckung. *Zeitschrift des Deutsch-Österreichischen Alpenvereins* 17, 163–187 (1886)
- Chen, J. Y.: Recent Development of Geodesy in China. *AVN International Edition* 5, 26–33 (1988)
- Ding, Yongjian: The Study of the Thermo-Hydrological Environment of Glacial Development in the Karakorum N-Side. Lanzhou, China (unpublished manuscript) 1987.
- Dreimanis, A.: Vagners, U. J.: Bimodal distribution of rock and mineral fragments in basal tills, p. 237–50. In: Goldthwait, R. P. (ed.), *Till, a symposium*. Ohio State Univ. Press, 1971.
- Flint, R. F.: *Glacial and Quaternary Geology*. New York 1971.
- Gansser, A.: *Geology of the Himalayas*. London 1964.

- Gansser, A.: The Wider Himalaya, a Model for Scientific Research. The Royal Danish Academy Of Science And Letters, Matematisk-fysike Meddelelser 40, 14, Copenhagen (1983)
- Groß, G.; Kerschner, H.; Patzelt, G.: Methodische Untersuchungen über die Schneegrenze in alpinen Gletschergebieten. Zeitschrift für Gletscherkunde und Glazialgeologie 12, 2, 223–251, Innsbruck (1977)
- Hagen, T.: Report on the Geological Survey of Nepal (2): Geology of the Thakkhola including adjacent areas. Denkschr. Schweiz. Nat.-forsch. Ges. 86, 2, Zürich (1968)
- Hagen, T.: Report on the Geological Survey of Nepal (1): Preliminary Reconnaissance. Denkschr. Schweiz. Nat.-forsch. Ges. 86, 1, Zürich (1969)
- Herterich, K.: Zur Modellierung des letzten Eiszeitcyclus. Akademie d. Wiss. d. Lit. Mainz, Paläoklimaforschung 1988.
- Heuberger, H.: Untersuchungen über die letzte eiszeitliche Vergletscherung des Mount-Everest-Gebietes, Südseite, Nepal. Göttinger geogr. Abh., 81, Göttingen (1986)
- Höfer, H. v.: Gletscher und Eiszeitstudien. Sitz. Ber. d. Akad. d. Wiss. Wien, Math.-Phys. Kl. I, 79, Wien (1879)
- Höllermann, P.: Rezent Verwitterung, Abtragung und Formenbildung im oberen Suldenal (Ortlergruppe/Südtirol). Z. f. Geomorph., NF, Suppl. bd. 4, Berlin (1964)
- Kleblsberg, R. v.: Handbuch der Gletscherkunde und Glazialgeologie. 2 Bde. Wien 1948/49.
- Kuhle, M.: Klimageomorphologische Untersuchungen in der Dhaulagiri- und Annapurna-Gruppe (Zentraler Himalaya). Tagungsber. u. wiss. Abh. 42, 244–247, Dt. Geographentag 1979, Wiesbaden 1980.
- Kuhle, M.: Der Dhaulagiri- und Annapurna-Himalaya. Ein Beitrag zur Geomorphologie extremer Hochgebirge. Z. Geomorph., Suppl. Bd. 41, Bd. 1 u. 2, 1–229, 1–184. Berlin-Stuttgart (1982)
- Kuhle, M.: Der Dhaulagiri- und Annapurna-Himalaya. Empirische Grundlage. Ergänzungsband. Z. Geomorph. Suppl. Bd. 41, 1–383. Berlin-Stuttgart 1983a.
- Kuhle, M.: Zur Geomorphologie von S-Dickson Land (W-Spitzbergen) mit Schwerpunkt auf der quartären Vergletscherungsgeschichte. Polarforschung 53, 1, 31–57 (1983b)
- Kuhle, M.: Postglacial Glacier Stades of Nugssuaq Peninsula, West Greenland (70° 03'–70° 10' North). Late- and Postglacial Oscillations of Glaciers: Glacial and Periglacial Forms. 325–355. In memoriam H. Kinzl. Schroeder-Lanz, H. (ed.), Rotterdam 1983c.
- Kuhle, M.: Zur Geomorphologie Tibets. Bortensander als Kennformen semiarider Vorlandverglletscherung. Berliner Geogr. Abh. 36, 127–137, Berlin (1984)
- Kuhle, M.: DFG-Abschlußbericht über die Ergebnisse der Chinesisch/Deutschen Gemeinschaftsexpedition nach S-Tibet und in die Nordflanken von Shisha Pangma und Mount-Everest (Chomolungma) 1984. pp. 1–52, 1985a.
- Kuhle, M.: Ein subtropisches Inlandeis als Eiszeitauslöser. Südtibet- und Mt. Everest-Expedition 1984. Georgia Augusta, 35–51, Göttingen 1985a.
- Kuhle, M.: The Upper Limit of Glaciation in the Himalayas. GeoJournal 13, 4, 331–346 (1986a)
- Kuhle, M.: Schneegrenzbestimmung und typologische Klassifikation von Gletschern anhand spezifischer Reliefparameter. Peterm. Geogr. Mitt. 1, 41–51, Taf. 2 (1986b)
- Kuhle, M.: Die Vergletscherung Tibets und die Entstehung von Eiszeiten. Spektrum der Wiss. Sept. 86, 42–54 (1986c)
- Kuhle, M.: Former Glacial Stades in the Mountain Areas Surrounding Tibet – in the Himalayas (27°–29° N: Dhaulagiri, Annapurna, Cho Oyu) and in the Kuen Lun and Quilian (34°–38° N: Animachin, Kakitu, in the north), pp. 437–473. In: Joshi, S. C. (ed.), Nepal Himalaya: Geo-Ecological Perspectives. New Delhi 1986d.
- Kuhle, M.: Subtropical Mountain- and Highland-Glaciation as Ice Age Triggers and the Waning of the Glacial Periods in the Pleistocene. GeoJournal 13, 6, 1–29 (1987a)
- Kuhle, M.: Absolute Datierungen zur jüngeren Gletschergeschichte im Mt. Everest-Gebiet und die mathematische Korrektur von Schneegrenzberechnungen. Tagungsbericht des 45. Dt. Geographentages, Berlin 1985, 200–208, Stuttgart 1987b.
- Kuhle, M.: The Problem of a Pleistocene Inland Glaciation of the Northeastern Qinghai-Xizang Plateau. Reports on the Northeastern Part of the Qinghai-Xizang (Tibet) Plateau by Sino-W German Scientific Expedition, 250–315, China 1987c.
- Kuhle, M.: Zur Geomorphologie der nivalen und subnivalen Höhenstufe in der Karakorum-N-Abdachung zwischen Shaksgam-Tal und K 2-N-Sporn: Die quartäre Vergletscherung und ihre geökologische Konsequenz. Tagungsber. u. wiss. Abh. 46, Dt. Geographentag 1987, 308–311 Stuttgart 1988a.
- Kuhle, M.: Eine reliefspezifische Eiszeittheorie. Die Geowissenschaften 6, 5, 142–150 (1988b)
- Kuhle, M.: Topography as a Fundamental Element of Glacial Systems – A new Approach to ELA-Calculation and Typological Classification of Paleo- and Recent Glaciations. GeoJournal 17, 4, 545–568 (1988c)
- Kuhle, M.: Ice Marginal Ramps: An Indicator of Semi-arid Piedmont Glaciations. GeoJournal 18, 2 (1989)
- Kurowski, L.: Die Höhe der Schneegrenze mit besonderer Berücksichtigung der Finsteraarhorngruppe. Geogr. Abh. 5, 1, 115–160 (1891)
- Lichtenecker, N.: Die gegenwärtige und die eiszeitliche Schneegrenze in den Ostalpen. Verhandl. d. III. Intern. Quartär-Konferenz, Wien 1936, 141–147 (1938)
- Louis, H.: Schneegrenze und Schneegrenzbestimmung. Geographisches Taschenbuch 1954/55 414–418, Wiesbaden 1955.
- Mörner, N. A.: Faulting, fracturing, and seismicity as functions of glacio-isostasy in Fennoscandia. Geology 6, 41–45 (1978)
- Mörner, N. A.: The Fennoscandian Uplift and Late Cenozoic Geodynamics: Geological Evidence. GeoJournal 3, 3, 287–318 (1979)
- Müller, F.: Present and late Pleistocene equilibrium line altitudes in the Mt. Everest region – an application of the glacier inventory. World Glacier Inventory, IAHS-AISH Publ. no. 126, 75–94 (1980)
- Odell, N. E.: Observations on the rocks and glaciers of Mount Everest. Geogr. Journal 66, 286–315 (1925)
- Reichelt, G.: Über Schotterformen und Rundungsanalyse als Feldmethode. Peterm. Geogr. Mitt. 105, 15–24 Gotha (1961)
- Sugden, D. E.; Brain, S. John: Glaciers and Landscape. London 1976.
- Sun Zuozhe: Flat-topped Glaciers in the Qilian Mountains. Reports on the Northeastern Part of the Qinghai-Xizang (Tibet) Plateau by Sino-W German Scientific Expedition., 46–76, 1987.
- Tietze, W.: Über die Erosion von unter Eis fließendem Wasser. Mainzer Geogr. Studien 1, 125–142 (1961) (Panzer-Festschrift)
- Troitsky, L. et al.: Pleistocene glaciation chronology of Spitsbergen. Boreas 8, 401–407 (1978)
- Visser, Ph. C.: Wissenschaftliche Ergebnisse der niederländischen Expeditionen in den Jahren 1922, 1925, 1929/30 und 1935. In: Visser, Ph. G.; Visser-Hooff, J. (ed.), vol. 2, IV: Glaziologie, Leiden 1938.
- Wissmann, H. v.: Die heutige Vergletscherung und Schneegrenze in Hochasien mit Hinweisen auf die Vergletscherung der letzten Eiszeit. Akad. d. Wiss. u. d. Lit., Abh. d. math.-nat. wiss. Kl. Nr. 14, 1103–1407, Mainz (1959)
- Zheng Benxing: The influence of the uplift of the Himalayas on Quaternary Glaciers. (oral communication), 'The Neogene of the Karakorum and Himalayas' 23rd March 1988, Leicester.

## Topography as a Fundamental Element of Glacial Systems

### A New Approach to ELA\* Calculation and Typological Classification of Paleo- and Recent Glaciations

*Kuhle, Matthias, Prof., Dr., University of Göttingen, Institute of Geography, Goldschmidtstraße 5, D-3400 Göttingen, FR Germany*

**ABSTRACT:** The equilibrium line of glaciers as a climate-sensitive parameter is indispensable for the assessment of changes in climate through time. The methods previously developed for calculating the equilibrium line do not obtain, however, satisfactory accuracy. Using the statistical evaluation of data collected from 223 glaciers it is shown here that the inaccuracy of the prevailing methods generally results from the negligence of the specific glacier geometry.

In calculating realistic ELAs glaciers must be understood as dynamic systems whose variables, climatic environment and topography, are linked through feedback. The accompanying transformation in this dynamic system, which is expressed by the difference between a mathematical index and the ELA, can be exactly determined with a regression line. The climatically induced change in glacier geometry is the controlling factor, i.e. operator. The behavior of glacial systems in view of long-term climatic variations can first be understood when the details of the interdependency between topographical and climatic parameters are fully known, as will be demonstrated here.

#### Introduction

The glaciation of continents, its variability in time and space, and the associated climatic implications have long been an object of research: J. Walcher (1773) was the first to attribute changes in glaciers to climatic variations. Subsequently, several attempts were made to calculate a specific index by means of abstraction from the absolute size and configuration of glaciers. From the location of this glacier-index and its change over time it may be possible to draw direct conclusions as to the climatic conditions. First developed by Simony, Brückner, Richter, Kurowski, Finsterwalder and v. Höfer all such methods were derived on the basis of relatively little experience gained under temporal restrictions in spatially limited areas, using glaciers of the E and W Alps as examples. The technique of specific mass budget measurement developed by H. W. Ahlmann (1948) since the 1920s and the expansion of glaciological research to glaciations outside Alpine areas, especially

during the “International Hydrological Decade” (IHD, 1963–1973), as well as the publication of large scale maps of glaciers from all parts of the world provide us with a broad empirical basis to reexamine the suitability of these methods. In this context two aspects have to be considered in more detail: (1) to be of climatic significance it must be ensured that the method for determining a specific glacier index is independent with regard to the actual dimensions and geometric configuration (type) of the glaciers, (2) to be usable for paleoclimatic research the calculation method must be applicable to both former and recent glaciers with the same accuracy<sup>1)</sup>.

1) In previous studies concerning methods of ELA assessment (Gross et al. 1977; Braithwaite & Müller 1980; Hawkins 1985), for example, the applicability to various types of glaciers was not reflected. This was caused by the fact that nearly all examples given were of the firn basin type (cf. Fig 6). However, it was indicated that both piedmont glaciers and ice caps (Meier & Post 1962, 70) as well as avalanche caldron glaciers (Müller 1980, 82) have area ratios which differ significantly from those of the firn basin type.

\* ELA = Equilibrium Line Altitude

### Prevailing Methods of Determining Glacier Indexes

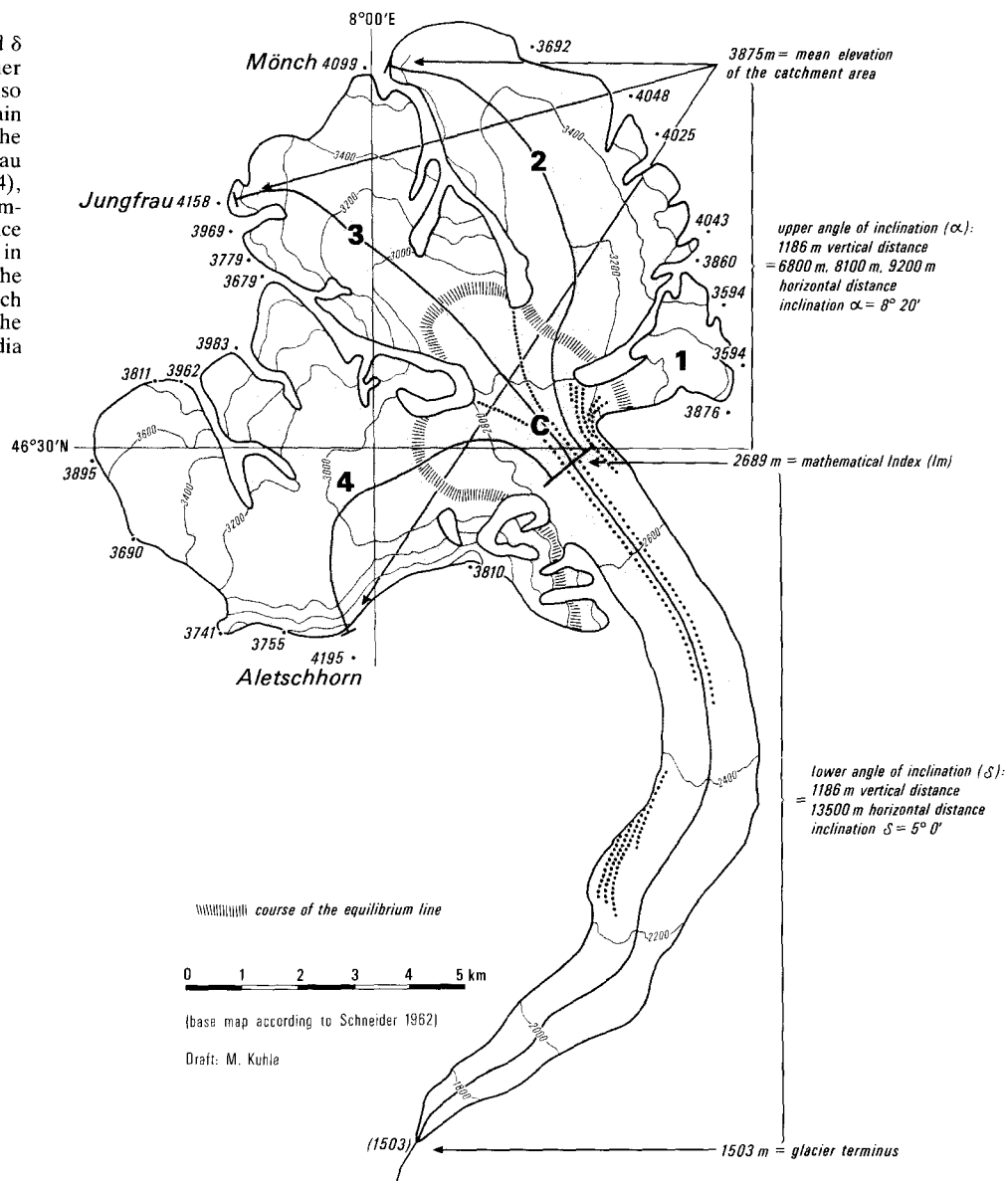
An initial approach to a specific glacier index was the "summit method" which F. Simony (acc. Drygalski & Machatschek 1942, 11) and subsequently Partsch (1882) and Brückner (1887) applied to the subrecent glaciers of the Alps. In this case, the average difference in elevation between glacier-free and perpetually firn- or glacier-covered summits is calculated. Enquist (1916) designated this as the "glaciation limit". Although this method is still being used for recent glaciers (Østrem 1966; Andrews & Miller 1972), reliable values for subrecent glaciations are not obtained. In the critical boundary zone between glaciated and unglaciated summits glacial erosion and accumulation is least distinct due to quantitative and temporal reasons and undergoes the greatest postglacial change as well. Thus, glacial evidence in the boundary zone of a former glaciation is least likely to be preserved. In addition, the climatic significance of the "glaciation limit" and its relationship to the ELA (= Equilibrium Line Altitude, i.e. the line, where ablation equals the accumulation is not yet sufficiently proven since the glaciation of summits) is greatly influenced by local topography (Andrews 1975, 49). Reliable indications of a former glaciation are, contrarily, accumulations and erosional features of ice bodies which originated in the zone of optimal glaciation. This is accounted for best by the area ratio method developed by E. Brückner (1886) and E. Richter (1888) using glaciers of the E Alps as examples. According to this method it is assumed that the zones of accumulation and ablation of a glacier have an areal ratio of 3:1 and that the resulting line separating the two represents the approximated value of the equilibrium line (in Brückner = firn line). Kurowski (1981) on the other hand, equates the area-weighted mean altitude of a glacier with its ELA (here named the snowline, however used in the modern sense of ELA), whereby he postulates that ablation and accumulation are linear functions of altitude above sealevel. R. Finsterwalder (1953) assumed that the relationship of ablation and accumulation to altitude is parabolic in calculating its ELA.

These methods were based more or less on theoretically fixed conditions for glacier mass budget because quantitative data necessary for an inductive method were not yet available. However, with the increasing information on specific mass and energy budgets of glaciers it became clear that the equilibrium line of a glacier represents a system in which several climatic factors are integrated. For example, the local variability of glacier indexes (cf. Andrews 1975, 21–28) shows that the climatic parameters constituent for glacier formation are not rigidly quantitatively fixed but are variable due to possible mutual compensation. An exact determination of the ELA is thus only possible by using the direct glaciological method (Ahlmann 1948), which is, however, limited to a few exemplary cases due to the great expenditure of work required (e.g. Storglaciären,

Schytt 1962; South Cascade Glacier, Meier & Tangborn 1965; Hintereisferner, Hoinkes 1970). In addition, this method is only applicable to recent glacier systems. This is true as well for the method of Lichtenecker (1938) and Visser (1938), which is also based on mass budget and assumes that the ELA lies in the zone of the highest lateral and medial moraines. This method yields excellent approximated values for recent and subrecent stades (Andrews, 1975, 54 f. Gross et al. 1977; Müller 1980). However it is not applicable to older phases of glaciation because lateral moraines of maximum alpine glaciations are always deposited on steep slopes subject to undercutting, i.e. the preservation of the highest glacial residuals is contingent upon relief and thus random (cf. Hawkins 1985).

Based on the voluminous quantitative glaciological data currently available (cf. Kasser 1967, 1973; Müller 1977) a promising study, in imitation of Brückner's method (1886), was made on the relationship between the mass balances of glaciers and the AAR (Accumulation Area Ratio, i.e. ratio between accumulation area and total glacier surface) with the aim of calculating the ELA for glaciers whose specific mass balances are unknown. Studies by Meier and Post (1962) on 475 North American glaciers yielded an AAR range of 0.5 to 0.8 for glaciers with balanced regimes. However, it must be taken into account here that the South Cascade Glacier, for example, with an AAR value of 0.58 has a specific net budget of zero (Meier & Post 1962, 70), while the Hintereisferner (Ötztaler Alps) with the same AAR of 0.58 (1952/53 to 1963/64, Hoinkes 1970, 59) has a negative net budget ( $b = -48.06 \text{ g/cm}^2$ ), resulting in a retreat of 27.3 m/yr (1959/60 to 1970, Kasser 1967, 1973; Müller 1977). The neighbouring Kesselwandferner with a steep crevassed tongue, on the contrary, has an AAR of 0.8 and a balanced regime (Gross et al. 1977, 232). Thus the area ratios of 0.5 to 0.8 only denote the range within which there is only one specific value at which a glacier attains a net budget of zero. In the case of the Hintereisferner an AAR between 0.5 and 0.8 signifies however a possible range in ELA of 250 m when the glacier only has a total vertical extension of 1238 m! Gross et al. (1977) consider an AAR of 0.67 (derived from eight selected Alpine firn basin glaciers) as a constant value for stationary glaciers. Wang Yinsheng et al. (1983, 23, Tab 6) calculated  $Sc/Sa$  (ablation area/accumulation area) surface ratios between 1:0.6 and 1:1.3, i.e. AAR values of 0.39 to 0.56, for glaciers of the E Tian Shan (Mt. Bogda region). Müller (1980, Tab 2) determined an average AAR of  $0.41 \pm 0.19$  ( $0.37 \pm 0.13$  for valley glaciers only) in the Mt. Everest region. On a scale of 0.37 to 0.8 for valley glaciers the ratio of accumulation to total surface area does not prove to be generally predictable. ELAs derived from an assumed AAR of  $0.6 \pm 0.1$  (Andrews 1975; Gross et al. 1977; Porter 1981; Hawkins 1985) can thus be regarded as rough approximated values and are only of limited climatic significance. The cause for this must be the lack

Fig 1  
 Determination of the angles  $\alpha$  and  $\delta$  using the Aletsch glacier (Berner Oberland, Switzerland; see also cross-section, Fig 2a). The main catchment area is formed by the Ewigschneefeld (2), the Jungfrau firn (3) and the large Aletsch firn (4), while the Grunegg firn (1) is of comparatively subordinate importance for nourishment and thus not used in the calculation of the angle  $\alpha$ ; the same is true for the middle Aletsch glacier (5) which does not reach the main valley glacier C: Concordia place



of a variable, the neglect of which gives rise to the unpredictable variation in the AAR values.

One factor essential to the formation of glaciers is topography which is, however, ignored in area ratio calculations. Müller (1980, 82) attributed the extremely low AAR values in the Mt. Everest region with an average of 0.41 to the topographical setting and the resulting specific type of nourishment (in the Mt. Everest region avalanche and firn caldron glaciers with secondary nourishment are prevalent, cf. Fig 6). Gross et al. (1977) excluded those glaciers surrounded by high backwalls and with sharp breaks in slope from their comparative studies because unpredictable deviations in the area ratio are the rule in such cases.

In case of specific mass balances, which treat glaciers as climate- (not topography-) controlled equilibrium systems, the influence of the topographical setting is

expressed only indirectly in the path of the curve for the specific mass balance (e.g. reduction in the positive balance in the area of the surrounding backwall; wind redistribution of snow; see also Young 1975). When, however, no direct observations are made or possible and a rigid mathematical method is used for the assessment of the ELA, it must be assured that the calculation is not affected by the distorting influence of topographic controls. A fundamental change in the topographical setting of a glacier, i.e. in the glacier geometry and type of nourishment (see Fig 6), is often connected with the transition from the former to recent glaciation of a region. In the Tibetan Himalayas, for example, the type of glaciation changed from recent avalanche and firn caldron glaciers to an ice stream system (Kuhle 1982, 1987), i.e. from predominantly secondary avalanche nourishment to primary snow accumulation. Hence, the

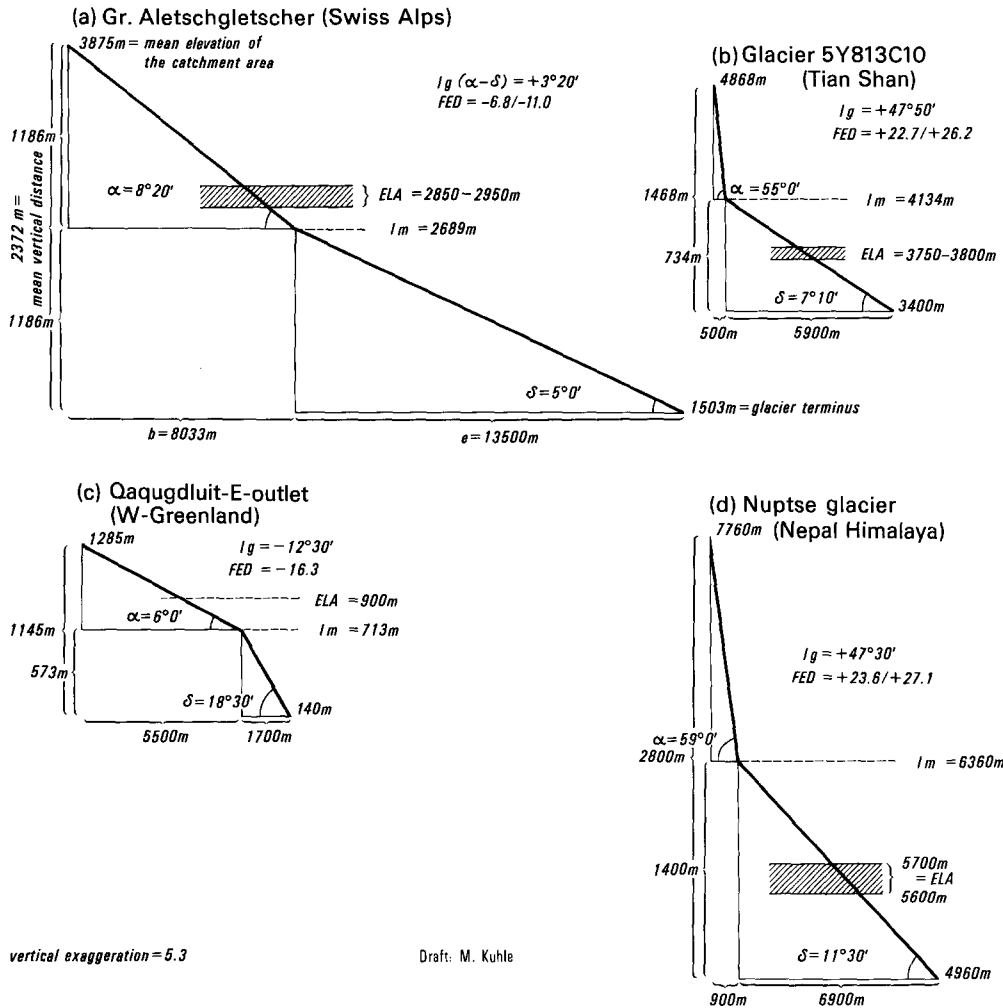


Fig 2  
 Diagram of exemplary angle differences ( $I_g$ ) and equilibrium line deviations (FED) of modern glaciers

deduction of the area ratios of more extensive subrecent glacier stades based on the area ratios of recent glaciers from the same region is impermissible in case the area ratios are dependent upon the type of glacier. In addition, the inferred area-elevation curves and thus the ELA values can be considerably different for the same glacier outline through ambivalent reconstructions of the surface contours for paleo-ice bodies (Hawkins 1985, 208). Consequently, the AAR method does conflict with both of the criteria for glacier index assessment given at the beginning.

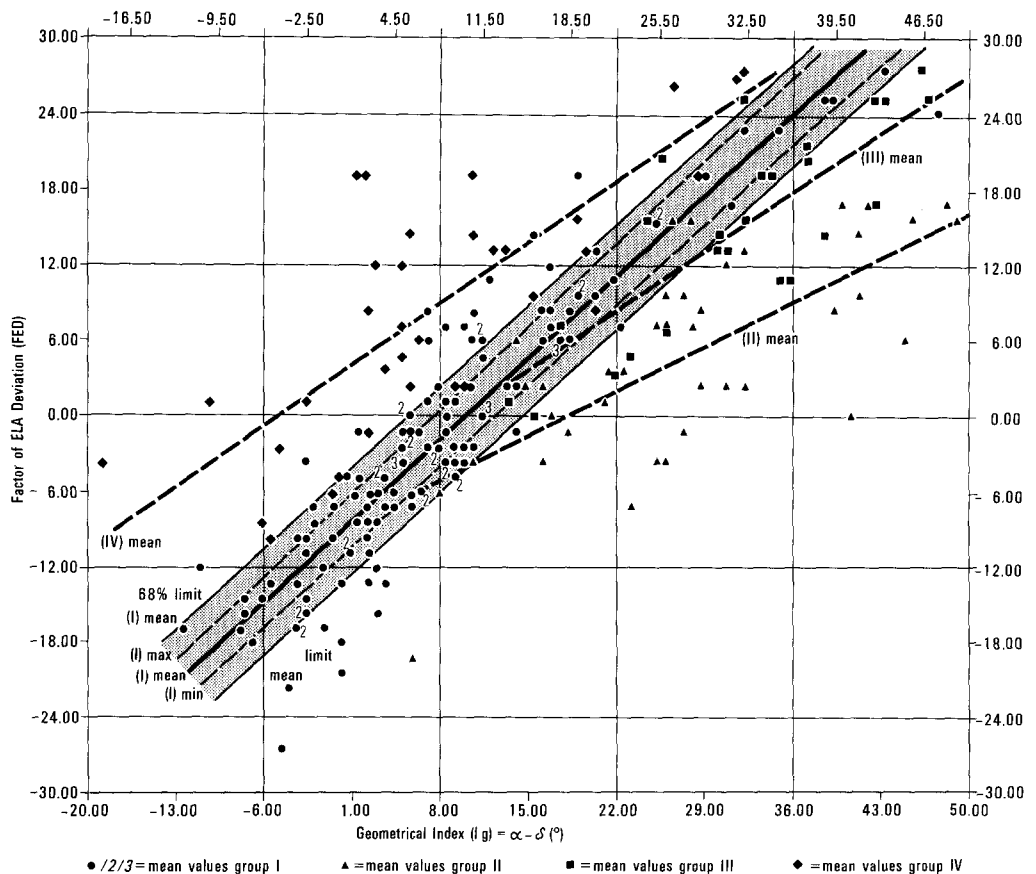
In the first instance, only the glacier outline, i.e., topographical data, can be inferred from subrecent glaciers, whereas the accompanying climatic parameters represent the desired unknown quantity. Only through the elimination of the influence which the topography has on glaciers is it possible here to determine a purely climate dependent index which approximately corresponds to the ELA. Also applying the method of v. Höfer (1879), which is recommended by UNESCO/IASH (1970 a) and uses the mathematical mean between

the average altitude of the catchment area and the glacier terminus, both factors are mixed so that the resulting shifts in the ELA do not only reveal climatic changes but changes in glacier geometry as well. To clear up these methodical uncertainties and to guarantee the interpretability of the calculated ELAs as climatic indexes, the relationship between topography and glacier behavior must be completely understood.

### Conception of the Factor of Equilibrium Line Deviation (FED)

To check and quantify the dependency of the ELA on glacier geometry a method was developed which (a) yields a glacier-specific mathematical index having the same accuracy for both recent and former glaciers, (b) depicts glacier geometry with its fundamental elements, and (c) clarifies the interdependency between the geometric index, mathematical index, and ELA via a suitable statistical analysis.

Fig 3  
Regression lines I, II, III and IV  
in the scatter diagram of the  
mean values for groups I-IV  
(Tab 1, col. 11+12)



Draft: M. Kuhle

(a) *Mathematical index ( $I_m$ )*

The method of determining a mathematical index is based on two quantities which can be determined for both former and recent glaciers with the same accuracy. First, the average summit elevation above a base value is calculated. The base value is a rough approximation of the ELA determined with the calculated mean between the highest backwall elevation and the glacier terminus

$$I_m = \frac{\text{highest summit of catchment area (m asl)} - \text{terminus (m asl)}}{2} + \text{terminus (m asl)}$$

Only the major summits of the catchment area (i.e. no points from continuous ridges) or in the case of plateau glaciers the highest points on the ice surface which lie above the base value will be regarded for the calculation of the average summit elevation. (In rare cases, the base value can lie too high, i.e. higher than the summits of a tributary component; e.g., large dendritic glaciers extending over great distances which have variations in ELA and whose individual catchment areas have very differing altitudes. For instance, the primary base value for the Muldrow glacier (Mt. McKinley) is 3554 m, so that the surrounding ridge of the Brooks glacier would be cancelled out for the most part. In this case, the mean

must be calculated from all three main components, i.e. the Muldrow, Traleika and Brook glaciers, to be 3193 m). The mathematical mean calculated with the average summit elevation and the lowest ice margin position is designated in the following as the mathematical index

$$I_m = \frac{\text{average summit elev. (m asl)} - \text{terminus (m asl)}}{2} + \text{terminus (m asl)}$$

(b) *Equilibrium line altitude (ELA)*

The ELA values (Tab 1, col. 8 and 9) were obtained in different ways. For several glaciers they were already available from longterm studies (Kasser 1967, 1973; Müller 1977). These ELAs deviate in part from the values given by Braithwaite and Müller (1980, 265, Tab 1). In such cases, both values were taken into account. Data on direct observations from Swiss glaciers were available (Müller et al. 1976). However, the values given here solely concern 1973 and thus can only be taken as conditionally representative for the corresponding long-term ELA, i.e. they are only used as an informal reference point. Emphasis was rather given to

values obtained with the Lichtenecker method (1938) which agreed very well with the long-term ELA of glaciers determined with specific mass balances (cf. Müller et al. 1976; Gross et al. 1977; Müller 1980). The Lichtenecker method was also applied to all other glaciers for which only a one-year or no direct observation was made. There were, in part, great deviations in the ELA values especially for compound glaciers facing different directions. In these cases, minimum and maximum values were given.

(c) *Geometrical index ( $I_g$ ) and the factor of equilibrium line deviation (FED)*

The next step was the attempt to discover a regular relationship between the mathematical index and the ELA. The initial idea here was that the mathematical calculation divides the continuum of a glacier between the level of the summit elevation and the terminus into two halves, taking only the vertical and not the horizontal extension into account. Fundamentally, the separation of an upper, surficially larger catchment area from a lower ablation area, which is surficially smaller due to the conical confluence of the ice, is to be expected. This corresponds to the fact, that in most cases the accumulation area of stationary glaciers is greater than the ablation area. However, the specific topography in which the glacier is formed remains disregarded. Hence, the mathematical index, for example, for a glacier with a high surrounding ridge and a gently inclined tongue would be too high and thus would divide a very steep, surficially underrepresented upper zone with low accumulation and ice formation potential from a level, oversized lower zone. In such a case, the ELA would be lower than  $I_m$  (Fig 2b, d). The opposite is true for a gently inclined plateau glaciation with steep outlet glaciers. Using a vertical averaging method the upper zone would be too large in comparison to the lower zone – the mathematical index would then lie below the ELA (Fig 2c). In order to be able to check this hypothesis comparatively, the decisive inclination relationships of the glacier must be represented. With respect to the mathematical index, the horizontal distance parallel to slope in the direction of the highest point of the catchment area, but only to the average summit elevation, is measured from the corresponding contour line on the surface of the glacier (Fig 1). In the case of compound glaciers with several components this procedure is repeated for each of the corresponding catchment areas. (In the case that the highest point of a tributary catchment area does not quite reach the mean summit height, the calculation of the angle must be done with the highest point of the catchment area).

The horizontal from the glacier terminus up to the level of  $I_m$  is calculated in the same way. The angles are obtained with the tangent, whereby  $\alpha$  denotes the upper angle of inclination and  $\delta$  the lower (Fig 1 and 2a; Tab 1, col. 4 and 5). The geometrical index ( $I_g$ ) of a glacier is

calculated by  $\alpha - \delta$  (Tab 1, col. 6) and is set in relation to the equilibrium line deviation ( $I_m - ELA$ ). Assuming that the interdependency of angle difference and equilibrium line deviation outlined above does exist, the amount of deviation ( $I_m - ELA$ ) must act linearly proportional to the vertical distance of the glaciers out of geometrical necessity. In order to eliminate absolute dimensions the factor of equilibrium line deviation (FED; Tab 1, col. 11) is expressed in percent of the vertical:

$$FED = \frac{(I_m - ELA) \cdot 100}{\text{vertical distance}}$$

(d) *Distortional effects*

In order to reveal the dependency of the ELA deviation on  $I_g$  explained in Sect. (c) effects leading to distorted results are specified and named as far as possible.

Steeply breaking off or calving tongues, for example, would have to result in an irregular raising of the mathematical index and thereby in an increase in the amount of deviation ( $I_m - ELA$ ). In the same way, noncanalized broadly flowing ablation zones (piedmont glaciers) cause the mathematical index to be relatively too high and thereby result in greater equilibrium line deviations. On the other hand, a thick debris cover on the ablation zone helps to preserve the ice mass, i.e. the glacier tongue reaches relatively lower altitudes, whereby the mathematical index is lowered, and the deviation factor decreases. Since this effect would have to be evident in dependency on the relative size of the debris-covered glacier surface, its percentage in relation to the total surface of the ablation zone was first estimated. In doing so, the thickness of the debris cover had to be disregarded. In addition, it can be expected that with very shallowly inclined tongues a cover of 75%, for example, has less of an effect on the amount of deviation than with steeper tongues which only need a short horizontal distance to acquire a greater vertical extension in a shorter time. Thus, it becomes clear that equal percentages of debris cover do not necessarily have to be accompanied by the same change in equilibrium line deviation. As shown with the following correlation, the deviation was not affected in linear proportion to the relative amount of debris cover due to this complexity. However, a general reduction in the amount of deviation can be ascertained for percentages of cover greater than 25%. Therefore, a classification of the degree of cover was abandoned. Distortion of the equilibrium line deviation is likewise to be expected with catchment areas with an average summit height over 7000 m. As telemetric temperature measurements on precipices in the Mt. Everest region have shown (Kuhle 1986b), there are virtually no temperatures above 0° C in ice or rock over 7000–7100 m alt. Thus the zones above 7000–7100 m are, according to the definition of Shumskii (1964, 407), in the recrystallization zone.



Tab 1 Geometrical indexes, mathematical indexes and equilibrium line deviation of modern glaciers\*)

1	2	3	4	5	6	7	8	9	10	11	12
A 01	Hintereisferner	Fm	11°50'	6°20'	+ 5°30'	2936	2950–3050	I 2969 1952/53–64/65 E 2995 1955–1964 E 2951 1965–1974 K/N 2972 1952/53–7475 A 2910±20 1953–1975	1	– 1.1/– 5.2	I
A 02	Kesselwandferner	Fm	9°30'	14°50'	– 5°20'	3047	3100–3150	E 3094 1953–1975	1	– 6.3/–13.0	IV
A 03	Hochjochferner	Fm	17°20'	13°20'	+ 4°00'	2984	3000–3050		1	– 1.7/– 7.0	I
A 04	Langtaufererferner	Fm	18°30'	11°30'	+ 7°00'	2922	2900–3000		1	+ 1.9/– 6.7	I
A 05	Gepatschferner	Fm	7°40'	11°30'	– 3°50'	2720	3000–3050		1	–19.4/–22.9	I
A 06	N Guslarferner	Fm	18°20'	12°20'	+ 6°00'	3064	3050–3080		1	+ 1.9/– 2.2	I
A 07	Taschachferner	Fm	12°30'	16°00'	– 3°30'	2830	3050–3100		1	–14.7/–18.0	I
A 08	Mittelbergferner	Fm	10°30'	17°20'	– 6°50'	2748	2950–3000		1/2	–15.6/–19.5	I
A 09	Marzellferner	Fm	20°20'	10°40'	+ 9°40'	2946	2950–3060		2	– 0.3/– 9.6	I
A 10	Schalferner	Fm	14°20'	8°40'	+ 5°40'	2937	2950–3050		2	– 1.3/–10.9	I
A 11	Diemferner	Fm	14°20'	10°50'	+ 3°30'	2998	3000–3100		2	– 0.3/–13.1	I
A 12	Gurglerferner	Fm	7°00'	12°30'	– 5°30'	2782	2900–2980		2	–10.1/–17.0	I
A 13	Langtalerferner	Fm	17°20'	7°00'	+10°20'	2896	2850–2950	I/K 2907 1962/63–69/70 E 2878 1963–1970 A 2850±30 1963–1970	2	+ 5.0/– 1.2	I
A 14	Rotmoosferner	Fm/Fk	24°30'	13°20'	+11°10'	2825	2800–2850		2	+ 2.5/– 2.5	I
A 15	Gaißbergferner	Fm/Fk	26°40'	12°20'	+14°20'	2899	2850–2900		2	+ 5.3/– 0.1	I
A 16a	W Vernagtferner 1969	Fm	14°00'	11°50'	+ 2°10'	3055	3050	E 3054 1965–1975 A 3080±30 1966–1975	3	– 0.7	IV
A 16b	E Vernagtferner 1969	Fm	17°50'	11°20'	+ 6°30'	3161	3100–3150	E 3054 1965–1975 A 3080±30 1966–1975	3	+ 9.2/+ 1.7	IV
A 17	Untersulzbach Kees	Fm	15°10'	11°50'	+ 3°20'	2766	2620	H 2620	4	+11.7	IV
A 18	La Cudera	Fm	18°30'	21°00'	– 2°30'	2821	2850–2900	M 2907 Ø 1973	5	– 4.4/–11.9	I
A 19	Silvrettagletscher	Fm	25°30'	9°20'	+16°10'	2809	2750–2780	I/K 2784 1960/61–69/70 N 2757 1959/60–74/75 E 2776 1961–1975 A 2760±30 1960–1975 M 2860 Ø 1973	5	+ 7.8/+ 3.8	I

Tab 1 Geometrical indexes, mathematical indexes and equilibrium line deviation of modern glaciers\*)

1	2	3	4	5	6	7	8	9	10	11	12
A 20	Ochsentalergl.	Fm	27°50'	18°30'	+ 9°20'	2754	2750–2800		5	+ 0.4/ -5.1	I
A 21	SW Vermuntgletscher	Fm	22°40'	13°20'	+ 9°20'	2752	2750–2800	M 2840 Ø 1973	5	+ 0.3/- 7.2	I
A 22	Jamtalferner	Fm	22°40'	12°50'	+ 9°50'	2758	2750–2800		5/6	+ 1.0/- 5.4	I
A 23	WLarainferner	Fk	37°30'	15°10'	+22°20'	2822	2720–2750		6	+13.0/+ 9.2	I
A 24	Vedretta di Scersen Inferiore	Fm	29°00'	9°30'	+19°30'	2950	2750–2800		7	+17.6/+13.2	IV
A 25	Vedretta di Scersen Superiore	Fm/Fk	32°00'	15°10'	+16°50'	3173	3050		7/8	+ 8.2	I
A 26	Tschierva Vadret	Fm/Fk	26°30'	15°10'	+11°20'	2955	2850–2900	M 3150 Ø 1973	7	+ 6.1/+ 3.2	I
A 27	Roseg Vadret	Fm/Fk	19°40'	11°40'	+ 8°00'	2884	2850	M 3150 Ø 1973	7	+ 2.3	I
A 28	Morteratsch Vadret	Fm/Fk	26°30'	9°20'	+17°10'	2881	2700–2800	M 3010 Ø 1973	7	+ 9.7/+ 4.7	I
A 29	Rhonegletscher	Fm	9°20'	11°50'	- 2°30'	2657	2800–2850	M 2950 Ø 1973	9	- 7.9/-11.5	I
A 30	Triftgletscher	Fm	13°40'	16°00'	- 2°20'	2485	2700–2750	M 2873 Ø 1973	9	-13.0/-16.1	I
A 31	Griesgletscher	Fm	8°40'	8°50'	- 0°10'	2795	2840–2872	I/K/N 2872 1961/62–74/75 A 2840±50 1962–1975 M 3020 Ø 1973	10	+ 0.6/-11.6	IV
A 32	Oberaletsch-Beichgletscher	Fm/Fk	27°50'	6°30'	+21°20'	2926	2850–2950	M 3170 Ø 1973	11	+ 4.8/- 1.5	II
A 33	Fieschergletscher	Fm	8°50'	9°20'	- 0.30'	2716	2900–2950	M 3193 Ø 1973	12	- 8.8/-11.2	I
A 34	Mittelaletschgl.	Fm	29°00'	12°30'	+16°30'	3034	2850–2950	M 3120 Ø 1973	11	+11.9/+ 5.4	I
A 35	Aletschgletscher	Fm	8°20'	5°00'	+ 3°20'	2689	2850–2950	M 3145 Ø 1973	11	- 6.8/-11.0	I
A 36	Unteraargletscher	Fk	30°30'	5°20'	+25°10'	2804	2650–2700	M 2957 Ø 1973	12	+ 8.6/+ 5.8	II
A 37	Oberaargletscher	Fm/Fk	26°30'	8°20'	+18°10'	2892	2780–2850	M 3007 Ø 1973	12	+ 9.5/+ 3.6	I
A 38	Gauligletscher	Fm	19°00'	10°20'	+ 8°40'	2818	2750–2850	M 2910 Ø 1973	12	+ 5.2/- 2.4	I
A 39	Rosenlaugletscher	Fm	15°30'	25°30'	-10°00'	2725	2650–2750		12	+ 4.5/- 1.5	IV
A 40	Oberer Grindelwaldgl.	Fm	24°30'	22°40'	+ 1°50'	2509	2680–2750		12	- 7.4/-10.5	I
A 41	Unterer Grindelwaldgl./without Ischmeer	Fm/Fk	25°30'	17°20'	+ 8°10'	2551	2600–2650	M 2840 Ø 1973	12	- 1.9/- 3.8	I
A 42	Langgletscher	Fm	23°30'	12°00'	+11°30'	2883	2850–2900	M 3000 Ø 1973	11	+ 1.9/- 1.0	I
A 43	Gamchigletscher	Lk	48°00'	22°40'	+25°20'	2669	2400–2500	M 2520 Ø 1973	11	+19.5/+12.3	I

Tab 1 Geometrical indexes, mathematical indexes and equilibrium line deviation of modern glaciers\*)

1	2	3	4	5	6	7	8	9	10	11	12
A 44	Gornergletscher	Fm	19°40'	8°20'	+11°20'	3105	3000–3200	M 3225 Ø 1973	13/14	+ 4.8/- 4.4	I
A 45	Findelengletscher/ without Adlergl.	Fm	13°10'	8°40'	+ 4°30'	3063	3100–3200	M 3455 Ø 1973	13/14	- 2.6/- 9.5	I
A 46	Schwarzberggletscher	Fm	30°30'	10°10'	+20°20'	3176	3000–3030	K 3030 1956–1967 M 3170 Ø 1973	13	+14.1/+12.2	I
A 47	Hohlaubgletscher	Fm	24°30'	16°00'	+ 8°30'	3195	3190	K 3190 1956–1967 M 3160 Ø 1973	13	+ 0.5	I
A 48	Allalingsgletscher	Fm	17°20'	12°20'	+ 5°00'	3266	3190	K 3190 1956–1967 M 3293 Ø 1973	13	+ 4.8	IV
A 49	Gh. del Belvedere	Fk/Lk	45°00'	16°50'	+28°10'	3095	2700–2750		13	+17.2/+13.3	II
A 50	Hohberggletscher	Fm	21°50'	24°30'	- 2°40'	3469	3450	M 3560 Ø 1973	13	+ 1.2	IV
A 51	Zmuttgletscher	Fm/Fk	37°30'	8°30'	+29°00'	3088	2850–3050	M 3090 Ø 1973	15	+14.2/+ 2.3	II
A 52	Glacier de Zinal	Fm/Fk	26°40'	10°10'	+16°30'	2956	2880–3200	M 3111 Ø 1973	16	+ 3.9/- 9.9	II
A 53	Glacier de Ferpècle (Plat. d' Herens)	Fm	15°30'	13°20'	+ 2°10'	2855	3000–3100	M 3200 Ø 1973	16	- 9.5/-16.0	I
A 54	Glacier du Mont Miné	Fm	13°10'	15°30'	- 2°40'	2802	3000–3100	M 3210 Ø 1973	16	-12.0/-18.1	I
A 55	Glacier de Moiry	Fm	15°30'	12°50'	+ 2°40'	2961	3000–3050	M 3100 Ø 1973	16	- 5.1/- 9.3	I
A 56	Haut Glacier d' Arolla	Fm/Fk	29°00'	8°10'	+20°50'	3053	2920–3000	M 3150 Ø 1973	15	+13.5/+ 5.4	I
A 57	Glacier du M. Collon	Fm	19°40'	21°40'	- 2°00'	2883	2950–3000	M 3100 Ø 1973	15	- 6.7/-10.2	I
A 58	Glacier de Tsjiore Nouve	Fm/Fk	23°30'	15°30'	+ 8°00'	2974	3000–3100	M 3320 Ø 1973	15	- 1.9/- 9.4	II
A 59	Glacier d'Otemma	Fm	20°20'	5°50'	+14°30'	3037	3000–3100	M 3126 Ø 1973	15/17	+ 3.2/- 5.4	I
A 60	Glacier du Giétro	Fm	14°00'	16°00'	- 2°00'	3117	3200	M 3220 Ø 1973	17	- 7.0	I
A 61	Glacier du Brenay	Fm	17°50'	8°50'	+ 9°00'	3181	3150–3300	M 3293 Ø 1973	17	+ 2.6/- 9.9	I
A 62	Glacier de Cheilon	Fk	42°10'	9°30'	+32°40'	3183	3000–3100	M 3160 Ø 1973	17	+18.2/+ 8.3	II
A 63	Glacier de Corbassière	Fm	14°50'	8°40'	+ 6°10'	2970	3000–3150	M 3200 Ø 1973	17	- 1.9/-11.5	I
A 64	Glacier de Boveire	Fm/Fk	26°30'	16°50'	+ 9°40'	3122	3150–3200	M 3220 Ø 1973	17	- 2.8/- 7.9	I
A 65	Hohwänggletscher	Fl	16°50'	35°30'	-18°40'	3215	3250	M 3300 Ø 1973	15	- 4.0	IV

Tab 1 Geometrical indexes, mathematical indexes and equilibrium line deviation of modern glaciers\*)

1	2	3	4	5	6	7	8	9	10	11	12
A 66	Glacier de la Dent Blanche	Fl	51°20'	24°30'	+26°50'	3600	3200	M 3240 Ø 1973	16	+26°5	IV
A 67	Glacier du Trient	Fm	20°20'	27°50'	- 7°30'	2610	2800-2900		18/19	-11.7/-17.9	I
A 68	Glacier du Tour	Fm	16°00'	21°50'	- 5°50'	2805	2850-3000		19/20	- 3.3/-14.3	IV
A 69	Gl. d'Argentière	Fm/Fk	35°30'	23°30'	+10°10'	2654	2850-2900		19	- 8.5/-10.7	I
A 70	Mer de Glace	Fm/Fk	12°30'	9°10'	+ 3°20'	2642	2850-3000		19	- 8.4/-14.4	I
A 71	Gl. des Bossons	Fm	21°50'	26°30'	- 4°40'	2864	2900-3000		21	- 1.2/- 4.5	IV
A 72	Gl. du Taconnaz	Fm	30°30'	30°30'	± 0°00'	2838	2900-3000		21	- 2.5/- 6.5	IV
A 73	Gl. de Bionnassay	Fm/Fk	26°30'	21°00'	+ 5°30'	2854	2850-3000		21	+ 0.2/- 6.6	I
A 74	Glacier de Miage	Fk	45°00'	16°00'	+29°00'	3156	2850-3000		21	+25.7/+13.1	IV
A 75	Gl. de Tré la Tête	Fm	18°30'	10°40'	+ 7°50'	2857	2850-2950		21	+ 0.4/- 5.4	I
A 76	Gl. de la Lex Blanche	Fm/Fk	30°30'	24°30'	+ 6°00'	2985	3000		21	- 1.0	I
A 77	Glacier du Miage	Fk	32°00'	9°30'	+22°30'	2977	2900		21	+ 3.2	II
A 78	Gl. du Brouillard	Fl	33°30'	27°50'	+ 5°40'	3077	3000-3050		21	+ 3.6/+ 1.3	IV
A 79	Glacier de Fréney	Fl	30°30'	27°50'	+ 2°40'	3203	3050		21	+ 8.7	IV
A 80	Gl. de la Brenva	Fm/Fk	30°30'	19°40'	+10°50'	2821	2850-2900		21	- 1.0/- 2.8	I
A 81	Gl. de Frébouze	Fm/Fk	33°40'	22°40'	+11°00'	3075	2900-2950		19	+16.4/+11.6	IV
A 82	Glacier de Triolet	Fm/Fk	37°30'	17°50'	+19°40'	3054	2850-2900		19	+15.6/+11.8	IV
A 83	Glacier de Saleina	Fm	18°30'	18°30'	± 0°00'	2682	2850-3000		20/22	- 8.9/-16.9	I
B 01	Tunsbergdalsbreen	Zf	4°30'	4°00'	+ 0°30'	1150	1382	K/N 1382 1966/67-71/72	23/24	-18.1	I
B 02	Tuftebreen	Zf	6°10'	17°20'	-11°10'	1389	1500-1550		24	- 9.8/-14.2	I
B 03	Nigardsbreen	Zf	6°50'	11°10'	- 4°20'	1110	1487-1570	I/K/N 1487 1962/63-74/75 A 1570±30 1963-1975	24/25	-24.0/-29.1	I
B 04	Storglaciären	Fm	26°40'	8°40'	+18°00'	1527	1466-1490	I/K/N 1490 1959/60-74/75 I 1466 1959/60-64/65	26	+ 7.4/+ 4.5	I
C 01	Gibsonbreen	Fm	18°30'	7°40'	+10°50'	549	500- 525		27 75/76	+ 8.2/+ 4.0	I
C 02	Ayerbreen	Fm	12°00'	6°40'	+ 5°20'	590	550		27 75/76	+ 6.9	IV
C 03	Scott Turnerbreen	Fm	16°20'	5°10'	+11°10'	573	525- 550		27 75/76	+ 7.4/+ 3.6	I
C 04	Tillbergfonna	Fm	16°50'	6°10'	+10°40'	600	550		27 75/76	+ 8.3	I
C 5	Svendsenbreen	Fm	19°10'	6°30'	+12°40'	683	600- 625		27 75/76	+16.1/+11.3	IV
C 06	Bogerbreen	Fm	16°50'	6°30'	+10°20'	634	575- 600		27 75/76	+ 8.8/+ 5.1	I
C 07	Larsbreen	Fm	8°30'	10°50'	- 2°20'	569	575- 600		27 75/76	- 1.0/- 5.4	I

Tab 1 Geometrical indexes, mathematical indexes and equilibrium line deviation of modern glaciers\*)

1	2	3	4	5	6	7	8	9	10	11	12
C 08	Longyearbreen	Fm	25°30'	6°10'	+19°20'	628	550– 575		27 75/76	+11.2/+ 7.6	I
C 09	Tufsbreen	Fm	14°00'	6°30'	+ 7°30'	597	550		27 75/76	+ 7.9	I
C 10	Frostisen/ Skandsdalsbreen	Zf	5°30'	6°40'	– 1°10'	365	420– 450		28/75	– 9.6/–14.9	I
C 11	Frostisen/ Studentdalenbreen	Zf	12°50'	11°20'	+ 1°30'	428	420– 450		28/75	+ 1.8/– 4.8	I
C 12	Jotunfonna/middle Tordalenbreen	Zf	9°10'	11°20'	– 2°10'	472	520		28/75	–10.8	I
C 13	Jotunfonna/ Elicher Tordalenbr.	Zf	6°30'	9°30'	– 3°00'	478	520		28/75	– 9.0	I
C 14	Manchester/ Southhamptonbreen	Fm	14°50'	4°00'	+10°50'	506	400		29/75	+18.9	IV
C 15	Hörbyebreen	Fs/Fm	12°20'	3°10'	+ 9°10'	483	450– 470		29/75	+ 4.3/+ 1.7	IV
C 16	Bertilbreen	Fm	19°00'	5°10'	+13°50'	498	460– 500		29/75	+ 5.1/– 0.3	I
D 01	Qaqugdloit/E-outlet (70°6'N/51°34'W)	Zf	6° 00'	18°30'	–12°30'	713	900		30 77/78	–16.3	I
D 02	Qaqugdloit/E-outlet (70°5'N/51°34'W)	Zf	5°50'	13°10'	– 7°20'	692	850– 900		30 77/78	–14.3/–18.9	I
D 03	Qaqugdloit/E-outlet (70°8'N/51°34'W)	Zf	17°50'	8°00'	+ 9°50'	873	850		30 77/78	+ 2.9	IV
D 04	Qaqugdloit/NE-outlet (70°10'N/51°38'W)	Zf	10°20'	4°10'	+ 6°10'	929	850		30 77/78	+14.2	IV
D 05	Qaqugdloit/NNW-outlet (70°10'N/51°49'W)	Zf	11°20'	6°10'	+ 5°10'	949	850– 875		30 77/78	+14.0/+10.6	IV
D 06	Qaqugdloit/W-outlet (70°7'N/51°54'W)	Zf	17°20'	11°30'	+ 5°50'	869	875		30 77/78	– 0.8	I
D 07	Qaqugdloit/S-outlet (70°5'N/51°47'W)	Zf	7°50'	6°20'	+ 1°30'	898	900– 950		30 77/78	– 0.3/– 8.7	I
D 08	Qaqugdloit/S-outlet (70°4'N/51°46'W)	Zf	6°00'	14°20'	– 8°20'	725	875– 900		30 77/78	–15.8/18.4	I
D 09	Nūgssuaq/Sermerssuaq (70°20'N/51°41'W)	Zf	7°40'	8°20'	– 0°40'	988	1000–1100		31 77/78	– 1.3/–12.5	I
D 10	Nūgssuaq/Sermerssuaq (70°21'N/51°52'W)	Zf	9°10'	8°30'	+ 0°40'	986	1000–1100		31 77/78	– 1.4/–11.7	I
D 11	Nūgssuaq/Sermerssuaq (70°22'N/52°0'W)	Zf	10°50'	5°50'	+ 5°00'	1058	1050–1100		31 77/78	+ 0.7/– 3.8	I
D 12	Nūgssuaq/Sermerssuaq (70°22'N/52°7'W)	Zf	10°10'	7°20'	+ 2°50'	1114	1150–1200		31 77/78	– 3.5/– 8.4	I
D 13	Nūgssuaq/Sermerssuaq (70°23'N/52°12'W)	Zf	15°10'	10°10'	+ 5°00'	1170	1200		31 77/78	– 3.2	I
D 14	Nūgssuaq/Sermerssuaq (70°31'N/51°56'W)	Zf	8°30'	5°10'	+ 3°20'	845	1100		31/32 77/78	–15.8	I
D 15	Nūgssuaq/Sermerssuaq (70°29'N/51°54'W)	Zf	10°10'	6°40'	+ 3°30'	945	1100–1150		31 77/78	–11.2/–14.7	I
D 16	Nūgssuaq/Sermerssuaq (70°35'N/52°20'W)	Zf	13°20'	4°40'	+ 8°40'	1212	1200–1250		33/34 77/78	+ 0.9/– 2.8	I

Tab 1 Geometrical indexes, mathematical indexes and equilibrium line deviation of modern glaciers\*)

1	2	3	4	5	6	7	8	9	10	11	12
D 17	Nûgssuaq/Sermerssuaq (70°27'N/52°28'W)	Zf	11°30'	4°40'	+ 6°50'	1083	1100		31/34 77/78	- 1.2	I
D 18	Nûgssuaq/Sermerssuaq (70°32'N/52°4'W)	Zf	15°10'	6°40'	+8°30'	1078	1100-1150		32 77/78	- 1.6/- 5.3	I
D 19	Nûgssuaq/Sermerssuaq (70°34'N/52°5'W)	Zf	14°00'	7°40'	+ 6°20'	1050	1100-1200		32 77/78	- 2.8/- 8.3	I
E 01	Blue Glacier (47°50'N/123°45'W)	Fm	20°20'	11°10'	+ 9°10'	1798	1719-1860	I/K 1719 1963/64-66/67 A 1860±90 1964-1968	35	+ 7.6/- 5.9	I
E 02	Peyto Glacier	Fm	13°10'	7°30'	+ 5°40'	2589	2630-2666	A 2630±30 1965-1975 K/N 2666 1965-1975	36	- 4.5/- 8.4	I
E 03	Lemon Creek Glacier (58°50'N/134°20'W)	Fm	5°30'	11°50'	- 6°20'	950	1075		37	-13.9	I
E 04	Worthington Glacier (61°10'N/145°40'W)	Fm	10°50'	10°30'	+ 0°20'	1248	1310		38	- 5.3	I
E 05	Bear Lake Glacier (60°10'N/149°20'W)	Fm	14°20'	8°40'	+ 5°40'	942	925- 950		39	+ 1.5/- 0.7	I
E 06	McCall Glacier (69°20'N/143°45'W)	Fm	11°10'	7°30'	+ 3°40'	1937	1925-2068	N 2068 1968/69-71/72	40	+ 1.0/-10.7	I
E 07	Muldrow Glacier	Fs	20°20'	2°20'	+18°00'	2489	2134-2439		41/42	+11.3/+ 1.6	I
E 08	Peters Glacier	Fs	24°30'	5°00'	+19°30'	2560	2195-2300		43/44	+11.3/+ 8.1	I
E 09	Peters Dome-N-Gl.	Fk	33°40'	8°10'	+25°30'	1995	1982-2104		41	+ 0.8/- 6.8	II
E 10	Ruth Glacier	Fs	10°30'	2°00'	+ 8°30'	1907	1650		45-47	+ 7.7	I
E 11	Kahiltna Glacier	Fs	14°20'	2°10'	+12°10'	2179	1677-1829		41/44 48-51	+13.0/+ 9.0	I
E 12	Tokositna Glacier	Fs	16°50'	2°30'	+14°20'	1743	1500-1615		46-48	+ 8.3/+ 4.1	II
E 13	Yentna/Lacuna Gl.	Fs	12°30'	2°00'	+10°30'	1646	1650-1829		48 52/53	- 0.1/~ 6.5	II
E 14	Dall Glacier	Fs	7°50'	3°00'	+ 4°50'	1304	1400-1550		52-55	- 4.3/-11.1	I
E 15	Chedotlothna Gl.	Fs/Fk	21°00'	2°30'	+18°30'	1777	1550-1700		52/55	+12.3/+ 4.2	I
E 16	Surprise Glacier	Fs	6°40'	4°10'	+ 2°30'	1371	1372-1524		54	± 0.0/-12.6	I
E 17	Glacier (62°57'N/151°50'W)	Fk	33°40'	5°50'	+27°50'	1897	1677-1829		52	+14.6/+ 4.5	II
E 18	Herron Glacier	Fs/Fk	32°00'	4°50'	+27°10'	2469	2000		48/52 56	+15.4	II
E 19	Foraker Glacier	Fk	35°30'	4°20'	+31°10'	2510	1982-2287		44/56 48	+16.2/+ 6.9	II
E 20	Straightaway Gl.	Fk	20°20'	4°00'	+16°20'	2297	2195-2287		44	+ 3.9/+ 0.4	II
E 21	Buckskin Glacier	Fs	21°00'	3°10'	+17°50'	1539	1350-1460		43/47 57	+ 8.9/+ 3.7	I
E 22	Kanikula Glacier	Fs/Fk	21°50'	4°30'	+17°20'	1423	1311-1524		46/49 48	+ 5.2/- 4.7	II
E 23	Malaspina Glacier	Fs	33°40'	1°20'	+32°40'	2108	900-1000	O 1000	58/59	+28.7/+26.3	IV

Tab 1 Geometrical indexes, mathematical indexes and equilibrium line deviation of modern glaciers\*)

1	2	3	4	5	6	7	8	9	10	11	12
E 24	Bering Glacier	Fs	2°30'	0°50'	+ 1°40'	1480	900–1000	O/F 1000 1949	58/60	+21.6/+17.9	IV
E 25	Kaskawulsh Glacier	Fs	2°50'	1°40'	+ 1°10'	1973	2150–2300		58	– 7.3/–13.5	I
F 01	Ndo. Soirococha NW-Gl.	Fl	37°40'	26°30'	+11°10'	4751	4700–4720		61	+ 7.7/+ 4.7	I
F 02	5455 m-peak-N-Gl.	Fl	37°40'	33°40'	+ 4°00'	4855	4800–4850		61	+ 5.9/+ 0.5	IV
F 03	5435 m-peak-N-Gl.	Fl	37°40'	35°30'	+ 2°10'	5009	4850		61	+19.0	IV
F 04	5540 m-peak-N-Gl.	Fl	48°00'	32°00'	+16°00'	4953	4850		61	+ 9.7	IV
F 05	Panta o Chacha- cumayoc-N-Gl.	Fl	45°00'	32°00'	+13°00'	4970	4850		61	+13.3	IV
G 01	Glacier 5Y813B 8	Fk	35°30'	10°10'	+25°20'	4259	3950–4000	P	62	+17.6/+14.7	I
G 02	Glacier 5Y813B 11	Fk/Lk	55°00'	11°10'	+43°50'	4393	4000–4050	P	62	+29.2/+25.5	I
G 03	Glacier 5Y813B 17	Fk/Lk	55°00'	15°30'	+39°30'	4370	4000–4050	P	62	+26.4/+22.9	I
G 04	Glacier 5Y813C 10	Fk	55°00'	7°10'	+47°50'	4134	3750–3800	P	62	+26.2/+22.7	I
G 05	Glacier 5Y725B 8	Fk/Lk	45°00'	16°00'	+29°00'	4157	3800–3850	P	62	+21.1/+18.1	I
G 06	Glacier 5Y725B 10	Fk	39°30'	8°10'	+31°20'	4202	3850–3900	P	62	+20.3/+14.5	I
G 07	Glacier 5Y725E 10	Fk/Lk	48°00'	9°20'	+38°40'	4388	3950–3990	P	62	+26.7/+24.3	I
H 01	Fedtschenko Gl.	Fs	4°40'	2°10'	+ 2°30'	4385	4600–4750	B 4600	63	– 7.3/–12.3	I
H 02	Notgemeinschaftsgl.	Fs	8°10'	3°10'	+ 5°00'	4794	4800–4900	B 4800	63	– 0.2/– 4.4	I
H 03	Tanimas 2 Gl.	Fm	15°10'	8°10'	+ 7°00'	4945	4800	B	63	+ 6.5	I
H 04	Tanimas 3 Gl.	Fm	22°40'	5°40'	+17°00'	4980	4700–4800	B	63	+14.9/+ 9.6	I
I 01	Dunde-SE-outlet	Zf	11°30'	14°50'	– 3°20'	5003	5060		64	–12.8	I
I 02	Dunde-SSW-outlet	Zf	10°50'	10°50'	± 0°00'	4975	5100		64	–19.8	I
I 03	Dunde-middle SSW-outlet	Zf	9°20'	11°30'	– 2°10'	5024	5100		64	–15.5	I
I 04	Dunde-SSW-outlet	Zf	10°30'	11°50'	– 1°20'	5084	5150–5200		64	–12.2/–21.6	I
I 05	Dunde-N-outlet	Zf	18°20'	11°10'	+ 7°10'	5086	5080		64	+ 1.1	I
I 06	Dunde-N-outlet/ 2nd from W	Zf	17°20'	7°00'	+10°20'	5046	5050–5080		64	– 0.7/– 6.2	I
I 07	Dunde-N-outlet/ 2nd from E	Zf	7°40'	6°20'	+ 1°20'	4985	5050		64	–10.7	I
I 08	Dunde-EN-outlet	Zf	5°40'	8°40'	– 3°00'	4935	5050		64	–16.2	I
K 01	Halun Glacier	Fm/Fk	27°50'	8°40'	+19°10'	5342	5000–5050		65	+20.9/+17.9	I
K 02	Ha Lang Glacier	Fm/Fk	21°50'	6°20'	+15°30'	5220	5000–5050		65	+16.4/+12.7	I
L 01	Batura Glacier	Fk	26°40'	3°10'	+23°30'	4669	4800–5100	R 5000	66	– 3.1/–10.2	II
L 02	Minapin Glacier	Fk	32°00'	9°50'	+22°10'	4274	4100–4200		67	+ 4.5/+ 1.9	II
L 03	Pisan Glacier	Lk	48°00'	16°50'	+31°10'	4850	4200		67	+13.3	III
M 01	Bazhin Gl.	Lk	51°40'	12°50'	+38°50'	5354	4600–4900	D 4700–4800	68	+17.9/+10.8	III
M 02	Shaigiri-Gl.	Fk/Lk	48°00'	17°20'	+30°40'	5404	4900	D	68	+14.0	III

Tab 1 Geometrical indexes, mathematical indexes and equilibrium line deviation of modern glaciers\*)

1	2	3	4	5	6	7	8	9	10	11	12
M 03	Hanging Glacier	Lk/FI	51°40'	27°50'	+23°50'	5716	4900	D	68	+19.4	III
M 04	Chhungphar/ Chongra-Gl.	Lk	39°50'	12°20'	+27°30'	4720	4600-4900	D	68	+ 3.2/- 4.9	II
M 05	Sachen Gl.	Lk	42°10'	9°30'	+32°40'	4706	4600-4700	D	68	+ 3.9/+ 0.2	II
M 06	Rakhiot-Gl.	Fk	32°00'	9°30'	+22°30'	5065	4750-4800	D	68	+ 8.3/+ 7.0	I
M 07	Dhaulagiri-S-Gl.	Fk/Lk	32°00'	18°30'	+13°30'	5602	5500-5600		69	+ 3.2/+ 0.06	III
M 08	Dhaulagiri-E-Gl.	Fk/Lk	27°50'	25°30'	+ 2°20'	5194	5500-5600		69	- 8.8/-11.6	I
M 09	Dhaulagiri-N-Gl.	Fk/Lk	25°30'	10°00'	+15°30'	5539	5500-5600		69	+ 1.1/- 1.7	III
M 10	Roc Noir-NNE-Gl.	Fk	37°30'	14°10'	+23°20'	5659	5500-5550		69	+ 5.1/+ 3.5	III
M 11	Lower Barun Glacier	Fm/Fk	13°10'	7°20'	+ 5°50'	5623	6000-6050		70	-17.7/-20.1	II
M 12	Khumbu Glacier	Fk	39°50'	7°30'	+32°20'	6432	5600-5720	L 5720	70/71	+27.2/+23.2	III
M 13	Barun Glacier	Fk	30°30'	4°30'	+26°00'	5841	5800-6000		70	+ 2.2/- 8.6	II
M 14	Lhotse Glacier	Lk	59°00'	12°20'	+46°40'	6585	5600-5750	L 5750	70/71	+29.6/+25.1	III
M 15	Lhotse Shar/Imia Gl.	Lk	45°00'	7°50'	+37°10'	6154	5700-5730	L 5730	70/71	+20.9/+19.5	III
M 16	Amal Dablang Gl.	Lk	59°00'	10°10'	+48°50'	5646	5300-5400	L 5400	70/71	+19.5/+13.9	II
M 17	Chhukung Glacier NE-component	FI	39°50'	19°00'	+20°50'	5615	5450-5570	L 5570	70/71	+13.9/+ 3.8	IV
M 18	Hunku Nup Glacier	Fk	39°50'	7°10'	+32°40'	5785	5560-5600		70	+25.3/+20.8	I
M 19	Hunku Glacier	Fk	51°30'	10°10'	+41°20'	6045	5800		70	+14.5	II
M 20	Makalu-W-Glacier (with Chago Gl.)	Lk	51°40'	14°00'	+37°40'	6619	5900-6100		70	+25.0/+18.0	III
M 21	Lhotse Nup Gl.	Lk	59°00'	15°10'	+43°50'	6360	5600-5700	L 5700	70/71	+27.1/+23.6	III
M 22	Nuptse Glacier	Lk	59°00'	11°30'	+47°30'	6360	5600-5700	L 5700	70/71	+27.1/+23.6	III
M 23	Hunku Shar Gl.	Fk/Lk	33°40'	7°10'	+26°30'	5965	5850-5900		70	+ 9.3/+ 5.3	II
M 24	Changri Shar Gl.	Lk	55°00'	9°30'	+45°30'	5985	5700-5750	L 5700	70/71	+17.7/+14.6	II
M 25	Changri Nup Gl.	Lk	48°00'	6°10'	+41°50'	5833	5600-5800	L 5620	70/71	+17.8/+ 2.5	II
M 26	Gyubanare Glacier	Lk	45°00'	5°10'	+39°50'	5868	5650-5800	L 5670	70	+12.0/+ 3.7	II
M 27	Lungsampa/Ngozumpa Glacier	Fk	29°00'	4°20'	+24°40'	6058	5580-5650	L 5580	70	+17.4/+14.8	III
M 28	Sumna Glacier	Lk	39°50'	7°20'	+32°30'	6060	5650-5750	L 5750	70	+17.3/+13.1	III
M 29	W-Col-W-Glacier (S of Hunku Gl.)	Fk	48°00'	12°30'	+35°30'	5980	5750-5800		70	+25.0/+19.6	I
M 30	Nangpa Lunag Gl.	Lk	45°00'	4°20'	+40°40'	5704	5600-5800	L 5800	70	+ 5.3/- 4.9	II
M 31	Pangbug Glacier	Lk	55°00'	5°50'	+49°10'	5789	5500-5600	L 5600	70	+19.3/+12.6	II
M 32	Dingjung Glacier	Lk	51°20'	8°50'	+42°30'	5666	5400	L 5400	70	+16.3	II
M 33	Langmoche Glacier	Lk	48°00'	19°40'	+28°20'	5572	5300-5500	L 5500	70	+11.6/+ 3.1	II
M 34	Kangshung Glacier	Lk	39°50'	5°30'	+34°20'	6127	5500-5600		70/72	+20.3/+17.0	III
M 35	Tuo Glacier	Lk	59°00'	18°30'	+40°30'	5653	5300-5400	L 5300	70/71	+20.2/+14.5	II
M 36	Lobuche Glacier	Fk	29°00'	14°20'	+14°40'	5566	5500-5570	L 5570	70	+ 5.8/- 0.4	II



Tab 1 Geometrical indexes, mathematical indexes and equilibrium line deviation of modern glaciers\*)

1	2	3	4	5	6	7	8	9	10	11	12
M 37	SE-Tsola Gl.	Lk	63°40'	18°30'	+45°10'	5492	5300–5450	L 5450	70	+10.3/+ 2.3	II
M 38	W-Rongbu Gl.	Fk	39°50'	3°30'	+36°20'	6206	5860–6200	G 5900–6100	72	+16.4/+ 5.0	III
M 39	E-Rongbu Gl.	Fk	22°40'	5°00'	+17°40'	6318	6200		72	+ 7.2	III
M 40	Rongtö Glacier (Gyachung-Kang-NE-Gl.)	Fk	37°30'	6°10'	+31°20'	6141	6100		72	+ 2.8	II
M 41	Gyachung Kang Gl.	Fk	48°00'	5°20'	+42°40'	6414	6000–6050		72	+17.8/+15.6	III
M 42	Gyabrag Glacier (Nangpa La-N-Gl.)	Fk	26°40'	4°30'	+22°10'	6064	5850–6100	G 6100	70/72	+ 9.9/- 1.7	III
M 43	Drolambao Glacier (Trakarding tongue)	Fk/Lk	24°30'	6°00'	+18°30'	5509	5400–5650		73	+ 5.6/- 7.2	II
M 44	Ripimo Shar Glacier	Fk	35°30'	6°50'	+28°40'	5506	5450		73	+ 3.0	II
M 45	Dropga Nagtsang Gl.	Fk	32°00'	6°00'	+26°00'	5722	5500–5650		73	+14.6/+ 4.7	II
M 46	Zemu Glacier	Fk	30°30'	4°10'	+26°20'	5617	5400	C 5400	74	+ 7.0	III

\*) Table Key

- (1) Regional association and notation
  - A = Alps
  - B = Scandinavia
  - C = W Spitsbergen
  - D = W Greenland
  - E = North America/Alaska
  - F = South America
  - G = Tian Shan
  - H = Alai Pamir
  - I = Kuen Lun
  - K = Anyemaquen
  - L = Karakoram
  - M = High Himalayas
- (2) Name of the glacier and/or coordinates of the terminus
- (3) Glacier type according to the terminology of Schneider (1962)
  - (Zf) = central firn cap
  - (Fm) = firn basin type
  - (Fs) = firn stream type
  - (Fk) = firn caldron type
  - (Lk) = avalanche caldron type
  - (Fl) = flank glaciation/wall glaciation
- (4) Angle  $\alpha$  (°)
- (5) Angle  $\delta$  (°)
- (6) Geometrical index ( $I_g$ ) =  $\alpha - \delta$
- (7) Mathematical index ( $I_m$ )
- (8) Equilibrium line altitude
- (9) Literature sources for equilibrium line values (A–R)\*\*)
- (10) Maps (1)–(74)\*\*\*)
- (11) Maximum and minimum amounts of the factor of equilibrium line deviation:  $FED = \frac{(I_m - ELA) \times 100}{\text{vertical distance}}$
- (12) Group affiliation (I/II/III)

\*\*\*) References for equilibrium line values (Tab 1, col. 9)

- (A) Braithwaite, R. J.; Müller, F. (1980)
- (B) Finsterwalder, R. (1932)
- (C) Finsterwalder, R. (1933)
- (D) Finsterwalder, R. (1938)
- (E) Gross, G.; Kerschner, H.; Patzelt, G. (1977)
- (F) Hermes, K. (1965)
- (G) Heuberger, H. (1956)
- (H) Jiresch, E. (1982)
- (I) Kasser, P. (1967)
- (K) Kasser, P. (1973)
- (L) Müller, F. (1970)
- (M) Müller, F.; Caffisch, T.; Müller, G. (1976)
- (N) Müller, F. (1977)
- (O) Sharp, R. P. (1951)
- (P) Wang Yinsheng; Qiu Jiaqi (1983)
- (R) Zhang Xiangsong; Chen Jinming; Xie Zichu; Zhang Jinhua (1980)

\*\*\*) Maps (Tab 1, Col. 10)

- (1) Karte d. Ötztaler Alpen/Blatt Weisskugel-Wildspitze; ÖAV 1951; Feldarbeiten 1942/43–1950.
- (2) Karte d. Ötztaler Alpen/Blatt Gurgl, DÖAV 1949; Feldarbeiten 1938/1943 u. 1948.
- (3) Vermagtferner 1:10000, Blatt 3 (1938–1969), Kom. f. Glaz. d. Bayerischen Akad. d. Wiss., München 1972. – In: Kasser, P., Fluctuations of Glaciers 1965–1970, 1973.
- (4) Luftbildkarte "Großvenediger" 1:10000. Pillewizer, W. (ed.): Glaziologie und Kartographie. W. Pillewizer Festschrift, Geowiss. Mitt. 21, Wien 1982.
- (5) Landeskarte der Schweiz (LKS) 1:25000 / Blatt 1198; Gletscherstand 1956.
- (6) LKS 1:25000 / Blatt 1178; Gletscherstand 1959.
- (7) LKS 1:50000 / Blatt 268; Aufnahme 1934–1948
- (8) LKS 1:50000 / Blatt 269; Aufnahme 1965
- (9) LKS 1:50000 / Blatt 255; Gesamtnachführung 1960, Nachträge 1965
- (10) LKS 1:50000 / Blatt 265; Gletscherstand 1959
- (11) LKS 1:50000 / Blatt 264; Gletscherstand: Gletscherzunge 1970 übrige Gletscher 1957–70
- (12) LKS 1:5000 / Blatt 5004; Gesamtnachführung 1969/71, Einzelnachträge 1971/74
- (13) LKS 1:50000 / Blatt 284; Gesamtnachführung 1968
- (14) LKS 1:25000 / Blatt 1348; Gletscherstand 1963
- (15) LKS 1:25000 / Blatt 1347; Gletscherstand 1967
- (16) LKS 1:50000 / Blatt 283; Gesamtnachführung 1961, 1968
- (17) LKS 1:25000 / Blatt 1346; Gletscherstand 1964
- (18) LKS 1:50000 / Blatt 282; Ausgabe 1954
- (19) Carte Touristique 1:25000, Massif du mont blanc (1); Institut Géographique National 1975.
- (20) LKS 1:25000 / Blatt 1344; Gletscherstand 1960
- (21) Carte Touristique 1:25000, Massif du mont blanc (2); Institut Géographique National, Paris 1975.
- (22) LKS 1:25000 / Blatt 1345; Gletscherstand 1961
- (23) Norge Norway 1:50000 / Blatt 1318 II; Gletscherstand 1966
- (24) Norge Norway 1:50000 / Blatt 1418 III; Gletscherstand 1966
- (25) Norge Norway 1:50000 / Blatt 1418 IV; Gletscherstand 1966
- (26) Topografisk Karta över Sverige 1:100000 / Blatt 29 I: Kebnekaise; Gletscherstand 1961
- (27) Svalbard 1:50000 / Blatt E 9; Norsk Polarinstitut, Oslo.
- (28) Svalbard 1:100000 / Blatt C 8 / Billefjorden; Norsk Polarinstitut, Oslo 1970/71
- (29) Svalbard 1:100000 / Blatt C 7 / Dicksonfjorden; Norsk Polarinstitut, Oslo 1972

- (30) Danmark / Grönland 1:50000 / Blatt 70 V. 20; Geodetic Inst. Copenhagen 1958
- (31) Danmark / Grönland 1:50000 / Blatt 70 V.2K
- (32) Danmark / Grönland 1:250000 / Blatt 70 V.2 / Umanak; Stand 1948/1953
- (33) Danmark / Grönland 1:50000 / Blatt 70 V.2E
- (34) Danmark / Grönland 1:50000 / Blatt 70 V.2J
- (35) "Nine Glacier Maps" 1:10000; Am. Geogr. Soc., Spec. Publ. no. 34 (1960); Sheet no. 2; Gletscherstand 1957
- (36) "Peyto Glacier" 1:10000; Part of 82 N 10/E; Inland Water Directorate, 1975; Gletscherstand August 1966. In: Müller, F., Fluctuations of Glaciers 1970–1975, 1977.
- (37) "Nine Glacier Maps" 1:10000; Am. Geogr. Soc., Sec. Publ. no. 34 (1960); Sheet no. 1; Gletscherstand September 18, 1957
- (38) "Nine Glacier Maps" (. . .); Sheet no. 5; Gletscherstand May 17, 1957
- (39) "Nine Glacier Maps" (. . .); Sheet no. 7; Gletscherstand July 8, 1957
- (40) "Nine Glacier Maps" (. . .); Sheet no. 9; Gletscherstand Aug. 26, 1958
- (41) Mount McKinley, Alaska 1:50000, B. Washburn, Gletscherstand 1951. In: Schweiz. Stifftg. f. alpine Forschung (ed.) Berge der Welt 1960/61.
- (42) Alaska Topographic Series (ATS) 1:250000 / Mt. McKinley; Gletscherstand 1952–1958
- (43) ATS 1:63360 Mt McKinley (A-2); Stand 1952
- (44) ATS 1:63360 Mt McKinley (A-3); Stand 1952
- (45) ATS 1:63360 Talkeetna (C-1); Stand 1951+53
- (46) ATS 1:63360 Talkeetna (C-2); Stand 1953–54
- (47) ATS 1:63360 Talkeetna (D-2); Stand 1952
- (48) ATS 1:63360 Talkeetna (D-3); Stand 1952
- (49) ATS 1:63360 Talkeetna (C-3); Stand 1951–54
- (50) ATS 1:63360 Talkeetna (B-3); Stand 1951–54
- (51) ATS 1:250000 / Talkeetna; Gletscherstand 1954–58
- (52) ATS 1:63360 Talkeetna (D-4); Stand 1952
- (53) ATS 1:63360 Talkeetna (C-4); Stand 1952/53
- (54) ATS 1:63360 Talkeetna (C-5); Stand 1952+57
- (55) ATS 1:63360 Talkeetna (D-5); Stand 1952
- (56) ATS 1:63360 Mt McKinley (A-4); Stand 1952
- (57) ATS 1:63360 Talkeetna (D-1); Stand 1951–54
- (58) ATS 1:250000 / Mt. St. Elias; Stand 1961
- (59) ATS 1:250000 / Yakutat; Stand 1948–59 und 1963
- (60) ATS 1:250000 / Bering Glacier; Stand 1957
- (61) Cordillera Vilcabamba, Perú / Blatt Panta 1:25000. E. Spiess; In: Schweiz. Stifftg. f. Alpine Forschung (ed.), Berge der Welt, Bd. 15, Zürich 1965.
- (62) Glacial Topographic Map of Mt. Bogda Region, 1:50000. Journ. of Glaciology and Cryopedology 5, 3 (1983).
- (63) Fedtschenko Tanimasgebiet / Blatt Süd und Nord / 1:50000, Finsterwalder, R.; Biersack, H.; Notgemeinschaft d. Dt. Wiss., 1930.
- (64) The Map of Dunde Glacier, 1:50000, Academia Sinica, 1982.
- (65) Climatic Geomorphological Map of Anyemaqen Region, 1:100000, by Wang Jin-Tai and Gu pei; Gletscherstand 1981
- (66) The Map of Batura Glacier, 1:60000; compiled by the Inst. of Glaciol. and Cryopedol. and Desert Research, Academia Sinica, Lanchow 1978; Prof. Papers on the Batura Glacier, Karakoram Mountains 1980.
- (67) Minapin (Rakaposhi Range) NW-Karakorum, 1:50000; Stand 1954, Schneider, H.-J., Berlin 1967.
- (68) Karte der Nanga Parbat-Gruppe, 1:50000; Deutsche Himalaya Expedition 1934. In: Finsterwalder, R., et al. (eds.). Die geodätischen, gletscherkundlichen u. geographischen Ergebnisse d. Dt. Himalaya Exp. 1934 zum Nanga Parbat. Berlin 1938.
- (69) Geomorphologische Karte des Dhaulagiri- und Annapurna-Himalaya 1:85000 von M. Kuhle; Grundlage: One Inch (1:63360) Topographic Map, Survey of India, Aufnahme 1958–1967; Kuhle, M.: Der Dhaulagiri- und Annapurna-Himalaya. Z. F. Geomorphologie, Suppl. Bd. 41, Stuttgart/Berlin 1982.
- (70) Khumbu Himal (Nepal) 1:50000, E. Schneider et al., Aufnahme 1955–1963. Hellmich, W. (ed.) Forschungsunternehmen Nepal Himalaya.
- (71) Chomolangma-Mount Everest 1:25000, E. Schneider et al., Stand 1955. (ed.) by Dt. Alpenverein u. Österr. Alpenverein and Dt. Forschungsgemeinschaft, 1957.
- (72) Qomolangma Feng Region 1:50000, "Mount Jolmo Lungma Scientific Expedition 1966–1968", Academia Sinica, China.
- (73) Rolwaling Himal (Gaurisankar), Nepal, 1:50000, E. Schneider et al., Aufnahme 1960–1968. Hellmich, W. (ed.) Forschungsunternehmen Nepal Himalaya.
- (74) Karte des Zemu-Gletschers (Sikkim-Himalaya) 1:33333, Finsterwalder, R.; Wien, K.. In: Bauer, P. Um den Kantsch. Der zweite deutsche Angriff auf den Kangchendzönga 1931. München 1933.

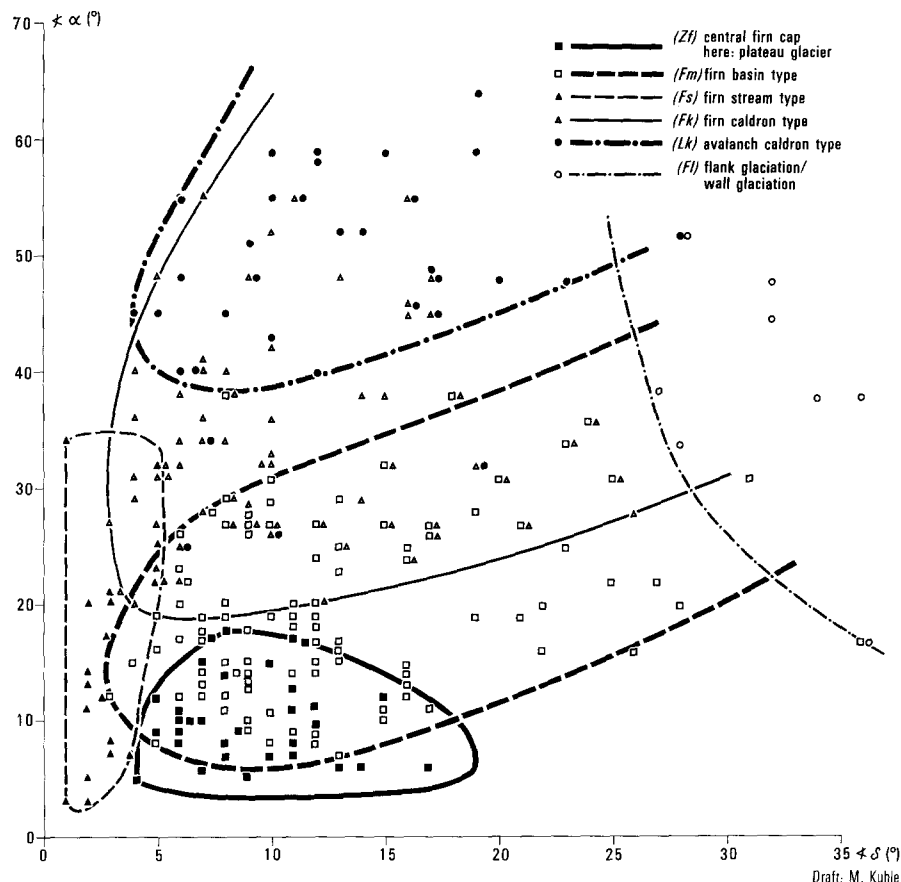
#### Images

- (75) Svalbard, Serie 1148 / S60, 1:50000, vom 7./9. Juli 1960; Norsk Polarinstitut, Oslo.
- (76) Svalbard, Serie 1248 / S61, 1:40000, vom 23.–25. 8. 1961, Norsk Polarinstitut, Oslo.
- (77) Grönland, Serie 520, 15. 7. 1948; Geodetic Institute, Denmark.
- (78) Grönland, Serie USN VJ-62 DET. "A" 77/148, 5. 6. 1953, "A" 98/145, 24. 6. 1953; Geodetic Institute, Denmark.

Firn and ice formation occur comparatively slowly here and dependent on the growing overburden pressure of accumulating snow masses. Particularly the long-term accumulation of snow at high altitudes is usually checked by lacking depositional surfaces and intensive wind drifting – the empirical upper boundary of glaciation is achieved here (Fig 6, 7; Kuhle 1986b). Therefore, in catchment areas over 7000 m an accumulation capability which is too low relative to the average summit elevation and consequently disproportionally short glacier tongues are to be expected. This would have to be expressed in an increase in equilibrium line deviation through the resulting increase in  $I_m$ . In the consistent classification of catchment areas over 7000 m undertaken here it is however problematic that mass balances are not always negative but also positive, as in some cases on leeward slopes. Moreover, there is a regional and meridian-parallel variation in the upper boundary of glacier-for-

mation, corresponding to that of the recrystallization zone (cf. Shumskii 1964, Fig 122). A general limitation to catchment areas over 7000 m, as in the case presented here, is only preliminary. This is acceptable here because all examples originate from the Himalayas and other glaciations which partly extend into the recrystallisation zone: for example Antarctica and the inland ice of central Greenland (Shumskii 1964, 408) are not used in this comparison. In summary, it is maintained that the specified, influencing distortional effects do show a tendency of increasing or decreasing the equilibrium line deviation, but only contingently allow conclusions on the absolute amounts. Other distortional effects which may affect the equilibrium line deviations like the regional variability of activity indexes (cf. Andrews 1975, 21–30) are conceivable, but are too complex and uncalculable especially regarding subrecent glaciations, and thus it is not possible to consider them. It is also to be assumed

Fig 4  
Glacier-typological scatter diagram  
based on the angles  $\alpha$  and  $\delta$  (Tab 1,  
col. 4+5)



that the glaciers chosen for comparison are in various stages of mass balance (negative, equalized, positive) with which a variation in the deviation factors must also be related. Thereby, it should be emphasized that concerning the amounts of equilibrium line deviation only integral values can be obtained (i.e. random variables) whose empirical dependency on the angle differences can only be expressed through a large number of glaciers with a more or less wide range of variation and not through a strictly functional correlation of both factors using individual cases. This range of variation in the equilibrium line deviation has advantages in reconstructing subrecent glaciations. Since the climatic and other parameters are never to be deduced a priori with the required exactness for using them in ELA calculation, the method of reconstruction must reflect the disregard of these parameters in the form of a corresponding inaccuracy. A greater accuracy can only be acquired with complementary studies, such as pollen analysis. Methods with which a calculation of a subrecent or recent ELA is designed for a definitive value from the outset can obtain this "accuracy" only through an averaging method with which the variations through marginal influences are omitted (see discussion of AAR method above). This eliminates the possibility for a subsequent specification of the values corresponding, for instance, to the regional climatic or

topographic relationships, as they can be at least tendentially evaluated in individual cases.

### Correlation of Equilibrium Line Deviation and Geometrical Index

Concurring with the previous considerations the 223 glaciers studied were divided into 4 groups (Tab 1, col. 12):

- Group I (n=130): Glaciers with ablation zones which are canalized by valley slopes, free of debris or have a debris cover of less than 25%, and have average summit heights less than 7000 m.
- Group II (n= 39): Glaciers whose ablation zones are more than 25% covered with debris and whose average summit heights are less than 7000 m.
- Group III (n= 21): Glaciers whose average summit heights are over 7000 m (all of the glaciers belonging to this group incidentally have ablation zones with debris cover over 25%).
- Group IV (n= 33): Glaciers with uncanalized, out-flowing, calving or interrupted ablation zones covered up to 25%

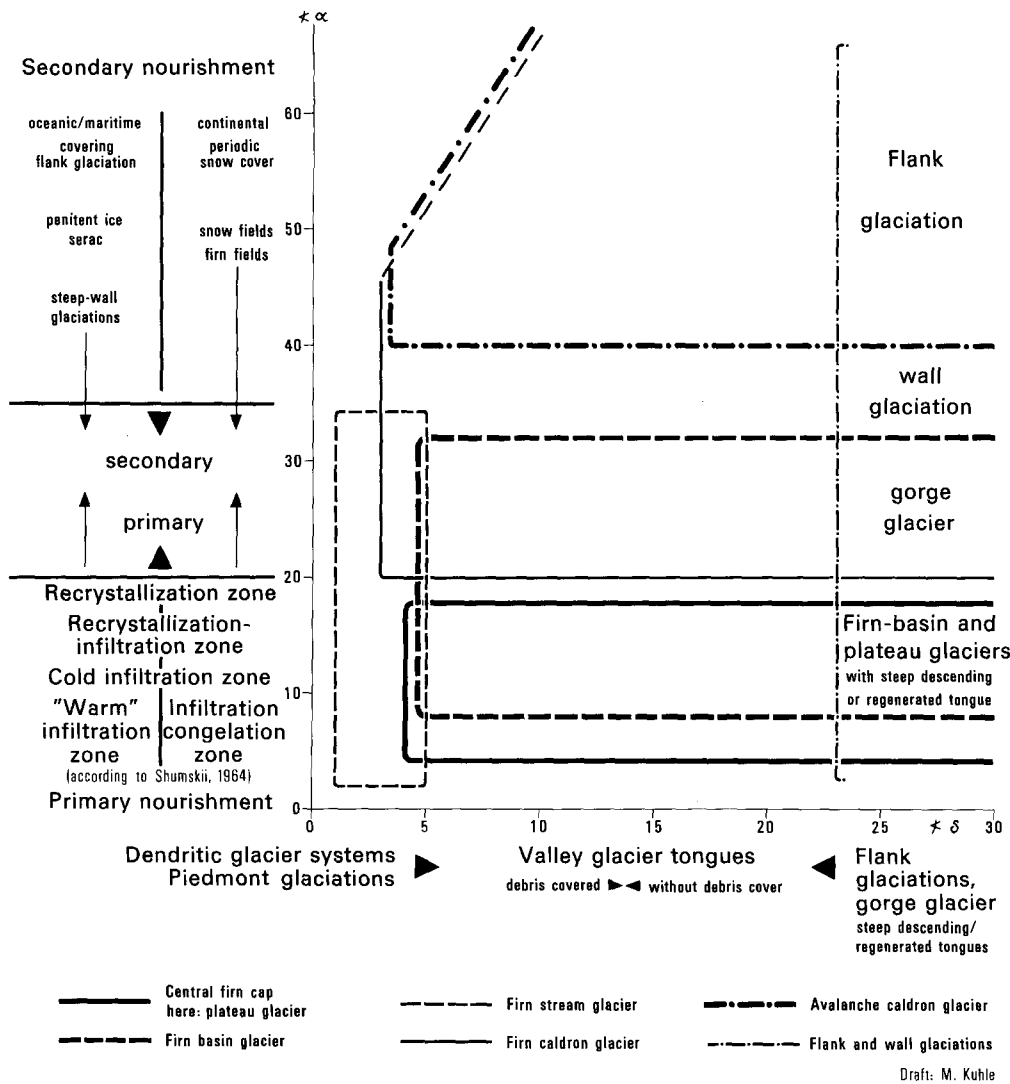


Fig 5 Idealized Glacier-typological scheme based on the angles  $\alpha$  and  $\delta$

with debris and with average summit heights under 7000 m (since a distortion of the FED through, for example, outflowing or interrupted ablation zones in the same direction is expected, these phenotypically fully opposed types were placed in the same group).

Three scatter diagrams of the maximum, minimum, and mean factors of the equilibrium line deviation were drawn for each group (y-axis = FED; x-axis =  $\alpha - \delta$ ), and a product-moment correlation after Pearson was done.

Group I, whose characteristics and number of value pairs ( $n=130$ ) are best suited for answering the previous questions, had a correlation coefficient or  $r^{xy}=0.916$  for the mean values (maxima  $r=0.915$ ; minima  $r=0.898$ ). The linear relationship of both random variables is thus highly significant. The measure of certainty B

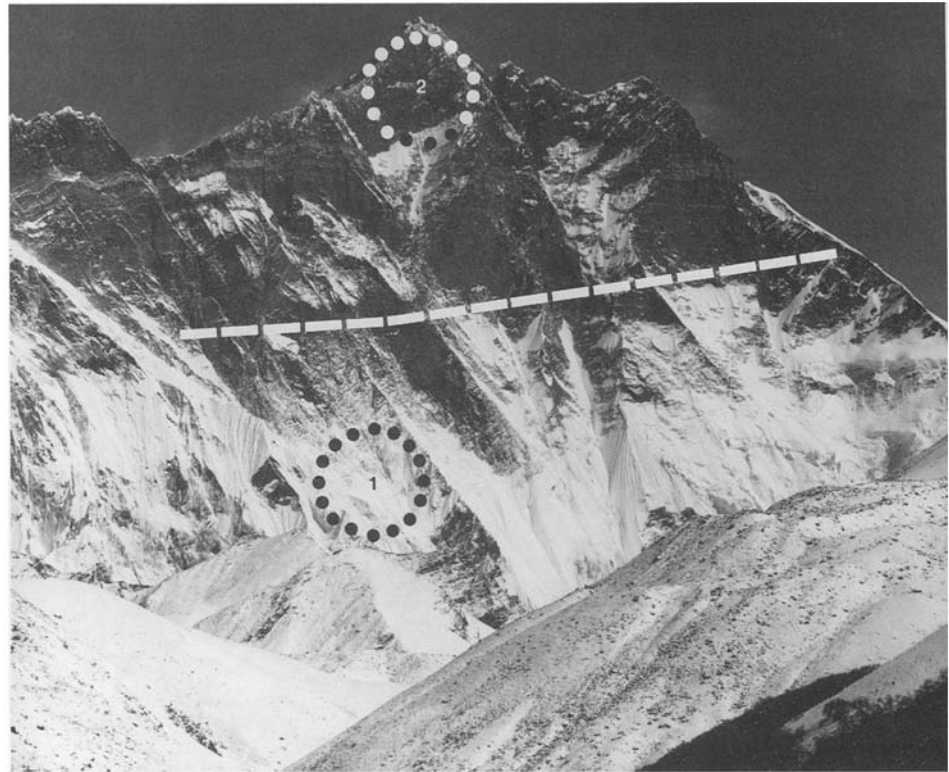
$$B = \frac{\text{explained portion of variance}}{\text{total variance}}$$

amounts to 0.84 for the mean values; i.e. 84% of the variance in the ELA deviation given by the empirical values is explained by the angle difference with linear regression (cf. Bahrenberg and Giese 1975, 149). This means that the remaining 16% of the variation can be traced back to the influence of the still unquantified distortional factors. Corresponding to a standard error of estimation (SEE) of 4.3, around 68% of the mean values lie in the range of  $\pm 4.3$  y of the average regression lines (Fig 3). The distance from the maximum and minimum regression lines to the mean regression line amounts to  $\pm 2.15$  y with a comparable SEE (max.=4.4 y; min.=4.8 y). Hence, 68% of the maximum/minimum value pairs (with an average interval of 4.3 y) are found within a range of around 13.5 y, and finally 95% of the mean values lie within  $\pm 8.6$  y of the accompanying regression line.

Group II, III, and IV clearly have a linear relationship between the variables (x/y), whereby the correlation coefficients are however generally lower, and the standard deviations higher:

Fig 6

South face of the 8501-m-high Lhotse photographed from 4300 m asl. The 7.5-km-long wall section is located 27°57'N and 86°57'E in the Mahalangur Himalaya. Above 7100 m altitude glaciation ends, independent of the wall inclination. Only sporadic remains of the first winter snow, which extends down below the timberline, is able to cling to the steep wall surface composed of basset edges of metamorphic rock. The upper glacier boundary coincides with the 0° C line at 7100 m asl. The 0° C line was determined with 1800 telemetric infrared surface-temperature measurements in 1982 and 1984 on the summits in the Mahalangur Himal. Regression analysis with a correlation coefficient of  $r_{xy} = -0,82$  yielded a boundary situated between c. 7000 m and 7200 m asl (dashed line). In the measured field at 6000–6125 m asl (dotted circle 1) surface temperatures of  $-0^{\circ}$  to  $-4^{\circ}$  C were measured under sunny weather conditions between 12<sup>00</sup> and 13<sup>00</sup> hours from Oct. 24 to Nov. 4, 1982, whereas at 8200–8500 m asl (dotted circle 2) temperatures of  $-16^{\circ}$  to  $-38^{\circ}$  C were measured. (Photo: Oct. 24, 1982, 12<sup>00</sup> hours; M. Kuhle)



Mean values of Group II:  $r=0.74$ ;  $SEE=5.4$

Mean values of Group III:  $r=0.81$ ;  $SEE=4.8$

Mean values of Group IV:  $r=0.76$ ;  $SEE=6.3$

In addition, their gradients deviate from those of regression line I (Fig 3). Considering the unavoidable quantitative inhomogeneity of the group characteristics and the comparatively small number of value pairs, nothing else could have been expected. However, the theoretical presumptions are generally confirmed through the relative arrangement of the regression lines: (a) The regression line of the mean values of Group II (over 25% of the ablation zone covered with debris) clearly runs below those of Group I, i.e., with equal x-values lower y-values are intersected. (b) The regression line of Group III lies between those of I and II. The course above II first confirms the presumed effect of catchment areas over 7000 m, i.e., the relative increase in the y-values. The course below I shows contrarily that the positive shift of the mean values caused by the level of the catchment area is not capable of balancing or overcompensating the negative shift caused by the debris cover over 25% of the ablation area (see characteristics of Group III above).

Individual glaciers, however, with catchment areas around 8000 m attain or penetrate even the zone of the "normal glacier" (I) (cf. Fig 2d with b; with corresponding angle differences the Nuptse glacier with a catchment area at 7760 m alt. in spite of its 80% debris cover over the ablation zone has a slightly larger FED than the

5Y813C10 glacier with a bare tongue and a catchment area at 4868 m alt.) and are all characteristically above the accompanying (III) regression lines of the mean values, whereas the glaciers with catchment areas between 7000–7500 m alt. are found below. (c) The regression line for Group IV (outflowing or interrupted ablation areas) runs clearly above I, i.e., with equal x-values larger y-values are intersected.

#### *Application of the factor of equilibrium line deviation to former glaciation*

The calculation of equilibrium line deviations for subrecent glaciers must involve the reconstruction of three values: (a) the altitude of the glacier terminus, (b) the average summit elevation above the base value, and (c) the glacier level in the zone of the mathematical index ( $I_m$ ). The last value is obtained from lateral moraine relicts, striation boundaries, or interpolation between both. With this information the horizontals b and c (Fig 1 and 2a) of the subrecent glacier can be determined. In calculating the equilibrium line deviation ( $I_m - ELA$ ) it is advisable in the heuristic viewpoint to presume a variance spectrum of 8.6 (FED) units (Fig 3, screened zone). Thereby, at least the mean value and the average maximum and/or minimum range of variation of the subrecent position of the snowline is achieved with 68% probability. For glaciers which fall in one of

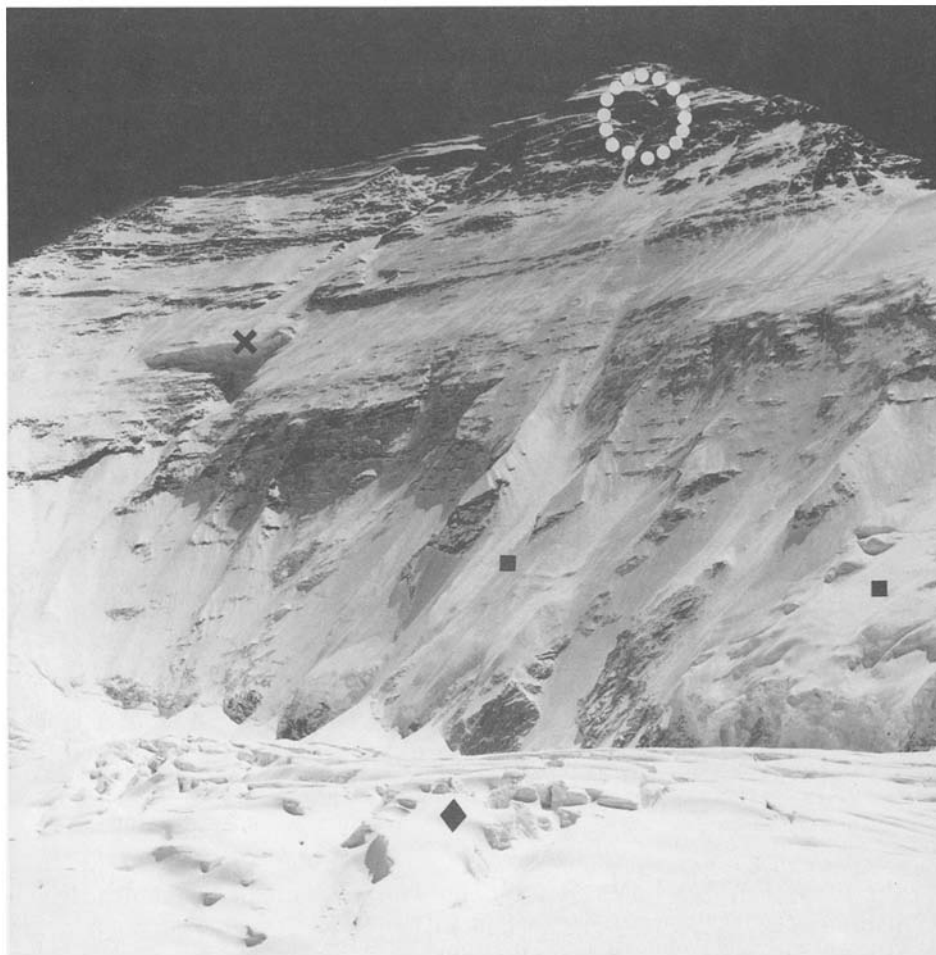


Fig 7  
NNW face of 8848 m high Mt. Everest (Chomolungma, 27° 59' N/86° 56' E) photographed from the upper firn basin of the central Rongbuk Glacier at 6010 m asl. The snow and firn cover (◆) extending up to the foot of the wall at 6450 m asl belongs to the level at which snow transformation primarily occurs through the type of metamorphism close to the melting point. Within the lower 800 m (■) of the NNW face of Mt. Everest as well, the seasonal, midday warmth leads to a snow-to-ice consolidation through settling, sintering, and ice formation between grains. This process allows snow, firn and ice to cling to the wall in spite of the steepness. Pressure compaction here is less than in the level firn basin. Above ca. 7000–7200 m altitude flank glaciation and glacier formation cease. The 0° C boundary is attained (cf. Fig 6), and mostly very low temperatures make the metamorphic processes, which occur at lower altitudes, impossible. Metamorphism through molecular diffusion of cold snow, as it occurs in the central plateau regions of Antarctica, requires the overburden pressure of thick snow accumulation and, thus, sufficiently long time. Here the relief makes this impossible, because the very cold and therefore physically dry snow is, at this altitude, not only shifted (as on the ice surfaces in Antarctica and Greenland) but also blown away. Only in stable lee positions, as in the Norton couloir, do seracs (×) over 100 m in thickness have a chance to form above 7200 m altitude. The snow and firn thicknesses necessary for glacier formation under extremely cold conditions accumulate on shallowly dipping rock ledges in the wind shadow. Whereas only slightly negative temperatures were recorded at the foot of the wall under sunny weather conditions in 1984, the author registered temperatures of  $-28^{\circ}$  to  $-36^{\circ}$  C at the summit (dotted circle) in September and October. Corresponding to prevailing westerly winds, the snow blown from the NNW and SSW faces of Mt. Everest toward the E does not contribute to the nourishment of the central Rongbuk and Khumbu glaciers. (Photo: Sept. 30, 1984, 16.30 hours; M. Kuhle).

snow and firn thicknesses necessary for glacier formation under extremely cold conditions accumulate on shallowly dipping rock ledges in the wind shadow. Whereas only slightly negative temperatures were recorded at the foot of the wall under sunny weather conditions in 1984, the author registered temperatures of  $-28^{\circ}$  to  $-36^{\circ}$  C at the summit (dotted circle) in September and October. Corresponding to prevailing westerly winds, the snow blown from the NNW and SSW faces of Mt. Everest toward the E does not contribute to the nourishment of the central Rongbuk and Khumbu glaciers.

the special groups II, III, and IV a rough but tendential estimation of the direction and amount of deviation is possible with the corresponding regression lines (Fig 3). Example: Suppose that the *Hinterseiferner* (Ötztaler Alps) in its present form was the object in reconstructing a subrecent ELA. Using the regression line (I) of the mean values and its standard deviation (see above) the FED at an angle difference ( $I_g$ ) of  $+5^{\circ} 30'$  is 8.8 to  $-0.2$  (cf. Fig 3; intersect. of  $+5^{\circ} 30'$  with the upper and lower 68% line). Thereby, the former ELA can be calculated to be 2939–3045 m using

$$ELA = I_m - \frac{FED \cdot \text{vertical distance}}{100}$$

(the empirical value of the ELA, based on measurements between 1952/53 to 1974/75 is at 2950 to 3050 m; Kasser 1973; Müller 1977; Gross et al. 1977). The ratio of the range of variation of the reconstructed ELA of 106 m to the average vertical (1238 m) is 1:12.

On the other hand, when the area ratio method is applied in the same case without anticipating assumptions, e.g., concerning the climatic regime, which is not known in case of subrecent glaciers, at least AAR values between 0.5 and 0.8 would have to be assumed (Meier 1962, 70; Porter 1975). The ratio of the related variation in the ELA of 250 m (2770–3020 m; Hoinkes 1970, Tab 2) to the average vertical of the glacier is, on the contrary, 1:5!

#### Glacier Typology Based on Surface Geometry

The proof that there is a significant correlation between glacier geometry and the ELA also evidences that topography is a fundamental element of glacial systems. The climatic parameters critical for the mass balances of glaciers belong to a relatively independent subsystem and can be analyzed independently, but are

insufficient for inferring glaciers in their concrete manifestation. A system with which the glacier as a whole can adequately be described is first obtained at a higher level of integration by linking climatic parameters with topographical parameters. There are various approaches to typologically classify the variability in glaciers contingent on the specific topography. Among these are the relief-contingent classification of land ice (J. K. Charlesworth 1957), the digital glacier classification of UNESCO (1970), and the glacier typification by H. J. Schneider (1962), which is based on the form of the catchment area. In each of these cases, glaciers are classified based on formal criteria separating them into discrete groups. However, it is an essential point of this study to describe the continuous transition in topography, i.e., glacier geometry, which accompanies the primarily climate-induced expansion or retreat of a glaciation. This conception would correspond to the method of H. W. Ahlmann (1948) by which the different glacier configurations are quantified and made comparable to one another by plotting a so-called "normal curve" (= the vertical extension of a glacier is divided into 10 equal intervals on the abscissa, and the respective percentages of surface area are entered on the ordinate). This method has the disadvantage of being very time-consuming and presents the difficulty, especially for subrecent glaciations, of determining the exact surface area and contours.

Since the description of glacier geometry can be reduced to the angles  $\alpha$  and  $\delta$ , as has been proven sufficient with regard to equilibrium line deviation, it was checked whether this could also be used as a meaningful characterization of glaciers. To show the phenotypes, the localities of the 223 glaciers were each given signatures on the  $\alpha/\delta$  coordinates. These signatures (Tab 1, col. 3) correspond to the terminology of Schneider (1962): (1) central firn cap (Zf), (2) firn basin type (Fm), (3) firn stream (Fs), (4) firn caldron (Fk), (5) avalanche caldron (Lk), and flank glaciation/wall glaciation (Fl). (Schneider's ice stream system (7) did not prove to be distinguished, since it represents a more quantitative than a qualitative variation of the firn stream type (3); Schneider 1962, 281). When two types of nourishment appear to participate equally in the formation of a glacier, this would be marked with the corresponding combination of symbols (Fig 4).

The distribution of glacier symbols in the  $\alpha$  (y-axis)/ $\delta$  (x-axis) diagram has two basic attributes (Fig 4): (1) the individual types form coherent groups with clear concentration zones, and (2) no one type has a numerically exclusive range – all zones are overlapped on the periphery by other groups. The empirical continuity of types, which exhibits successive quality differences, is thereby adequately substantiated. An attempt at schematizing this in an idealized way through extrapolation of the values on hand is made in Fig 5. (The zone of the central firn cap consists here only of values from plateau glaciers with outlet tongues.

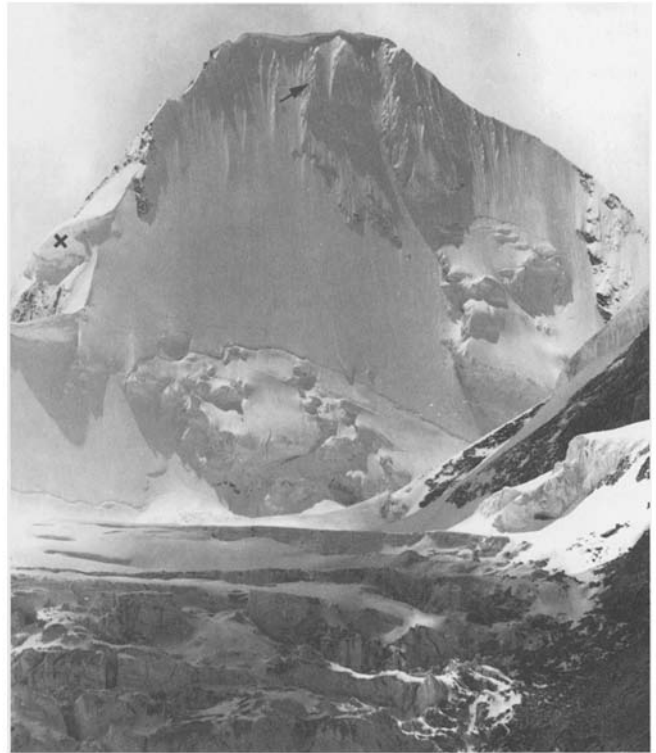


Fig 8 ENE face of the 6714 (6697)-m-high Lingtrense (28°02'N/86°51'E) photographed from the central Rongbuk Glacier. Independent on the exposure to the wind, as the view of the S face with a serac (X) which has a greater exposure to the wind shows, the 6000 to 7000 m high summits are covered with flank glaciations. The extreme steepness of the walls evidence the meaningless of the degree of inclination for the ice cover at this altitude; the temperatures drop below freezing sufficiently often so that adhesion to the rock and metamorphism of new snow are possible (in contrast, cf. Fig 6, 7). Avalanche tracks and the flowage of seracs substantiate that the central Rongbuk Glacier is nourished by this wall. Up to an altitude of c. 7000–7200 m, the steep faces in the Mt. Everest region contribute largely to glacier nourishment. Snowfall and hoar-frost also add to flank glaciation at this altitude. This is shown by the formation of ribbed firn (→) on the upper 120 m of the wall. (Photo: Sept. 24, 1984, 14.20 hours; M. Kuhle).

According to definition, however, continental glaciations also belong to this type (Schneider 1962). Taking them into account would presumably effect an expansion of the Zf zone into that of the Fs type up to a  $\delta$  of 1°. It is to be mentioned here that the overlapping zones are mainly composed of transitional types – which cannot be defined as one or the other since the transition is continuous – or are composed of glaciers of one type containing at least some elements of another type – for example, obvious firn caldron components are linked to an obvious firn stream glacier. Specifying data on the characteristics of the accumulation and ablation areas were able to be related to the absolute values of the angles  $\alpha$  and  $\delta$ . Up to an angle of  $\alpha = 20^\circ$  primary glacier nourishment can be regarded as predominant. Between 20° and 35° a proportionally increasing mixture

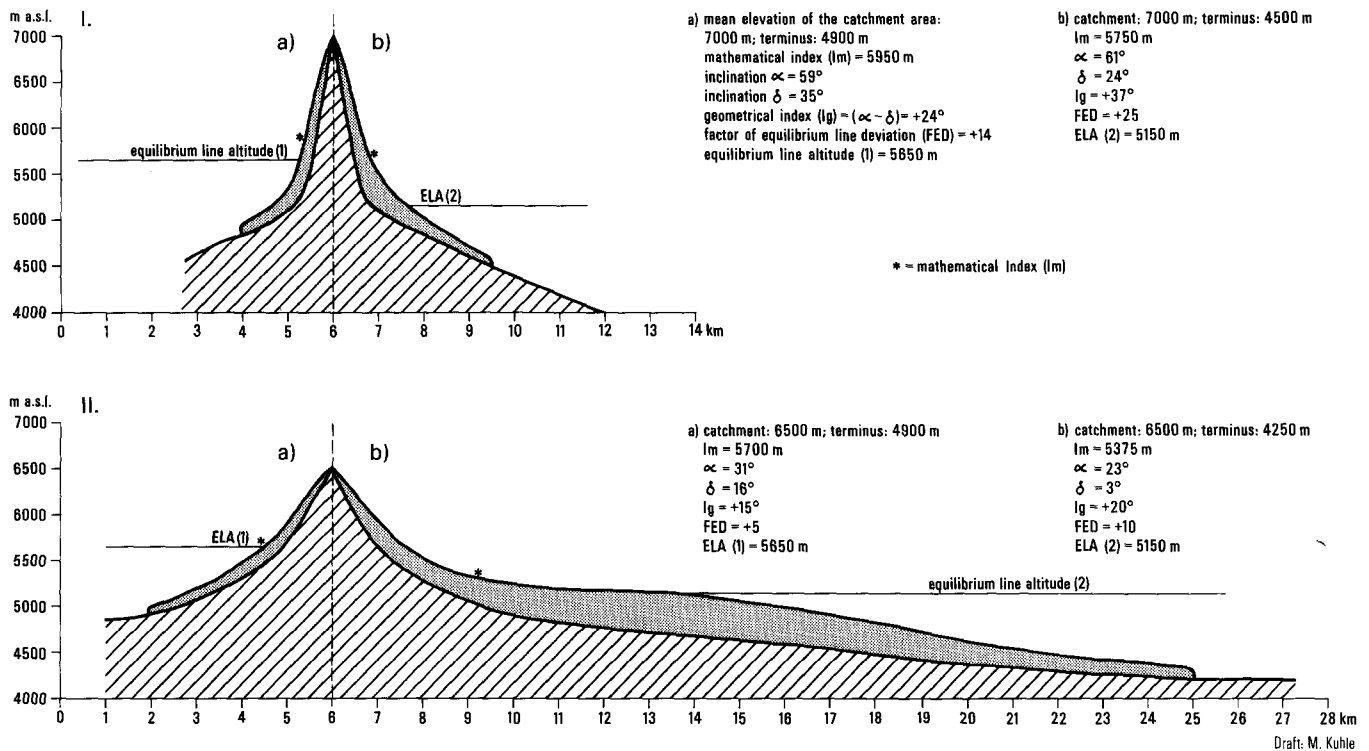


Fig 9 Dependency of the intensity of glaciation on topography: I corresponds to the relief of the main chain of the Himalayas, II to the relief within the central Tibetan plateau. Under equal climatic conditions the glacier termini of Ia and IIa reach the same altitude although the feeding ground of Ia is 500 m higher; this can be put down to the smaller accumulation capacity of the steeper feeding ground of Ia ( $\alpha = 59^\circ$ ). When reducing the ELA by 500 m Ib only reaches 4500 m while IIb flows down to 4250 m. The FED was calculated using regression line I (Fig 3).

with secondary nourishment is characteristic. Above  $35^\circ$  the former decreases to the advantage of the latter. The classification of thermodynamic ice formation processes worked out by Shumskii (1964, Fig 122) is interesting here insofar as phenomenological differences in numerically identic glaciers can also be explained with the related differentiation in maritime/oceanic and continental zones. Thus, regarding the firn caldron type, for example, steep walls in an oceanic climate can be occupied by thick flank ice, seracs, and wall ice flowing down into gorges (Fig 8), whereas in continental climates only thin snow and firn fields are observed, or at very high absolute altitudes the walls extend up into the recrystallization zone and are thus only periodically covered with snow (Fig 6 and 7; Kuhle 1986b).

In comparison, the  $\delta$  values allow an evaluation of the configuration of the tongue – but here as well the given boundaries (Fig 5, x-axis) are only to be understood as major tendencies along a continuous transition.

### Topography and Climate-Elements of a Glacial Feedback System

Shifting of the topographic setting of glaciers is primarily caused by climatic changes and thus proceed-

ing expansion or retreat of the ice body. However, the linkage between climatic and topographic parameters is not dominated by one or the other but acts in the way of a true feedback system (cf. Ashby 1964). The amount of increase in surface area evoked by an initial lowering of the ELA is the decisive factor for the effect which topography has on the climate. On the S slopes of the Himalayas, for example, an ELA depression of 500 m still remains within the zone of high relief and thus effects a comparatively slight enlargement of the catchment areas and no significant change in glacier geometry (Fig 9 I a–b). In Central Tibet, however, such an ELA depression of 500 m causes the small steep alpine glaciers to reach the level of the high plateau where they build up coalescing piedmont glacier lobes (Fig 9 II a–b) and finally an inland ice sheet (cf. Kuhle 1986a, 1987 and this volume). The very small recent glaciation of the Tibetan plateau as compared to that one of the Alps resulted in the view that the glaciation of Tibet did only increase as insignificantly during the Pleistocene and fell behind in relation to the glaciation of the Alps; the reason being the aridity (v. Wissmann 1959). Due to the influence of topography, however, similar climatic conditions can result in very different intensities of glaciation, as is shown in Fig 9. Thus, topographical parameters are of the same influence on glacial formation as are climatic



parameters. Therefore, differences in the actual and former dimensions of glaciations do not necessarily depict solely climatic but also topographical differences and variations. Topographically induced enlargement of a glacier has climatic consequences though: the Tibetan debris and rock surfaces, which presently absorb 80% of the solar radiant energy and thus heat up the atmosphere, changed during the Pleistocene glaciation into cooling surfaces by reflecting 95% of the energy. The induced negative shift of temperature leads once again to a lowering of the ELA and a further expansion of the glaciated area. (The 2–2.4 million km<sup>2</sup> inland glaciation of Tibet was apparently build up by this kind of a self-boosting process. Due to the subtropical situation in the case of extreme radiation transparency in the atmosphere at great altitudes where the irradiation is three to four times more than in higher latitudes the impact on the earth's thermal balance was so severe that the Tibetan ice sheet induced the onset of the ice age (Kuhle 1986a, 1987 and this volume).

It can be generally said that the surface effectiveness of a shift in the ELA is all the greater, the smaller the values are, which the angles  $\alpha$  and  $\delta$  in glacier geometry have. The concrete effect that the topographically controlled surface growth has on the climate is, on the other hand, determined by the altitude above sea level and latitude as a function of the solar radiant energy.

## Conclusions

A regular interdependency between glacier geometry and mass balance is proven by the highly significant correlation between the geometrical glacier index ( $I_g$ ) and the factor of equilibrium line deviation FED.

Particularly concerning paleoglaciers which are only accessible in their entirety, glaciers must thus be treated as complex systems whose fundamental components contain both climatic and topographic parameters. To be able to purely climatically interpret regional and temporal shifts in the ELA the distorting influence of the specific topographical setting must hence be excluded. This has not previously been done when using the customary methods for approximately calculating the ELA. The accuracy achieved when calculating equilibrium line deviation affected by the heterogenous glacier geometry depends on the number of value pairs used in the investigation. Through the increasing availability of long-term mass balance data and the production of large scale glacier maps the accuracy of predications will improve further. The expansion and retreat of glaciations is accompanied by a continuous change in the topographical setting. The variations of glacier geometry which are quantitatively given on the  $\alpha/\delta$  coordinate axes (Fig 6) indicate (a) a change in the factor of equilibrium line deviation and (b) that identical amounts of shift in the ELA cause differing amounts of change in the surface of catchment areas depending on whether the shift in the ELA occurs in an area with high or low relief (Fig 9). Since a change from rock and debris surfaces to permanent snow cover induces a significant change in the atmospheric temperature balance, the variability in glacier geometry has a distinct effect on the climate. The impact on the climate increases at identical surface areas dependent upon the solar radiation with altitude above sea level, and with low latitudes. The investigation of the feedback between topographical and climatic parameters of glacial systems in their respective global positions appears to be of fundamental importance in understanding paleoclimatic evolution (Kuhle 1986a, 1987 and this volume).

## References

- Ahlmann, H. W. son: Glaciological Research on the North Atlantic Coasts. Royal Geographical Society London, Research Series 1, 83 (1948)
- Andrews, J. T.: Glacial systems. An approach to glaciers and their environments. Duxbury Press, North Scituate, MA 1975.
- Andrews, J. T.; Miller, G. H.: Quaternary history of northern Cumberland Peninsula, Baffin Island, N.W.T., Canada: Part IV: Maps of the present glaciation limits and lowest equilibrium line altitude for north and south Baffin Island. Arctic and Alpine Research 4, 1, 45–59 (1972)
- Ashby, W. R.: An Introduction to Cybernetics. Methuen, New York 1964.
- Braithwaite, R. J.; Müller, F.: On the parameterization of glacier equilibrium line altitude. World Glacier Inventory, IAHS–AISH Publ. No. 126, 263–271 (1980)
- Brückner, E.: Die Hohen Tauern und ihre Eisbedeckung. Zeitschrift des Deutsch-Österreichischen Alpenvereins 17, 163–187 (1886)
- Brückner, E.: Die Höhe der Schneelinie und ihre Bestimmung. Meteorologische Zeitschrift 4, 31–32 (1887)
- Charlesworth, J. K.: The Quaternary Era. London 1957.
- Drygalski, E. v.; Machatschek, F.: Gletscherkunde. Enzyklopädie der Erdkunde. Wien 1942.
- Enquist, F.: Der Einfluß des Windes auf die Verteilung der Gletscher. Bulletin of the Geological Institute, Uppsala, 14, 1–108 (1916)
- Finsterwalder, R.: Wissenschaftliche Ergebnisse der Alai-Pamir Expedition. Teil 1. Geodätische, topographische und glaziologische Ergebnisse, 1, Berlin 1932.

- Finsterwalder, R.: Gletschergeschwindigkeitsmessungen und gletscherkundliche Bemerkungen. In: Bauer, P. Um den Kantsch, 141–143, München 1933.
- Finsterwalder, R.: Die geodätischen, gletscherkundlichen und geographischen Ergebnisse der Deutschen Himalaya-Expedition 1934 zum Nanga Parbat. Teil II: Gletscherkunde, 106–157, Berlin 1938.
- Finsterwalder, R.: Die zahlenmäßige Erfassung des Gletscherrückganges an Ostalpengletschern. Zeitschrift für Gletscherkunde und Glazialgeologie 2, 2, 189–239 (1953)
- Flint, R. F.: Glacial and Quaternary Geology. John Wiley & Sons, New York 1971. (Chs. 4, 18)
- Gross, G.; Kerschner, H.; Patzelt, G.: Methodische Untersuchungen über die Schneegrenze in alpinen Gletschergebieten. Z. f. Gletscherkunde u. Glazialgeologie 12, 2, 223–251 (1977)
- Hawkins, F.: Equilibrium-line altitudes and paleoenvironment in the Merchants Bay area, Baffin Island, N.W.T., Canada. Journal of Glaciology 13, 109, 205–213 (1985)
- Hermes, K.: Der Verlauf der Schneegrenze. Geographisches Taschenbuch 1964/65, 58–71, Wiesbaden 1965.
- Heuberger, H.: Beobachtungen über die heutige und eiszeitliche Vergletscherung in Ost-Nepal. Z. f. Gletscherkunde u. Glazialgeologie 3, 349–364 (1956)
- Heuberger, H.: Die Schneegrenze als Leithorizont in der Geomorphologie. In: Höhengrenzen in Hochgebirgen; Arb. a. d. Geograph. Inst. d. Univ. d. Saarlandes 29, 35–48 (1980)
- Höfer, H. v.: Gletscher- und Eiszeitstudien. Sitzungsber. d. Akad. d. Wiss. Wien, Math.-Nat. Kl. 1, 79, 331–367 (1879)
- Hoinkes, H.: Methoden und Möglichkeiten von Massenhaushaltsstudien auf Gletschern. Ergebnisse der Messreihe Hintereisferner (Ötztaler Alpen) 1953–1968. Zeitschrift für Gletscherkunde und Glazialgeologie 6, 1/2, 37–90 (1970)
- Jiresch, E.: Die geodätischen und kartographischen Arbeiten am Untersulzbachkees (Venedigergruppe) von 1974 bis 1982. In: Glaziologie u. Kartographie; W. Pillewizer Festschrift. Geowiss. Mitt. 21, 67–112, Wien (1982)
- Kasser, P.: Fluctuations of Glaciers 1959–1965. A contribution to the IHD. IASH (ICSJ)-UNESCO, Louvain 1967.
- Kasser, P.: Fluctuations of Glaciers 1965–1970. IASH (ICSJ)-UNESCO, Paris 1973.
- Kuhle, M.: Der Dhaulagiri- und Annapurna-Himalaya. Ein Beitrag zur Geomorphologie extremer Hochgebirge. Zeitschrift für Geomorphologie, Supplement Bd. 41, 1–229 (1982)
- Kuhle, M.: Die Vergletscherung Tibets und die Entstehung von Eiszeiten. Spektrum der Wissenschaft 9, 42–54 (1986a)
- Kuhle, M.: The Upper Limit of Glaciation. GeoJournal 13, 4, 331–346 (1986b)
- Kuhle, M.: Subtropical Mountain- and Highland-Glaciation as Ice Age Triggers and the Waning of the Glacial Periods in the Pleistocene. GeoJournal 14, 4, 393–421 (1987)
- Kurowski, L.: Die Höhe der Schneegrenze mit besonderer Berücksichtigung der Finsteraarhorngruppe. Geographische Abhandlungen 5, 1, 115–160 (1891)
- Lichtenecker, N.: Die gegenwärtige und die eiszeitliche Schneegrenze in den Ostalpen. Verhandl. d. III. Intern. Quartär-Konferenz, Wien 1936, 141–147, 1938.
- Louis, H.: Schneegrenze und Schneegrenzbestimmung. Geographisches Taschenbuch 1954/55, 414–418, 1955.
- Meier, M. F.: Mass budget of South Cascade Glacier, 1957–60. U. S. Geol. Survey Prof. Paper 242–B, 206–211 (1961)
- Meier, M. F.; Post, A. S.: Recent variations in mass net budgets of glaciers in western North America. Commission of Snow and Ice Symposium of Obergurgl 1962. IASH, Publ. 58, 63–77 (1962)
- Meier, M. F.; Tangborn, W.: Net budget and flow of South Cascade glacier, Washington. Journal of Glaciology 5, 41, 547–566 (1965)
- Müller, F.: Inventory of glaciers in the Mount Everest region. In: Perennial Ice and Snow masses, 47–59; UNESCO Technical Papers in Hydrology 1 (1970)
- Müller, F.; Cafilisch, T.; Müller, G.: Firm und Eis der Schweizer Alpen. Gletscherinventar. Geogr. Inst., ETH Zürich, Publ. 57, 1976.
- Müller, F.: Fluctuations of Glaciers 1970–1975. IASH (ICSJ)-UNESCO, Paris 1977.
- Müller, F.: Present and late Pleistocene equilibrium line altitudes in the Mt. Everest region – an application of the glacier inventory. In: World Glacier Inventory, IASH-AISH Publ. 126, 75–94, 1980.
- Østrem, G.: The height of the glaciation limit in southern British Columbia and Alberta. Geogr. Annaler, Ser. A, 48, 126–138 (1966)
- Partsch, J.: Die Gletscher der Vorzeit in den Karpathen und den Mittelgebirgen Deutschlands. Breslau 1882.
- Porter, S. C.: Quaternary glacial record in Swat Kohistan, West Pakistan. Bull. Geol. Soc. Am. 81, 1421–1446 (1970)
- Porter, S. C.: Glaciological evidence of climatic change. In: Wigley, T. M. L.; Ingram, M. J.; Farmer, G., (eds.) Climate and history studies in past climates and their impact on man. Cambridge 1981.
- Richter, E.: Die Gletscher der Ostalpen. J. Engelhorn, Stuttgart 1888.
- Schneider, H.-J.: Die Gletschertypen. Versuch im Sinne einer einheitlichen Terminologie. Geographisches Taschenbuch, 276–283, Wiesbaden 1962.
- Schytt, V.: Mass balance studies in Kebnekajse. Journal of Glaciology 4, 33, 281–286 (1962)
- Sharp, R. P.: Accumulation and ablation on the Seward-Malaspina Glacier system, Canada-Alaska. Geol. Soc. Am. Bul. 62, 726–744 (1951)
- Shumskii, P. A.: Energiia oledeneniia i zhizn lednikov (Energy of glaciation and the life of glaciers). Geografiz, Moscow 1947; transl. by W. Mandel, The Stefansson Library, New York 1950.
- Shumskii, P. A.: Principles of Structural Glaciology. translated from the Russian by D. Kraus; Dover Publ., Inc., New York 1964.
- UNESCO/IASH: Perennial ice and snow masses. A guide for compilation and assemblage of data for a world inventory. Technical Papers in Hydrology 1, 1–59 (1970a)
- UNESCO/IASH: Perennial ice and snow masses. A contribution to the International Hydrological Decade. Technical Papers in Hydrology, Paris (1970b)
- Visser, P. C.: Wissenschaftliche Ergebnisse der Niederländischen Expeditionen in den Karakorum und die angrenzenden Gebiete in den Jahren 1922–1935. Vol. II, Glaziologie, 1–216, 1938.
- Walcher, J.: Nachrichten von den Eisbergen in Tirol. Wien 1773.
- Wang Yinsheng; Qiu Jiaqi: Distributive Features of the Glaciers in Bogda Region, Tian Shan. Journ. of Glaciology and Cryopedology 5, 3, 17–24 (1983)
- Wissmann, H. v.: Die heutige Vergletscherung und Schneegrenze in Hochasien mit Hinweisen auf die Vergletscherung der letzten Eiszeit. Akad. d. Wiss. u. d. Lit., Abh. d. math.-nat. wiss. Kl., No. 14, 1103–1407. Mainz 1959.
- Wu Guanghe; Zhang Shunying; Wang Zhongxiang: Retreat and Advance of Modern Glaciers in Bogda, Tian Shan. Journ. of Glaciology and Cryopedology 5, 3, 143–152 (1983)
- Young, G. J.: Accumulation and ablation patterns as functions of the surface geometry of a glacier. Snow and Ice- Symposium, Proceedings of the Moscow Symposium, August 1971, IASH-AISH Publ. 104, 134–138 (1975)
- Zhang Xiangsong; Chen Jinming; Xie Zichu; Zhang Jinhua: General features of the Batura glacier. Professional Papers on the Batura Glacier, Karakoram Mountains, 8–27, 1980.

## The Pleistocene Glaciation of Tibet and the Onset of Ice Ages – An Autocycle Hypothesis

Kuhle, Matthias, Prof. Dr., University of Goettingen, Institute of Geography, Goldschmidtstraße 5, D-3400 Goettingen, FR Germany

**ABSTRACT:** During seven expeditions new data were obtained on the maximum extent of glaciation in Tibet and the surrounding mountains. Evidence was found of moraines at altitudes as low as 980 m on the S flank of the Himalayas and 2300 m on the N slope of the Tibetan Plateau, in the Qilian Shan. On the N slopes of the Karakoram, Aghil and Kuen Lun moraines occur as far down as 1900 m. In S Tibet radiographic analyses of erratics document former ice thicknesses of at least 1200 m. Glacial polishing and knobs in the Himalayas, Karakoram etc. are proof of glaciers as thick as 1200–2000 m. On the basis of this evidence, a 1100–1600 m lower equilibrium line altitude (ELA) was reconstructed for the Ice Age, which would mean 2.4 million km<sup>2</sup> of ice covering almost all of Tibet, since the ELA was far below the average altitude of Tibet. On Mt. Everest and K2 radiation was measured up to 6650 m, yielding values of 1200–1300 W/m<sup>2</sup>. Because of the subtropical latitude and the high altitude solar radiation in Tibet is 4 times greater than the energy intercepted between 60 and 70° N or S. With an area of 2.4 million km<sup>2</sup> and an albedo of 90% the Tibetan ice sheet caused the same heat loss to the earth as a 9.6 million km<sup>2</sup> sized ice sheet at 60–70° N. Because of its proximity to the present-day ELA, Tibet must have undergone large-scale glaciation earlier than other areas. Being subject to intensive radiation, the Tibetan ice must have performed an amplifying function during the onset of the Ice Age. At the maximum stage of the last ice age the cooling effect of the newly formed, about 26 million km<sup>2</sup> sized ice sheets of the higher latitudes was about 3 times that of the Tibetan ice. Nevertheless, without the initial impulse of the Tibetan ice such an extensive glaciation would never have occurred. The end of the Ice Age was triggered by the return to preglacial radiation conditions of the Nordic lowland ice. Whilst the rise of the ELA by several hundred metres can only have reduced the steep marginal outlet glaciers, it diminished the area of the lowland ice considerably.

*'Very likely the future will see greater changes in the glacial map of eastern Central Asia than in that of any other part of the world.'* Richard Foster Flint (1967, p. 421)

### The State of Research up to 1975, together with Investigations Subsequently Carried Out

A synopsis of older results and views on the Pleistocene glacier cover in Tibet has been provided by v. Wissmann's compilation (1959; the author himself has, however, never set foot in the high regions of Asia). It is echoed in the recent Chinese literature in Shi Yafeng et al. (1979), and has also been reproduced by Climap (1981 Map entitled "Last Glacial Maximum"). These authors speak of a from 10% to maximally 20% ice covering of the mountains and plateaux of Tibet. But time and time again, from as long ago as the turn of the

century, there have been single researchers like v. Loczy (1893), Dainelli & Marinelli (1928), Norin (1932), De Terra (1932), v. Handel-Mazzetti (1927) and others (cf. Kuhle 1987a), who described ancient ice-margin sites scattered throughout the high regions of Asia. According to the author's calculations, they presented ELA (equilibrium line altitude) depressions of more than 1000 m, and thus indicate locally much more significant glacier formations than the v. Wissmann scheme had acknowledged. However, these authors neither drew nor gave voice to such conclusions. Other early researchers like Tafel (1914), Prinz (1927), Trinkler (1932), Zabirot (1955) (cf. Kuhle 1987a), making more or less direct use of the data they obtained by observation, reconstructed larger glacier areas which, depending on the great altitude of mountains or plateaux respectively, had built up at only a few hundred metres of ELA depression.

The author has been fortunate in being able to carry out nine expeditions and research visits since 1973, some

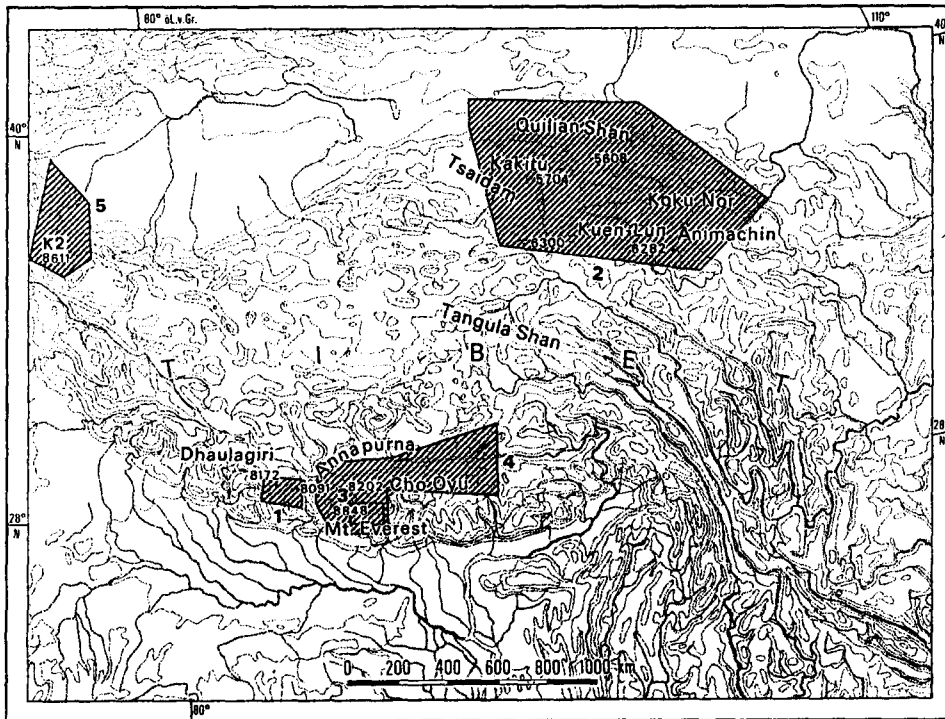


Fig 1  
Research areas in High Asia visited  
in the course of seven expeditions

1: 1976 u. 1977

2: 1981

3: 1982

4: 1984

5: 1986

Draft: M. Kuhle (1986)

of which extended to seven months, with the purpose of reconstructing the extent of glaciers in Asia during glacial periods<sup>1</sup>). Two of these were to the arid East Zagros Mountains, the others to Tibet and its flanking mountain systems (Fig 1). By now the location and number of areas under investigation permit representative data on the glacier areas to be made for the whole of Tibet. They are supported by data from some earlier authors, and are in glaring contrast to the negligible ice-cover published by Climap as late as 1981 (see above). Apart from the Tianshan the glaciation of Tibet during the last Ice Age is given as approximately  $2.4 \times 10^6$  km<sup>2</sup> (Fig 2), and is estimated to include central thicknesses of about 2.7 km (Fig 3 and Fig 4). There was thus inland ice with a central dome of about 7000 m asl in Tibet, the details of which are to be demonstrated below. Breaking up on the edges, it discharged through the surrounding mountains as steep outlet glaciers.

#### Evidence of a Large-Scale Glacier Cover on the Tibetan Plateau

Three areas covered by boulder-clay and erratics, or by erratics alone, may be adduced:

In S Tibet, at 28° 50' N / 87° 20' E (Fig 1, No. 4), there is the Lulu Valley; it cuts deeply into hydrothermally decomposed basalt (50% pyroxenes, pseudomorphically replaced by dolomite and chlorite). Between 4400 and 4950 m the valley floor is filled with boulder

clays, which extend far (170 m) up the sides in some places. In its very fine intermediate material there are some isolated deposits of very coarse 2-mica granite components (Fig 5). Transported over long distances from the N, tens of metres thick, and spread over tens of kilometres, these glacial diamictites should be regarded as ground moraines. A convergence with a mud-flow must be ruled out for sedimentological, petrographic and topographic reasons (Kuhle 1987b).

The second example is also provided from a finding in S Tibet. That is so because throughout Tibet the ELA attained its highest level here during the Ice Age, and still does so now. The evidence of a glacial cover that extends over entire areas thus receives the greatest possible extrapability, particularly to the N towards which the ELA in any case inclines for planetarian reasons. At 29° 41' N / 90° 12' E, N of the Tsangpo Valley, there is a 5300 m high pass known as the Chalamba La. It is, in other words, situated at the point at which the valley network of the Transhimalaya leads out of the Central Plateau of Tibet. Up to at least 200 m above the depression that forms the pass, lying on dark rhyolite bedrock with chlorite but without potassium feldspar, there are superimposed, light-coloured, tectonically-marked granite erratics with potassium feldspar components, but lacking chlorite. On both sides of the Chalamba La steep valleys lead down immediately about 1000 m (to 4300 m asl); according to these moraine finds the valleys must have been filled with glacier ice well above the pass and up to 1200 m at least. This proves the

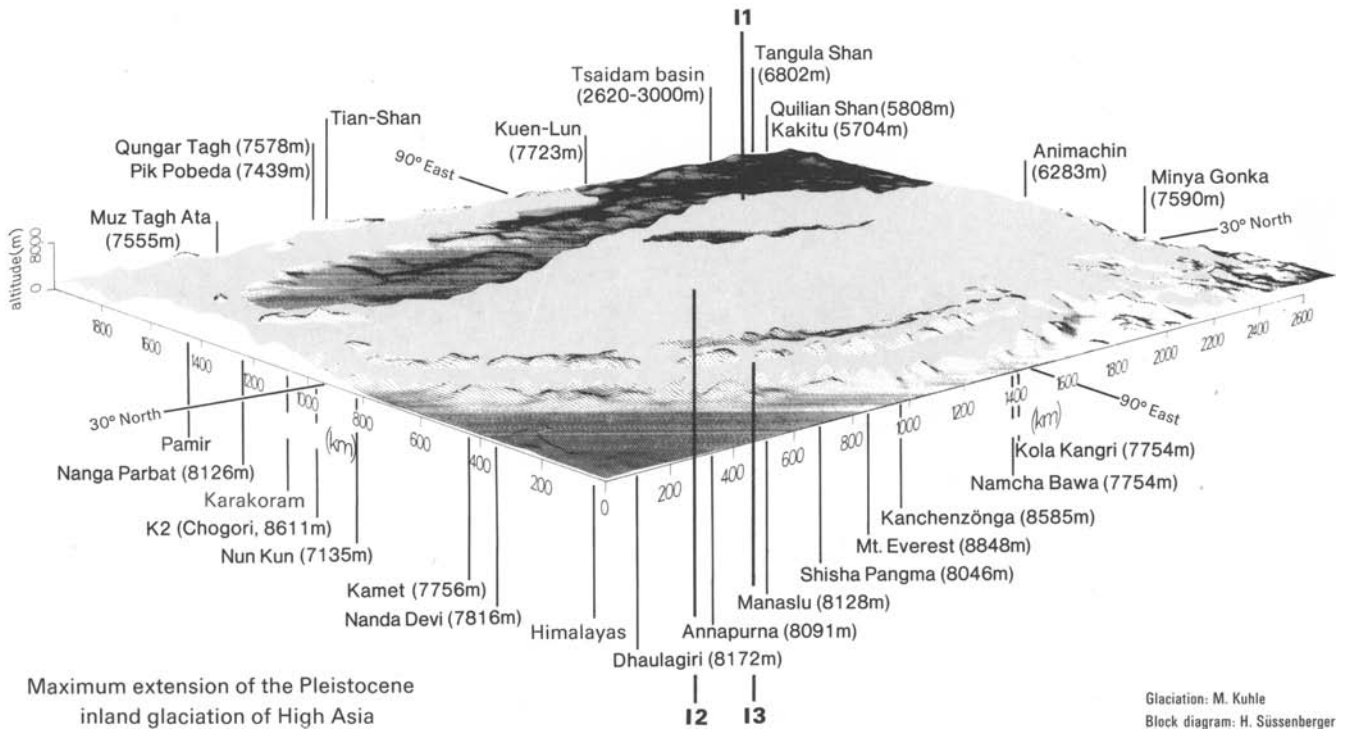


Fig 2 The  $2,4 \times 10^6$  km<sup>2</sup> continental ice-sheet on the Tibetan highland with its centres I1, I2, I3. Only peaks reaching more than 6000 m project above the glacier surface (exaggeration 15-times)

existence of a ramified network of ice streams, subordinate stream surfaces of which have moved over and across the counter gradients of divides with their saddles. The nearest bedrock granite is known to occur 80–100 km further E, and is part of the Lhasa Pluton (Gansser 1964). The direction of transportation and the glacier direction given by the valley system point to

numerous, quasi-parallel outlet glaciers of substantial thickness. This is confirmed by roches moutonnées, which rise to 5600 m together with rough crest-lines and peaks which begin only above the latter. The outlet glaciers have left the central Tibetan inland ice by way of an interposed section of the ice-stream network (Fig 2, I 2) and at this longitude (about 89° E) just missed the

Fig 3 The cross section of Tibet

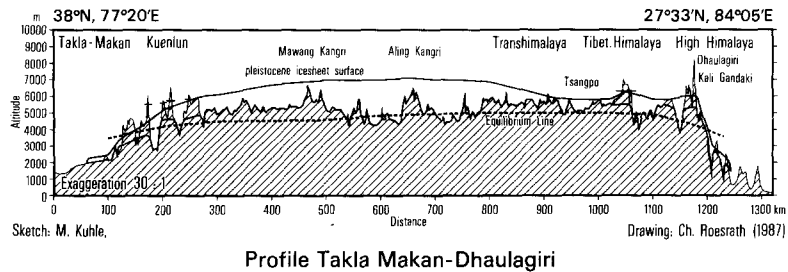


Fig 4 The cross section of Tibet

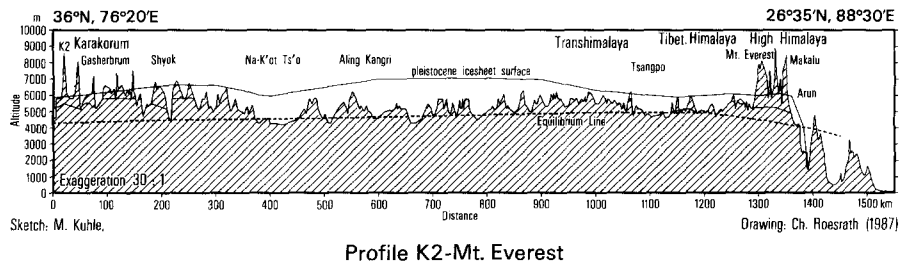




Fig 5 Erratic 2-mica granites on basaltic bedrocks in S Tibet ( $28^{\circ}51'N/87^{\circ}21'E$ , 4900 m asl). The Lulu Valley is set in bedrock basalts. The floor of this valley is covered by ground-moraines containing granite blocks. The largest ones measure up to  $4,3 \times 2,6 \times 2,2$  m. Photograph by M. Kuhle 31. 8. 1984

Tsangpo isobath at 3800 m (Kuhle 1987b). The final extremity of the outlet glacier concerned came to its end at 3900 m asl inwards of a side valley, a mere 6–10 km from the Tsangpo, exactly like that of the westerly, parallel valley of the Orio Matschu ( $29^{\circ}23'N / 89^{\circ}37'E$ ). Evidence of this may be found in the over 120 m high lateral moraines which coalesce in terminal moraine walls.

From these a sander root or outwash cone emerges. The deposits in the side-valley that joins the main valley near Lhasa ( $29^{\circ}43'N / 91^{\circ}04'E$ ) must also be seen in this context of moraine findings as evidence of ELA depressions of at least 1075–1200 m in S Tibet. They are situated at 4250 and 3950 m asl.

Another finding of erratics in the Shaksgam Valley on the W edge of Tibet ( $36^{\circ}06'N / 76^{\circ}28'E$ ) (Fig 1, No. 5) is evidence of a relief-filling glacier cover rarely presented in such an unmistakable way. This is the most

arid part of High Asia, with less than 40 mm of precipitation annually at 4000 m asl. The area in question is a cross-section of the Muztagh Valley in the area of its confluence in the Karakoram N slope to the N of the 8616 m high K2, which has been ground down to a glacial trough up to an altitude of 1200 m above the valley floor (Fig 6). At altitudes between 4400 m and 4700 m gneiss and granite as well as dolomite erratics (90% Do, 5% Ca, micritic and sparitic) have been found on roches moutonnées of 90% pure calcite (Fig 8), standing 600 m above on a transfluence pass that leads from the Shaksgam to the Muztagh Valley. These erratic blocks have been transported over a long distance following the Shaksgam Valley. More than 1.5 m long, they occur singly as well as in the context of bands of lateral moraine material. Gneiss and granite appear on the inner side of the Shaksgam Valley. These blocks required transport along the valley at a high level in order to be deposited here.



Fig 6 Glacier polishing on the right flank of the Shaksgam Valley in dolomite bedrocks ( $36^{\circ}09'N/76^{\circ}36'E$ , 4100 m asl, Karakoram-N-slope, Aghil-S-slope). It proves a minimum thickness of the Shaksgam Glacier of 1200 m (-----). It was one of the big pleistocene W-Tibetan outlet-glaciers. Photograph by M. Kuhle 30. 8. 1986

On the outward side of the valley in the W the transfluence pass is bounded by a 4730 m high polished (i.e. to its top) glacial horn – a massive rock of micritic calcite. Up-valley and to the E of the saddle, the glacially-polished calcareous rock flanks of the intermediate divide rise to more than 500 m above the floor of the transfluence pass. Clearly situated above the polished band, its uppermost section is a roughened and earlier crest-line which rose above the high, or even only late, glacial ice stream network like a nunatak. The great thicknesses of ice are confirmed by very small-scale relief and at the same time by softly polished roches moutonnées on the pass. They are only brought about through ground polishing in the subglacial region where the melting point is reached as a result of ice-pressure. Now, as well as during the glacial period, the mean annual temperature at the glacier surface was and is about  $-10^{\circ}\text{C}$  at the equilibrium line. At the time of the main Ice Age the corresponding glacier surface of this locality was in the glacier supply area, c. 1000 m above the equilibrium line. This is an indication that the forms of the roches moutonnées transfluence pass are most likely testimony of the late Ice Age. Corresponding grooves can be found on the orographically right-hand side of the Shaksgam Trough and on the 5466 m high ‘Shaksgam Horn’ 25 km up-valley and up to 1200 m above the rocky floor of this large W Tibetan longitudinal valley (Fig 6). This is the area in which a distributary stream of the Shaksgam Glacier system buried the 4863 m high Aghil Pass ( $36^{\circ} 11' \text{N} / 76^{\circ} 36' \text{E}$ ) under a 500 m thick cover, thus communicating with the Yarkand ice-stream network system. Glacier polishings in the massive limestones on the orographic left-hand in the Aghil Valley and in the granite on the right are evidence of this. Below 3700 m well preserved striae in the quartzite are encrusted with iron-manganese (Fig 7). Others can be found on sandstone outcrops at about 3600 m, and roches moutonnées with polishings on metamorphosed schist outcrops were found at 3400–3600 m near Illik ( $36^{\circ} 23' \text{N} / 76^{\circ} 42' \text{E}$ ). That is the trough-shaped confluence area of the upper Yarkand Valley. Besides many other forms of polishing (Kuhle 1987a, c) these exemplary data are evidence of a W Tibetan Karakoram – Aghil – Kuen Lun ice-stream network at the time of the main Ice Age. The ice fillings of the central longitudinal valleys (Shaksgam and Yarkand Valley) (Fig 6) were large outlet glaciers – attaining thicknesses like Alpine glaciers during the Pleistocene – (cf. Fig 3 and 4), which had flowed down from the Central Plateau ice.

In addition to the findings of erratics mentioned above, roches moutonnées fields in Central Tibet are evidence of the ice-cover: in north-central Tibet (Kuhle 1987c) S of the Kuen Lun Pass ( $35^{\circ} 33' \text{N} / 93^{\circ} 57' \text{E}$ ) there are roches moutonnées in metamorphic sandstones and crystalline schists at 4800–5350 m; in the S Tibetan Latzu Massif ( $28^{\circ} 55' \text{N} / 87^{\circ} 20' \text{E}$ ) in basalts at 5000–5500 m asl, and 100–120 km to the W, N of the Menlungtse Group at  $28^{\circ} 32' \text{N} / 86^{\circ} 09' - 25' \text{E}$  in meta-

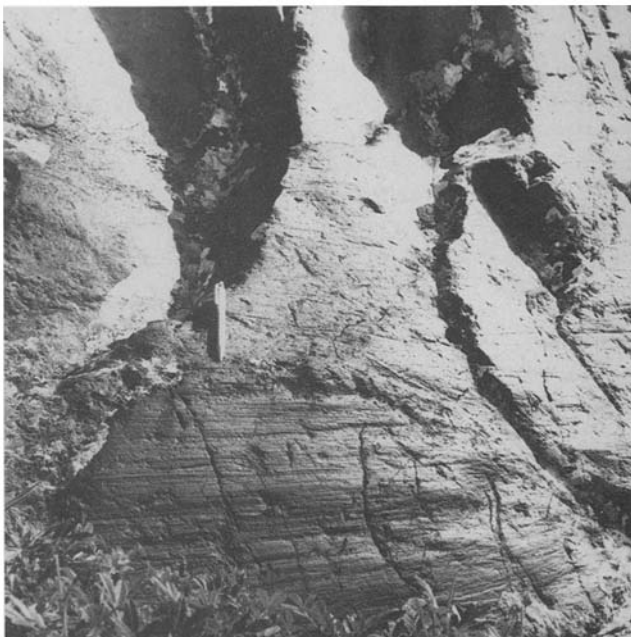
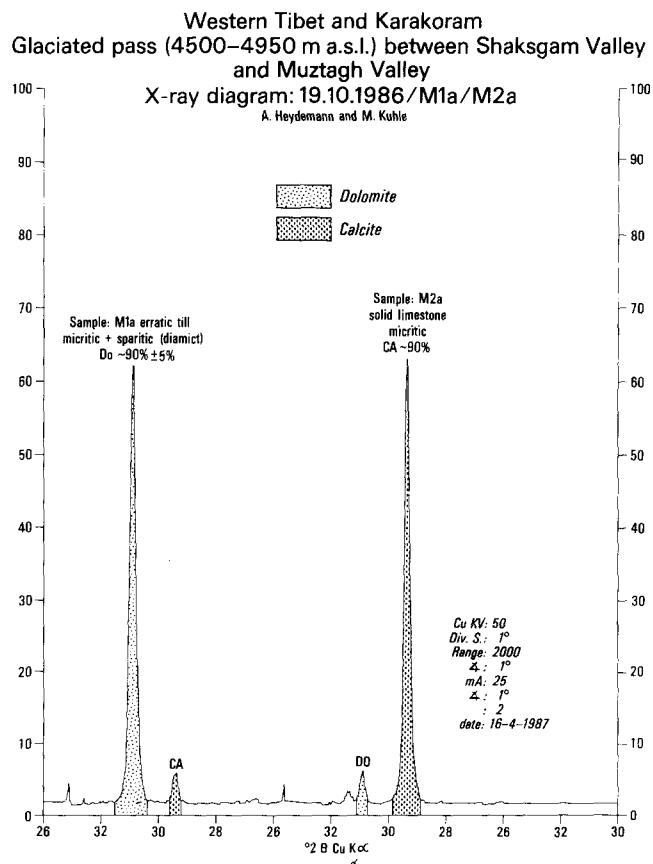


Fig 7 Glacier polishing with striae and polish marks on the right flank of Aghil Valley ( $36^{\circ}13' \text{N} / 76^{\circ}38' \text{E}$ , 3700 m asl, NW Tibet, Aghil-Kuenlun) in metamorphic bedrocks. Photograph by M. Kuhle 27. 8. 1986

Fig 8 Erratic till and solid rock



morphic sediments between 4400 m and 5100 m, to name another example, or – another 50 km away – roches moutonnées in the Shisha Pangma foreland (28° 37' N / 85° 49' E). Although pebble fillings now frequently give them the appearance of box profiles (Fig 6), the predominantly trough-shaped valleys of N and S Tibet are of an appropriate character to prove the existence of what was once probably a more than 2000 m thick inland ice cover (Fig 3 and 4).

### The Lowest Positions of Marginal Ice around the Tibetan Plateau and Depression of the Equilibrium Line

Determined by the position of 46 glaciers, the present climatic line of equilibrium (ELA) on the S edge of Tibet, S and N of the Dhaulagiri and Annapurna Himalaya (Fig 1, No. 1) lies at about 5550 m asl. It was calculated in accordance with v. Höfers method (1879) and that of Louis (1955, which has a mathematical equivalent in the 'maximal method' developed by Kuhle, 1982), as well as in accordance with the Lichtenecker method (1938) (Kuhle 1982, 1986a). Going into detail, the climatic equilibrium line N of the main crest of the Himalaya is at 5620 m, and S of it at 5490 m, i.e. only 130 m lower in the humid monsoon position (6000–2000 mm p.a. at 1600–3000 m) than on the dry N side in the rain shadow (270 mm p.a. at 2700 m asl). Moraines of the *main glacial* period are to be found on the S slope down to 1100 m in the Mayangdi Khola (28° 23' N / 83° 23' E) and the Thak Khola (Kali Gandaki; 28° 24' N / 83° 36' E) (Kuhle 1979/80, 1982). Using five valley glaciers, two of which were large outlet glaciers flowing simultaneously from the N slope of the Himalaya, the equilibrium line was calculated as being at 4060 m asl. In this

$$ELA_{\text{Depr.}} = \frac{tp-ti}{Si} \quad (\text{m asl}) \text{ and}$$

$$Si = Sp - S_{\text{Depr.}} \quad (\text{m asl})^2.$$

By means of glacial positions of ice margins, still evident in 31 terminal moraines, it was possible to establish the equilibrium line north of the main crest as being at about 3980 m asl. The large number of glacier margins is explained by the very deeply incised former transverse valley of the Thak Khola (Kali Gandaki), together with a catchment area of the S Tibetan Mountains that is only a little higher than 6000 m. The transverse valley cuts through at almost 2000 m asl, and N of the main crest it has only reached the 2700 m line. It follows that here the hanging glaciers, as well as those from longitudinal valleys, having been outlet glaciers of the S Tibetan inland ice and the ice-stream network as well (Fig 2, I 3), though reaching the main valley, no longer coalesced into a single tongue (Kuhle 1982, Fig 8). An integral equilibrium line for this section of the S Tibetan Plateau edge would be 4200 m. This is the

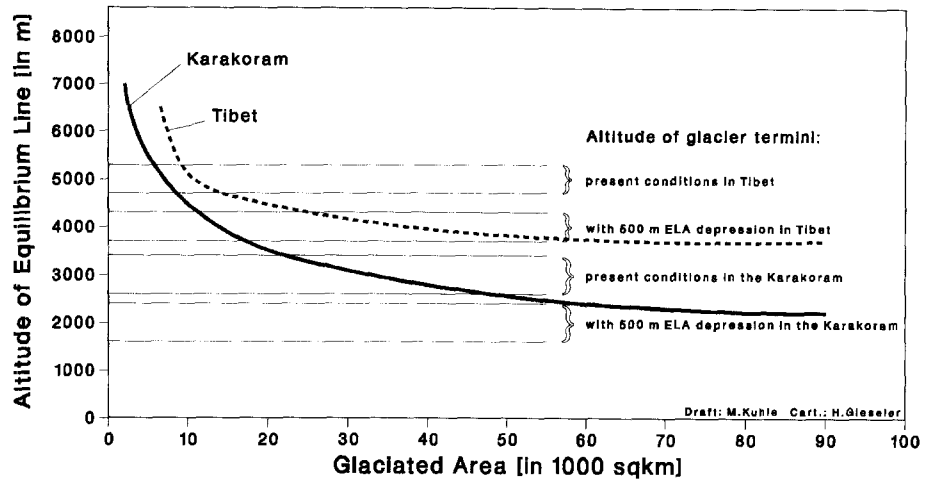
equivalent of a depression of the equilibrium line of 1530 m. This calculation even includes the Late-Glacial position of the ice margin of the Jhong Khola Glacier (Muktinath Basin) at 3250 m (near Kingar: 28° 49' N / 83° 50' E; see map in Kuhle 1982, Fig 184 and Fig 38). It is situated in a very dry valley N of the main Himalayan crest, and is evidence of an equilibrium line at about 4450 m, the equivalent of a local equilibrium line depression of only 1210 m (Kuhle 1979/80, 1982). Since then this moraine has been confirmed by Iwata et al. (1982, p. 87). Yamanaka (1982) has dated the minimum age of the corresponding glacier basin as being  $8670 \pm 200/210$  (C 14). This Late Glacial Age and the same equilibrium line depression brings it into line with other moraines like the terminal moraine at Ghasa ('Ghasa Stadium' I, after Kuhle 1979/80, 1982, Fig 91, 92) in the Thak Khola (Kali Gandaki) transverse valley.

The positions of marginal ice and the extent of sometimes large – almost up to 60 km (58 km) long – outlet glaciers flowing down from the S Tibetan ice which have been reconstructed here, are based on terraces of river-side moraines that may rise as high as 570 m and lie up to 1060 m above the valley bottoms, as well as on well-marked terminal moraines with erratics. Moreover, there are trough profiles with glacier striae descending as far as 1700 m to the evergreen forest (with *Quercus semecarpifolia*, *inter alia*) and grooves as evidence of glacier thicknesses of 1600 m in the central Mayangdi Khola (28° 08' N / 83° 23' E) to give just one example (Kuhle 1979/80, 1982). It must be emphasized that in its glacial drop to 3980 m asl the equilibrium line N of the main crest ran more than 1000 m below the average level of valley floors of the S Tibetan mountains (Tibetan part of the Himalaya) (Kuhle 1982, Fig 184). Even when the Late Glacial equilibrium line ran at an altitude of 4450 m, there was still a difference of 600 m. This had to lead to a glacial filling of the entire Tibetan Himalaya, which overwhelmed the relief – as is evident from the ubiquitous smoothly polished intermediate valley divides – and extended to an ice-stream network and further N to the formation of inland ice (Fig 2, I 3).

340 km further W on the N side of Mt. Everest, and again on the dry leeward side, conditions are the same (Fig 1, No. 4). In this area (28°–29° 50' N / 85° 24'–91° 13' E) investigations established a recent macro-climatic equilibrium line at almost 5900 m by means of 15 values that are based on fieldwork. The Chinese map for snow lines and glacier and snow equilibrium lines (Xie Zichu, 1:2 000 000) indicates values between 5500 m and 5900 m for this area, so that in consequence a level of 5700 m is to be assumed. Evidence of the maximum equilibrium line depression of the area puts this at 1180 m (or, if taken in relation to the map, at only 980 m); it was arrived at by reconstruction of eight ice margin positions. The climatic equilibrium line accordingly ran at 4700 m asl (Kuhle 1984/85). It is, however, probably a matter of ice-margin positions which had already receded, i.e. Late Glacial ice margin



Fig 9  
Correlation of equilibrium line  
altitude and glacier area



positions which were the only ones to be found in this area, consisting of vast areas altitudes of 5000 m to 6500 m and never dropped below 4200 m. It is likely that glacial margin positions from the High Glacial period can only be found near the terminal points of outlet glaciers which formerly flowed through the High Himalaya. The Bo-Chu or Sun Kosi glaciers of the High Glacial period (28° 50' N / 86° 09' E) may serve as an example. Located on the Tibetan Plateau, which emerges here from the High Himalaya in 5000-5500 m high, continuous and large remnants, it was supplied by the N, E and SW flank of the Shisha Pangma, as well as by the Menlungtse group. It descended to at least 1600 m (near Kodari: 27° 56' N / 85° 56' E) and is evidence of a climatic equilibrium line at 4300 m, a level that is still 300 m too high by comparison with the Dhaulagiri and Annapurna area (see above). Evidence of the minimal glacier end exists in the form of perfectly preserved polishings on outcrops of the metamorphosed sheets of Kathmandu and Nawakot.

As had been discovered in 1982, the ice-streams of the Cho Oyu-, Everest- and Lhotse S slopes flowed down similarly far and coalesced to form the Dudh Kosi Glacier. The glacier tongue smoothed the gorge between Nangbug and the mouth of the Surke Drangka, and may well have passed by the Lumding Drangka confluence as far down as 1800 m (27° 38' N / 86° 42' E). There is evidence (Fig 1, No. 3) of glacial bank formations with disturbed glaciolimnic sands at Namche Bazar, Nyambua Thyang, Chu Chhutawa and Julming (27° 44' - 50' N / 86° 42' E) (cf. Heuberger 1986, p. 30). Just like the Mayangdi, Thak Khola and Bo Chu glaciers, the Dudh Kosi Glacier, too, was a large inland-ice glacier or ice-stream network outlet-glacier, which to some extent was fed by tributaries from the Tibetan ice. It was brought about by the confluence of the Nangpa La (28° 06' N / 86° 35' E; 5700 m) W of the Cho Oyu, and the later re-routed Rongbuk Glacier, which had couse down from the Lho La (28° 0' N / 86° 53' E; 6010 m) W of Mt. Everest.

There is evidence of overflows from the present N to the Himalaya S side, thanks to attrition from below, supra-glacial weathering, below the W shoulder of Mt. Everest at an altitude of 6500 m (500 m above the transfluence pass; Fig 4). In the N forefield of the present northward-draining Rongbuk Glacier, the gradient of the lateral moraines accordingly tilt so that at an ice-level on 900 m above the valley floor the gradient begins to face S. This 180° re-orientation of the Rongbuk Glacier explains the total absence of older frontal moraines as little as 8 km down valley from the present glacier tongue from the Neo-Glacial ice-marginal deposits at the Rongbuk monastery. They had never been formed. Even during the Late-Glacial period the glacier still drained to the S (Fig 4). These continuing over-spills (Fig 2, I3) into the steep S ramp of the Himalaya also explain the slight thickness of the Ice-Age Rongbuk Glacier. Its highest traceable strip of lateral moraines runs a mere 600 m above the recent glacier surface. A further heightening of the ice became impossible through an overspill into the steep S side that was only 5 km away.

In the S part of the highland as well, with a mean altitude of 4800–5000 m and valley floors of 4200 m at the lowest, the reconstructed equilibrium line depression to at least 4720–4300 m asl (see above) had to lead to relief-filling glaciation. Its level was determined by the topographic proximity to the steep S edge of Tibet alone. The result was an approximately 900–1200 m thick ice-stream network.

How unproblematic or cogent a glacier-filling of this mountain landscape is, whose main valley floors fail to reach the equilibrium line by perhaps 600 m, is shown by a comparison with the Ice Age Alps: the Rhone Valley, for example, having been infilled with 2000 m of ice, finds its valley floor to be 1600 m below the main Ice Age equilibrium line (cf. Fig 9).

In 1987 the investigations on the S fringe of Tibet were extended to the extreme SW edge of the Highland,

to Nanga Parbat and to the S slope of the Karakoram (Fig 1, No. 6).

The present almost 60 km long glaciers end here in the catchment area of the Indus Valley at altitudes of at least 2500–2600 m (Hunza-Karakoram). They are thus the ones to descend most deeply in the whole of High Asia. On Nanga Parbat they reach 2900–3600 m asl. During the last Ice Age, however, all the tributary glaciers from the Karakoram S slope and the Nanga Parbat group united in a  $12 \times 10^4$  to  $18 \times 10^4$  km<sup>2</sup> ice-stream network – the Indus ice-stream network. At 980 m asl its largest outlet-glacier reached the lowest common ice-marginal position at Sazin at the mouth of the rivers Daret and Tangir, a little above the bend of the Indus (35° 34' N / 73° 28' E). There are two graded series of lateral moraines more than 100 m in height, with a final bend of the terminal moraine. These series of moraines occur at a distance of about 10 km from one another, each flanking the Indus valley over several kilometres. The moraine ramps consist of typical glacial diamictites of polymict composition. Down-valley the valley cross-section becomes a V-shaped valley gorge. Up-valley from the position of the ice-margin a concave, worn-down U-profile takes over and eventually expands to a trough profile with well-preserved striae on the flanks. Sixty km up-valley, at about 1100 m asl, there is a basin-shaped opening – the 'Chilas Chamber'. Here remnants of lateral moraines on the orographic left bank provide evidence of the prehistoric in-filling with ice. Exactly opposite the Chilas settlement glacial polishing on the orographic righthand side provides evidence of a minimum glacier thickness of 450–550 m. Between Chilas and the lowest moraines, the subsidence of the valley glacier edge during the late High Ice Age is retraced by stable lines of light coloured glacio-limnic bank sediments. In some places the limnites were dammed back into the side-valleys.

The next 60 km along the NE slope of Nanga Parbat are characterised by ground moraine covers, which coat the roches moutonnées fields, and by several hundred-metre-deep deposits of platform and lateral moraines. This wealth of moraines may be explained by the immense supply of scree from the steeply descending Nanga Parbat glaciers. For the SE flank of Nanga Parbat (Rupal Valley) which (by way of the Astor Valley) had also connection to the Indus Valley the author was able to provide evidence of an ice-stream network of a glacier thickness of 900–1200 m. Apart from polishing on the flanks, which in many places reaches up hundreds of metres, the Bunji moraines are an important feature of the following valley section and up to the mouth of the Ice Age Gilgit Glacier where it debouches into the Indus Glacier (1228 m asl). Thrust into this side valley of Bunji, this orographic moraine on the left bank corresponds to those in the opening of the Astor Valley. They are 400 m high. Subsequently in 1987 the Gilgit-Hunza part of the glacier stream was reconstructed up to

the 58 km long Batura Glacier with the help of diamictites and glacial polishings.

Below Gilgit the tributary glaciers of Batkor and Bagrot joined up. Their Late-Glacial advances are provisionally classified by the author as belonging to the Ghasa Stadium (I) (cf. Kuhle 1986b, c); they reached the Gilgit Valley outside the equally old terminal basin of Gilgit at an altitude of 1300–1380 m. The former is caused by the steepness of the valley, and the latter by the high altitude of the catchment area (Rakaposhi 7788 m). Thanks to glacial polishings (together with striations extending as far down as 1900 m asl at Rakaposhi (36° 15' N / 74° 24' E) the Hunza Glacier component can be reconstructed up to 1600–1800 m above the floor of the valley. It is an exemplary demonstration of glaciation of Pleistocene-Alpine dimensions, with a central-montane thickness of at least 2000 m for this part of the area under investigation. The approaching Shishal Glacier provided a link with the N side of the Karakoram and presented a connection with the Shishal Glacier system (see above). The Pleistocene predecessors of the Hispar-Biafo Glacier produced the S transverse connection with the Muztagh-Karakoram ice. Consisting of acute and wide angles, the ice-stream network was subject to a great deal of friction, and therefore tended to dome-shaped prominence. On the E edge of the Karakoram, approximately at the Pangong Tso (33° 45' N / 79° E) and further N on the Depsang Plateau (35° 25' N / 78° 20' E), it gradually merged with the compact inland ice cover of Central Tibet (Fig 2).

By contrast with the recent glaciers in the Indus Valley catchment, which tend to terminate at about 3400 m, the equilibrium line depression for the lowest prehistoric ice-margin at about 1000 (980 m) is calculated to be 1200 m<sup>3</sup>). Compared with a contemporary equilibrium line at 4600–5000 m, this implies an Ice Age line at 3400–3800 m in the area under investigation. The exponential increase in the area under glaciation, together with the depression of the equilibrium line, is shown in Fig 9; it is established for the first 500 m of the depression of the equilibrium line altitude (ELA).

This implies that here also, on the extremely arid W edge of Tibet, where the mean annual precipitation of stations (Misijaer, Gilgit, Chilas; 1961–70) in valley floor locations is a mere 142.5 mm p. a., there is evidence of relief-filling glaciation which completely masked it all. Its equilibrium line ran 1200–1600 m below the average altitude of W Tibet.

TL-datings of tills and glaciolacustrine sediments immediately upvalley of the terminal moraine at the village Sazin near the mouth of the rivers Daret and Tangir at 980 m asl (see above) and further up in the basin of Chilas (at 1000–1200 m asl) carried out by Schroder and Saqid Khan (1988) indicate (in the context of the authors findings) that this glaciation existed at least up to 37–55 Ka BP.

During the 1986 expedition to the N slope of the Karakoram and to K2 (Fig 1, No. 5) the author invest-

igated the even more arid part of NW Tibet as far as the N ramp of the Aghil and Kuen Luen ridges and down to the desert-like Tarim Basin (cf. above). The long-term mean annual precipitation at the stations was 67.3 mm p. a., and at 2500 m asl it is 4–5° C colder than on the Karakoram S side. At an altitude of 3090 m the station of Tashikuergan measured 3.1° C during the period 1957–80. The lowest moraines of the last glacial maximum are at 2000–1900 m asl. Tens of kilometres long, these chains of median moraines extend the transverse valleys of the Kuen Lun (37° 20' N / 77° 05'–35' E) S of the Yeh Cheng far out into the mountain foreland, (Fig 3, left). The very extensive and thick moraines are 400–700 m high. Made up of in parts very large, poly-mictic, faceted blocks with rounded edges which are embedded in a loamy ground mass, they also include in many places stratified glacio-fluvial drift and rhythmic limnites that have been thrust in as well (Kuhle 1987a). 30–40% of the rough blocks are adjusted to the direction of movement. The extreme thickness and the flexures of these diamictites exclude convergent mud-flow deposits, as does their granite, phyllite and limestone composition. Their ground-plan morphology is one of elongated ramps, which bend to form frontal moraines around terminal basins. Even exaration striations at the foot of the inner slopes of the moraines have been handed to us. These are forms which have been deposited by the large Tibetan outlet glaciers in the course of the repeated glaciations of the Pleistocene (see below). During inter-glacial periods – as again now – renewed processing of continental frost scree took place in the highland. Outside the recent moraines described above there are more extensive, wide-ranging terminal glacier basins. They have remained untouched by the superimpositions of the last Ice Age and reach another 200 m further down.

The glacier cover of the last glacial period of the area is shown in Fig 3, left. The depression of the equilibrium line during the last glacial period amounted to 1300 m, so that the equilibrium line in the area under investigation (Fig 1, No. 5) ran at about 3900 m asl (3700–4100 m).

Like the area treated above, the more humid NE area (Fig 1, No. 2), too, stands for the N fringe of Tibet (Kuhle 1981). It does not have a key function for the reconstruction of the ice cover to the same degree as on the S fringe (Fig 1, Nos. 1, 3, 4). The altogether highest levels of the equilibrium line (see above) are reached in the S, where they are in most marked contrast to a formerly very large glacier area. Due to present aridity, and thus insufficient likelihood of an extensive Ice Age glaciation, the W edge of the plateau is also more brittle. The 450×820 km area under investigation in the NE, however, completes the Tibetan profiles from S and W. During an expedition in the year 1981, the Ice Age glaciation was reconstructed on the basis of 35 representative positions of ice margins (end moraine complexes) (Kuhle 1987c). In the extreme N, on the edge of the

Gobi Desert, as for instance at 39° 50' N / 97° 33' E, as well as at 39° 49' N / 97° 49' E, the glaciers flowed down to 2150 m. This corresponds to a depression of the equilibrium line by 1225 m to 3375 m asl. The equilibrium line depression by 1450 m to 3250 m which also occurred during the last Ice Age (at 39° 23' N / 98° 49' E) presents an extreme value<sup>4</sup>).

On the basis of these values the equilibrium line depression from its highest altitudes in S Tibet to its N edge here amounted to 1470 m (4720–3250 m). The S to N distance being 1500 km, this makes for a good accordance with the temperature equivalence, in which 100 m vertical distances is equal to 100 km of horizontal distance.

A mapping of the reconstructed equilibrium line heights in NE Tibet during the last Ice Age (Kuhle 1987c, p. 302) showed one isochion running S of the Tsaidam Depression at 4100 m, i. e. 100–400 m below the mean altitude of the plateau there. This must have led to a self-accumulating formation of inland ice (Fig 2). Polishing limits are evidence of a thickness of at least 500–700 m of ice in the area concerned (Kuhle 1987c). The existence of a total ice cover has been proved by lodgement till covers with locally prominent rough granite blocks; such granite block loams occur for instance in a valley on the N edge of the plateau, extend over the 4500 m high Oh La Pass and rise another 200 m along the slopes, dropping to 3950 m in the S in the plateau area proper (35°25'N/99°25'E) (Kuhle 1987c, p. 256).

North of the Tsaidam Depression, approximately at the latitude of the Kukuror (36°30'–50°N/98°–100°E), the equilibrium line has descended to 3750–3650 m. Towards the Qilian Shan's N slope it fell to 3400 m and further (see above). At a median altitude of this most northerly complex of plateaux and mountains of still more than 4000 m, the equilibrium line depression alone – apart from findings of ground moraines – allows conclusions to be made concerning the most northerly inland ice-complex I1 (Fig 2). In the W and E it was linked to I2 by bridges of glaciated mountain chains. At its centre was the 5704 m high Kakitu mountain range (38°09'N/96°29'E), the forelands of which are covered by a lodgement till measuring tens of metres in depth with five varieties of granite, sandstones and metamorphics. A 150 m deep core boring has been carried out in the foreland of the Kukuror Shan (Qinghai Nanshan; Chaka Basin, 3170 m asl, 36°48'N/99°04'E). It manifests a multitude of alternating deposits of stratified advance scree, ground moraine and limnic sediments of terminal basins, thus rendering likely the passage of 8 to 11 Pleistocene glaciations of the foreland and, in consequence, of the interior of Tibet (Kuhle 1987c, p. 261, Fig 6).

Concerning the dating: the Würm Age date of the last complete glacier cover described above has been established through the interlocking of recent outwash plains with the Ice Age limnites of the Tsaidam

Depression. These sediments were secured in 1981 by boring 10–180 m below the present sediment surface (36°48'N/96°27'E; 2806–2706 m asl) and found to date from 35 120–47 270 years BP (C 14 analyses by M. A. Geyh, Hannover, FR Germany). According to further radio-carbon datings in the Kakitu Massif (38°02'N/96°24'E) (Kuhle 1986b, pp. 456–7: samples taken by J. Hövermann) and in the Animachin (34°43'N/100°12'E) (Kuhle 1987c, p. 300, Fig 12/13), the more wide-ranging end of High to Late Ice Age glacier cover in Tibet had been completed by approximately 9400 to 8600 BP. This is also supported by the date – older than 8670 C14 years BP by Yamanaka (1982) (mentioned above) for the age determination of the moraine located by the author in S Tibet (Jhong Khola, 28°48'N/83°51'E) at 3250 m (Kuhle 1979/80, 1982).

A Holocene, Neo-Glacial glacier advance was established for two stages, in accordance with the 14–16-step stadial scale developed in the Dhaulagiri-Himal (Kuhle 1982): the Nauri Stadium (V) 4165 ± 150 C 14 years ago, and for the Dhaulagiri Stadium (VI) 2050 ± 105 to 2400 ± 140 years ago (Kuhle 1986 b, c). In the Khumbu Himalaya (N of Cho Oyu; 27°52'N/86°42'E), the Nauri Stadium (V), averaged for seven glaciers, reached an equilibrium line depression of 560 m. N of the Dhaulagiri and Annapurna Himalaya (28°43'N/83°45'E) Stadium V was found to have experienced an equilibrium line depression of 570 m on 17 glaciers, whilst descending to not quite 400 m on the S side (28°35'N/83°45'E) (calculated on the basis of eight glaciers; Kuhle 1982). A reconstruction of the equilibrium line depression on the Animachin Massif in NE Tibet (34°48'N/94°33'E) during the Nauri Stadium (V) worked out at only 240 m. This is an indication of the equilibrium line reactions in response to short-term climatic changes being less significant in N Tibet than in S Tibet.

Especially the younger, Late-Glacial positions of the ice margins, but possibly even the Neo-Glacial advances, may provide a conception of the extent of glaciation on the Tibetan Plateau during the Early-Würm ice age. According to the author's hypothesis, it was the cause of the global triggering of the Ice Age proper (see below).

### **The Overall Picture of Glaciation in Tibet down to the Lowest High Glacial Positions of the Ice Margin**

Fig 2 shows the reconstruction of the maximum glaciation in Tibet, with an area of about  $2.4 \times 10^6$  km<sup>2</sup>. In the central part it formed a compact inland ice, the outflows of which descended through the surrounding mountains for tens of kilometres. They terminated at the steep edges of the high plateau.

To be on the safe side, the 50–70 m high, glacio-fluvial gravel terraces E of 84°–85° E, which lie on the valley floor at 3800–3900 m asl, will be classified as High Glacial deposits. They thus indicate a glacier-free

Tsangpo section, which separated the glacier complexes I3 and I2 as far W as 84° E. Still further W they merged once again (cf. Fig 3 and 4). According to the reconstruction of an equilibrium line depression as low as 600 m below the average plateau altitude and the resulting self-elevation of the inland ice (Fig 3 and 4), a glacial filling seems likely, even in the case of this more easterly Tsangpo section. This would assign these terraces – like the varve clays in the deepest parallel valleys to the Late Ice Age. Nevertheless this valley section is to be regarded as free of ice until there is firm evidence to the contrary as a result of determining the age of terraces (Fig 2, N of Annapurna to Namcha Bawa). The second ice-free area is the Tsaidam Depression. In the block diagram perspective and exaggeration it is made to seem a merely narrow strip below I1.

Running in a NW direction from Mt. Everest to K2, and from Dhaulagiri to the W Kuen Lun (Fig 3 and 4), the profile shows that the Ice Age ELA had been upvaulted parallel to the present one – in the sense of a modified 'principle of uniformitarianism'. Over S Central Tibet it attained an altitude of fully 4700 m (see above). Nonetheless, an equilibrium line depression of at least 1200 m led to a drop below 83–86% of the plateau surface. The accumulating ice necessarily led to the infilling of the in-set valleys, which account for the remaining 14–16%. This resulted in the formation of ice, which grew higher through positive feedback, attaining an approximate thickness of 2700 m. Glacier thicknesses, ascertained by means of polishings and erratics, reach 1600 m in the Himalaya, and 700–1200 m in Central and N Tibet. In the W Karakoram even thicknesses of 2000 m have been observed (see above). However, these are minimum values, which may well have risen to 2500–3000 m in Central Tibet thanks to the compact ground-plan extending over 1500–3000 km. The high viscosity of cold, continental glacier ice with annual temperatures of around  $-10^\circ$  C at ELA-altitude (Kuhle 1987a) is bound to have been conducive to the build-up of ice. An average thickness of c. 1000 m would imply that  $2.2 \times 10^6$  km<sup>3</sup> of water had been bound up in the ice-sheet of Tibet. This corresponds to a lowering of sea-level by about 5.4 m (calculated on the basis of data provided by Flint 1971).

Fig 9 shows how the glacier area in Tibet relates to an equilibrium line depression of only 500 m. At the same time it permits an estimation of conditions if the equilibrium line drops by 1200 m, and makes plausible the cupola-shaped build-up of the inland ice to a considerable thickness. With the ice held back by mountain barriers, build-up had been assisted by the slow spread of its run-off, and its freezing to the sub-surface. At a later stage the pressure-induced melting point was passed. Run-off from the central inland ice-sheet via a zone of ice-stream networks in the highland rims and down to the tongues of the outlet glaciers gradually increased until an equilibrium had been achieved. This was the end of the build-up of ice.

Glacial isostasy in Tibet – an indirect proof: this must result in a glacio-isostatic drop of about 700 m (730 m) (density difference of ice versus material of the earth's mantle ( $\Delta g = 1:3.7$  at an ice thickness of 2700 m). Since deglaciation occurred about 9000 years ago (see above) remnants of glacio-isostatic uplift with a falling phase should still be recoverable – as in Central Scandinavia (Mörner 1978) or the Pleistocene glaciation of North America (Andrews 1970) – the latest tectonic map to be published in China (Beijing 1987) does indeed show rates of uplift of more than 10 mm/year for Central Tibet. This value is two to three times higher than what had been established for the much younger High Himalayas<sup>5)</sup>, which had actually been uplifted much more rapidly, as the evidence of antecedent valleys demonstrates (Kuhle 1982a). Epirogenetically slow rather than fast, the tectonic uplift of Tibet can accordingly attain more substantial rates of uplift than the Himalayas<sup>6)</sup> *only due to the reduction of glacio-isostatic pressure*. This is further, albeit indirect, evidence for the ice in Tibet. This is the point at which to have recourse to the discussion of the 1932 Swedish triangulation by Norin (1982). This showed that since the Survey of India in 1861 the profile by way of Leh and into SW Tibet had undergone an uplift of 37 m. This implies a rate of uplift of 521 mm/year (37 m/71 years). In the Scandinavian centre of uplift such extreme rates of uplift only took place around 10–8 Ka (Mörner 1978, Fig 1) and decreased to the present vestigial uplift by about 4 Ka. This permits the analogous conclusion that in the region of the Na-K'ot Ts'o (Fig 4), which is represented by that profile of uplifting, the Tibetan ice persisted several thousand years longer than the Scandinavian inland ice.

**Measurements Regarding the Radiation Balance in Tibet in the Light of the Energy Balance of the Ice Age**

From August until November 1984 and 1986 climatic parameters were measured on Mt. Everest and Shisha Pangma in S Tibet (28°N; Fig 1, No. 4), as well as on K2 in NW Tibet (36°N; Fig 1, No. 5). Eight climatic stations were installed for that purpose at altitudes varying from 3800 m to 6650 m asl. At the same time, portable, hand-operated instruments allowed comparative measurements to be carried out in other places<sup>7)</sup>. In this context measurements of radiation and radiation balance on rock or scree, as well as on glaciers, are of interest. Approximately 25000 representative data on global radiation, return-radiation and albedo were obtained. When weather conditions were such that radiation was not impeded by any cloud, the values of incoming radiation were between 1000 and 1300 W/m<sup>2</sup>, which is approximately the solar constant at the upper limit of the atmosphere in relation to the corresponding position of the sun at the time (Fig 10 and 11). Theoretical incoming radiation on September 21st as a mean value, is about

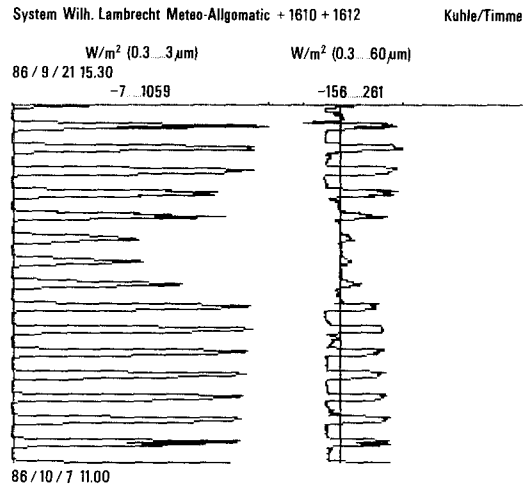


Fig 10 Radiation and radiation balance on K2 (Karakoram 36°03'N/76°32'E) above firn (rough)

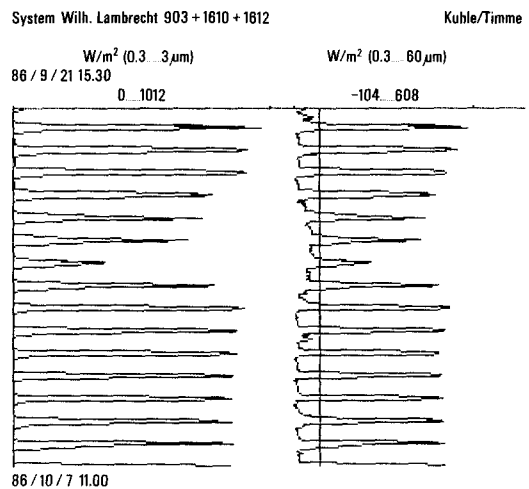
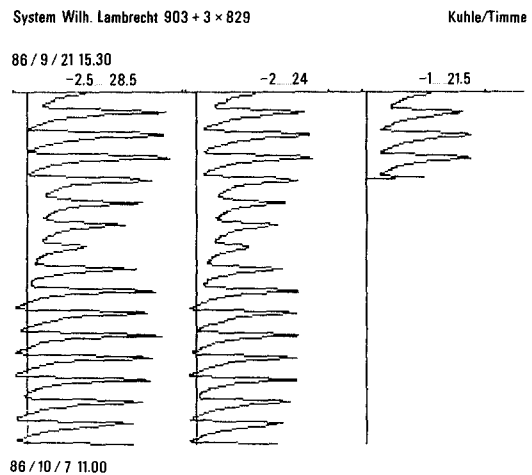
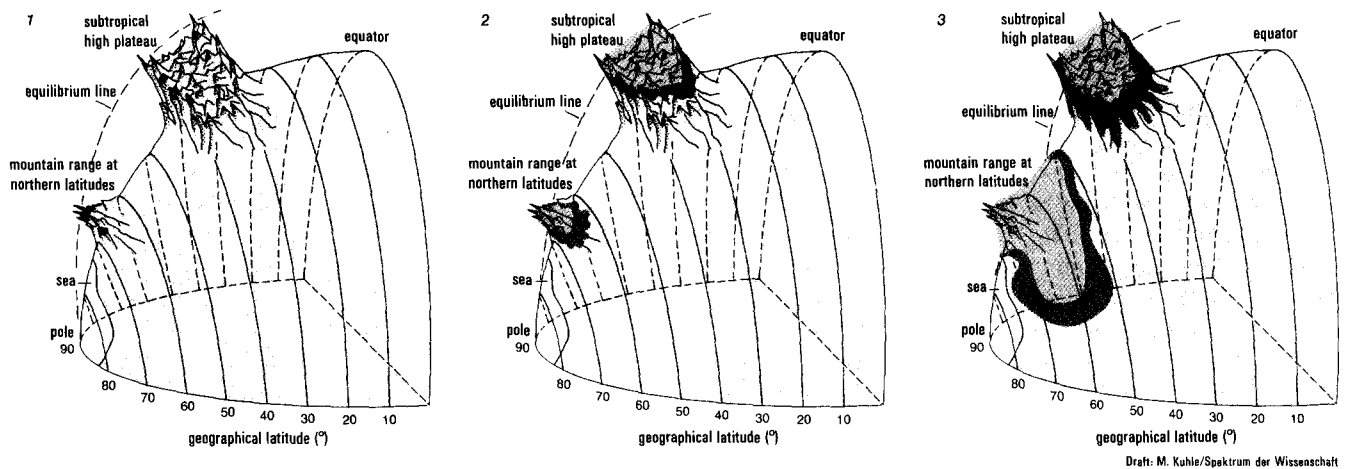


Fig 11 Radiation and radiation balance on K2 (Karakoram 36°06'N/76°32'E) above light scree (rough)

Fig 12 Soil temperature on K2 (Karakoram 36°06'N/76°32'E) light scree (see Fig 10) (depth: 1, 5, 10 cm).





**Fig 13** Strongly schematized presentation of the principle of the relief related origin and termination of ice ages. The causative intensification of the cooling-down process emanates from a subtropical high plateau (such as the Tibetan High Plateau) due to the fact that the initial lowering of the equilibrium line by c. 500 m leads to the glaciers descend by 1000 m from the mountains, thus suddenly glaciating large plateau areas (step 1 to 2). Mountain chains at higher latitudes experience the same amount of equilibrium line lowering as a result of the cooling-down by 3,5° C during that change in the parameters of the earth's orbit. But, since the altitudinal distance of the present glaciation to the height of the foreland areas is too great, glaciation has as yet had little effect on area and thus on reflection (2). As the subtropical high plateau has undergone large-scale glaciation and the transformation of a formerly very effective 'heating panel' into an area of reflection, the further cooling down of the atmosphere caused in this way leads to a renewed lowering of the equilibrium line. The consequence is a chain reaction-like, worldwide enlargement of glacier areas. This particularly advanced very fast in all those places where the lowering of the glaciation line reaches the flat mountain forelands (step 2 to 3). The sequence of additions of mountain foreland glaciation depends on the particular altitudinal distance of pre-Ice Age hanging glacier ends from the altitudinal level of the foreland. Although, due to the conditions of radiation, the cooling effect per glacier area is greatest in the sub-tropics, the areal gain of glaciers increases significantly with the decreasing equilibrium line at higher latitudes (3). The reason for this is the fact, that the equilibrium line dips towards the polar regions, and that starting point of equilibrium line heights comes progressively lower towards the lowlands. In the end the ice areas of the high latitudes outnumber those of subtropical high plateaus and mountains by approximately 8:1, by which time their cooling effect has increased around twofold. Nonetheless, such far-reaching glaciation would not have occurred without the impact of the subtropical inland ice. The cooling, which reacts upon the subtropical plateau ice as well can hardly result in any further increase of the area of ice there because the glaciers cannot reach the lowlands when flowing over the edge of the plateau (step 2 to 3). In a reverse process (3 → 1) the end of the Ice Age begins in the N and S lowland plains: on the return to normal values of solar radiation and a rise in temperatures by those initial 3,5° C the corresponding rise in the equilibrium line by 500 m and the rise in the glacier ends thus by 1000 m becomes particularly effective for areas of flat lowland glaciation (step 3 to 2). Whilst lowland ice areas experience extreme reductions, thus forcing a global warming-up, the surface areas of the subtropical highland ice will remain almost constant, because only the steeply descending outlet of glacier tongues on the margins will become shorter on the initial upward move of the equilibrium line, whereas the reduction in glaciation is far from reaching the flat plateau ice proper (step 3 to 2). Only when the further warming-up of the earth has been initiated and progressed through the disappearance of lowland ice, will the subtropical highland areas also be freed from ice (step 2 to 1).

1180 W/m<sup>2</sup> at the latitude of the area under investigation (30°N). With an atmosphere approximately transparent to radiation, incoming radiation at Tibetan altitudes produces an energy input at least four times higher than that obtained between 60° and 70° of northerly latitude of the Pleistocene North European inland ice centre (cf. Bernhardt & Philipps 1958). Apart from the much lower angle at which the sun strikes the earth's surface, radiation losses through diffuse reflection of the atmosphere down to sea-level (Lauscher 1956) are about 7%. A radiation loss of this magnitude is in part brought about, and indeed increased, by the low angle of incidence in so far as it prolongs the distance in denser atmospheric layers as compared with a vertical incidence. On the expanses of rock and scree, which now make up 99% of the area of Tibet, albedo values of 15–20% of the global radiation were recorded (Fig 11). The increase in the temperature of the scree

(transformation into long wave radiation, Fig 12) is accordingly high. Thus Tibet is now the most effective heat surface of the earth for the hot season. On glacier surfaces, especially on the snow surfaces of the feeding areas, 85–90% of the short wave radiation (0.3–3 μm) is reflected (Fig 10). As incoming radiation increases, so does the reflection caused by the transparency of the high altitude atmosphere. At 6600–7000 m asl, i.e. at the altitude of Tibet's Pleistocene ice dome, the 'greenhouse effect' no longer applies (Fig 3 and 4). About 97% of the highland area was covered by ice, thus transforming the heat surface into a cooling surface with a 70% energy loss of that extremely high subtropical incoming radiation (Figs 10, 11). With an inland ice surface of 2.4 × 10<sup>6</sup> km<sup>2</sup> it implies a global cooling effect, equal to that of an at least 9.6 × 10<sup>6</sup> km<sup>2</sup> (4 × 2.4 × 10<sup>6</sup>) Nordic inland ice – i.e. an ice-sheet of more than twice the size of the N European Weichsel Ice (Fig 13).

### The Cooling Effect of the Tibetan Ice

In line with the author's theory (Kuhle 1981, 1987b) that the Tibetan Ice must have exerted a considerable global cooling influence, the hypothesis was mathematically examined by Lautenschlager et al. (1987, pp. 8–40) by using the above data of glacier expansion and radiation balance in conjunction with the T21 Model. According to the Hotelling T<sup>2</sup> Test of surface temperature, the cooling influence of the Tibetan Ice starts off very high in the test hierarchy. This test hierarchy consists of 10 parts, and assesses all the other globally reconstructed factors, such as ice-sheets on land and sea as well as on ice-free land and sea surfaces, along with their albedo and their role in the system of atmospheric circulation at about 18 Ka. In this test hierarchy the Tibetan Ice starts off with a significance of approximately 10 to the second power above the 99.9% confidence interval. It dominates the remaining nine influences to such an extent that together they were the cause of only the remaining scarcely three powers of ten (i.e. little more than half) of the total cooling down of the main Ice Age period.

### A Relief-Specific Ice Age Theory Based on Global Radiation Geometry (Fig 13)

The specific geometry of the earth and the position of the earth's axis in relation to the sun, which has been stabilized by rotation, together result in a radiation balance that provides the sub-tropics with many more times the energy than occurs at high latitudes. It causes the inclination of the equilibrium line from the sub-tropics towards the poles. From this there followed the formation of large expanses of ice in flat or lowland places where the equilibrium line approached sea-level during periods of prehistoric equilibrium line depressions. This was the case in high latitudes unfavoured by radiation. On the other hand, locations on the globe which are favoured by radiation, i.e. the lower latitudes, require even higher elevations the greater their proximity to the equator, in order to permit the formation of glaciers. This led to the mountain and highland ice which was unable to reach the sub-tropically warm plains and lowlands there, thereby terminating with their ablation areas on the steep highland margins.

This relationship of shallow-ended lowland ice in areas not favoured by radiation to steep-edged ice on mountains and highlands in the sub-tropics is the foundation on which the possibility of a relief-specific Ice Age cycle is founded. The comparatively small spatial expanse of ice in the sub-tropics as a function of the

necessary high altitude above sea-level, which at the same time is coupled with those locations on steep edges, is compensated for from the same root: a global radiation several times greater than that hitting the ice regions of the lowlands. The pre-condition for the triggering of an ice age is the adequate – i.e. relative to the necessary altitude above sea-level – and considerable size of a mountain highland favoured by sub-tropical radiation, which thus makes it a rare feature in earth history. Such a case, and with it the readiness of the earth for an ice age, occurred with the uplifting of the  $2.4 \times 10^6$  km<sup>2</sup> area of the Tibetan Highland. Proven findings of moraines from that time, plus the reconstructions of their positions, must permit a later ratification of the kind of orogeny that extended up into the vicinity of the equilibrium line during the Permo-Carboniferous glaciation, for instance.

It is characteristic of the structure of this mechanism of Ice Age auto-cycles that the degree of cooling and thus of global radiation, depends on the extent of the sub-tropical highland glaciation. The fixed proportion of sub-tropical ice to lowland ice also guarantees that the cooling process, which had built up as a result of self-intensification, is to be reversed from the earlier shrinking end of the lowland ice in the manner described above.

The approach of the sub-tropical plateau uplift does not require the principle of the Milanković Cycle for the triggering of the Ice Age. Continuing uplift by another 500 m, which corresponds to that of the Milanković cooling by c. 3.5° C, would ensure the glaciation of the Tibetan Plateau even without this extra-terrestrially induced cooling. Admittedly a 500 m uplift, and the consequence of one third of Tibet being under cover of ice, would not be sufficient to trigger the Ice Age. It is likely that an uplift of 900–1000 m is required, so that the amount of global cooling may also be obtained through the Milanković effect by way of a very much larger initial Tibetan ice. It is, however, indispensable for the re-warming. Only the rising of the equilibrium line by these 500 m can lead to the loss of area occupied by lowland ice necessary for this.

This demonstrates that an extra-terrestrial influence over a short period merely caused the short-cycle to be followed by the Pleistocene cold periods, but not by the Ice Age itself, and it must be stressed that the occurrence of these short cycles of about  $10 \times 10^4$  years will not come to an end through the loss of global readiness for an ice age. This will be the case when the uplift phase, primarily of the Tibetan Plateau and other mountains and highlands favoured by radiation, has been completed, and regions distant from the equilibrium line have been aggraded.

## Footnotes

- 1) Six expeditions were financed by the German Research Society (DFG), and in part by the Max Planck Society and the Academia Sinica, two by the State of Lower Saxony and the University of Göttingen, and one privately.
- 2) ELA<sub>Depr.</sub> = depression of the equilibrium line; tp = recent terminus of the glacier-tongue; ti = prehistoric terminus of the glacier-tongue; Si = prehistoric equilibrium line; Sp = recent equilibrium line; S = equilibrium line = ELA
- 3) Porter (1970) also found the depression of the equilibrium line in the Swat Kohistan, 100 km farther W, to have been about 1200 m, by contrast with a present ELA of 4200 m at approximately 3000 m asl.
- 4) An equilibrium line depression of 1430 m (with a maximum value of 1575 m) in NE Tibet was established for an older glaciation (Riss) on the basis of five margins (Kuhle 1987c).
- 5) Schneider (1957, pp. 468 & 475) puts the uplift of the NW Karakoram at 12000 m since the end of the Late Tertiary, which corresponds to 3–4 mm/y for Tibet and the Himalaya. Gansser (1983, p. 19) gives an integral value of 10–15 mm/y for Tibet and the Himalaya and separately for the Himalaya alone of 4–8 mm/y (oral communication, 1982).
- 6) As Fig 3 shows, the ice burden decreased in the direction of the outlet glaciers on the rim of the Tibetan Highland as a function of its steep gradient curves. On the one hand this serves to lessen the uplift, thanks to the reduction in pressure in contrast to Central Tibet, and on the other hand mountains like the Himalaya were merely affected by ice filling the valleys. This led to a comparatively linear ice burden, whereas the Central Plateau carried an extensive ice-sheet.
- 7) The author wishes to thank J.-P. Jacobsen, Diplomgeograph, for help with obtaining data during the 1984 expedition, and H. Diedrich, J.-P. Jacobsen and A. Schulze, Diplomgeograph, for such assistance during the 1986 expedition.

## References

- Andrews, J. T.: A Geomorphological Study of Post-Glacial Uplift with Particular Reference to Arctic Canada. *Canadian J. of Earth Sciences* 7, 2, 703–715 (1970)
- Bernhardt, F.; Philipps, H.: Die räumliche und zeitliche Verteilung der Einstrahlung, der Ausstrahlung und der Strahlungsbilanz im Meeresniveau. *Die Einstrahlung. Abh. Meteor. Hydrol. Dienst* 15, 1–227 (1958)
- Cline, R. (ed.): Climap Project: Seasonal Reconstructions of the Earth's Surface at the Last Glacial Maximum. *The Geol. Soc. of America*: 1–88 and maps, New York 1981.
- Dainelli, G.; Marinelli, O.: Le condizioni fisiche attuali. *Risultati Geol. e Geogr. IV; Relazioni scientifiche della Spedizione Italiana De Filippi nell' Himalaya, Caracorum e Turkestan Chinesa* (1913–14), Ser. II, Bologna 1928.
- De Terra, H.: Geologische Forschungen im westlichen Kunlun und Karakorum-Himalaya. *Wiss. Ergebn. d. Dr. Trinklerschen Zentralasien Expedition, II*, Berlin 1932.
- Flint, R. F.: *Glacial and Quaternary Geology*. London 1967.
- Flint, R. F.: *Glacial and Quaternary Geology*. New York 1971.
- Gansser, A.: *Geology of the Himalayas*. London 1964.
- Gansser, A.: The Wider Himalaya, a Model for Scientific Research. *Mat. Fys. Medd. Dan. Vid. Selsk.* 40, 14, 3–30 (1983)
- v. Handel-Mazzetti, Frh. H.: Das nordostbirmanisch-westyünnanische Hochgebirgsgebiet. *Karsten-Schenck, Vegetationsbilder* 17, 7–8 (1927)
- Heuberger, H.: Untersuchungen über die eiszeitliche Vergletscherung des Mount-Everest-Gebietes, Südseite, Nepal. *Göttinger Geogr. Abh.* 81, 29–30 (1986)
- Höfer, H. v.: Gletscher- und Eiszeitstudien. *Sitzungsber. d. Akad. d. Wiss. Wien, Math.-Nat. Kl.* 1, 79, 331–367 (1879)
- Iwata, S.; Yamanaka, H.; Yoshida, M.: Glacial Landforms and River Terraces in the Thakkhola Region, Central Nepal. *J. of Nepal Geol. Soc.* 2, spec. iss. 81–94 (1982)
- Kuhle, M.: Klimageomorphologische Untersuchungen in der Dhaulagiri- und Annapurna-Gruppe (Zentraler Himalaya). *Tagungsber. u. wiss. Abh.* 42. Dt. Geographentag 1979, Wiesbaden 42, 244–247 (1980)
- Kuhle, M.: Erste Deutsch-Chinesische Gemeinschaftsexpedition nach Tibet und in die Massive des Kuen-Lun-Gebirges. *Tagungsber. u. wiss. Abh.* 43. Dt. Geographentag 1981, Mannheim 43, 63–82 (1981)
- Kuhle, M.: Der Dhaulagiri- und Annapurna-Himalaya. Ein Beitrag zur Geomorphologie extremer Hochgebirge. *Z. f. Geomorph., Suppl. Bd.* 41, 1 u. 2, 1–229 u. 1–184 (1982)
- Kuhle, M.: DFG-Forschungsbericht mit Ergebnissen der Chinesisch-Deutschen Gemeinschaftsexpedition nach S-Tibet und in die N-Flanke des Mt. Everest (Chomolungma) 1984, 1–52, 1985.
- Kuhle, M.: Schneegrenzbestimmung und typologische Klassifikation von Gletschern anhand spezifischer Reliefparameter. *Petermanns Geogr. Mitt.* 130, 41–51 (1986a)
- Kuhle, M.: Absolute Datierungen zur jüngeren Gletschergeschichte im Mt. Everest-Gebiet und die mathematische Korrektur von Schneegrenzberechnungen. *Tagungsber. d. 45. Geographentages, Berlin* 1985, 45, 200–208 (1986b)
- Kuhle, M.: Former Glacial Stades in the Mountain Areas Surrounding Tibet – in the Himalayas (27°–29°N: Dhaulagiri, Annapurna, Cho Oyu and Gyachung Kang areas) in the South and in the Kuen Lun and Qilian Shan (34°–38°N: Animachin, Kakitu) in the North, pp. 437–473. In: Joshi, S. C. (ed.) *Nepal Himalaya: Geo-Ecological Perspectives*. New Delhi 1986c.
- Kuhle, M.: Zur Geomorphologie der nivalen und subnivalen Höhenstufe in der Karakorum-N-Abdachung zwischen Shaksgam-Tal und K2-N-Sporn: Die quartäre Vergletscherung und ihre geoökologische Konsequenz. 46. Dt. Geographentag 1987, München, *Tagungsber. u. wiss. Abh.* 46 (1987a) (in print)
- Kuhle, M.: Subtropical Mountain- and Highland-Glaciation as Ice Age Triggers and the Waning of the Glacial Periods in the Pleistocene. *GeoJournal* 1987, 14, 4, 393–421 (1987b)
- Kuhle, M.: The Problem of a Pleistocene Inland Glaciation of the Northeastern Qinghai-Xizang Plateau (Tibet), pp. 250–315. In: Hövermann, J.; Wang Wenying (eds.) *Reports on the Northeastern Part of the Qinghai-Xizang (Tibet) Plateau by the Sino-W. German Scientific Expedition*. Beijing 1987c.
- Lauscher, F.: Strahlungs- und Wärmehaushalt. *Ber. Dt. Wetterdienst* 4, 22, 21–29 (1956)
- Lautenschlager, M.; Herterich, K.; Schlese, U.; Kirk, E.: Simulation of the January Climate 18 000 YBP. *Report MPG-Inst. f. Meteorologie* 9, 87, 11, 1–42 (1987)
- Lichtenecker, N.: Die gegenwärtige und die eiszeitliche Schneegrenze in den Ostalpen. *Verhandl. d. III. Intern. Quartär-Konferenz Wien* 1936, 141–147, 1938.
- Louis, H.: Schneegrenze und Schneegrenzbestimmung. *Geogr. Taschenb.* 1954/55, 414–418, Wiesbaden 1955.
- v. Loczy, L.: Die wiss. Ergebnisse der Reise des Grafen Blazschényi in Ostasien 1877–1880, 3. Abschn. *Geologie*. 1, 307–836, Wien 1893.
- Mörner, N. A.: Faulting, Fracturing and Seismicity as Functions of Glacio-Isostasy in Fennoscandia. *Geology* 6, 41–45 (1978)
- Norin, E.: Quaternary Climatic Changes within the Tarim Basin. *Geogr. Review* 22, 591–598 (1932)



- Norin, E.: The Pamirs, K'unlun, Karakorum and Chang T'ang Regions. Sino-Svedish Expedition. I. Geography 54, III, 1, 1-61, 1982.
- Porter, S. C.: Quaternary Glacial Record in Swat Kohistan, West-Pakistan. Geol. Soc. of America Bull. 81, 5, 1421-1446 (1970)
- Prinz, G.: Beiträge zur Glaziologie Zentralasiens. Mitt. a. d. Jahrb. d. Kgl. Ungar. Geolog. Anst. 25, 127-335 (1927)
- Schneider, H.-J.: Tektonik und Magmatismus im NW-Karakorum. Geolog. Rundschau 46, 426-476 (1957)
- Schroder, J. F.; Saqid Khan, M.: High magnitude geomorphic processes and Quaternary chronology, Indus Valley and Nanga Parbat, Pakistan. Zeitschr. f. Geomorph. Suppl. Bd. Leicester Symposium, March 21 st-23 rd. 1988 on "The Neogene of the Karakoram and Himalayas." (in print)
- Shi, Yafeng; Wang Jing-tai: The Fluctuations of Climate, Glaciers and Sea Level since Late Pleistocene in China. Sea Level, Ice and Climatic Change. Proceedings to the Canberra Symposium, 12/79 13, 1, 1979.
- Tafel, A.: Meine Tibetreise. Eine Studienreise durch das nordwestliche China und durch die innere Mongolei in das östliche Tibet. 2 Bde., Karte, Stuttgart 1914.
- Trinkler, E.: Geographische Forschungen im Westlichen Zentralasien und Karakorum-Himalaya. Wiss. Ergebnisse d. Dr. Trinklerschen Zentralasien-Expedition I, 1-133, Berlin 1932.
- v. Wissmann, H.: Die heutige Vergletscherung und Schneegrenze in Hochasien mit Hinweisen auf die Vergletscherung der letzten Eiszeit. Akad. d. Wiss. u. d. Lit., Abh. d. math.-nat. wiss. Kl. 14, 1103-1407 (1959)
- Xie Zichu: Qinghai-Glacier Map (ELA). Science Press, Beijing 1984.
- Yamanaka, H.: Radiocarbon Ages of Upper Quaternary Deposits in Central Nepal. Sci. Rep. Tohoku Univ., 7th ser. (Geogr). 32, 1, manuscript, 1932.
- Zabirov, R. D.: Oledenenie Pamira. Moskau 1955.

The new geography of the northern countries

# Norden · Man and Environment

Edited on behalf of the Geographical Society of Northern Finland and the Dept. of Geography, Univ. of Oulu, Finland

by Uuno Varjo, Oulu/Finland and Wolf Tietze, Helmstedt/Germany

535 pages with 387 figures and 110 tables, 17 × 25 cm, hardcover, DM 118.—

A quarter century ago, the famous book "A Geography of Norden", ed. by A. Sømme, was published. The present new version of a similar geography of the northern countries has now been written by distinguished specialists. It will be of great interest to geographers, environmentalists and economists world-wide.

Contents: The historical shaping of the Nordic countries — The seas of Norden — Geology and geomorphology of Norden — Climate and hydrology of Norden — Biogeography of Norden — Physical geography of Iceland — Population and settlement of Norden — Primary occupations of Norden — Reindeer herding in Norden — Manufacturing and services in Norden — The social geography of Norden — The population, settlement and economy of Iceland — The Faeroes — Svalbard and Jan Mayen — Greenland — The geographical regions of Norden



**Gebrüder Borntraeger Verlagsbuchhandlung**  
Johannesstr. 3 A, D-7000 Stuttgart (Germany)

US Agents: Lubrecht & Cramer Ltd., Rd 1, Box 244, Forestburgh, NY 12777, USA

## On the Geoecology of Southern Tibet\*

### *Measurements of Climate Parameters Including Surface- and Soil-Temperatures in Debris, Rock, Snow, Firn, and Ice during the South Tibet- and Mt. Everest Expedition in 1984*

*Kuhle, Matthias, Prof., Dr.; Jacobsen, Jens-Peter, Dipl.-Geogr.,  
Universität Göttingen, Geographisches Institut,  
Goldschmidtstraße 5, 3400 Göttingen, FR Germany*

#### Radiation and Radiation Balance

Between 8 September and 23 October 1984 incoming radiation (0.3–3.0  $\mu\text{m}$ ) was measured with a Thies actinograph at heights between 5000 m and 6500 m at six stations for a total of 30 days (Fig 1). These were as follows:

- 1) Shisha Pangma Base Camp 28° 36'N 85° 45'E 5000 m 4 days
- 2) Shisha Pangma Camp I 5300 m 1.5 days
- 3) Shisha Pangma Camp II on the Yepokangara glacier (Fig 2) at 5540 m 1.5 days
- 4) Central Rongbuk glacier (orographic right paraglacial valley on Mt. Everest N slope) 28° 05'N 86° 52'E at 5500 m (Camp I) 10 days
- 5) East Rongbuk glacier medial moraine (Mt. Everest N slope) 6040 m (Camp II) almost 5 days
- 6) East Rongbuk glacier (Camp III) at 6500 m 7.5 days

On 21 September (the beginning of autumn) a theoretical value of global radiation of 1180 W/m<sup>2</sup> is possible at these heights in this region, ignoring the transmission absorption of the atmosphere. Since this date lies halfway through the expedition this may be taken as a mean for this value during the expedition. Fig 1 gives the decrease of global radiation during the period and shows that with values over 1200 W/m<sup>2</sup> these theoretical values for the upper limit of the atmosphere were reached at comparable solar altitudes. This shows the extreme transparency of the atmosphere above 5000 m.

Simultaneous observations of such high global radiation values were made on a Dirmhirn Starpyranometer (0.3–3.0  $\mu\text{m}$ ; measurement period 9 September to 3 November 1984), Lambrecht radiation-balance meter (0.3–60  $\mu\text{m}$ ; same period) and a Thies radiation-balance meter (0.3–60  $\mu\text{m}$ ; 10 October to 20 October 1984) (Fig 3). The values above 1200 W/m<sup>2</sup> are the result of reflection from the lower surfaces of small amounts of cloud (2/8) and from ice pyramids (Fig 2) (Fig 3 middle row: East Rongbuk glacier at 6040 m).

Fig 3 also shows the way the albedo depends on the surface. For comparable incident radiation values this reaches 180–290 W/m<sup>2</sup> with sporadic patches of mat vegetation, almost 500 W/m<sup>2</sup> from bright quartz sand and over more than 600 W/m<sup>2</sup> between ice pyramids (Fig 2). Reflected energy reaches even higher levels from bare firn. In the area of the glacier catchment the snow surface at 6650 m reflected more than 850 W/m<sup>2</sup> from an incoming radiation of less than 1000 W/m<sup>2</sup> (Fig 4 and 5, foreground). Fig 6 presents the albedo values (per cent) of specific materials from the Mt. Everest region. The albedo from dark debris amounted to about 14–16%, so that in comparison to the fresh snow cover the difference in albedo reaches 80% at the most. Generally, a difference of about 70% was measured between unglaciated surfaces and glacier catchments.

The low albedo values of the debris can be seen in its high soil temperatures measured at the same time; e.g. at Shisha Pangma at 5540 m where the soil temperatures at 1 cm in gravel reached 20° C (Fig 13). Fig 14 shows such a value of about 30° C measured on Mt. Everest at

\* Paper discussed at the International Tibet-Symposium at Göttingen, October 8–11, 1985

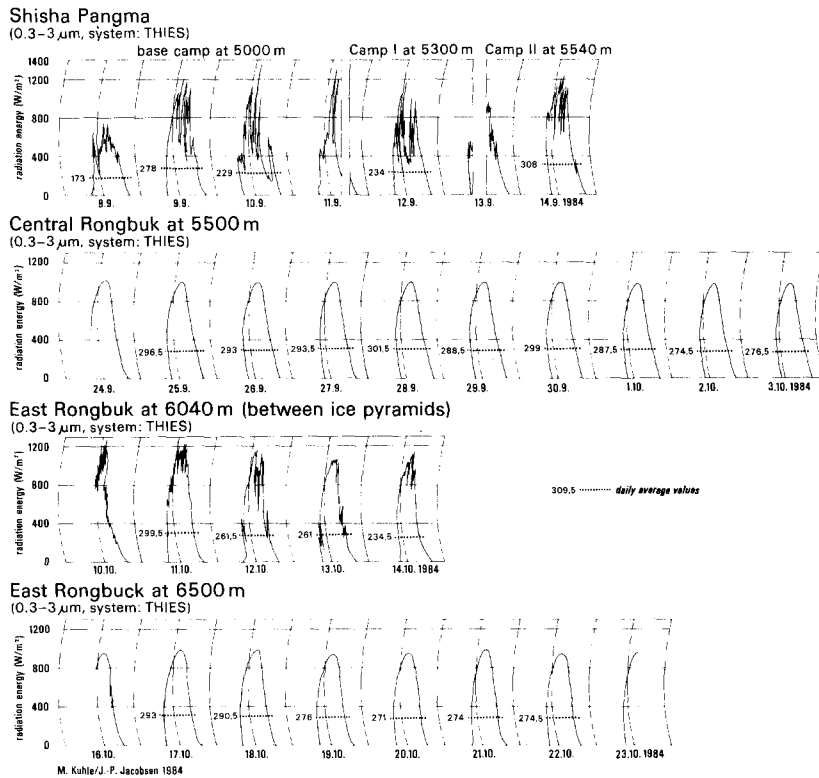


Fig 1  
Global radiation in S Tibet and on the N slope of the Himalaya (Shisha Pangma, Mt. Everest) between 28°N and 28°35'N

Fig 2 Ice pyramids of the glacier tongue of the Yepokangara glacier at 5600 m (28°25'N 85°46'E). The retreating glacier tongue is disintegrating into these c. 30 m high ice pyramids (scale provided by figure of man). Such glaciomorphological forms are characteristic of the subtropical radiation energy conditions in S Tibet in the precipitation shadow of the High Himalayas and are much more strongly developed than on the leeside S slope of the Himalayas. Photo: M. Kuhle, 13 September 1984



1.25 pm on a cloud-free autumn day. No doubt, soil temperatures especially in small depth depend on both incident radiation (cloud cover) and wind velocity (Fig 7–11).

#### Cloud Cover, Wind Direction and Velocity, Relative Humidity, Air Temperature, and Soil Temperatures at 1 cm, 5 cm and 10 cm

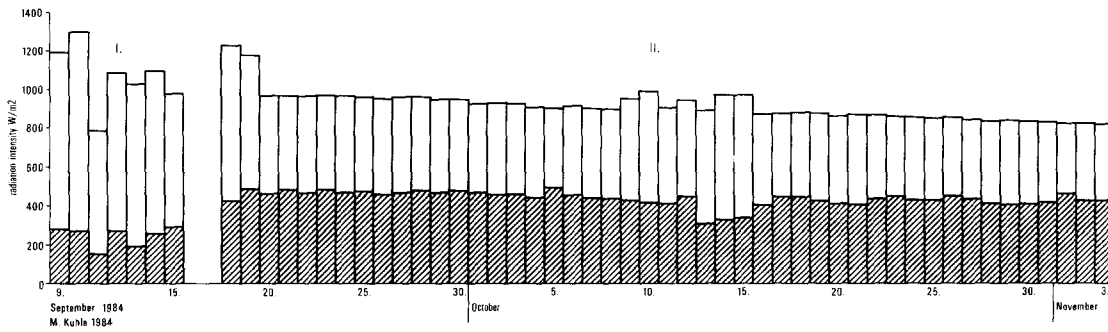
Fig 7–11 show continuous fixed measurements at the following locations and dates: Fig 7 Shisha Pangma Base Camp (5020 m, 28°36'N 85°45'E) 7 to 16 September; Fig 8–11 Mt. Everest Base Camp (5170 m, 28°11'N 86°51'E) from 8 to 11 September and on Himalaya N slope from 17 September to 4 November 1984.

These illustrations show the daily freeze-thaw alternations up to 10 cm deep in a representative year as the monsoon season changes to clear, cold and stormy autumn days. Moisture first enters the surface material; then follow the solifluction movements of debris of 4 to 8 cm/year measured by this expedition on slopes of 30° on scree-cones, debris slopes and morainic slopes.

Fig 12 to 17 present the observations and measurements obtained by portable instruments. The values from Shisha Pangma at 5300–5640 m and those from Rongbuk glacier on Mt. Everest were obtained at the same time as those on Fig 7–11. These provide for a comparative interpretation and the determination of rates of altitudinal change (lapse rates). Values repre-

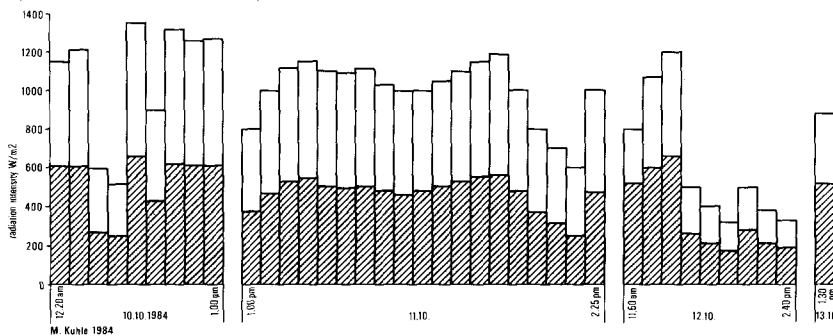
**Radiation and Radiation Balance (daily maxima)**

I. at Shisha Pangma at 5000m a.s.l.: 30cm above till partly covered with alpine meadow  
 II. at Mt. Everest at 5160m a.s.l.: 30cm above light quartz sand  
 (Star-shaped Pyranometer according to Dirmhirn, Albedometer 0.3-3um and Radiation Balance Meter 0.3-60um, LAMBRECHT)



**Radiation and Radiation Balance at East Rongbuk (6040m a.s.l.)**

30cm above firn between ice pyramids  
 (Radiation Balance Meter 0.3-60um, THIES)



**Radiation and Radiation Balance**

(Radiation Balance Meter 0.2 0.3-60um, THIES)

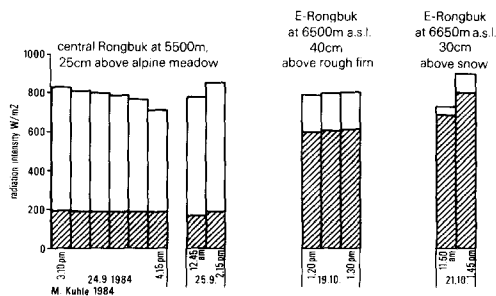


Fig 3 Global radiation and radiation balance in S Tibet on the Himalaya N slope (Shisha Pangma, Mt. Everest) between 28° N and 28° 35' N

representative of the S Tibetan area and the Tibetan Himalaya in the lee of the High Himalayas are provided by the measurements at Latsu (29°N 87°40'E) between 4030 m and 5000 m and at Nilamu (28°11'N 85°58'E) at 4300 m from 25 August until 7 September.

The following characteristic tendencies are recognizable:

- a) Cloud cover decreases from 8/8 to 0/8.
- b) From mid-September the wind direction ceases to vary and becomes stable from a prevailing SSE to SE point.
- c) In the areas near the valley floors the wind velocity, which reached only a few metres per second reached up to 20 m/sec in the autumnal post-monsoon period. The up to 100 m long snow banners streaming from the peaks which were observed from the beginning of

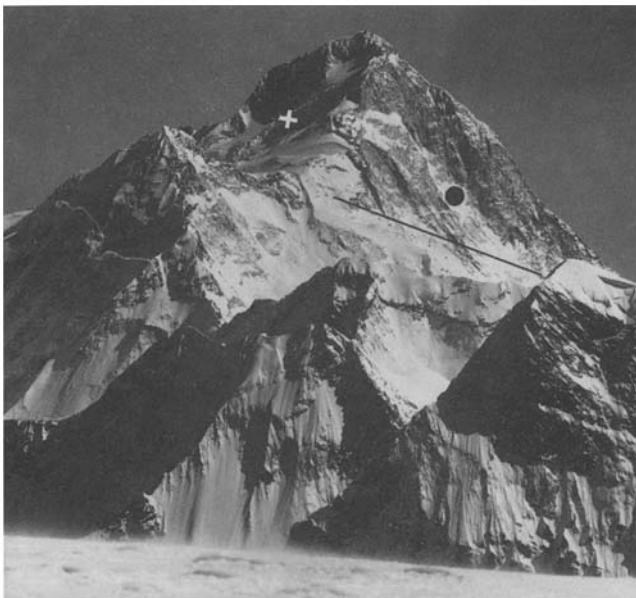
October became very much longer, clearly influenced by the jet-stream velocities which probably reached 30 or even 40 m/sec. These cleared the rock surfaces above 7200 m of snow and were effective in forming the upper limit of glaciation (see below).

- d) The relative humidity (and since temperature decreases also occurred, the absolute humidity) decreased from 60–90% in the monsoon period to 10–20% in the autumnal post-monsoon period. At the same time sudden excursions of humidity to 80 or 90% or more became steadily less regular and frequent (Fig 7–11). These suddenly increased humidity periods were associated with veering of wind from SE to W, NW and N and its simultaneous decrease in velocity; during them cloud cover increased from 0/8 to 1/8 and as much as 5/8.



Fig 4 View of Lhotse, 8501 m (27°58'N 87°00'E), from the N (● white) from Rapiu La (6500 m). Although the E spur (● black) of Mt. Everest is of similar steepness and is covered with cornices and ice wall some decametres thick, the metamorphite of the Lhotse wall (● white) reaching over 7200 m is unglaciated and is blown almost free of snow (cf. Fig 5). Photo: M. Kuhle, 19 October 1984

Fig 5 View of Makalu, 8481 m (27°54'N 87°05'E), from the NNW from Rapiu La (6500 m). On this mountain, formed of massive tourmaline-granite in contrast to the metamorphic rocks of Mt. Everest, a clear upper glacial limit (—) can be seen. It runs between 7200 m and 7600 m on its W wall (●). The NE flank of the mountain lies in wind shadow and thus carries a hanging glacier in a cirque-like feature (x) at above 7600 m. Photo: M. Kuhle, 19 Oct. 1984



Radiation and radiation balance on Mt. Everest 1984 (0.3–60 μm; system: THIES)

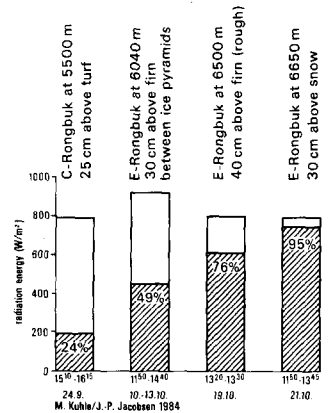


Fig 6 Radiation and radiation balance on Mt. Everest 1984

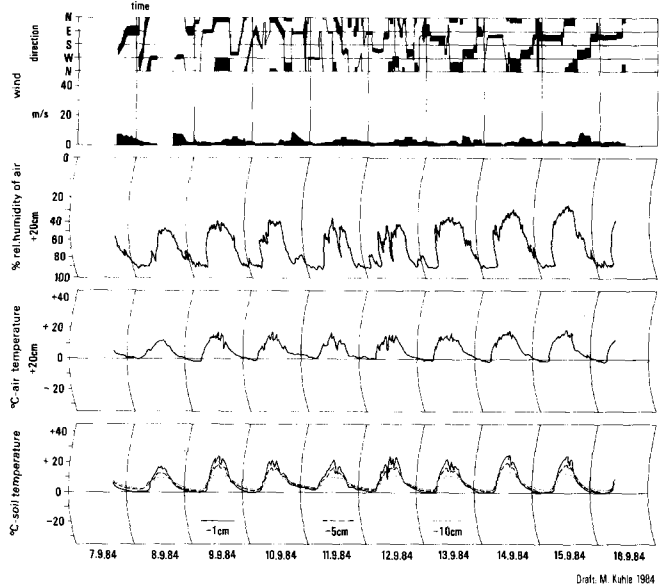


Fig 7 Measurements at the fixed base camp on Shisha Pangma N slope (28°35'N 85°46'E) at 5020 m on moraine debris with mat vegetation

e) Air temperature decreased as the solar altitude showed its seasonal decrease. On the debris surfaces of the valley floors and high plains at 5000 m these reached almost 20° C at midday and fell to only a few degrees below freezing at night. In October and November this same diurnal variation (about 20° C) is 10° C to 15° C lower down the scale. The maximum daily heating occurred on the upper moraine at 6500 m at 11,45 hr on 19 October when the air temperature at 2 m over the surface reached +7° C and at 2 cm above the ground +27° C. It is interesting that air temperatures were independent of the humidity increases referred to above. In each case there was no reduction in cooling at night during high humidities; it was rather slightly increased (Fig 9: 3–6 Oct.; Fig 11: 29 and 30 Oct).

Fig 8–11  
Measurements at the fixed Mt. Everest base camp in the Rongbuk valley (Himalaya N slope) on the tongue of the Rongbuk glacier at 5170 m (28°10'N 86°51'E) from 17 September to 4 November 1984

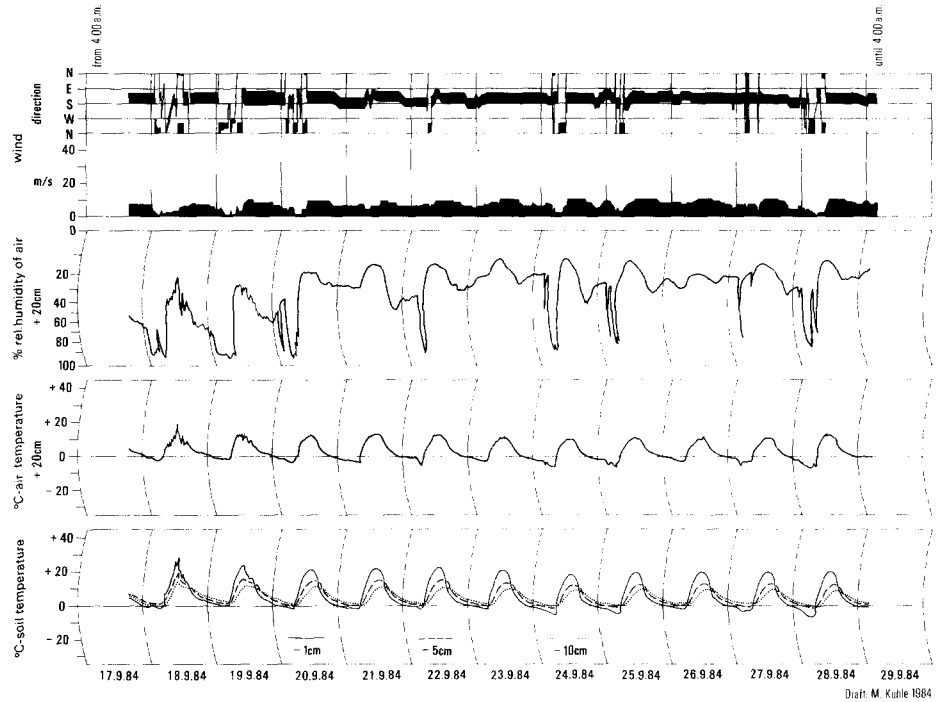


Fig 8

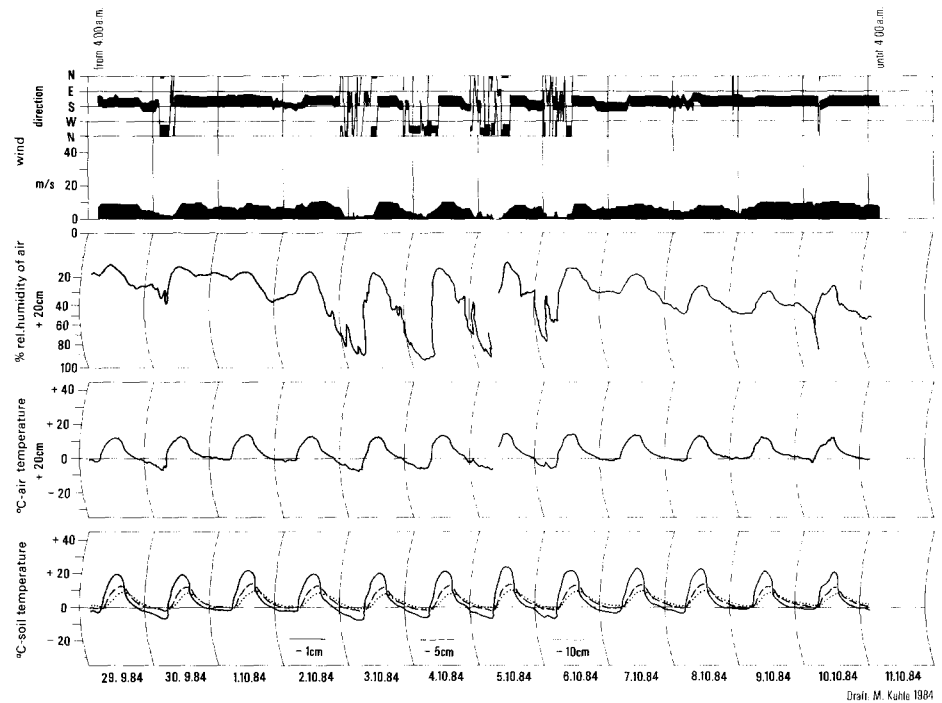


Fig 9

f) The diurnal variation of soil temperature, which follows the air temperature, is reduced as depth of observation increases from  $-1$  cm to  $-10$  cm. Periglacially active freezing in the debris began on 20 September at  $-1$  cm and on 29 September at  $-10$  cm (Fig 8). On the other hand the soil above  $-10$  cm no longer thawed after the beginning of November. Thus the periglacially active freeze-thaw layer traversed the upper 10 cm of soil in 45 days (cf. Kuhle 1985). This produces a new picture of the

relatively short seasonal transition period of periglacial processes in subtropical S Tibet at 5000 m. Not only is the period of periglacial soil movement here shorter than in temperate latitudes but, since the ground ceases to thaw down to 10 cm after a short time, it is also restricted in depth. The columns for Latsu (Fig 12) and Nilamu (Fig 13) make clear the relation between inversions of temperature and increasing attenuation of energy flux with depth. Thus at 05,15 hr on 26 August with  $15^{\circ}\text{C}$  at

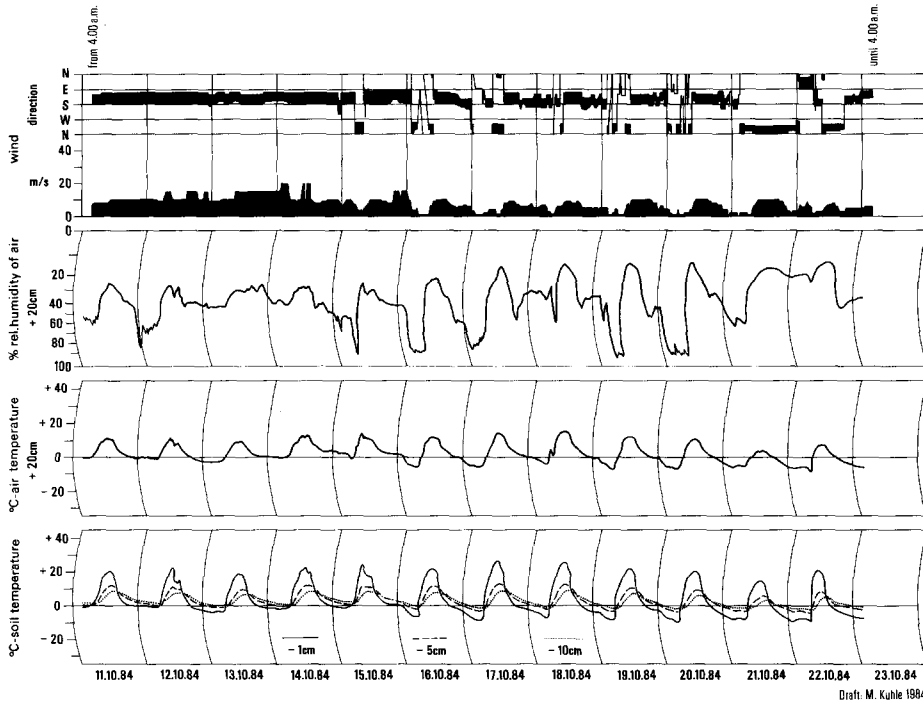


Fig 10

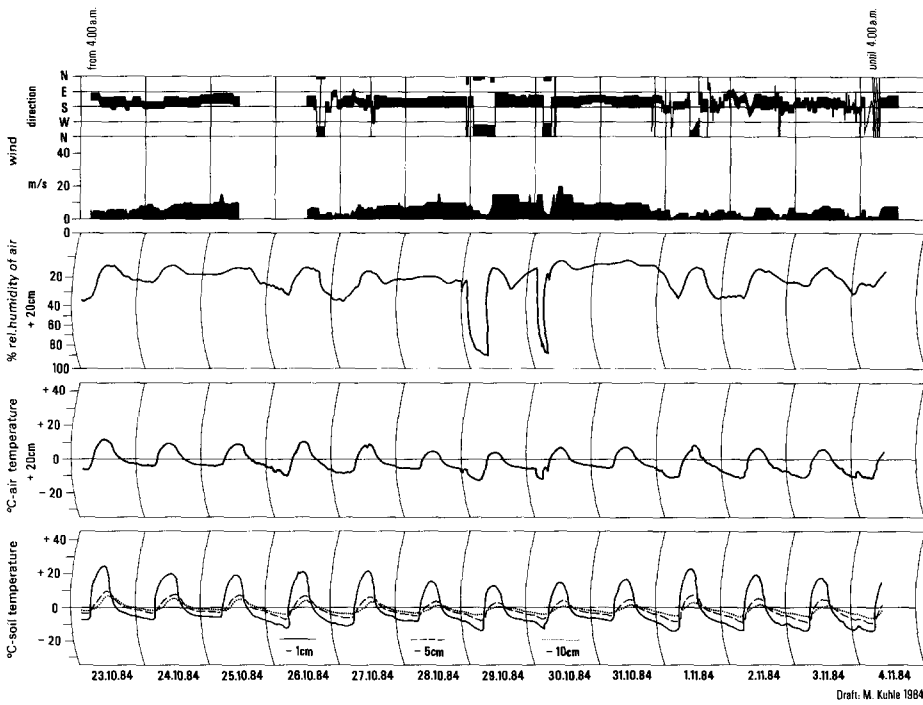


Fig 11

-10 cm but 12° C at -1 cm at 12,00 hr (am) in contrast it was only 13.5° C at -10 cm but 15.5° C at -1 cm.

- g) All the sinusoidal diurnal curves of air and soil temperature as well as relative and absolute air dryness (inverse humidity) are related in the same sense to the curve of air temperature. Soil temperatures show a lag because of its insulating effect on the flux of energy. Wind velocity varies independently of wind

direction and in this area is independent of time of day.

- h) The mean air temperature of -9° C to -11° C at the snowline (ELA) extrapolated from the values of Fig 7 to 17 shows that the S Tibetan glaciers of the N slope of the Himalaya and the Tibetan glaciers are cold-arid ice-flows. They are correctly contrasted by Shi Yafeng and Xie Zichu (1964) as continental rather than belonging to the more maritime monsoon influenced glaciers of obviously warmer regions.

Fig 12  
Measurements with hand transportable equipment in the Tibetan Himalaya S of the Tsangpo depression (29°03'N 87°42' E)

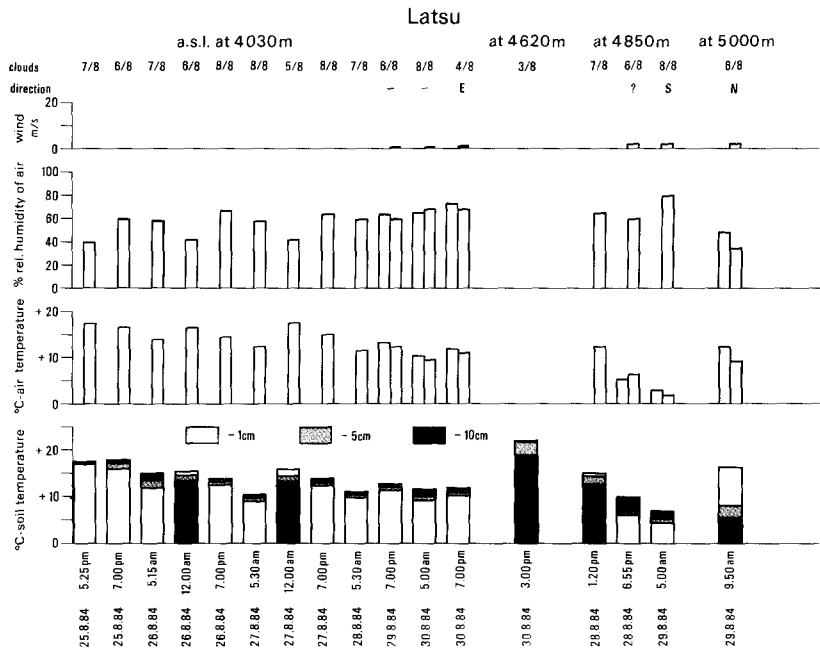
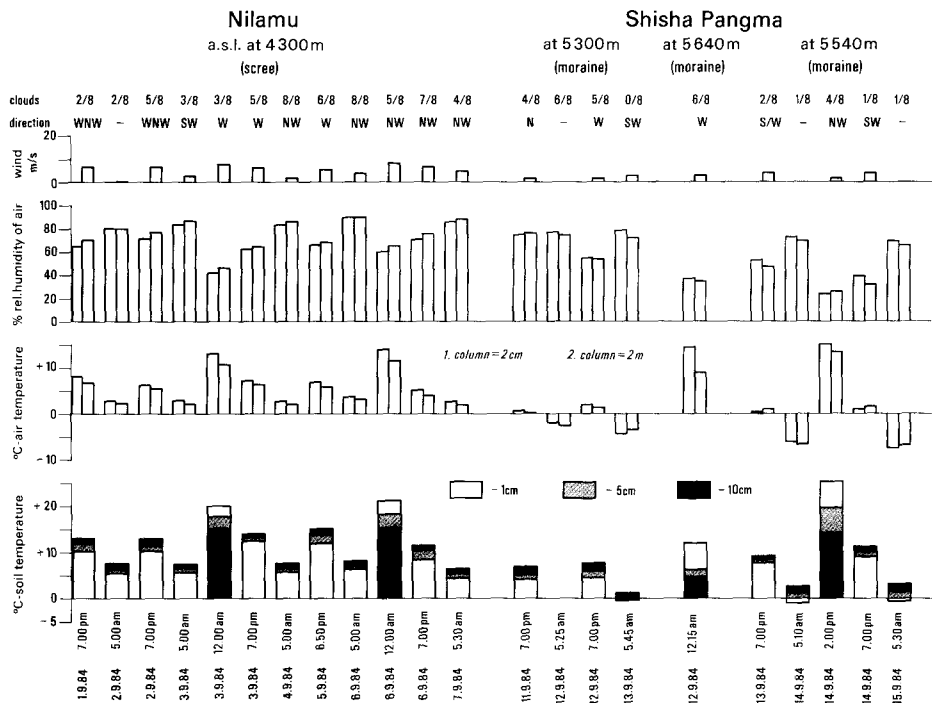


Fig 13  
Measurements with hand transportable equipment in the Tibetan Himalaya and on the N slope of the High Himalaya (28°12' to 40°N 85°40' to 86°10' E)



Draft: M. Kihle 1984

**Surface Temperatures on Mountain Slopes between 3800m and 8800m on Debris, Rock, Ice, Firn, and Snow**

In the post-monsoon periods of 1982 and 1984 at times between 18 September and 4 November measurements were made in the High Himalayas of the surface temperatures with all exposures; in more detail this was on the N and S slopes of the Mt. Everest group. These concentrated on collecting data during cloud free radiation weather situations because of the telemetric measu-

rement methods using passive infra-red detectors (Kuhle 1986a and 1986b). As the humidity measurements for the same periods show (Fig 8-11, 14-17) the air water content was then very small. This was not only because of the low temperatures measured at the same time as the specific humidities but also because of the low atmospheric density above 3800 m. Because of this transparency of the atmosphere to the transmission of energy (infra-red radiation between 8 and 14 μm) is almost complete so that there is almost no selective absorption



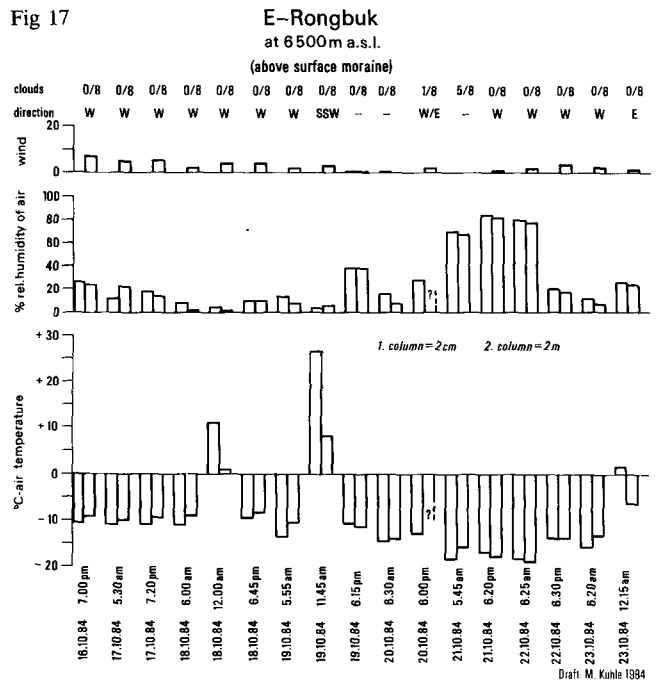
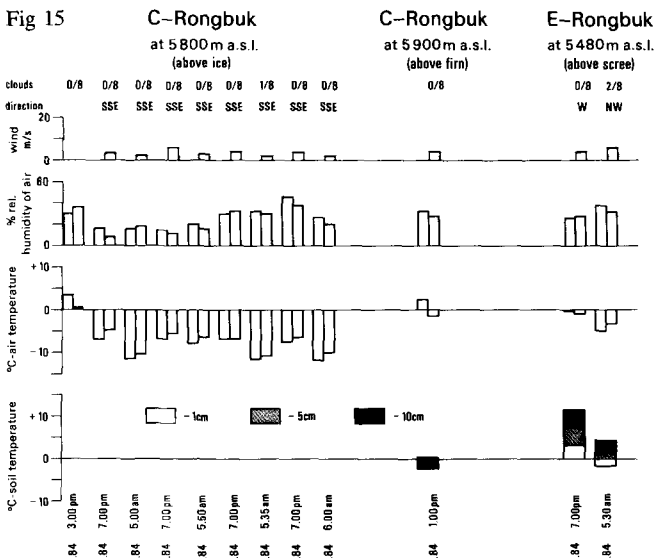
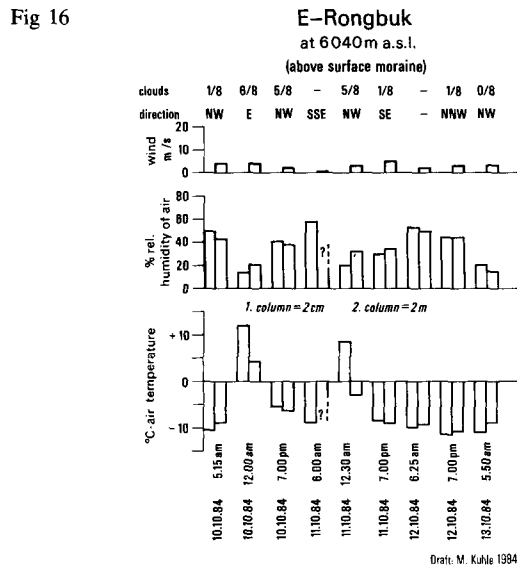
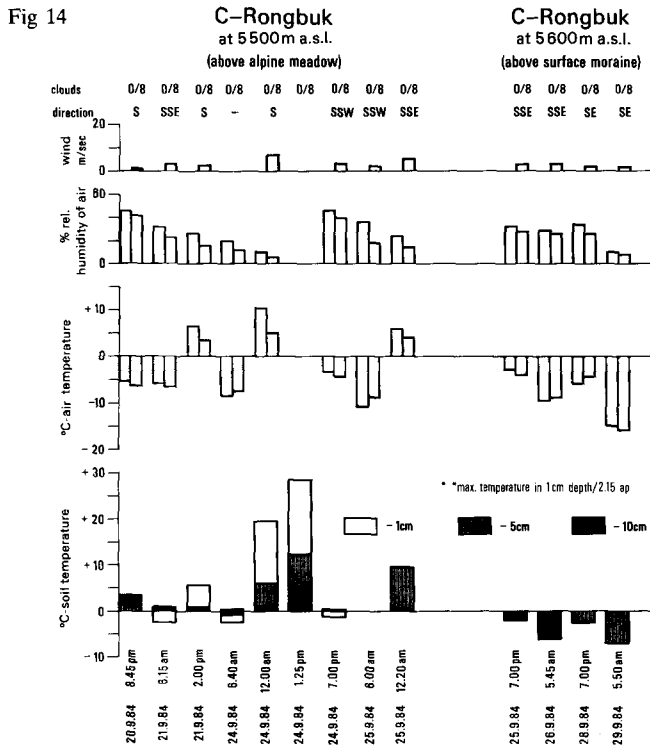


Fig 14-17 Hand portable and fixed measurements near and on the glaciers of the Mt. Everest N slope (Central and East Rongbuk glaciers between 5480 m and 6500 m, 28° to 28°08'N 86°50' to 58'E) from 20 September to 23 October 1984

by the air and thus the measured values represent the true surface temperatures.

Since the measurement techniques are described in previous works (Lorenz 1973; Kühle 1986 a+b) they are referred to only briefly. We used instruments with 100 m focal length concave mirrors and distances of 1500, 3000 and 6000 m. These were types R 380 RVC (Raynger, USA), Thermopoint 80 (AGA, FRG) and Raynger II HR (Raynger, USA). They are specially adapted for

extremely low temperatures. The concave mirrors focus the radiation on an electronic chopper and process the infra-red portions. Although the miniature R 380 RVC instrument required calibration over a black plate both the digital instruments were provided with corrections for specific conditions. The microprocessor controlled instruments are provided with telescopic sights and are accurate to ±1%. For calibration some of the surface temperatures were compared with resistance thermometer measurements on the same objects.

The results obtained are presented in Fig 19–29 and summarized in the table forming Fig 30. For statistical reasons the temperature gradients were not separated according to slope exposure so the rather inhomogeneous 1775 data points include all four or even eight compass directions. The regression analyses provided (Pearson product moment correlation) show R values correlation ranging from  $-0.82327$  to  $-0.66111$  with an overall value of  $R = -0.78000$  with a probable error of less than 1% (significance  $-0.00000$ ) so that meaningful conclusions can be drawn. These referred to both the temperature gradients per 100 m (A, B) and the position of the  $0^{\circ}$  C line on rock (Fig 19–21) and ice (Fig 22–24) surfaces between 11 hr and 15 hr local time (Fig 19, 22, 25) and between 15 hr and 11 hr (Fig 20, 23, 26). Fig 21 includes all values on rock surfaces and Fig 24 all such values on ice surfaces. Fig 25 and 26 include rock and ice substrates together, dividing the values between 11 hr and 15 hr from those between 15 hr and 11 hr. The curves of Fig 27 investigate all 1775 observations of surface temperatures of both surface types and time intervals.

Above and below the regression lines (the solid lines) of Fig 19 to 27 are shown by single (dashed) and double (dotted) standard errors of estimation (SEE). The former should include 66%, the latter 95%, of all possible surface temperatures. The height at which the double SEE line cuts the  $0^{\circ}$  C line is that for which there is a 95% probability that the temperature will not rise above freezing point. Similarly the intersection with the single SEE line shows the height at which melting rarely occurs on the slopes of the Himalayas. This is already at an altitude with a mean annual temperature of  $-25^{\circ}$  C or less. At this height, above the  $0^{\circ}$  C limit, there can be no snow settling or sintering process such as occurs in warmer, near freezing point areas i.e. no ice bridges can form between new snow nuclei. Firn formation by a temperature induced metamorphosis is absent. The snow remains dry and cohesionless and does not cling to the rock. It is easily blown from the summit pyramids by the storms at this altitude. Thus there is formed a glacier-free rocky altitudinal zone above that of the glaciers as the highest tier of the climato-geomorphological vertical zonation of the Earth (Kuhle 1986a, b; 1987).

This upper limit of the glacial zone is clearly developed on Mt. Everest, Makalu and Lhotse in the central Himalayas at some 7200 m. At this height bare rock comes to the surface (Fig 4 -----, Fig 5, 28, 29 -----). This height of the empirical upper limit of glaciation makes sense in terms of Fig 19–21 and 25 and especially of the curves of the combined data in Fig 27. In all these graphs the height of 7200 m comes between the  $0^{\circ}$  C intersections of the double SEE lines. In the middle of this height zone between 6600 m and 7700 m (Fig 27) the cold, cohesionless snow is almost completely blown away like dry wind-blown sand. This average height of the upper limit of glaciation varies with the exposure of the

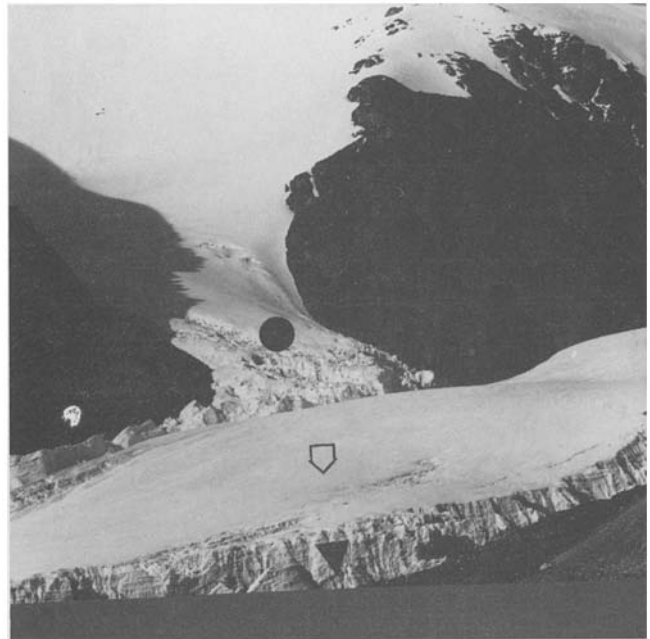


Fig 18 View from 6340 m over the East Rongbuk glacier (in shadow in foreground) towards the NE to its confluence with the Khartaphu glacier ( $28^{\circ}02'$  to  $30'N$   $86^{\circ}59'E$ ). The cross-sections of both the Khartaphu glacier ( $\square$ ) and that of the tributary cirque glacier ( $\bullet$ ) are both box-like, i.e. with almost vertical steep edges ( $\blacktriangledown$ ). This denotes a cold arid glacier flow mechanism (block flow movement). Such profiles occur at the snow line where mean annual temperatures of  $-9^{\circ}$  C to  $-10^{\circ}$  C are found. This is also the mean temperature of the glacier at about 10 m in the ice and indicates a cold continental type of glacier.  
Photo: M. Kuhle, 17 October 1984

mountain slopes to sun and wind and also, though only slightly, with the steepness of the rock walls.

Fig 30 provides the relationship between the height of the  $0^{\circ}$  C level based on the time of day and nature of the surface and the thermal zonation (temperature gradient). On rock surfaces this varies 870 m between day (representing the insolation between 11 hr and 15 hr) and night (low radiation balance between 15 hr and 11 hr). It varies twice as much on ice (1681 m). This height limit has a mean value of 5719 m on rock but some 800 m lower, 4913 m, on ice. The differential effect of the surface material is seen by the steeper gradient on rock (Fig 19–21). The less steep increase on ice surfaces may be explained by the loss of sensible heat below the  $0^{\circ}$  C line resulting from melting (which requires latent heat (Fig 22–24). This also explains the much lower mean level of the  $0^{\circ}$  C boundary over ice. The diurnal difference lies between these two extremes on a composite rock/ice surface. The distribution shown gives this as 953 m; the difference in height of the  $0^{\circ}$  C line between rock and ice is 593 m between 11 hr and 15 hr, and 1404 m between 15 hr and 11 hr. This illustrates both the greater absorption of heat by the dark rock surface and its greater heat capacity above freezing

INFRARED MEASUREMENTS: HIMALAYAS-TOTAL 1982+1984/M. KUHLE  
 DIAGRAM TEMPERATURE/ALTITUDE, 3800-8800M, 11-15 HOURS, ROCK  
 FILE NONAME (CREATION DATE=08/27/85)

06/27/85 PAGE 20

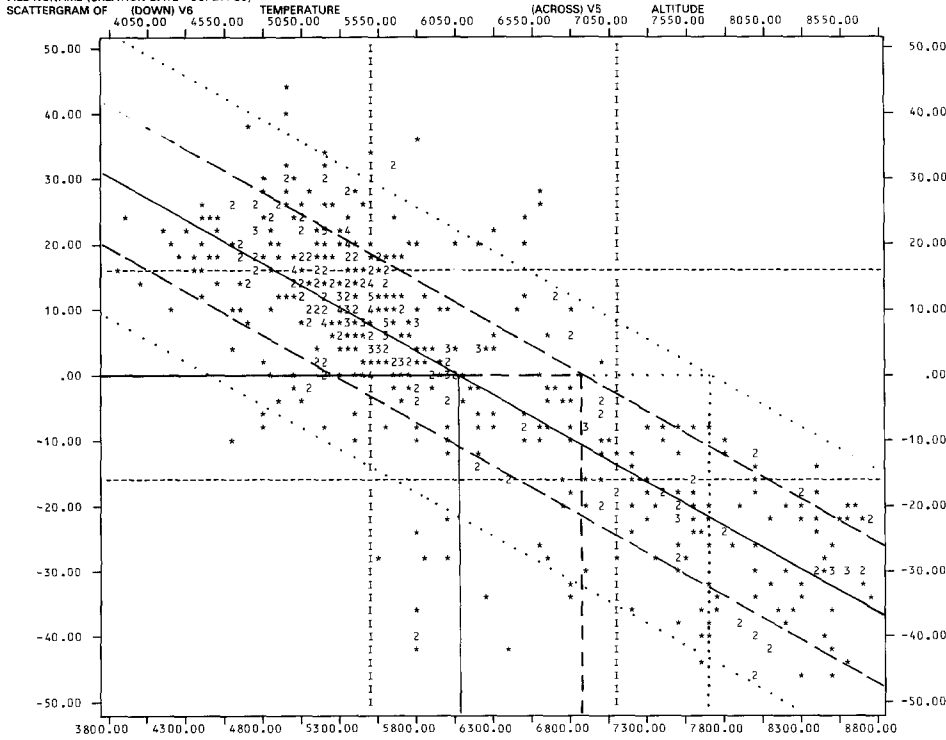


Fig 19

Fig 19-27  
 Telemetric infra-red measurements  
 in the Mt. Everest massif (High Hi-  
 malaya 27°57' to 28°10'N 86°45' to  
 87°E) on rock, debris, snow, firn and  
 ice surfaces of valley glaciers, valley  
 sides and the highest mountain slo-  
 pes

STATISTICS..

CORRELATION (R)-	-0.82327
STD ERR OF EST -	10.88582
PLOTTED VALUES -	554
R SQUARED -	.67778
INTERCEPT (A) -	82.13377
EXCLUDED VALUES-	5
SIGNIFICANCE -	.00000
SLOPE (B) -	-.01353
MISSING VALUES -	0

GRADIENT OF TEMPERATURE: 1.353°C/100M  
 0°C-LINE AT 6070M

INFRARED MEASUREMENTS: HIMALAYAS-TOTAL 1982+1984/M. KUHLE  
 DIAGRAM TEMPERATURE/ALTITUDE, 3800-8800M, 15-11 HOURS, ROCK  
 FILE NONAME (CREATION DATE=03/07/86)

03/07/86 PAGE 6

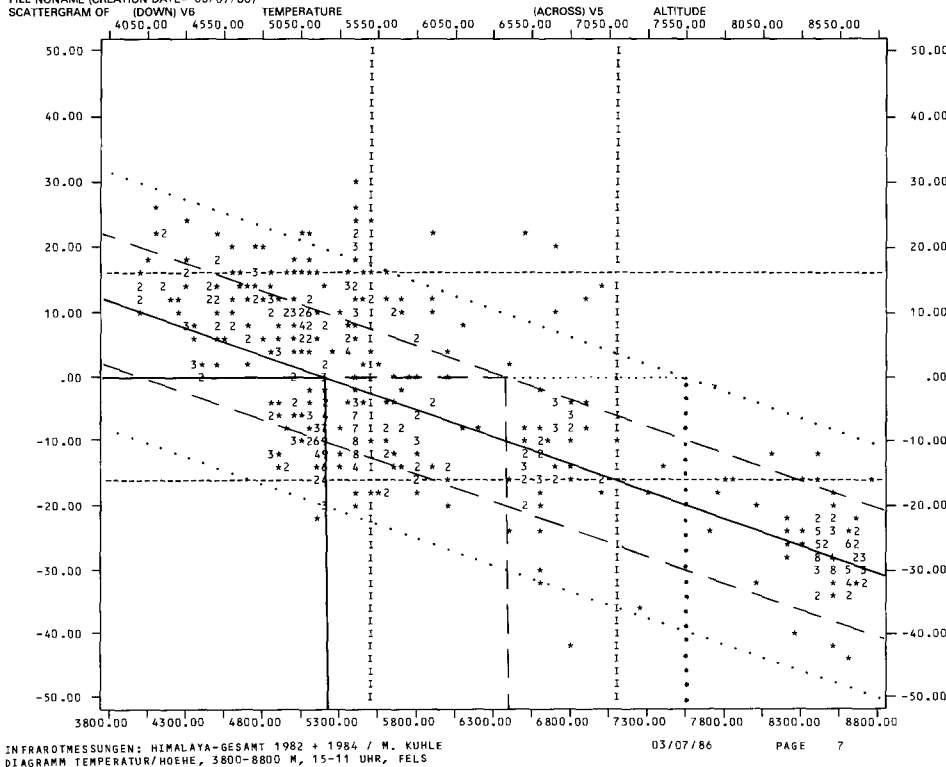


Fig 20

STATISTICS..

CORRELATION (R)-	-0.7599
STD ERR OF EST -	9.97278
PLOTTED VALUES -	536
R SQUARED -	.57759
INTERCEPT (A) -	44.24800
EXCLUDED VALUES-	3
SIGNIFICANCE -	.00000
SLOPE (B) -	-.00851
MISSING VALUES -	0

GRADIENT OF TEMPERATURE: 0.851°C/100M  
 0°C-LINE AT 5200M

INFRAROTMESSUNGEN: HIMALAYA-GESAMT 1982 + 1984 / M. KUHLE  
 DIAGRAM TEMPERATUR/HOEHHE, 3800-8800 M, 15-11 UHR, FELS

03/07/86 PAGE 7

Fig 21

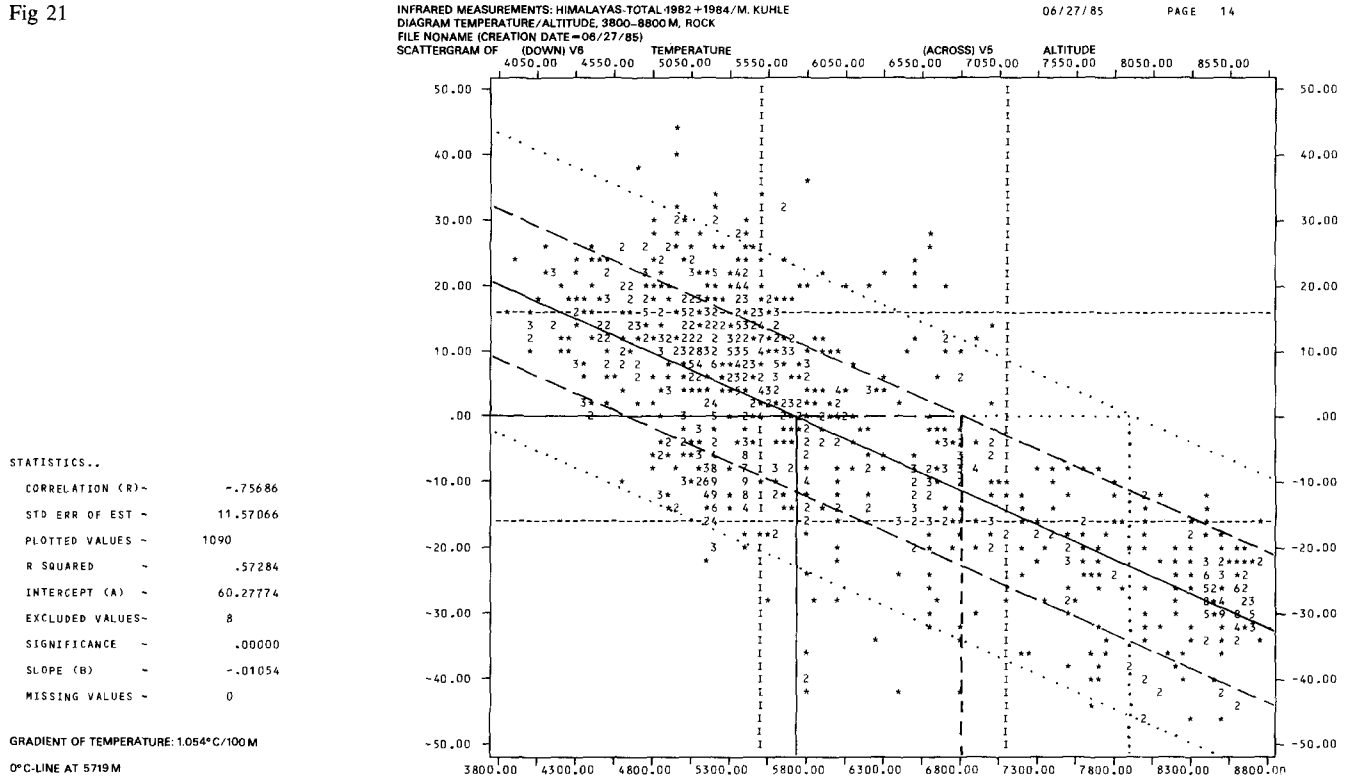
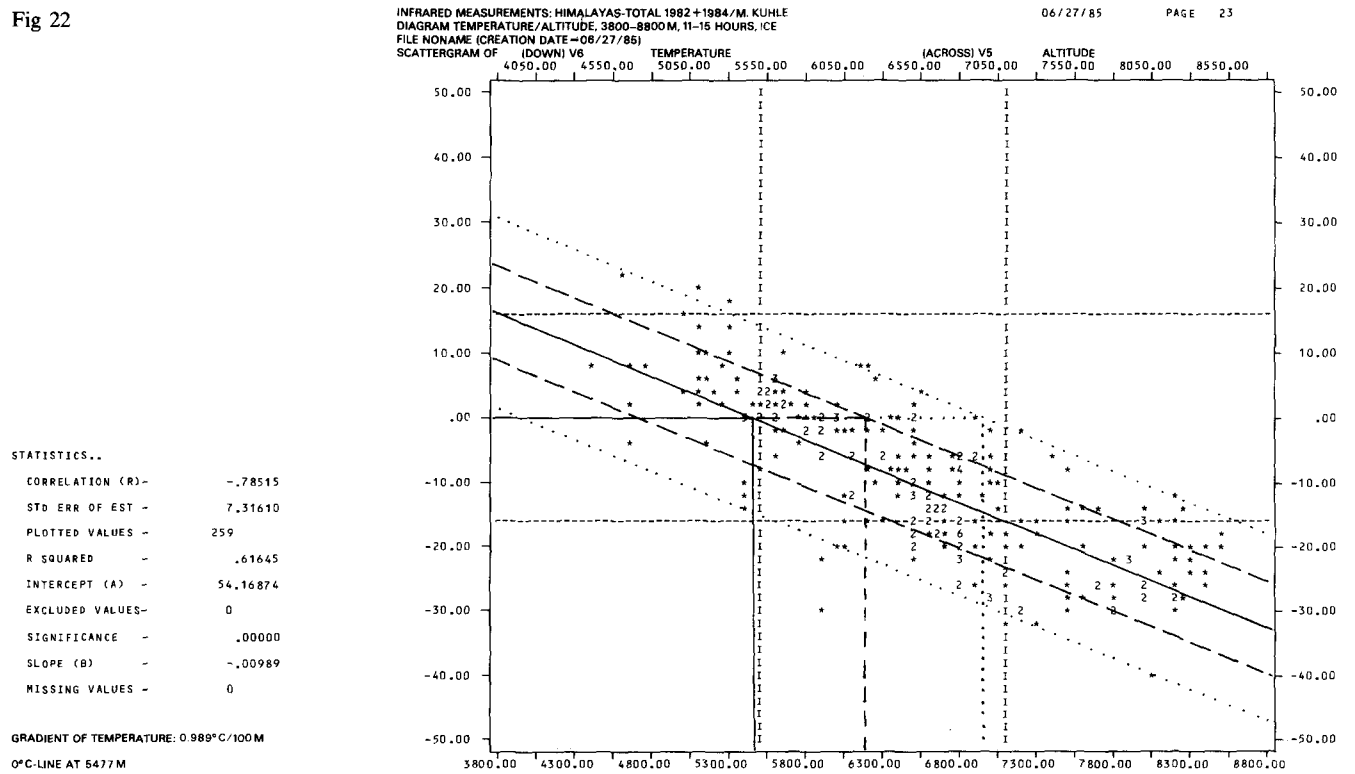


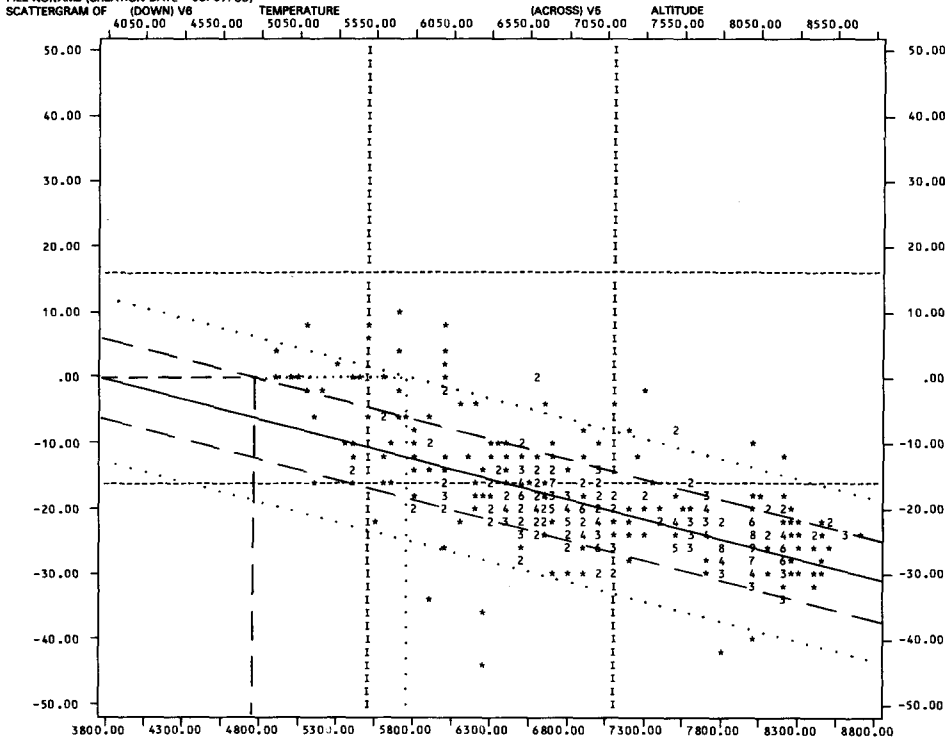
Fig 22



INFRARED MEASUREMENTS: HIMALAYAS-TOTAL 1982+1984/M. KUHLE  
DIAGRAM TEMPERATURE/ALTITUDE, 3800-8800 M, ICE  
FILE NONAME (CREATION DATE=03/07/88)

03/07/86 PAGE 9

Fig 23



INFRARED MEASUREMENTS: HIMALAYAS-TOTAL 1982+1984/M. KUHLE  
DIAGRAM TEMPERATURE/ALTITUDE, 3800-8800 M, ICE  
FILE NONAME (CREATION DATE=06/27/85)

06/27/85 PAGE 17

Fig 24

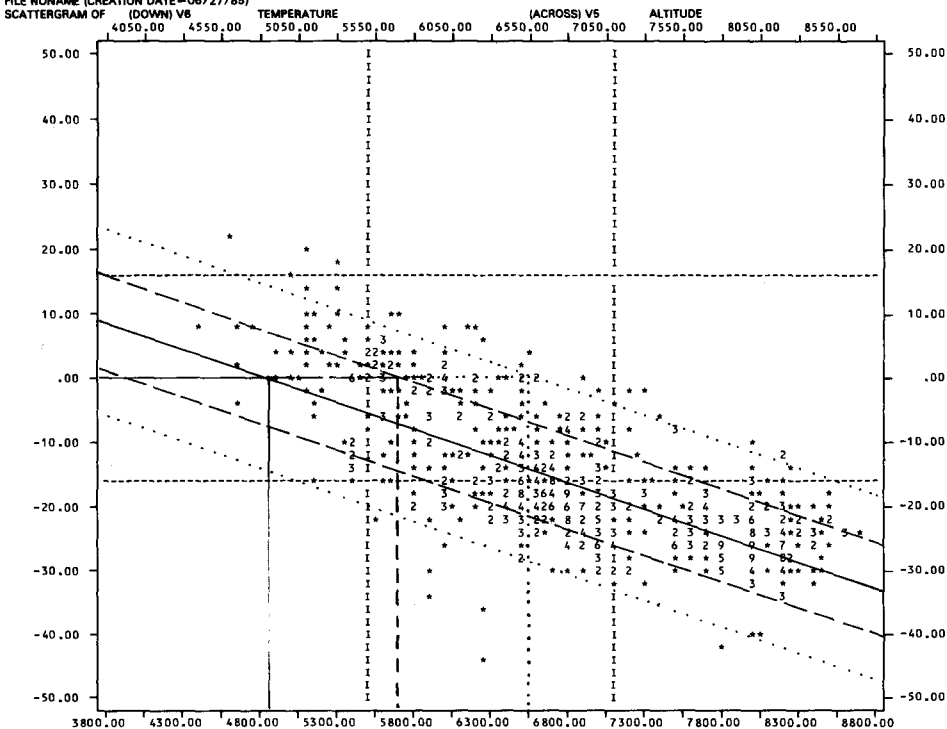


Fig 25

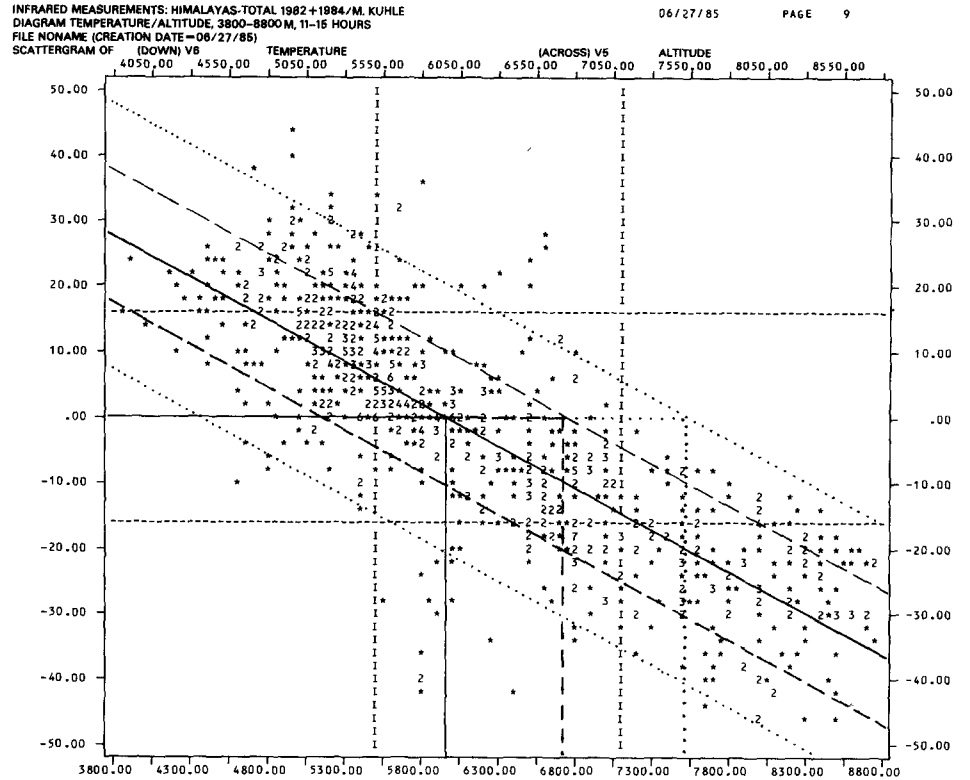
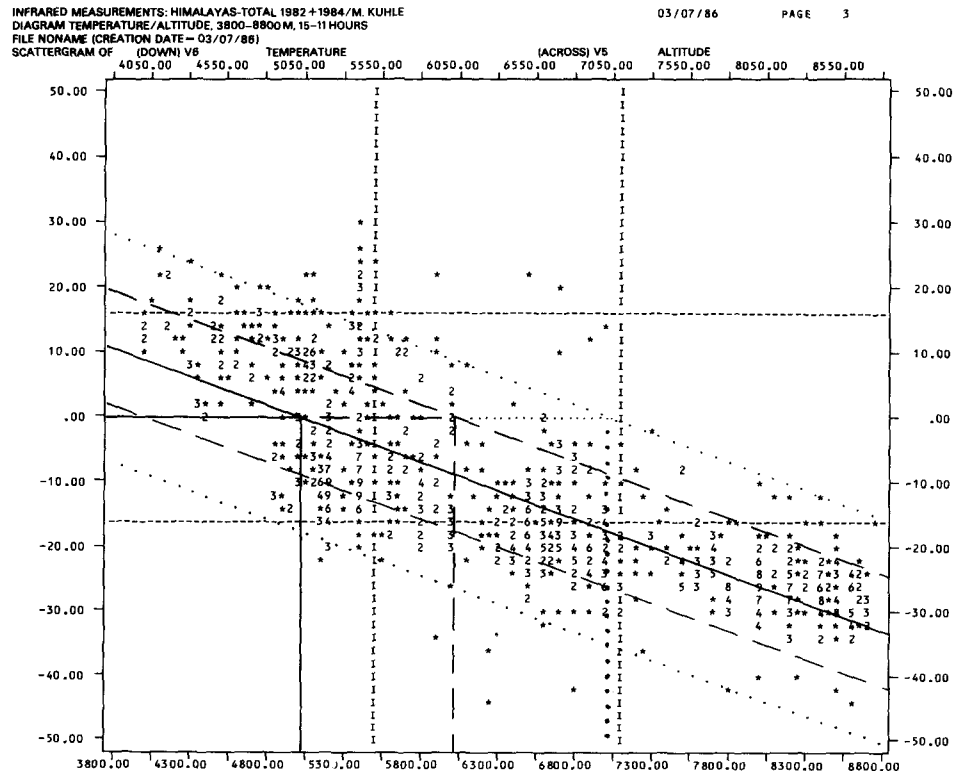


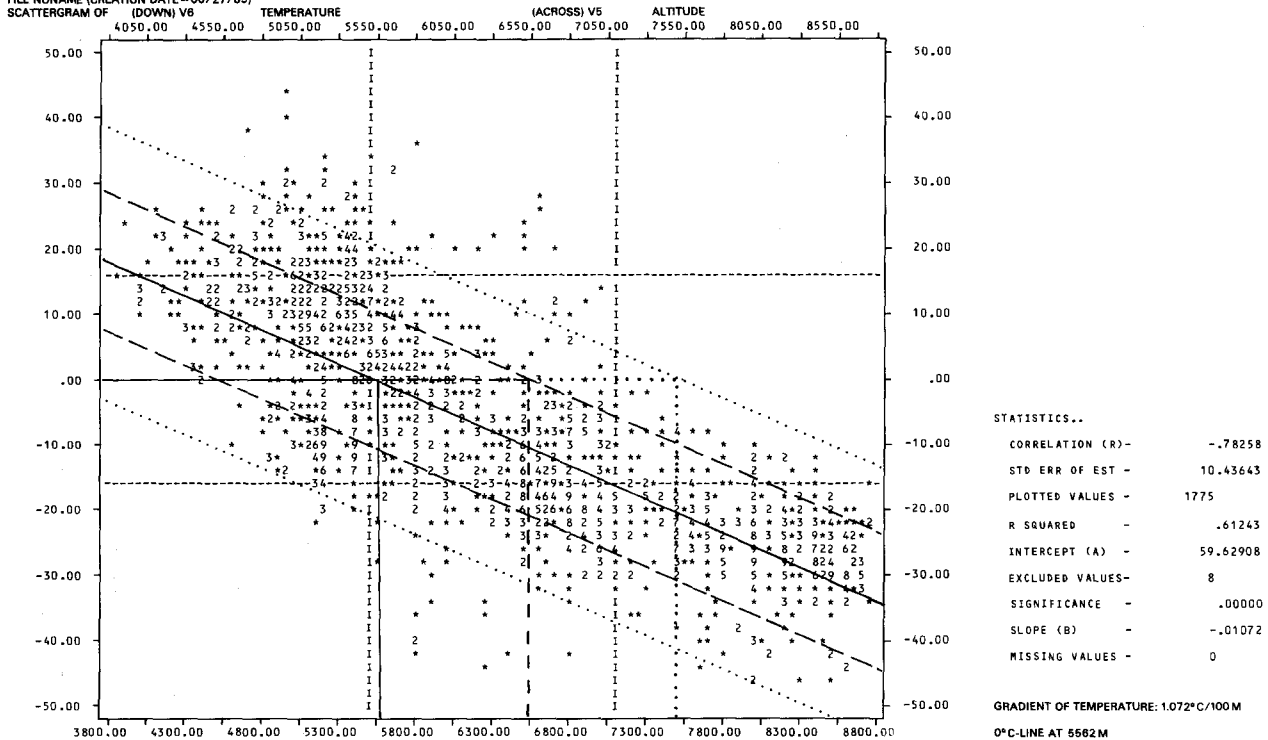
Fig 26



INFRARED MEASUREMENTS: HIMALAYAS-TOTAL 1982-1984/M. KUHLE  
DIAGRAM TEMPERATURE/ALTITUDE  
FILE NONAME (CREATION DATE=08/27/85)

06/27/85 PAGE 6

Fig 27



point. The daily average height of the 0° C line lies at 5719 m in contrast to 4913 m on surface of ice, firn and snow, i.e. a height difference of 806 m. This is also shown by the weakened temperature gradient over ice resulting from the loss of energy to latent heat during the melting process. The temperature gradient on rock surfaces is (according to time of day) between 0.23° C/100 m and 0.36° C/100 m greater than that on the ice surfaces; in the mean it is 0.2° C steeper (Fig 30).

The 7200 m upper glacial limit, which has been found by regression analysis and the application of single and double SEE values in the Mt. Everest, Makalu and Lhotse areas of the central Himalayas separates the zone of perennially snow-, firn- and ice-covered slopes from the seasonally snow-free rock (Fig 4, 5, 28, 29). Whereas by symmetry just as in the lower altitudinal zones of the High Himalayas as below the snow line (ELA) and far below the whole glacial region snow falls during winter remain lying; in the region above the upper glacial limit the snow falls in summer (during the monsoon precipitation; Fig 5 and 28). This does not melt like the snow at lower levels but is blown away during the winter. This region of glaciers is thus clearly bounded above and below. In the higher regions there are larger areas of rock and debris at the surface because the snow is blown away during the winter by the high velocity jet-stream (more than 45 m/sec) and prevented from compacting and adhering by the low temperatures. Only in areas of local lee eddies snow accumulations some decametres in

thickness occur and pressure compaction of the cold snow into ice of density 830 kg/m<sup>3</sup> result. It is here that small hanging glaciers and ice ledges over 100 m thick form over several decades in such cold conditions, far above the real climatic upper glacial limit of 7200 m (Fig 4 /, 5 /). The age of such cornices may be determined by the large number of annual layers. Because of the extreme extra - zonal conditions, recognizable small glacial features are far apart and separated by snow-free rock slopes (Kuhle 1986b).

These rock and local debris surfaces (as extending on the N ridge of Mt. Everest from the N saddle (Fig 28) as well as on the 8000 m Mt. Everest S saddle) above the upper glacial limit belong to a *pergelid* (eternally frozen) rock and dry debris altitudinal zone. It is this zone, and not that of the glaciers, that is the highest planetary altitudinal zone. It is confined solely to the high peaks of the Himalayas, the Karakoram (Kuhle 1987a, photo 3) and to a few peaks in the Vinson massif (in the Antarctic at 80° S) above 3500-4000 m. During the pleistocene glaciation this zone was rather more extensive. At that time, because of the general reduction in temperature, the thermal upper glacial boundary must also have been lowered (see below). The zone of pergelid rock and dry debris is characterized by purely temperature weathering in a region of negative temperature. The coarse blocky debris found there can only be produced by a process of rock destruction independent of that of freezing and thawing. The bonds between crystalline components of



Fig 28 Summit pyramid of Mt. Everest from the East Rongbuk glacier at 6300 m seen from the N; to the right the main summit at 8874 m, to the left the rock towers of the East Ridge (8390 m). Although the N flanks of the mountain (especially below the main peak) (○) slope gently and stepwise (mean slope 36° to 43°), rock forms large areas of the surface and there is no ice on the walls and no hanging glacier formation. Perennial snow only collects in the stable lee locations of chimneys and couloirs (×). It is there converted to firn on the walls and ice on the flanks. The upper limit of glaciation occurs on the metamorphic rocks of the mountain between 7000 m and 7600 m where the rock is kept clear by the wind. Where measurements were made on the peak (○) mean temperatures of -28° C to -36° C were observed in autumn 1984 under radiation weather conditions.  
Photo: M. Kuhle, 15 October 1984

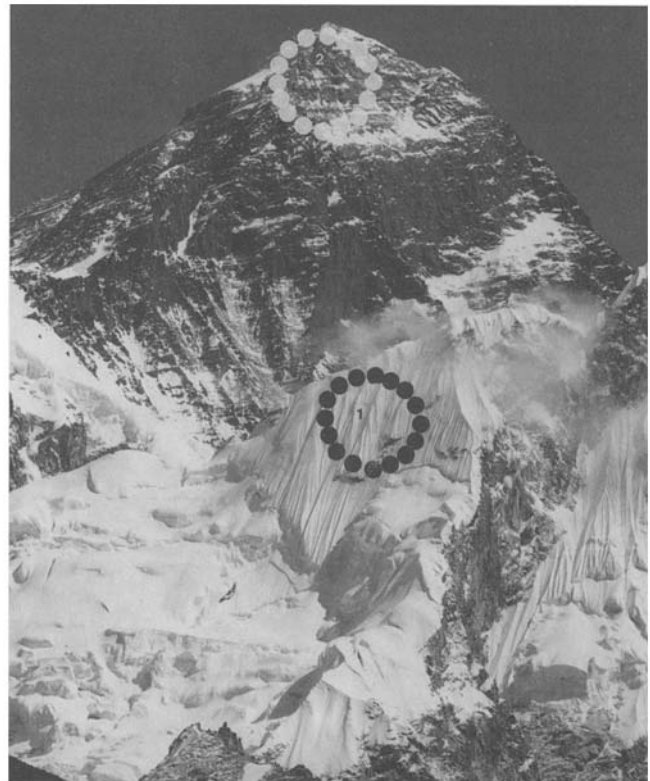


Fig 29 Mt. Everest viewed from the W at 5600 m. In the foreground the steep firn and glacier covered NW peak of Nuptse can be distinguished from the glaciated SSE slope of the WNW ridge of Mt. Everest. The locally only monsoon snow covered strata bands of the peak of Mt. Everest are not glaciated above 7000 to 7200 m. Under full sunshine conditions during 11 to 21 October 1982 measurements of surface temperatures on the firn between 6530 m and 6680 m (○) showed values of -7° C to 0° C but on rock between 8350 m and 8874 m (●) temperatures of -28° C to -46° C.  
Photo: M. Kuhle, 19 October 1982

the rocks with different coefficients of expansion are destroyed by the temperature oscillations of 15° C to 25° C below the freezing point. Probably because of the reduced elasticity of the rock at lower temperatures the intensity of the weathering is greater than that of the insolation weathering in warm arid regions (e.g. the Sahara). Whilst on Earth this weathering is found only on a few high peaks it is of supra-regional significance on other planets. Thus for example the oscillations of surface temperature on Mars at the landing place of Viking I average -38° C to -85° C (Stanek 1980).

At the glacial maximum the snowline (ELA) depression in the area of investigation was 1200 m (Kuhle 1987b). In September and October the author used three stations between 3960 m and 5330 m in similar moisture conditions on the K2 glacier to measure gradients of air temperature of 0.7° C/100 m to calculate the cooling of

the warmest month then of 8.4° C/100 m. In similar conditions Kuhn (1981; 1983) gave a lapse rate in the free air of 0.8° C/100 m which denotes a cooling of 9.6° C.

Since similar conditions of heat and mass balance apply to the thermal upper limit of glaciation and to the snowline (ELA) a comparable depression of 1200 m must have occurred. It cannot be excluded that such a depression of the upper limit of glaciation was a consequence of such steep gradients as 1.07 to 1.35° C/100 m (or even of 1.45 to 1.51° C/100 m according to Kuhle 1986a, Fig 1 and 2). It can thus be concluded that during the last glacial period there was a depression of the upper glacial limit of 620 to 1200 m to about 6000 m to 6580 m above present sea level. Thus on other less elevated mountain systems a pleistocene upper limit of glaciation must also be expected.



INFRARED MEASUREMENTS HIMALAYA 1982, 1984

material	time	0° C-line (a.s.l.)	temperature-gradient (° C/100 m)	number of values	altitudinal difference between 0° C-lines (m)	difference of temperature gradients (° C/100 m)
rock	11-15	6070	1.35	554	870	0.5
rock	15-11	5200	0.85	536		
rock	0-24	5719	1.05	1090	—	—
ice	11-15	5477	0.99	259	1681	0.37
ice	15-11	3796	0.62	426		
ice	0-24	4913	0.85	685	—	—
rock/ice	11-15	5966	1.31	813	953	0.43
rock/ice	15-11	5013	0.88	962		
rock/ice	0-24	5562	1.07	1775	—	—
rock	11-15	6070	1.35	554	593	0.36
ice	11-15	5477	0.99	259		
rock	15-11	5200	0.85	536	1404	0.23
ice	15-11	3796	0.62	426		
rock	0-24	5719	1.05	1090	806	0.2
ice	0-24	4913	0.85	685		

Drafr: M. Kuhle

Fig 30  
Table from the diagrams of Fig 19 to 27

## Summary

1) Radiation measurements over a period of c. 2.5 months in S Tibet and on the Himalaya S slope up to heights of 6650 m showed very high values. These are close to the theoretical solar-constant values for corresponding solar altitudes. Measurements of radiation balance over snow surfaces of the glacier catchment areas show that up to 90% of this energy is reflected, whereas over debris surfaces this value ranges from 16 to 24%, about 70% lower than the former.

2) Observations and measurements of cloud cover, humidity, wind direction and velocity showed the transition from the summer monsoon to the radiation conditions of autumn and winter. This results from a change from variable low velocity winds to storm winds from the S to SE, and from humidities of up to 90% to those no more than 40 to 10%. Associated with the seasonal decrease in temperature is a freezing of the debris above 5000 m from September to November to a maximum depth of a few decimetres. Although the frost at the end of September penetrated only a few centimetres, by the beginning of November the diurnal thaw penetrated no

deeper than 10 cm. Thus there were no more than 45 days of solifluction (periglacial) activity during this transitional season during which a 10–20 cm thick frost active layer moved downslope.

3) Data derived from telemetric measurements of surface temperatures between 3800 and 8800 m on debris, rock, ice, firn and snow on the slopes of the Himalayas were analysed statistically. The lapse rate of these temperatures was rather steeper than that of the free atmosphere, ranging from 0.85 to 1.35° C/100 m. Rock surfaces showed higher lapse rates (up to 1.35° C/100 m) than ice surfaces (up to 0.99° C/100 m). Simple and double SEE showed an absolute 0° C level on the Himalaya slopes at 7200 m. Average temperatures above this height are so low (less than –25° C) that, apart from sublimation and molecular diffusion, only very slow ice-bridge formation between the snow crystals can occur. Because high winds prevent the necessary persistence of snow cover (by deflation) there is at 7200 m an upper climatic limit to glacier formation. Above this level the highest altitudinal zone on Earth is formed of a pergelid rock and dry debris region. During the glacial period this empirical upper limit of glaciation was depressed parallel to the snowline (ELA) by between 620 m and 1200 m.

## References

- Bishop, C. B.; Ångström, A. K.; Drummond, A. J.; Roche, J. J.: Solar Radiation Measurements in the High Himalayas (Everest Region). *Journal of Applied Meteorology*, 5, 94–104 (1966)
- Häckel, H.; Häckel, K.; Kraus, H.: Tagesgänge des Energiehaushalts der Erdoberfläche auf der Alp Chukhung im Gebiet des Mt. Everest. *Khumbu Himal* (zweite Lieferung), 47–60, München 1970.
- Kuhle, M.: Permafrost and Periglacial Indicators on the Tibetan Plateau from the Himalaya Mountains in the south to the Quilian Shan in the north (28–40° N). *Z. f. Geomorph. N. F.* 29, 2, 183–192 (1985)
- Kuhle, M.: Die Obergrenze der Gletscherhöhenstufe, Oberflächentemperatur und Vergletscherung der Himalayaflanken von 5000–8800 m. *Z. f. Gletscherk.* 22, 2, 149–162 (1986a)
- Kuhle, M.: The Upper Limit of Glaciation in the Himalayas. *GeoJournal* 13, 4, 331–346 (1986b)
- Kuhle, M.: Physisch-geographische Merkmale des Hochgebirges: Zur Ökologie von Höhenstufen und Höhengrenzen. *Frankfurter Beiträge zur Didaktik der Geographie*. 10, 15–40 Frankfurt am Main (1987a)
- Kuhle, M.: Subtropical Mountain- and Highland-Glaciation as Ice Age Triggers and the Waning of the Glacial Periods in the Pleistocene. *GeoJournal* 13, 6, 1–29 (1987b)
- Kuhn, M.: Climate and Glaciers. Sea Level, Ice, and Climatic Change, *Proceedings of the Canberra Symposium*, Dec. 79, *IAHS*, 131, 3–20 (1981)
- Kuhn, M.: Die Höhe der Schneegrenze in Tirol, berechnet aus Fliris klimatischen Profilen. *Arbeiten zur Quartär- u. Klimaforschung. Innsbr. Geogr. Stud.* 8, Fliri Festschrift, Innsbruck (1983)
- Lorenz, D.: Die radiometrische Messung der Boden- und Wasseroberflächentemperatur und ihre Anwendung insbesondere auf dem Gebiet der Meteorologie. *Z. Geophys.* 39, 627–701 (1973)
- Shi Yafeng; Xie Zichu: The Basic Characteristics of the Existing Glaciers in China. *Acta Geographica Sinica* 30, 3, 1–38 (1964)
- Stanek, B.: *Planeten Lexikon*. 3. Aufl., Hallwag, Bern, Stuttgart 1980.

## The Petrography of Southern Tibet

### **Results of Microscopic and X-Ray Analyses of Rock Samples from the 1984 Expedition Area (Transhimalaya to Mt. Everest N Slope)**

*Heydemann, Annerose, Dr., University of Göttingen, Institute of Sedimentary Petrography, Goldschmidtstraße 1, 3400 Göttingen, FR Germany,  
Kuhle, Matthias, Prof. Dr., University of Göttingen, Geographical Institute, Goldschmidtstraße 5, 3400 Göttingen, FR Germany*

During the 1984 expedition to S Tibet more than 100 rock samples were collected from the country rocks and morainic components. Some of these samples were examined in thin section by microscopy and X-ray diffraction. 24 of these samples of glacial geological interest are chosen for treatment here. These deal mainly with far-travelled erratics deposited on country rocks of another type.

Kuhle (cf. pp. 459–469, this issue) has executed a glaciological treatment of certain petrographic analyses from the Transhimalaya and Tibetan Himalaya (Fig 1, samples 24. 8. 1984/1,2; 31. 8. 1984/1–2c). The remainder treated here (Fig 1,2 samples 2. 10. 1984/1–4, 23. 10. 1984/1–9, 2. 11. 1984/1–3) are from the immediate Mt. Everest N slope. Because 50 days of detailed work was possible there, the density of such samples is greatest on the Mt. Everest N slope. These mineralogical researches provide here a short account of the petrography and tectonic influences found in this highest part of the earth.

Other samples (not represented here) were obtained from the upper surfaces of moraines to investigate the intensity of weathering and for the determination of ages by differences in iron hydroxide occurrence. These include samples from other groups of mountains of S Tibet e.g. the Shisha Pangma N slope.

#### **Samples from the Transhimalaya North of the Tsangpo** (Samples 24. 8. 1984/1–2; Fig 1)

Chalamba La is an E–W pass at 5300 m 150 km W of Lhasa. The location of samples 24. 8. 1984/1+2 lies 400 m below the N–S trending ridge at Chalamba La. Sample 1 is from a dissected bench (29°42'N 90°14'E).

This is a rhyolitic rock with albite-oligoclase phenocrysts in a fine-grained groundmass (Fig 3). Partial chloritisation and carbonatisation indicates hydrothermal alteration. All the surrounding summits and peaks up to 6138 m are also formed of rhyolitic rocks.

Sample 2 is an erratic derived from the same place as Sample 1. It is a granitic rock with tectonic features (Fig 4). There are many large light-coloured and well-rounded granite blocks (with long axes up to 1 m long) transported here by valley glaciers at least 1200 m thick from the E (components of a network of ice streams). This spread of granite blocks occurs both in the saddle of the Chalamba La and up to 200 m on the slope above it.

#### **Samples from the Tibetan Himalaya i.e. the Ladake Shan South of the Tsangpo** (Samples 31. 8. 1984/1–2c; Fig 1)

Although the N slope of the Lazu massif is formed of phyllites the Lulu valley (28°44'–54'N 87°10'–25'E) is incised into basalts in its S slopes. These basalts are clearly stratified, flat-lying and with no columnar texture at right angles to the cooling surface. Sample 1, from this area, is a much-decomposed basaltic rock in which the pyroxenic components are hydrothermally chloritised and carbonatised (Fig 5).

A glacial till with large blocks extends from 5200 m in the Lulu valley down to its outlet at 4300 m into the Lulu basin. It lies as a far-travelled erratic-bearing layer above the basalt country rocks. Its fine-grained matrix contains light-coloured rounded granite blocks up to 3 m long which lie in the valley floor and up to 170 m above it on the valley slopes (Samples 2, 2a, 2b, 2c). Erratics 2a and 2c are tectonically modified biotite-granite (Fig 7

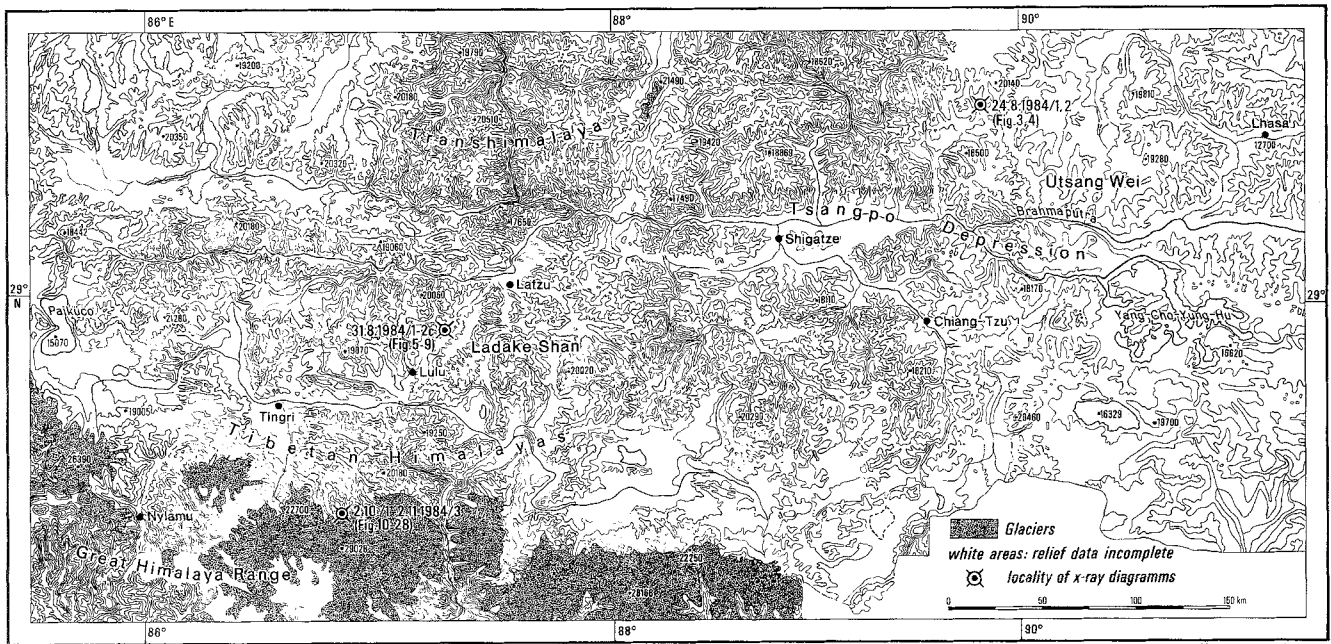
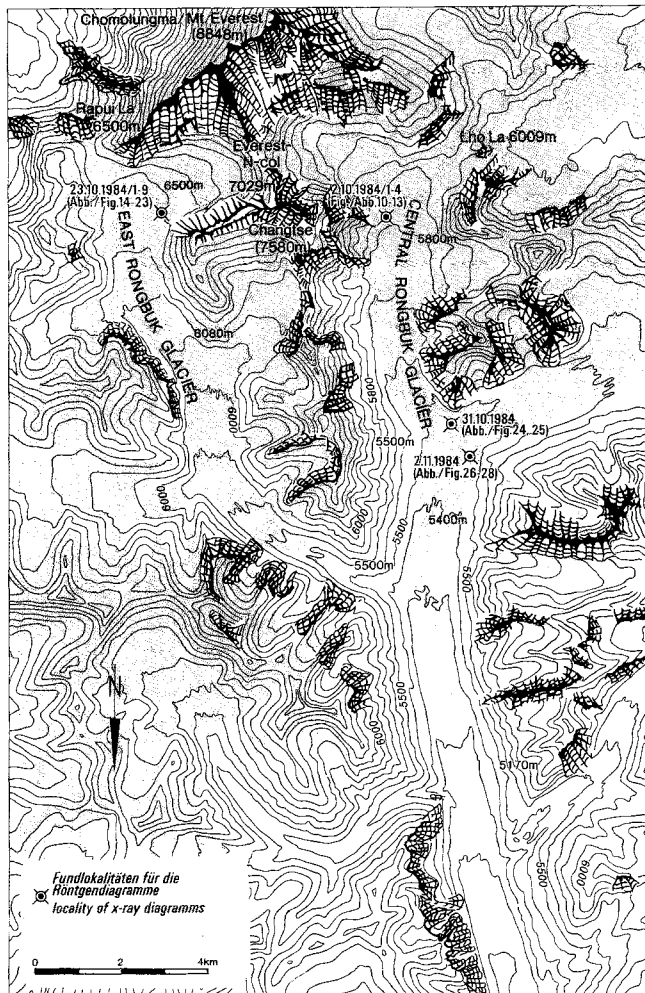


Fig 1 Localities at which the S Tibetan rock samples were collected

Fig 2 Rock sample localities on the N slope of Mt. Everest



and 9) and erratics 2 and 2b are similarly modified two-mica granite with varying muscovite-biotite relationships. In Sample 2 part of the biotite is already chloritised (Fig 6 and 8).

**Samples from the Source Basin of the Rongbuk Glacier in the North Slope of Mt. Everest**

27°58' -28°10'N 86°45' -87°E (Samples 2. 10. 1984/1-4; Fig 1 and 2

Rock samples from the Mt. Everest area were mainly investigated to provide further information on the petrography of the highest part of the earth. It is well known from the High Himalaya belt that it is made up of a number of irregularly spaced plutons emplaced at the top of the Tibetan slab into sedimentary series up to the Cretaceous (Deberon, F. et al.: Geol. Rundschau 74, 229-236 (1985).

Samples 2. 10. 1984/1-4 are from the medial (surface) moraine exactly where it thaws out at 5800 m. This medial moraine derives from the true right side lateral moraine of the central Rongbuk glacier below the 1800 m high NW wall of Changtse. Thus, the four samples provide information of the petrography of the peak of Changtse. Surface observations have already shown that granite intrusions occur here within a sedimentary series. The naked eye can detect a red contact metamorphism and schists show migmatization. Sample 1, a fine-grained biotite schist, is certainly derived from this sediment series (Fig 10).

The three other samples are granitic materials. Sample 2 (Fig 11) is from a tectonically modified two-mica granite with hardly any chloritisation of the biotite.

South Tibet and Mt. Everest  
X-ray diagram: 31.8.1984/1  
Decomposed basaltic bedrock 4,950 m a.s.l. Lazu massif, Lulu valley  
A. Heydemann and M. Kühle

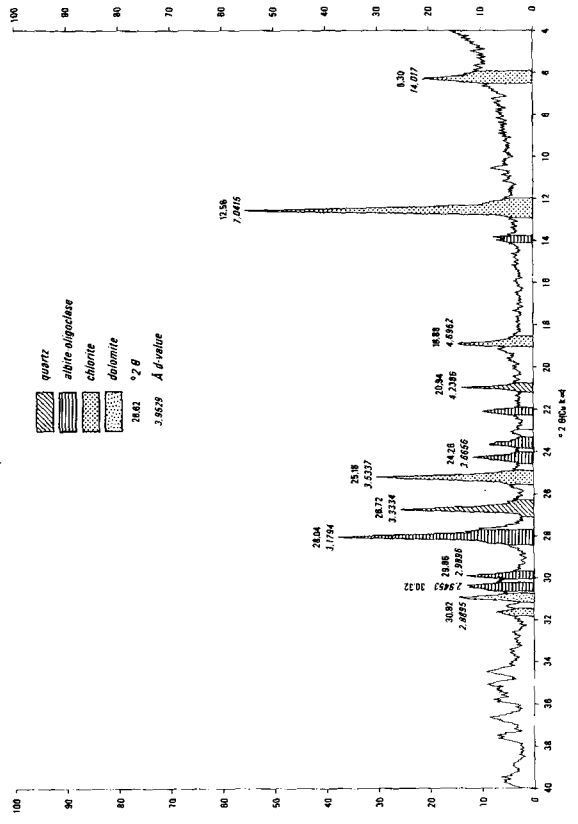


Fig 5

South Tibet and Mt. Everest  
X-ray diagram: 24.8.1984/1; 5300 m, Chalamba La  
rhyolitic rock (solid)  
A. Heydemann and M. Kühle

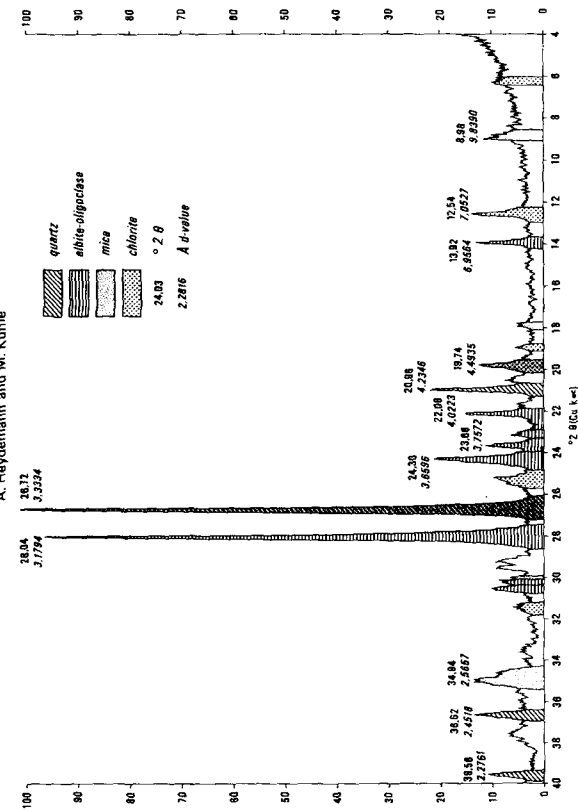


Fig 3

South Tibet and Mt. Everest  
X-ray diagram: 31.8.1984/2  
Erratic clast: Two-mica granite, 4,950 m a.s.l. Lazu massif, Lulu valley  
A. Heydemann and M. Kühle

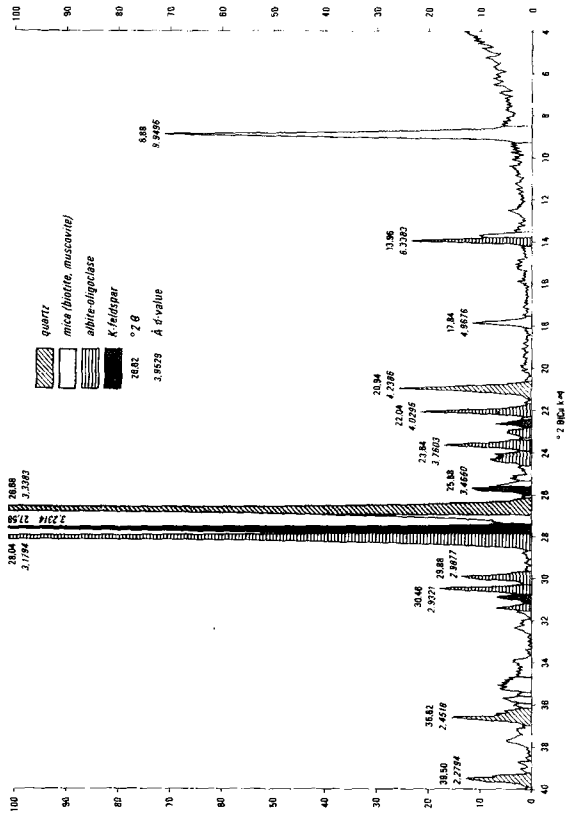


Fig 6

South Tibet and Mt. Everest  
X-ray diagram: 24.8.1984/2; 5300 m, Chalamba La  
Erratic clast: Granite (tectonometamorphic)  
A. Heydemann and M. Kühle

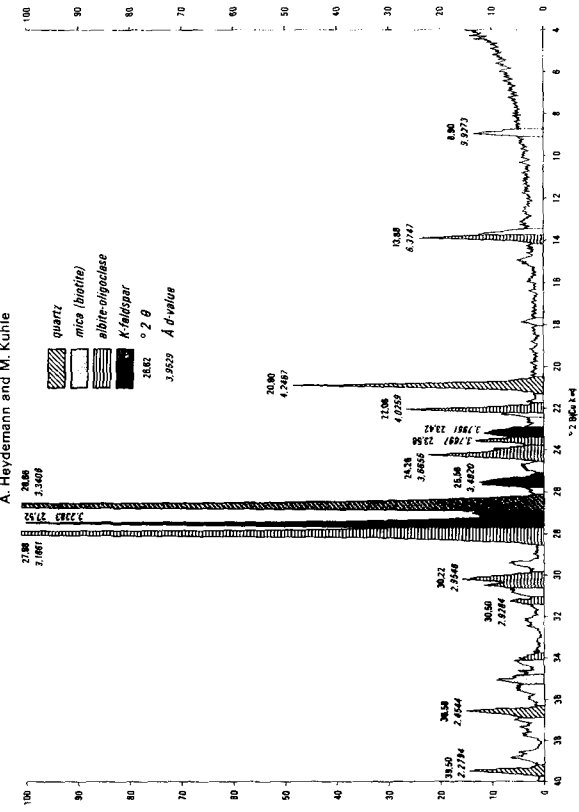


Fig 4

Fig 7

South Tibet and Mt. Everest  
 X-ray diagram: 31.8.1984/2a  
 Erratic clast: Biotite granite 4,950 m a.s.l. Latzu massif, Lulu valley  
 A. Heydemann and M. Kuhle

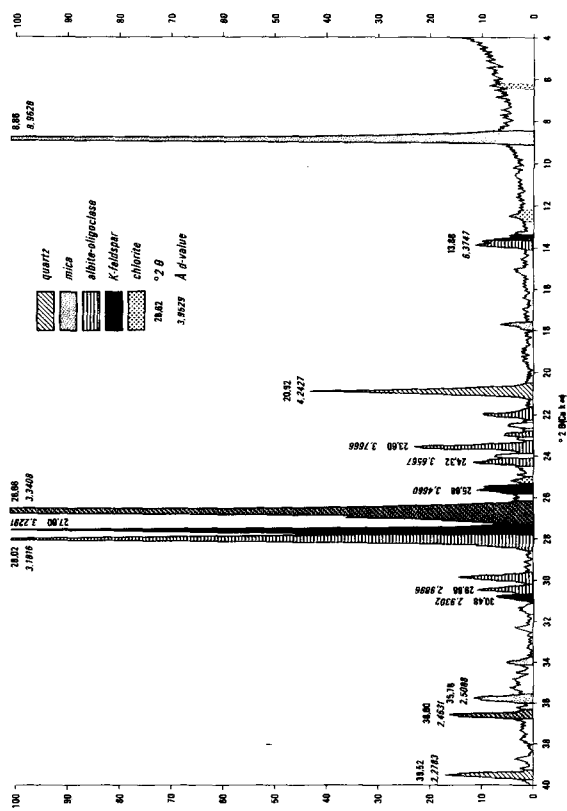


Fig 9

South Tibet and Mt. Everest  
 X-ray diagram: 31.8.1984/2c  
 Erratic clast: Biotite granite 4,950 m a.s.l. Latzu massif, Lulu valley  
 A. Heydemann and M. Kuhle

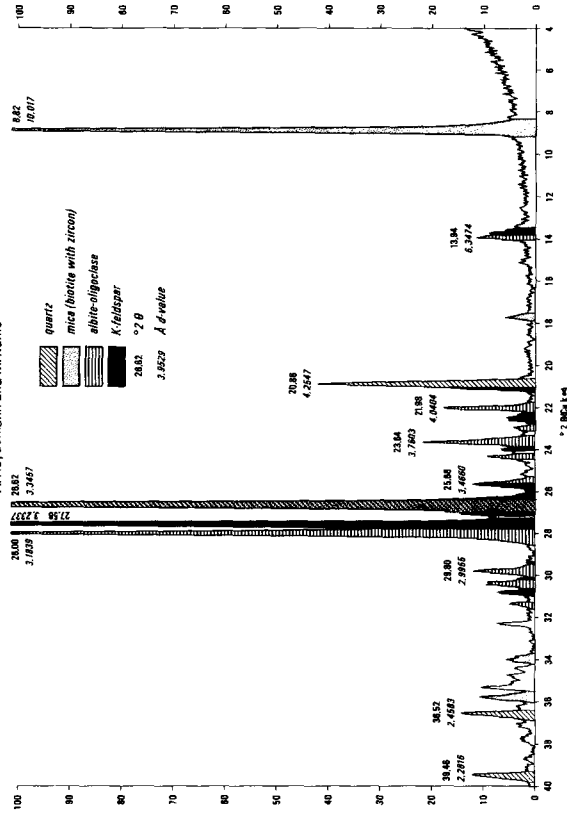


Fig 8

South Tibet and Mt. Everest  
 X-ray diagram: 31.8.1984/2b  
 Erratic clast: Two-mica granite, 4,950 m a.s.l. Latzu massif, Lulu valley  
 A. Heydemann and M. Kuhle

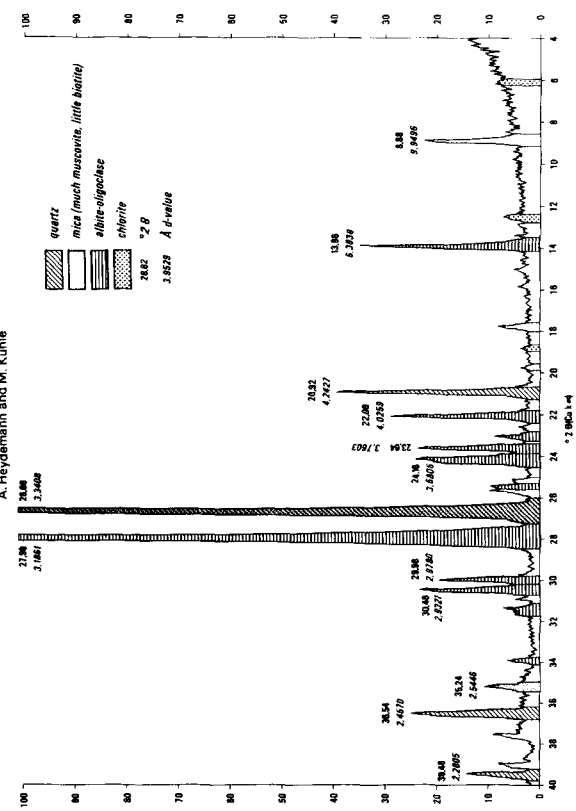


Fig 10

South Tibet and Mt. Everest  
 X-ray diagram: 2.10.1984/1  
 Biotite mica schist 5,800 m a.s.l. surface moraine Central Rongbuk Glacier  
 A. Heydemann and M. Kuhle

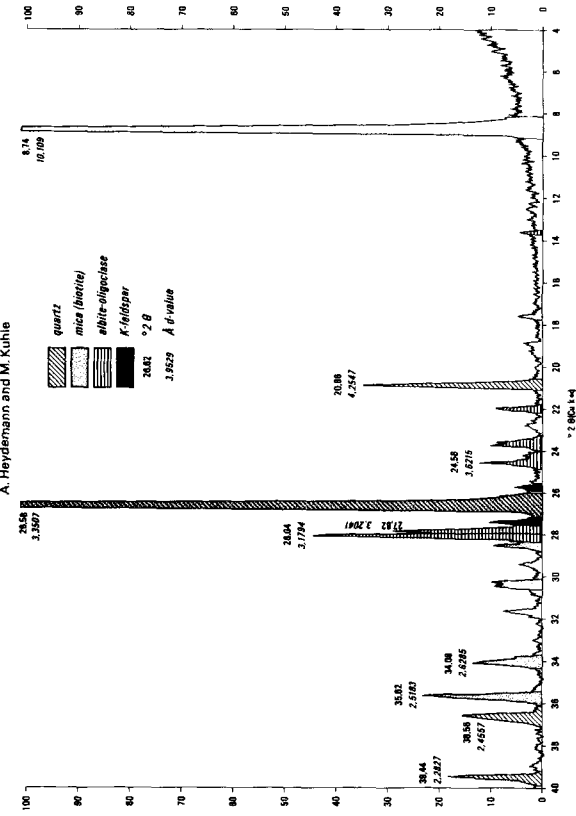


Fig 11 South Tibet and Mt. Everest  
X-ray diagram: 2.10.1984/2, Central Rongbuk Glacier, medial moraine  
Two-mica granite  
A. Heydemann and M. Kuhle

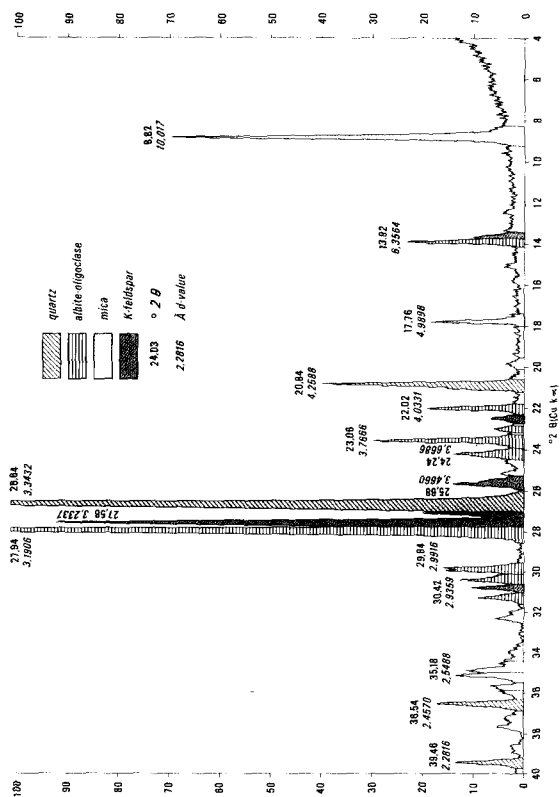


Fig 13

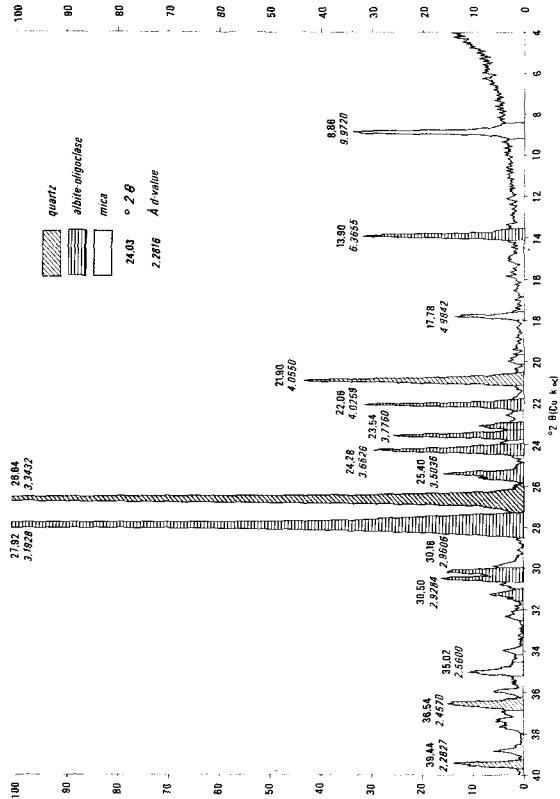


Fig 12 South Tibet and Mt. Everest  
X-ray diagram: 2.10.1984/3  
Makalu-Granite  
Central Rongbuk Glacier, medial moraine  
A. Heydemann and M. Kuhle

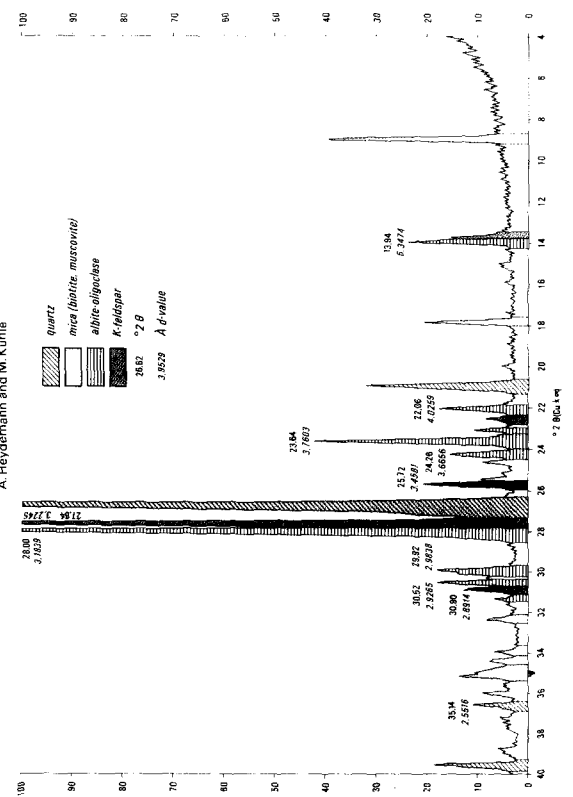
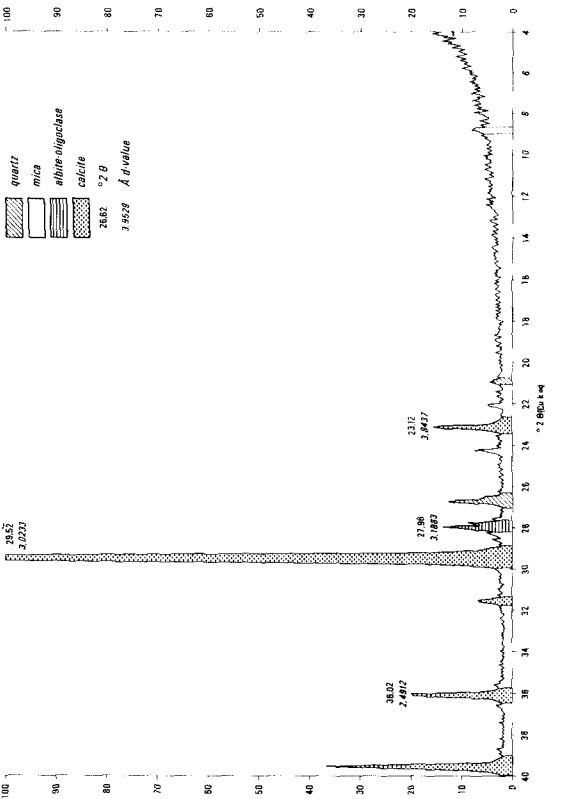


Fig 14

South Tibet and Mt. Everest  
X-ray diagram: 23.10.1984/1  
quartz-containing marble  
A. Heydemann and M. Kuhle



South Tibet and Mt. Everest  
X-ray diagram: 23.10.1984/2  
limestone mylonite  
A. Heydemann and M. Kuhle

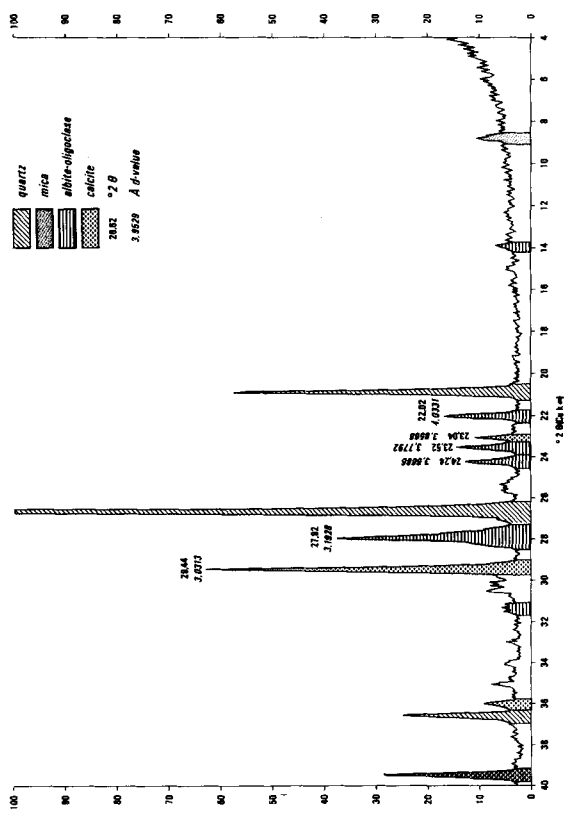
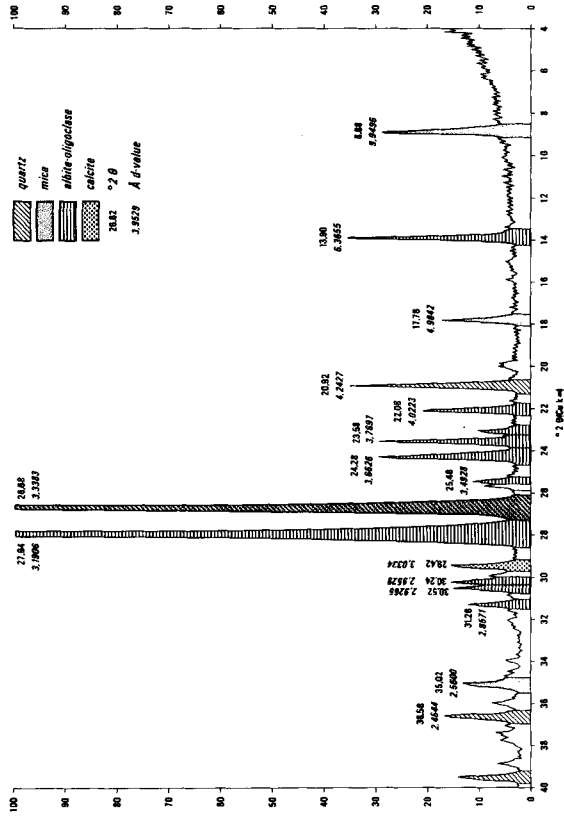


Fig 17

South Tibet and Mt. Everest  
X-ray diagram: 23.10.1984/4  
Granite (tectonometamorphic)  
A. Heydemann and M. Kuhle



South Tibet and Mt. Everest  
X-ray diagram: 23.10.1984/3  
Calcite marble  
A. Heydemann and M. Kuhle

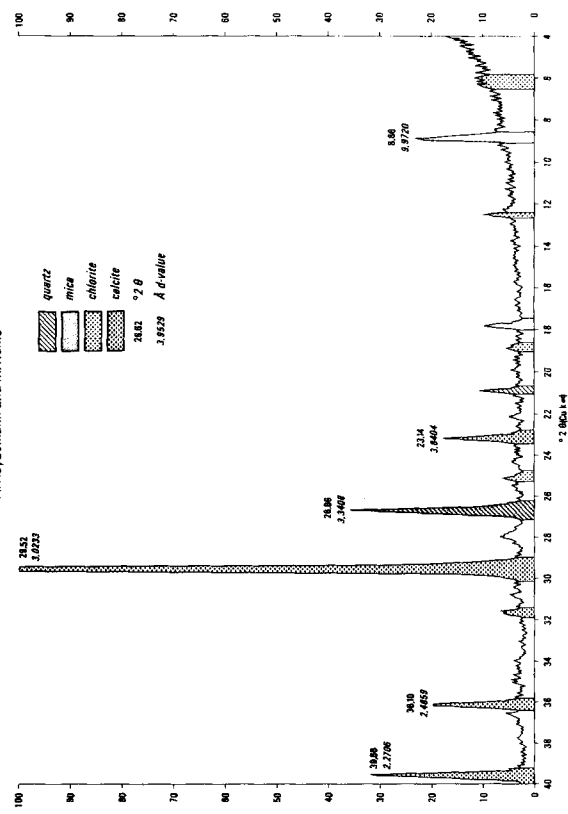


Fig 16

South Tibet and Mt. Everest  
X-ray diagram: 23.10.1984/5, East-Rongbuk Glacier, left lateral moraine; 6,500 m a.s.l.  
Cataclastic (sillimanite)  
A. Heydemann and M. Kuhle

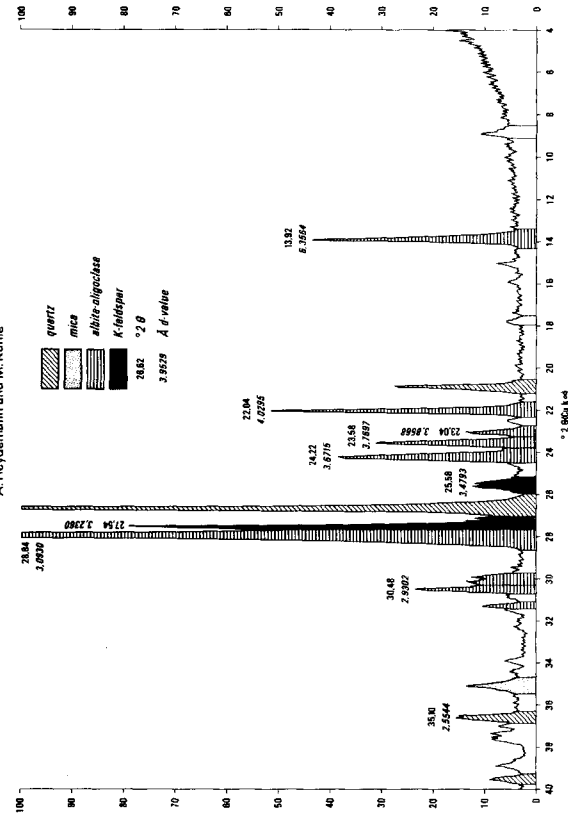


Fig 19



South Tibet and Mt. Everest  
X-ray diagram: 23.10.1984/8

Mica schist  
A. Heydemann and M. Kuhle

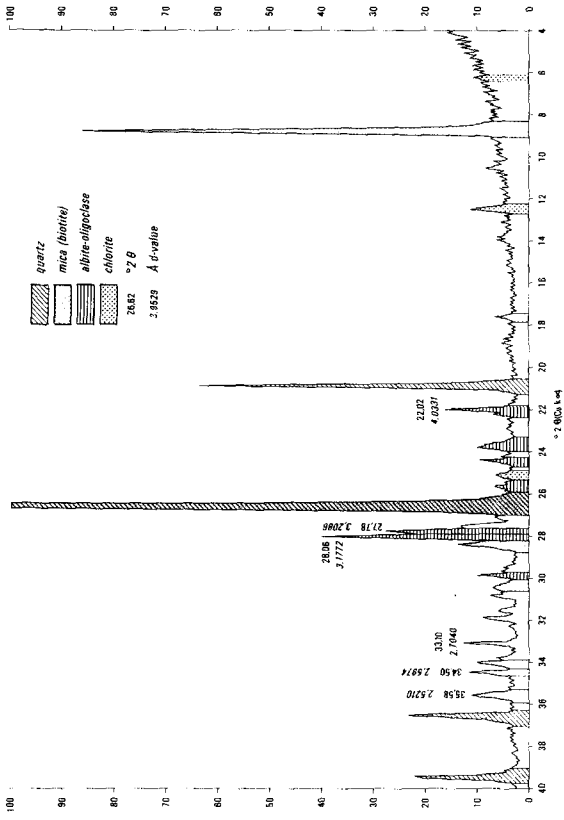


Fig 22

South Tibet and Mt. Everest  
X-ray diagram: 23.10.1984/6

quartz-containing limestone mylonite  
A. Heydemann and M. Kuhle

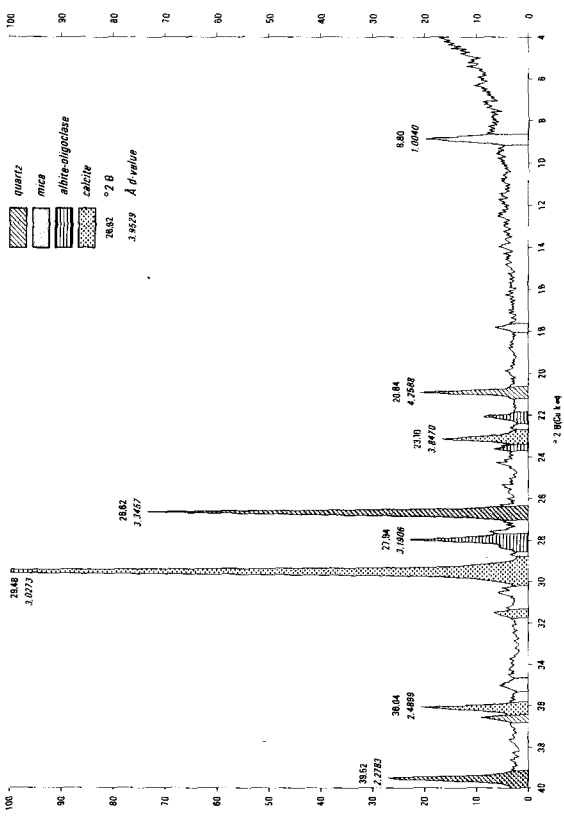


Fig 20

South Tibet and Mt. Everest  
X-ray diagram: 31.10.1984/1

Alkali granite  
A. Heydemann and M. Kuhle

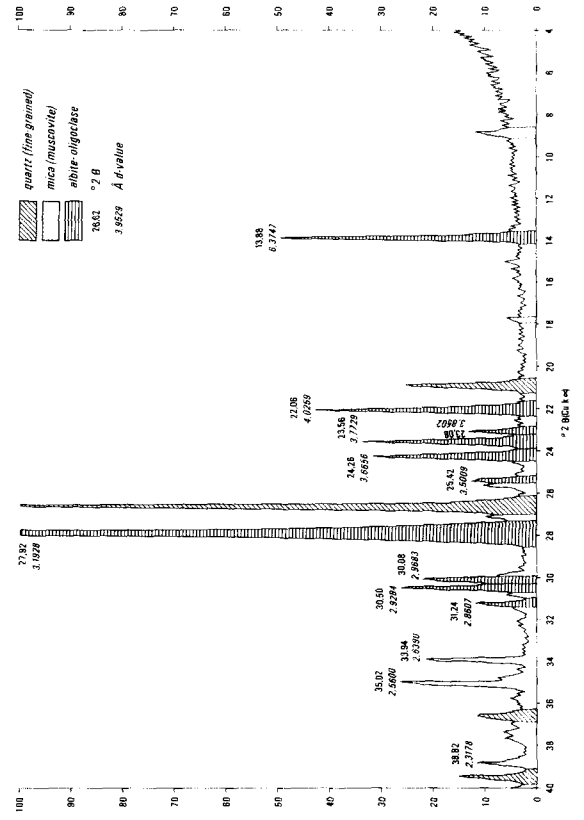


Fig 24

South Tibet and Mt. Everest  
X-ray diagram: 23.10.1984/7

Mica schist  
A. Heydemann and M. Kuhle

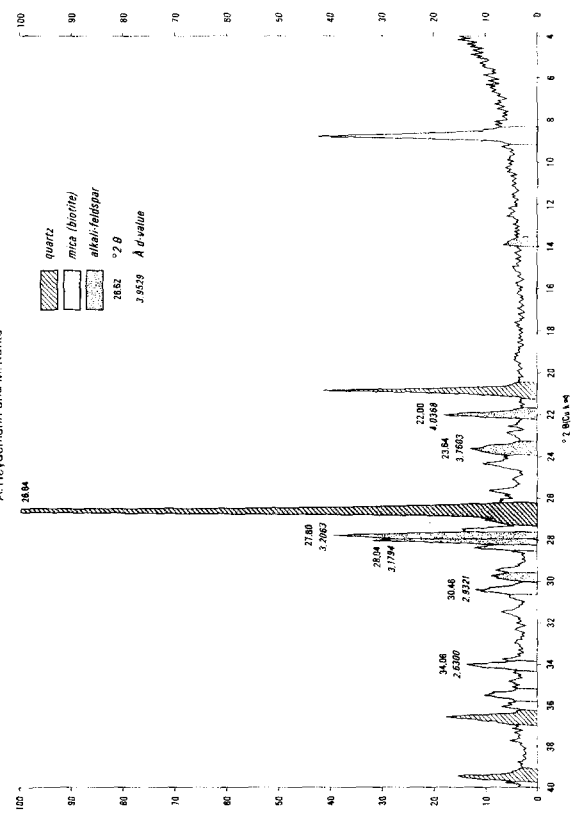


Fig 21

South Tibet and Mt. Everest  
X-ray diagram : 2.11.1984/2  
A. Heydemann and M. Kuhle

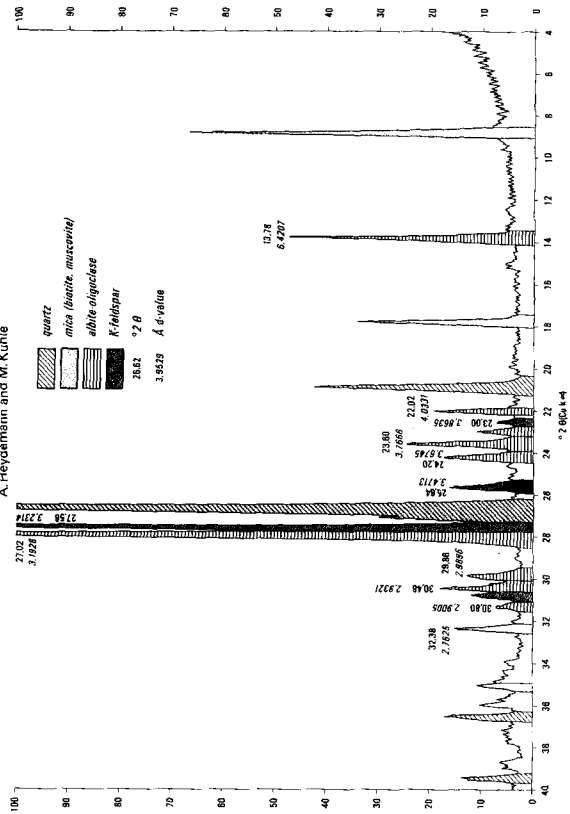


Fig 27

South Tibet and Mt. Everest  
X-ray diagram: 31.10.1984/2  
Cataclastite  
A. Heydemann and M. Kuhle

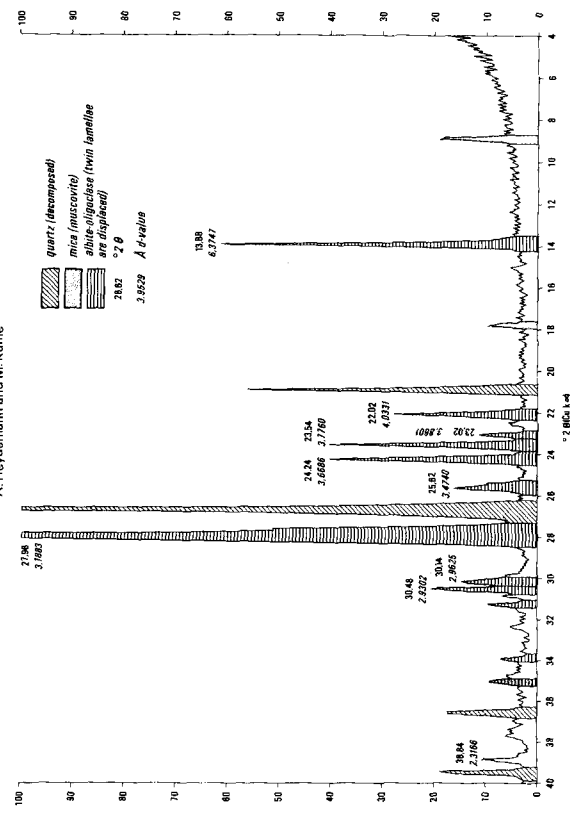


Fig 25

South Tibet and Mt. Everest  
X-ray diagram: 2.11.1984/3  
Mica schist  
A. Heydemann and M. Kuhle

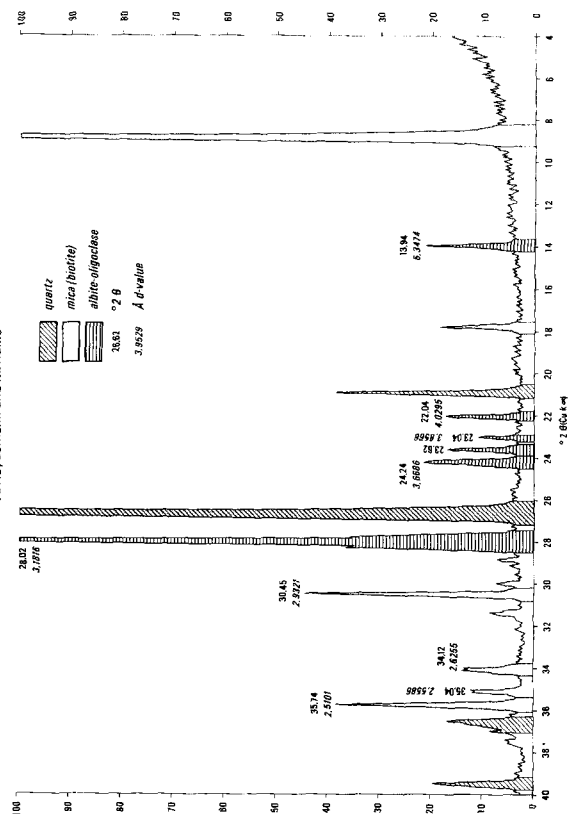


Fig 28

South Tibet and Mt. Everest  
X-ray diagram: 2.11.1984/1  
Granite  
A. Heydemann and M. Kuhle

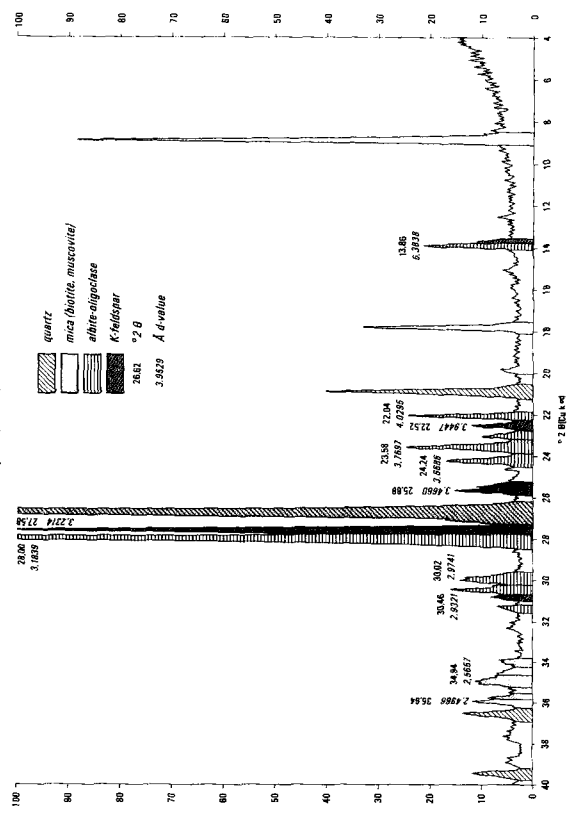
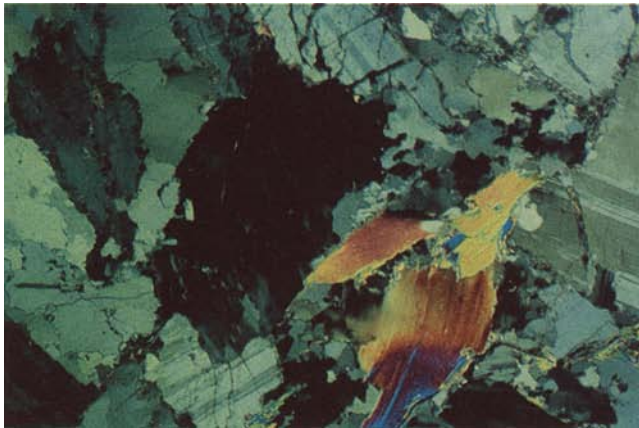
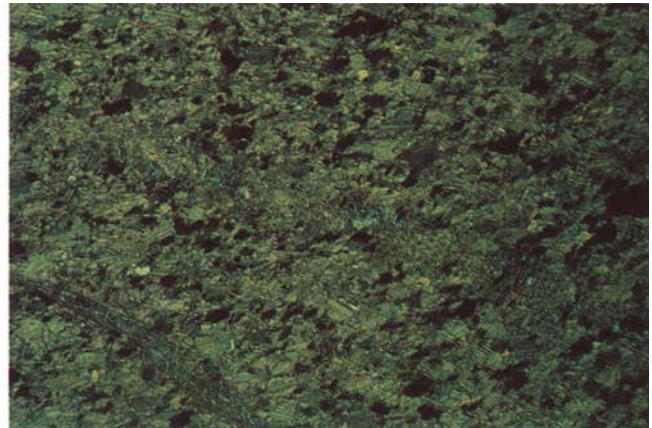


Fig 26



**Fig 18** Thin section of a strongly tectonically modified granite. (Sample 23. 10. 1984/4; see also Fig 17). An excerpt with crossed nicols (photo 2.7×4.1 mm). The quartz here occurs partially as tectonically broken crystals with a wavey extinction and partially as the result of stress factors they are interdigitated as clearly distinguishable minute crystals of various orientations. The feldspars, easily recognised by their twinning laminations, are also broken up, the fragments juxtaposed and the fracture lines partly rewelded. The micaceous components, here recognisable by the vivid interference colours, also show pressure effects with distorted bundles of mica.



**Fig 23** Thin section of a tectonically modified calcite-marble (Sample 23. 10. 1984/9). An excerpt with crossed nicols (photo 2.7×4.1 mm). The calcite crystals of the fine-grained marble all show pressure twinning. The quartz crystals are very small (< 100 μ) and well rounded and only part of them show wavey extinction. The slightly diagonal cleavage line shows broken and rubbed calcite crystals, appearing now as microcrystalline phases. The quartz components are recrystallised and appear here partly as linearly ordered aggregates formed of minute, variously ordered and interdigitated crystals.

Sample 3 is a similar two-mica granite with rare biotite and dominant muscovite (Fig 12). It is noticeable that tourmaline is subsidiary, and dissolved garnets are recognisable in the thin section. In the Everest area these tourmaline-bearing granites are known as Makalu granites where further to the SE they form the 8481 m peak of Makalu. Sample 4 (Fig 13) is a tectonically modified granitic rock showing recrystallisation phenomena. X-ray analysis shows no potash feldspar but only albite-oligoclase. This thin section also contains relicts of dissolved garnets.

#### **Samples from the Source Basin of the E Rongbuk Glaciers of the Mt. Everest N Slope**

(Sample 23. 10. 1984/1–9; Fig 1 and 2).

Samples 23. 10. 1984/1–9 are derived from the glacier-upwards true left bank lateral moraines of the N col of Mt. Everest between the N wall of Mt. Everest and the SSE wall of Changtse at 6500 m. These portions of rock have been carried by snow- and ice-avalanches from the two rock walls (1800 m and 1000 m high) and the summit pyramids and thus provide petrographic information on the summit region.

Samples 1–3, 6 and 9 must be attributed to series of carbonate rocks. Samples 1–3 and 9 are quartz-bearing calcite marbles modified tectonically and metamorphosed; they contain subsidiary soda-feldspar, mica, chlorite and epidote. In sample 9 some phlogopite occurs subsidiary to muscovite and chlorite (Fig 14, 16, 23).

Samples 2 and 9 represent calcite-mylonites, quartz rich resp. quartz-bearing. The calcite forms the 'lubricant' medium between the quartz grains; albite and mica are also subsidiary here (Fig 15, 20).

Sample 4 (Fig 16 and 18) is a granite almost modified to a kataklasite by tectonic modification. The thin section shows the fragmented quartz crystals (with wavey extinction) and similarly broken and rewelded feldspar crystals.

Sample 5 is a true kataklasite. Its quartz and feldspar crystals are broken, aligned and sheared. Tourmaline is a notable component of this kataklasite (Fig 19).

Samples 7 and 8 are also from a sedimentary series. They are fine-grained biotite mica-schists with biotite partly chloritised; green hornblende, epidote and traces of apatite are subsidiary here (Fig 21, 22).

#### **Samples from the Confluence of the Central and Western Rongbuk Glaciers on the North Slope of Mt. Everest**

(Samples 31. 10. 1984/1, 2 and 2. 11. 1984/1–3; Fig 1 and 2).

Samples 31. 10. 1984/1 and 2 were collected at 5740 m from the medial moraine of the Rongbuk glacier beyond the confluence ridge. They provide information about the rocks in situ in the 1000 m high steep slopes of this spur which rises to 6480 m. Sample 1 is a tourmaline-bearing alkali-granite which is fine-grained, metamorphosed and tectonically altered (Fig 24). Sample 2 is

a kataklasite of granitic composition, also tourmaline bearing (Fig 25).

Samples 2. 11. 1984/1-3 are from the medial moraine of the W Rongbuk glacier where it debouches on to the main stream; this shows they originate from the true left valley sides of the W glacier. Samples 1 and 2 are tectonically modified two-mica granites with residual garnet.

Sample 3 is again a representative of a sedimentary series, a fine-grained tourmalinised biotite schist (Fig 28).

*Summary:* Mineralogical investigations of rock samples from the Transhimalaya and Tibetan Himalaya allow the conclusion that during the last glaciations in this area there was long distance glacial transport. The samples from the Mt. Everest group, the highest region of the continental crust, provide an account of the petrological data collected from this area. They depict a juxtaposition of sedimentary series and granitic intrusive bodies and also extreme tectonic action deep into their crystalline structure.